disrupted-in-schizophrenia 1 (*disc1*) regulates development of the hypothalamus and its associated behaviours

Thesis submitted to the University of Sheffield for the degree of Doctor of Philosophy

Lucy Caroline Sharples
March 2020

Faculty of Medicine
Sheffield Institute for Translational Neuroscience
University of Sheffield

Institute of Molecular and Cell Biology
A*STAR, Singapore

Abstract

Understanding how the genetic risk factor *Disrupted-in-schizophrenia 1* contributes to neuropsychiatric disorders will help direct therapeutic efforts. *Disc1* functions in neurogenesis and neuronal migration. Defects in early neurodevelopment are thought to be a contributing factor in neuropsychiatric disorders. Our group previously demonstrated that ENU-generated *disc1*$^{Y472X/Y472X}$ mutants have alterations in hypothalamic development from 2 days post fertilisation. Critically, behaviours relating to the hypothalamic-pituitary-interrenal (HPI) axis such as stress responses were also perturbed in larvae and adult.

Here, we generated a novel *disc1*$^{exon6/exon6}$ CRISPR knockout line with a frameshift mutation closer to the human translocation breakpoint. Following mutant validation, we characterised previously identified hypothalamic markers and found altered expression of *retinal homeobox 3* and *steroidogenic factor 1* (*sf-1/ff1b)*. In addition, we identified increased expression of *oxytocin* in the developing hypothalamus. Behaviourally, a decrease in feeding and hunting behaviour was observed in both *disc1*$^{Y472X/Y472X}$ and CRISPR-generated *disc1*$^{exon6/exon6}$ mutant larvae. Sleep regulation was altered in *disc1*$^{Y472X/Y472X}$ only. Conversely, only *disc1*$^{exon6/exon6}$ mutants had maladaptive responses to acoustic and light stimuli as larvae, and to a novel environment as adults. These behaviours are associated with hypothalamic function and relevant to neuropsychiatric comorbidities such as eating disorders, insomnia, and anxiety.

Using immunostaining for phosphorylated ERK as a measure of neuronal activity, we noted that loss of *disc1* led to significant increases and decreases in neuronal activity in different neuronal populations in 7 dpf larvae. Regions of interest (ROIs) with increased activity included the forebrain and cerebellum, while ROIs with decreased activity included hypothalamic and connected regions. Finally, GSK-3β inhibition during a critical time window normalised *ff1b* expression in *disc1*$^{Y472X/Y472X}$ mutant embryos, with later effects on neuronal activity and feeding behaviour at larval stages. This study demonstrates the validity of zebrafish in neuropsychiatric disease research and characterises novel neurodevelopmental and hypothalamus-associated behavioural functions of *disc1*.

Acknowledgements

The doctoral process has been both challenging and rewarding. I would like to express my deepest gratitude to Dr Jon Wood for his continuous support and mentorship throughout these four years. I aspire to manage and provide guidance in the same manner over my future career. I am also grateful to Dr Sudipto Roy for welcoming me into his team, for his philosophical insights and for introducing me to many great scientists. I am indebted to Dr Caroline Wee for her endless knowledge and lessons in the lab, for inspiring and encouraging me throughout my project. I would like to extend a special thanks to Dr Ajay Mathuru and to Dr Ruey Cheng. I really appreciate how generous they have been with their time and advice. My move to Singapore was made easier thanks to the talented Yan Ling Chong, who set up injections prior to my arrival and supervised my transition into SR lab. Thank you to all other members of SR lab (past and present), for their guidance, support and friendship.

My passion for developmental neurobiology was sparked by Prof Marysia Placzek. I would like to thank her for her enthusiasm and input into this project. Thank you to Dr Suresh Jesuthasan for inspiring me to pursue a career in research, from the early days. This project would not have been possible without the contribution of the technical teams in SITraN and the Bateson Centre in Sheffield and IMCB's "fish house" in Singapore. I am thankful to the Agency of Science, Technology and Research (A*STAR) for funding my project and giving me the opportunity to present my findings at research conferences. Lastly, I would like to acknowledge my family who have supported me throughout this endeavour.

Declaration

I, Lucy Caroline Sharples, confirm that this thesis is my own work. I am aware of the University's Guidance on the Use of Unfair Means (www.sheffield.ac.uk/ssid/unfair-means). This work has not been previously presented for an award at this, or any other university.

Contents

List of Figures

List of Tables

Abbreviations

aa	Amino acids
AF7	Retinal arborisation field 7
AGRP	Agouti-related protein
ASD	Autism spectrum disorder
AVP	Arginine vasopressin
bp	Base pair
cH	Caudal hypothalamus
CNS	Central nervous system
CNV	Copy number variation
CRF	Corticotropin-releasing factor
D2R	Dopamine receptor D2
DA	Dopamine
DIG	Digoxigenin
DISC1	Disrupted-in-schizophrenia 1
dpf	Days post fertilisation
ERK	Extracellular signal-regulated kinase
GSK-3	Glycogen synthase kinase 3
GWAS	Genome wide association studies
HCRT	Hypocretin
HPA	Hypothalamic–pituitary–adrenal
hpf	Hours post fertilisation
HPI	Hypothalamic–pituitary–interrenal
IEG	Immediate early genes
kDa	Kilodaltons
LLR	Light-induced locomotor response
LOF	Loss of function
min	Minutes
MO	Morpholino

mpf	Months post fertilisation
MZ	Maternal zygotic
NPC	Neural progenitor cell
NRG1	Neuregulin 1
NTD	Novel tank diving
O/N	Overnight
OB	Olfactory bulb
OTP	Orthopedia
OXT	Oxytocin
PFC	Prefrontal cortex
phMRI	Pharmacological MRI
PO	Preoptic area
POMC	Proopiomelanocortin
PPI	Prepulse inhibition
PT	Posterior tuberculum
PTC	Premature stop codon
PVN	Paraventricular nucleus
ROI	Region of interest
RT	Room temperature
RX3	Retinal homeobox 3
SF-1	Steroidogenic factor 1
SMG	Sensorimotor gating
TH	Tyrosine hydroxylase
VMH	Ventromedial hypothalamic nucleus
VMR	Visual motor response
WISH	Wholemount *in situ* hybridisation

Chapter 1: General Introduction

1.1 Background

1.1.1 Neurodevelopmental basis of neuropsychiatric disorders

Neuropsychiatric disorders are common among the general population and include schizophrenia, bipolar disorder, and major depression. After many centuries of research, disease aetiology still remains unknown; however, increasing evidence points toward abnormal brain development as a key feature (Fatemi and Folsom, 2009; Insel, 2010). Schizophrenia affects 1% of the population and symptoms can be classified into positive (visual and auditory hallucinations, catatonia, paranoia), negative (withdrawal, anhedonia, depression, lack of motivation) and cognitive (memory, learning, processing) (Altschul, 1988). Even though these disorders are late onset, in the sense that behavioural symptoms only arise during early adulthood, it is common for cognitive symptoms to emerge during prodromal stages (childhood, late adolescence), prior to disease onset (Conroy et al., 2018). For example, a reduced intelligence quotient (IQ), slower motor development and social withdrawal/ play were reported in children who eventually developed schizophrenia (Khandaker et al., 2011; Welham et al., 2009).

Abnormalities in brain development could occur as early as the first trimester *in utero* and impinge on neurogenesis and neural circuitry formation (Fatemi and Folsom, 2009). There is also a high prevalence of minor facial abnormalities in patients with schizophrenia (Scutt et al., 2001), which could also indicate disturbances as early as gastrulation or during neural crest migration: contributing processes towards bone and cartilage morphogenesis (Drerup et al., 2009). In adults with schizophrenia, neuroanatomical differences become more pronounced and include enlarged lateral ventricles, prefrontal cortex and hippocampal atrophy, and white matter abnormalities (Buckley, 2005; Weinberger et al., 1979).

1.1.2 Environmental and genetic interplay

Neuropsychiatric disorders are idiopathic and hypothesised to arise via a multitude of pathways which converge towards similar symptoms (described above). Their underlying biological causes remain unknown, however a combination of interacting genetic and environmental risk factors is thought to be important. The need to identify highly heritable components that separately or in combination are causative of disease has been addressed using genome wide association studies (GWAS). GWAS provide supportive evidence towards a polygenetic and multifactorial model of inheritance (Ripke et al., 2014). Genetic overlap between schizophrenia, depression and bipolar disease is highlighted by common variants identified in patients with these different mental illnesses. Another

neurodevelopmental disorder which shares common variants with the aforementioned diseases is autism spectrum disorder (ASD) (Kilpinen et al., 2008), again reinforcing the neurodevelopmental hypothesis of neuropsychiatric disorders. There is also a strong environmental component. Certain experiences appear to increase the susceptibility of developing schizophrenia (e.g. cannabis use, exposure to urban living, developmental trauma). This reflects the multi-hit hypothesis where a single or multiple mutations would predispose carriers by causing minor disruptions in neurodevelopment which could increase an individuals' vulnerability to environmental risk factors (Davis et al., 2016).

1.1.3 Heightened susceptibility during critical time windows

Critical time windows are delineated by heightened susceptibility to risk factors that, at any other stage of development, would be considered harmless. Rapid brain growth and neuroplasticity in the first two years after embryonic fertilisation is considered a critical time window in humans. Neuroplasticity is the ability of the central nervous system (CNS) to change throughout life and is required for synaptic pruning, memory formation and storage (Hensch, 2005; Selevan et al., 2000). Maternal viral infection during the second trimester of gestation can lead to severe immune activation and can significantly increase the incidence of major affective disorders (Machon et al., 1997). Slightly later in development, childhood trauma and social isolation were identified as other developmental risk factors associated with schizophrenia and depression (Heim et al., 2008; Howes et al., 2017). Finally, another critical time window being increasingly studied is adolescence (Patton et al., 2018). These studies postulate that early insults followed by quiescent periods result in an increase in incidence of neuropsychiatric disorders in early adulthood and that time, rather than level of exposure, would be the largest determinant of vulnerability (Lewis and Levitt, 2002; Schloesser et al., 2007).

1.1.4 Conservation throughout vertebrates

To understand disease mechanisms, researchers turn to model organisms to investigate alterations in neural circuits, molecular pathways and associated behaviours caused by disease-associated mutations and environmental factors. The zebrafish is an attractive model organism as it offers a unique compromise between reduced complexity (only 10^5 neurons) and conserved neuroanatomy/ neurotransmitter systems. Although teleosts lack a cerebral cortex, there is a high degree of conservation in subcortical areas, that, incidentally, are heavily implicated in neuropsychiatric disorders (Geng and Peterson, 2019). Moreover, the pallium contains homologues for the mammalian amygdala (dorsomedial pallium) and hippocampus (ventral dorsolateral pallium) which are known to be affected in these disorders. Another region of interest (ROI) is the hypothalamus, which makes up a significant part of the larval zebrafish brain and is highly conserved throughout evolution. The

neurosecretory preoptic area (PO), equivalent to the paraventricular nucleus (PVN)/ supra-optic nucleus (SON) in mammals, also expresses *oxytocin* (*oxt), arginine vasopressin* (*avp*), *orthopedia* (*otp*) and *corticotrophin-releasing factor* (*crf*) neurons. The arcuate nucleus, as well as its cellular markers *proopiomelanocortin* (*pomc*) and *agouti-related protein* (*agrp*), is also conserved in the zebrafish hypothalamus. However it should be noted that some regions present in the zebrafish hypothalamus, such as the caudal periventricular hypothalamus, do not have a mammalian counterpart (Biran et al., 2015).

The ease of genetic manipulation combined with the rapidity of development of optically transparent zebrafish embryos allows for real time *in vivo* visualisation of neurodevelopment and make this model ideal for investigating the genetic basis of neurodevelopmental disorders. Furthermore, molecular and cellular changes can be correlated with quantifiable behavioural phenotypes in zebrafish larvae and adults. Indeed, larvae display locomotive behaviour and respond to their environment as early as 5 days post fertilisation (dpf). While zebrafish behaviours were initially viewed as simplistic and mainly driven by instinct, more recent studies have revealed the behavioural complexities of this model and how their behaviour is regulated by aversive learning, anxiety and emotionality (Jesuthasan, 2012; Speedie and Gerlai, 2008; Stewart et al., 2011).

1.1.5 Zebrafish models of neuropsychiatric disorders

Different genetic zebrafish models of neuropsychiatric disorders have been characterised. Morpholino (MO) antisense oligonucleotides targeting two risk genes, *disrupted-in-schizophrenia 1 (disc1)* and *neuregulin 1* (*nrg1)*, caused altered development of oligodendrocytes due to reduced numbers of *oligodendrocyte transcription factor* (*olig2*)-expressing precursor cells (Wood et al., 2009). Another study found that *nrg1* knockdown impairs mitosis in both the subventricular zone (SVZ) and the ventricular zone (VZ) (Sato et al., 2015). The latter gene is also linked to myocardial development, and in zebrafish may not be a valid model of schizophrenia as CRISPR-generated *nrg1* homozygote mutants only survived until juvenile stages. They also had reduced cardiomyocyte cell numbers and a dysregulated heartbeat due to inadequate innervation (Brown et al., 2018). Similarly, *Nrg1* knockout mutant mice have cardiac defects leading to early embryonic lethality (Gassmann et al., 1995). Although, $Nrg1^{+/-}$ heterozygote mutants do display multiple schizophrenia-related features (Karl et al., 2007; O'Tuathaigh et al., 2008; Stefansson et al., 2002).

ENU (N-ethyl-N-nitrosourea) mutagenesis has been used in TILLING (Targeting Induced Local Lesions in Genomes) screens to induce and identify point mutations in protein-coding regions. Two *disc1* ENU mutants were identified with two different nonsense mutations in exon 2: $disc1^{fh291}$ and $disc1^{fh292}$ (Draper et al., 2004), renamed $disc1^{L115X}$ and $disc1^{Y472X}$, respectively, referring to the change in amino

acid (aa) sequence. *disc1*$^{Y472X/Y472X}$ homozygous mutants developed strong defects in brain connectivity and morphological phenotypes at 24 hours post fertilisation (hpf) (De Rienzo et al., 2011). However, after multiple rounds of outcrossing, these observations were not reproducible, suggesting these phenotypes were due to additional ENU-induced mutations. For example, our group found only subtle developmental abnormalities such as altered hypothalamic progenitors and impaired behavioural and endocrine response to stress in larval and adult *disc1*$^{Y472X/Y472X}$ homozygous mutants (Eachus et al., 2017).

Schizophrenia, depression and other anxiety disorders are associated with impaired social functions (Iosifescu, 2012; Schmidt et al., 2011). Recently, a large scale CRISPR-based targeted mutagenesis study examined 35 schizophrenia and autism-associated genetic risk factors using an unsupervised machine learning assay to classify social interactions in mutant zebrafish (Tang et al., 2020). In particular, *alpha-1a adrenergic receptor a* (*adra1aa*) $^{-/-}$ and *alpha-1a adrenergic receptor b* (*adra1ab*) $^{-/-}$ mutants remained in tighter shoals and froze for prolonged periods of time. Notably, polymorphisms in the promoter of *ADRA1A* have been linked to schizophrenia in humans (Clark et al., 2005). A mutation in the *glucocorticoid receptor* (*gr*), which has been used to model clinical depression, led to increased cortisol levels due to aberrant negative feedback in *gr*^{S357} larvae. Behaviourally, locomotion was reduced, habituation was impaired, and the startle response was dysregulated. Importantly, long-term treatment with the antidepressant fluoxetine was able to rescue some of the defects (Ziv et al., 2013).

Chemically induced zebrafish models can be used to replicate neuropsychiatric endophenotypes (Gottesman and Gould, 2003) and are a powerful tool in this field of research. Acute treatment with the N-methyl-D-aspartate (NMDA) receptor antagonist MK-801 elicits phenotypes in zebrafish, such as hyperlocomotion, which can be reversed through co-administration of antipsychotics (Seibt et al., 2010). On the other hand, reserpine treatment (commonly used in rodents to model depression) affects the monoamine system and leads to hypolocomotion and a decrease in social interaction/ cohesion in zebrafish, representing depressive-like features (Kyzar et al., 2013). Finally, larvae treated with subconvulsive concentrations of pentylenetetrazol (PTZ), a GABA antagonist, have been used to model endophenotypes related to bipolar disorder (Ellis and Soanes, 2012). The activity of the hypothalamic–pituitary–interrenal (HPI) axis, the fish equivalent of the human hypothalamic-pituitary-adrenal (HPA) axis, was increased, leading to anxiety and stress-related behaviours such as an increase in darting and a maladaptive response to changes in illumination.

Antipsychotic and antidepressant medication can reverse some of the phenotypes described above, suggesting that these drugs affect neuronal signalling via highly conserved molecular targets

throughout vertebrates. In addition, zebrafish larvae are amenable to non-invasive drug administration into the medium that bathes them. Phenotype-based drug discovery is an exciting technique that can uncover new therapeutic targets. Indeed, a novel class of antipsychotics named 'finazines' acting on sigma-1 receptor were discovered using high throughput screening in zebrafish and retained activity in mammals (Bruni et al., 2016; Rennekamp et al., 2016). Moreover, in zebrafish models of ASD, behavioural phenotyping was successful in identifying estrogen receptors as promising targets to treat autism (Hoffman et al., 2016).

1.1.6 Limitations to the use of zebrafish in neuropsychiatric research

Despite its strengths for studying neurodevelopment and behaviour, there are limitations to using *Danio rerio* as a model to study neuropsychiatric disorders. Firstly, although 70-80% of disease-causing genes are conserved in zebrafish (Howe et al., 2013), genome duplication and aa differences in CNS receptors could have important pharmacological implications, especially when testing new compounds *in vivo* (Vardy et al., 2015).

Another genetic difference in zebrafish limits their ability to inbreed. Inbreeding, brother x sister or progeny x parent mating, is commonly used in animal research to generate genetically homogenous lines, where each progeny is considered a clone. Inbred animal models are used to investigate the contribution of exogenous factors (exposure to an event or a compound) towards a specific phenotype. Zebrafish, however, tend to show an increased susceptibility of inbreeding depression, referring to the reduced viability of progeny after multiple rounds (<13) of inbreeding (Shinya and Sakai, 2011). This difference is thought to arise from a lack of chromosomal sex determination in teleosts (Bradley et al., 2011), and therefore progeny arising from a single pair-mating event exhibits extensive genetic diversity.

Furthermore, various strains of zebrafish are used in animal research such as AB, Tüpfel Long-Fin (TL), Tübingen (TU), leopard and WIK. Morphological differences such as skin pigmentation, fin size as well as genetic differences define these strains. Recent studies have also elucidated several physiological and behavioural differences developing from larval stages and persisting into adulthood. In this project we had to use two strains of wild-type zebrafish, the TL strain in Sheffield and the AB strain in Singapore. It has been previously reported that AB and TL larvae show different motor responses to light-induced or dark-induces changes in locomotion (Liu et al., 2015; Gao et al., 2016). Moreover, the habituation, baseline HPI activity and shoal cohesion also appear to differ between these two strains (Segueret et al., 2016; van de Bos et al., 2017). It is important to take this into account when designing high throughput behavioural experiments to investigate neuropsychiatric endophenotypes.

A major component of schizophrenia such as auditory and visual hallucinations rely on self-reporting from patients, which poses a problem in any animal model lacking higher order communication and language functions (Russell, 1980). Lastly, zebrafish display nowhere near as many behavioural complexities as humans. It is therefore imperative to differentiate between animal "model" and "tool", with the latter more applicable here and still providing key insights into the pathophysiology of these disorders (Blaker-Lee et al., 2011). The zebrafish does have key advantages and can complement studies from its mammalian counterparts. For example, like humans, zebrafish are diurnal (vs. nocturnal mice and rats), indicating parallels between sleep regulation. Moreover, as in humans, the main corticosteroid synthesised and released in response to stress is cortisol, as opposed to corticosterone in mice and rats (Alsop and Vijayan, 2009).

1.1.7 Hypothalamic-related changes in neuropsychiatric disorders

The hypothalamus is an evolutionarily ancient part of the brain and a key regulator of whole-body energy homeostasis. Situated in the ventral forebrain and extending rostrally, the highly interconnected hypothalamic nuclei integrate multiple sensory inputs and coordinate different neuroendocrine outputs. Their primary role is to modulate sleep, appetite, and the stress response (see sections 4.1 and 6.1, for detailed introduction). Defects in the hypothalamus have been suggested to contribute to disease mechanisms underlying neuropsychiatric disorders and ASD. In patients with schizophrenia, bipolar and unipolar disorder, the volume of the hypothalamus (particularly the PVN and SON) was significantly increased compared to healthy controls and correlated positively with anxiety (Goldstein et al., 2007; Schindler et al., 2019). In ASD, grey matter density was found to be decreased in the hypothalamus of affected children. These abnormalities were associated with changes in the macrostructure, including increased volume of the 3rd ventricle, which lies adjacent to the hypothalamus (Wolfe et al., 2015). In addition to volumetric changes, changes in hypothalamic cell types have been reported in numerous human studies. For example, increases in the number of CRF^{+}, AVP^{+} and OXT^{+} neurons were reported in the PVN of patients with major depression and bipolar disorder (Bao et al., 2005; Purba et al., 1996; Raadsheer et al., 1994). Functional magnetic resonance imaging (fMRI) studies have enabled the visualisation of brain activity in these patients. Abnormal hypothalamic activation to aversive images was reported in bipolar patients (Malhi et al., 2004) and functional connectivity scores between the hypothalamus and other subcortical areas were reduced in patients with major depression (Liu et al., 2018; Wang et al., 2019). In the MK-801 induced mouse model of schizophrenia, neuronal activation in the hypothalamus was also significantly reduced (Zuo et al., 2009). In another model previously mentioned, *Nrg1*$^{+/-}$ mice, neurons in the PVN appeared to be hypersensitive to cannabinoid exposure (Boucher et al., 2007). These results suggest that the

pathophysiology of neuropsychiatric disorders is tightly associated with aberrant hypothalamic patterning and function.

In response to stress, the PVN of the hypothalamus releases CRF, acting on the pituitary and leading to release of adrenocorticotropic hormone (ACTH) into the vasculature. This triggers the synthesis and release of cortisol from the adrenal cortex, which can be used as a readout of stress. Cortisol provides negative feedback to the hypothalamus via multiple brain regions also linked to neuropsychiatric disorders such as the prefrontal cortex, amygdala, and hippocampus. There is ample evidence suggesting HPA axis hyperactivity in major depression. Indeed, hypersecretion of ACTH and cortisol have been reported, as well as altered peripheral levels of CRF in patients with depression (Drevets et al., 2008; Holsboer, 2000; Swaab et al., 2005). Impaired negative feedback signalling from glucocorticoid receptors (GR) is hypothesised to contribute to this hypersecretion (Pariante and Miller, 2001). Medication-naïve patients with first episode psychosis exhibited a blunted cortisol release when acutely stressed (van Venrooij et al., 2012). Furthermore, repeated stressful experiences are often referred to as "triggers" of these disorders. Chronic corticosterone (CORT) injections induced depressive-like behaviours in male rats (Gregus et al., 2005). Conversely, *Nrg1*$^{+/-}$ mice injected with CORT to mimic HPA activation were hyporesponsive to stress, characterised by blunted neuroendocrine and behavioural responses (Chohan et al., 2014). These findings demonstrate that HPA axis dysfunction is present in many neuropsychiatric disorders and that chronic activation of the HPA axis can trigger depressive-like endophenotypes in mammals. Aberrant HPA axis function characterised by either an increase or decrease in activity could therefore cause maladaptive responses to stressful situations.

1.1.8 *Disrupted-in-schizophrenia 1* (*DISC1*)

Disrupted-in-schizophrenia 1 (*DISC1*) is a protein-coding gene located on chromosome 1 and possibly the most widely studied genetic risk factor in neuropsychiatry. The balanced translocation of t (1;11) (q42.1; q14.3) was initially characterised in a Scottish pedigree with a high incidence of diagnosed schizophrenia, bipolar disorder and major depression (Millar et al., 2000). Linkage and association studies also uncovered *DISC1* single nucleotide polymorphisms (SNPs) in disease groups from Japan, Taiwan and Finland (Chubb et al., 2008; Ekelund et al., 2004; Hashimoto et al., 2006; Liu et al., 2006b). Another *DISC1* mutation, a 4 base pair (bp) frameshift mutation in exon 12, co-segregated with schizophrenia in a small North American pedigree (Sachs et al., 2005). The causality of this particular mutation was debated as concerns regarding the sample size were raised (Green et al., 2006). In addition, following the most recent neuropsychiatric GWAS, *DISC1* was not identified in the list of 108 susceptibility loci associated with schizophrenia (Ripke et al., 2014). Controversy in the field emerged,

with some researchers proposing to stop investigating this gene altogether (Sullivan, 2013). Others acknowledged its lack of involvement in schizophrenia *per se,* instead linking it to schizoaffective and depressive disorders (Porteous et al., 2014). Importantly, GWAS only identified relatively common variants from genetically heterogeneous disorders. Thus, high risk alleles present at low frequencies in the general population, such as the *DISC1* translocation, are excluded. However, *DISC1* mutations are highly penetrant and have a strong biological impact in neuropsychiatric disorders (Blackwood et al., 2001) and they remain one of the highest single linkage risk factors associated with schizophrenia, bipolar disorder and major depression to date.

DISC1 is expressed in the brain during early development, and expression analysis in carriers suggested a 50% reduction in *DISC1* mRNA and DISC1 protein levels in translocation carriers (Millar et al., 2005). Additionally, there was a complete loss of DISC1 protein in neurons derived from induced pluripotent stem cells (iPSCs) with biallelic frameshift mutations in *DISC1* leading to a premature stop codon (PTC) exon 8 (Srikanth et al., 2015). Therefore, the mechanism of action in the Scottish pedigree is likely to be haploinsufficiency. However, other groups reported that the putative truncated form of DISC1 forms a dimer with wild type DISC1 providing evidence for a dominant negative (DN) mechanism of action (Kamiya et al., 2005; Pletnikov et al., 2007). Another study reported that DISC1 can homodimerise, pointing to protein mis-assembly and the formation of toxic aggregates (Atkin et al., 2012), common to many CNS disorders. Therefore, the exact mechanism by which mutations in *DISC1* increase the risk of developing neuropsychiatric disorders still remains unknown; although it seems likely that different variants could function through different mechanisms.

1.1.9 Phenotypes in *Disc1* rodent models

Multiple strains of transgenic and/ or mutant *Disc1* rodent models have been generated to study the role of *DISC1*. Multiple phenotypes relating to the clinical symptoms of depression and schizophrenia have emerged from these studies, although there are discrepancies. Depressive-like endophenotypes such as reduced sociability and reward responsiveness were identified in the missense *Disc1*^{Q31L} mutants, whereas missense *Disc1*^{L100P} mutants recapitulated more schizophrenia-like endophenotypes such as deficits in sensorimotor gating and information processing (Clapcote et al., 2007). Sensorimotor gating was also abnormal in a transgenic mice expressing dominant-negative truncated DISC1 (DN-DISC1) under the αCaMKII promoter (Hikida et al., 2007); however, this was not the case in transgenic mice with inducible expression of a mutant form of human DISC1 lacking the C-terminus (hDISC1-ΔC) limited to the cerebral cortex, hippocampus and striatum (Pletnikov et al., 2008). Conflicting results were also reported when examining sociability of *Disc1* mutants. Some groups observed reduced social interactions in *Disc1* mutant mice (Clapcote et al., 2007; Li et al., 2007;

Pletnikov et al., 2008), whereas other groups reported no difference (Hikida et al., 2007). These differences in behavioural phenotypes could differ based on the location of disruption or perhaps the different methods used to generate the mouse lines.

In addition to behavioural features, pathological analysis of *Disc1* mutants revealed the presence of morphological features related to schizophrenia. For example, the volume of the lateral ventricles is significantly increased in *Disc1* mutants compared to wild type littermates (Hikida et al., 2007; Pletnikov et al., 2008; Shen et al., 2008). Furthermore, a reduction in total brain volume was reported in both *Disc1*^{Q31L} and *Disc1*^{L100P} mutants (Clapcote et al., 2007). A reduction in immunoreactivity for parvalbumin, another hallmark of schizophrenia, was demonstrated in the medial prefrontal cortex and hippocampus (Hamburg et al., 2016; Hikida et al., 2007; Shen et al., 2008). Finally, synaptic spines and dendritic complexity were significantly reduced in the hippocampus of DN-*Disc1* mice (Kvajo et al., 2008; Li et al., 2007), consistent with working memory deficits in this disorder.

1.1.10 Vertebrate conservation

The mammalian *DISC1* gene is located on chromosome 1 and is made up of 13 exons. The full length protein contains 854 aa. There are over 23 different reported transcripts in humans. In zebrafish, the *disc1* gene is located on linkage group 13, contains 998 aa and 4 different isoforms have been annotated. The DISC1 protein does not share overall homology with any other known protein and its tertiary structures are speculative due to the absence of any solved crystal structure. Proteomic studies have identified a highly conserved *C*-terminus containing α-helical coiled-coils, thought to be important in protein-protein interactions, suggesting its evolutionarily conserved role as a scaffold protein (Soares et al., 2011). The globular *N*-terminus is not well conserved with the exception of a string of 15 aa: the arginine rich motif (ARM). This motif is thought to play a crucial role in mRNA transport (Tsuboi et al., 2015).

1.1.11 Cellular and molecular role of DISC1

Numerous functions have been suggested for *DISC1*, including roles in neurogenesis, axon guidance, neuronal migration and synapse function. The DISC1 protein has no endogenous enzymatic activity, however it interacts with a myriad of binding partners (Camargo et al., 2007; Morris et al., 2003). The protein is reported to localise to the nucleus, cilia, centrosome, mitochondria, growth cone, synapse and dendrites (James et al., 2004; Miyoshi et al., 2003). The diverse subcellular distribution and interactome is indicative of its diverse roles in neurodevelopmental processes, such as progenitor proliferation, neuronal migration and differentiation (Chandran et al., 2014; Hennah et al., 2006; Mao et al., 2009). Some of DISC1's direct and indirect interactome consists of other proteins classed as risk

factors for psychiatric disorders such as NDEL1, PDE4 and NRG1 (Li et al., 2007; Seshadri et al., 2015), suggesting that DISC1 could act as a hub in common pathways underlying mental illness (Chubb et al., 2008).

1.1.12 Roles in neurodevelopment

Since its initial discovery, *DISC1* has been found to regulate a number of key neurodevelopmental processes. High levels of *Disc1* expression are observed during embryonic development and decrease postnatally (Nakata et al., 2009). *DISC1* plays a key role in neural progenitor cell (NPC) proliferation and the formation of new neurons (neurogenesis). During early development, neurons arise from multipotent cells found in the neuroectoderm. They go through rounds of proliferation and differentiate at particular timepoints by synchronously responding to external and internal cues. Most developing neurons undergo neural migration guided by molecular cue recognition (Chubb et al., 2008). Dynamic changes in gene expression occur to orchestrate these processes. As transcriptional changes slow, committed cells give rise to different mature cell types, each with a unique molecular fingerprint. During this period, the CNS is sensitive to both internal and external stimuli (Holmes et al., 2005).

Disc1 knockdown in embryonic mice led to premature differentiation of neurons in both primary neuronal culture and the cerebral cortex, depleting the number of neural progenitors (Ishizuka et al., 2011; Mao et al., 2009). At a molecular level, DISC1 is thought to modulate cell proliferation via Glycogen Synthase Kinase 3β (GSK-3β) inhibition (see section 7.1, for detailed introduction). Loss of *DISC1* reduced proliferation and migration in mouse NPCs. There was an increase in the proportion of cells in G0/G1 indicating cell cycle progression was stalled (Wu et al., 2017b). *Disc1* transgenic mice expressing two copies of truncated *Disc1* (exon 1-8) had reduced neural proliferation visualised by decreased BrdU labelling (Shen et al., 2008). At 24 hpf, the expression of phosphorylated histone H3 (phosH3), an M-phase marker, was increased in *disc1*^{Y472X} zebrafish mutants; however at 3 dpf, phosH3 expression decreased compared to controls, suggesting that *disc1* is also required to maintain NPCs during early zebrafish development (Eachus et al., 2017). Expression of *retinal homeobox 3* (*rx3*), a marker for hypothalamic progenitors, was also decreased at 3 dpf in these mutants, and a concurrent increase in *steroidogenic factor 1* (*sf-1/ ff1b)*$^{+}$ cells which differentiate from this lineage was also noted, further supporting the role of *disc1* in cell fate determination. *DISC1* expression persists into adulthood but becomes restricted to specific neural stem cell (NSC) niches such as the olfactory bulb, dentate gyrus and hypothalamus (Austin et al., 2003; James et al., 2004; Lipska et al., 2006; Schurov et al., 2004). Progenitor populations also persist into adulthood, playing a critical role in

neuroplasticity, and loss of *Disc1* can also reduce levels of adult neurogenesis (Faulkner et al., 2008; Kim et al., 2012; Mao et al., 2009; Ye et al., 2017).

DISC1 associates with microtubule-interacting proteins such as MIPT3 (Morris et al., 2003) and centrosome-associated ones such as NDEL1 (Shu et al., 2004). Overexpression of *DISC1* in *C.elegans* motor neurons caused axonal guidance defects (Chen et al., 2011). Silencing of *Disc1* by RNAi in cortical pyramidal neurons of embryonic mice inhibited neuronal migration by a failure to anchor dynein and dynactin to the centrioles (Kamiya et al., 2005). Further, *disc1* knockdown also affected the migration and differentiation of cranial neural crest cells in zebrafish embryos through transcriptional repression of *foxd3* and *sox10* (Drerup et al., 2009). Therefore, DISC1 plays a role in neurodevelopment through both neural proliferation and neuronal migration.

As previously proposed (see section 1.1.3), the neurodevelopmental effects from loss of *DISC1* could have adverse consequences on neural circuitry and cause behavioural hallmarks of neuropsychiatric disorders. Indeed, behavioural characterisation of mouse models with neurodevelopmental abnormalities also revealed anxiety-related and schizoaffective endophenotypes (Clapcote et al., 2007; Mao et al., 2009). Furthermore, neurobehavioural effects of *DISC1* disruption are time dependent. Transient expression of the *C*-terminal portion of DISC1 at postnatal day (P) 7 resulted in deficits in spatial working memory, depressive-like traits, and reduced sociability. Strikingly, there were no acute effects when expression was induced in adults (Li et al., 2007). Another study used the inducible expression of mutant human DISC1 (hDISC1) (Pletnikov et al., 2008) to investigate the effect of transient early prenatal or postnatal mutant hDISC1 expression (Ayhan et al., 2011). Selective early prenatal expression led to minor effects on behaviour. Depression-like behaviour was present in female mice with selective postnatal expression, while aggression was only detected in male mice expressing mutant hDISC1 throughout their life.

As well as the effect of varying *Disc1* expression, environmental stressors interact with *DISC1* and have implications for later behaviours. For example, in gene-environment (GxE) studies, *Disc1* mutant mice were exposed to prenatal polyinosinic: polycytidylic acid (Poly I:C) infection to induce a cytokine response prenatally. At adult stages, the GxE mice exhibited exacerbated deficits in sociability, anxiety and depressive-like traits compared to *Disc1* mice with no immune activation (Abazyan et al., 2010; Ibi et al., 2010). Other studies evaluated the effect of psychosocial stress on different *Disc1* mutant mice. Chronic social defeat administered to heterozygote $Disc1^{Q31L}$ and $Disc1^{L100P}$ mice exacerbated a number of behavioural phenotypes previously observed in homozygous $Disc1^{Q31L}$ and $Disc1^{L100P}$ mice (Hague et al., 2012). Another form of stress: isolation stress (IS) was administered during another

critical time window, in adolescence. DN-*Disc1* mice exposed to stress (GxE) displayed hyperactivity in the open field and anxiety-related behaviours compared to controls (DN-*Disc1* only or IS only). This was linked to hyper-responsiveness of the HPA with a failure to return corticosterone to baseline levels (Niwa et al., 2013). Similar studies have also been performed in zebrafish. Acute exposure to stress induced behavioural responses and increased plasma cortisol in wild type zebrafish larvae, while these responses were absent in in *disc1*^{Y472X} and *disc1*^{L115X} zebrafish larvae. This suggests that functioning of the HPI axis is impaired in *disc1* mutants (Eachus et al., 2017). These results suggest that the mechanisms through which *Disc1* contributes to affective disorders also involves environmental interactions and could explain the incomplete penetrance and variety of clinical diagnoses in translocation carriers from the Scottish pedigree (Millar et al., 2000).

1.2 Hypothesis

In light of the background information aforementioned, we hypothesised that loss of *DISC1* confers vulnerability to neuropsychiatric disorders due to deficits in early neurodevelopment. Particularly, alterations in cell proliferation and differentiation are affected in a *DISC1*-dependent spatiotemporal manner, according to its expression profile. Given that *disc1* is widely expressed in the developing brain, we hypothesised that mutations in *disc1* lead to brain-wide developmental consequences and are not solely localised to the periventricular hypothalamic cells identified in a previous study (Eachus et al., 2017). Such developmental changes would be expected to have far reaching effects on activity of neural circuits and behaviour.

1.3 Objective and Aims

The objective of this project was to determine how the variation of a highly penetrant genetic risk factor for neuropsychiatric disease, namely *Disrupted-in-schizophrenia 1* (*DISC1*), affects the early development of the brain and particularly the hypothalamus. This will contribute to elucidating why there is an increased susceptibility of developing schizophrenia, bipolar and major depressive disorders in populations with mutation or SNPs in *DISC1.* It will therefore expand knowledge about mechanisms and the pathophysiology of neuropsychiatric disorders.

The primary aim of this project was to characterise phenotypes in *disc1* mutant larvae and adults. Initial findings from our group suggested that neuroendocrine function was compromised in *disc1*^{Y472X} and *disc1*^{L115X} mutants from 5 dpf, as a result of mispatterning of the *rx3*$^{+}$, *ff1b*$^{+}$ hypothalamic cells populations observed at 2 dpf (Eachus et al., 2017). We set out to generate another *disc1* mutant zebrafish model using CRISPR/ Cas9 genetic engineering, to create a loss of function mutation and address existing discrepancies around severity of phenotypes in the literature (De Rienzo et al., 2011; Eachus et al., 2017; Wood et al., 2009). We specifically targeted exon 6 of *disc1,* a locus proximal to

the human equivalent breakpoint in intron 8 of *DISC1*. Following validation, we investigated the expression *rx3, ff1b* and *pomc* in CRISPR-generated *disc1*^{exon6} and compared results with ENU-generated *disc1*^{Y472X} zebrafish embryos.

Another aim was to investigate whether altered hypothalamic development in *disc1* mutants affected key neural circuits and contributed to hypothalamus-associated behavioural hallmarks of neuropsychiatric disorders such as arousal, sleep, feeding and anxiety-related behaviours. To uncover the magnitude of the role of *disc1* in establishment of neural circuitry, we wanted to consider other affected brain areas, and avoid focussing on the hypothalamus exclusively.

A major objective of all disease-modelling studies is to rescue or at least ameliorate deficits induced by genetic or environmental insult. As Disc1 is known to bind and inhibit GSK-3β (Mao et al., 2009), we planned to use pharmacological inhibition of GSK-3β in *disc1*^{Y472X} mutant embryos to investigate its potential therapeutic effects.

1.4 Experimental Plan

We set out to generate the tools necessary for achieving these aims. To generate a *disc1* CRISPR/ Cas9 null zebrafish mutant, we co-injected guide RNA (gRNA) targeting exon 6 and *Cas9* mRNA to produce double strand breaks (DSB) in the zebrafish genome. We raised the injected F0 generation until adulthood and selected the most appropriate allele. We outcrossed the F0 to AB wild types and incrossed identical (16 bp deletion) siblings to achieve a stable F2 generation. Progeny from this generation was used for further characterisation. We ensured a simple and cheaper method of genotyping by restriction digestion analysis rather than by sequencing as in the ENU mutants.

We repeated some of the characterisation work performed on the *disc1*^{Y472X} line (Eachus et al., 2017) by investigating the hypothalamic/ pituitary expression of *rx3, ff1b* and *pomc* using probes and RNA *in situ* hybridisation. This also involved investigating the response to dark/ light flashes in larvae and the response to stress in adult zebrafish.

To investigate if other hypothalamic-associated behaviours were affected, we characterised other behavioural parameters. At larval stages, we measured locomotion during pseudo-natural daytime and night-time to study sleep behaviours. Next, we measured food intake by fluorescently dying *Paramecia* (zebrafish prey) and measuring gut fluorescence, post-ingestion. We used another measure, quantification of prey captures, to assess hunting behaviour. Then, we measured locomotion in response to unanticipated acoustic stimuli during the night, using the night-time arousal (NTA) test. In adults, we investigated innate fear by quantifying swimming behaviour using the novel tank diving (NTD) assay.

To determine whether brain activity was affected and avoid biased selection of hypothalamic neuronal populations, we used a previously developed method (Randlett et al., 2015) to measure whole brain neuronal activity in *disc1* mutants and identified aberrant neuronal circuits. Briefly, following rapid fixation at larval stages, we performed immunofluorescence against the immediate early gene (IEG): phosphorylated extracellular signal-regulated kinase (pERK). This provided information about baseline brain activity. We scaled up this experiment, to image 30-40 larval brains per condition and used predesigned methodology (Randlett et al., 2015) to create brain activity maps. These maps were normalised and computationally compared to a pre-annotated larval brain atlas (stackjoint.com/zbrain). Once neuronal populations with significant differences in brain activity were identified, we designed the necessary antisense RNA *in situ* probes against these hits. RNA *in situ* hybridisation was performed at earlier stages, to assess if deficits arose from a developmental origin.

Once robust phenotypes were established, we selected a commercially available GSK-3β inhibitor: CHIR99021, previously applied between 1-2 dpf in *disc1*^{Y472X} mutants, and which successfully rescued the expression of the hypothalamic marker *ff1b* (see section 7.2.1). We investigated the long-term effects of CHIR99021 on brain activity and larval behaviour in the *disc1*^{Y472X} line.

Another unresolved issue in this field is both the tissue distribution and subcellular localisation of endogenously expressed DISC1 protein orthologues. To this end, a zebrafish-specific polyclonal antibody was synthesised in order to localise zDisc1 expression in wild type zebrafish embryos and investigate whether *disc1* mutations lead to null knockout mutants. A polypeptide comprising the *N*-terminus of the zDisc1 protein, previously expressed and purified from bacterial cells, was sent for rabbit immunisation prior to starting the project. Once the serum returned, we purified the zDisc1(*N*)-specific antibodies and tested their specificity in both *in vitro* (western blotting) and *in vivo* (immunofluorescence) experiments.

Chapter 2: Materials and Methods

2.1 Buffers and Solutions

Name	**Composition**
E3 Medium	5 mM NaCl, 0.17 mM KCl, 0.33 mM $CaCl_2$, 0.33 mM $MgSO_4$
PEI	1 mg/ml polyethylenimine (PEI) (Polysciences Inc., #23966)
Phosphate Buffered Saline (PBS)	137 mM NaCl, 2.7 mM KCl, 10 mM Na_2HPO_4, 1.8 mM KH_2PO_4
20X Tris buffered saline (TBS)	400 mM Tris, 2.742 M NaCl, pH 7.6 with HCl
TBST	1X Tris-buffered saline (TBS), 0.1% Tween 20
5X Laemmli Buffer	250 mM Tris HCl (pH 6.8), 50% glycerol, 10% sodium dodecyl sulfate (SDS), 25% β-mercaptoethanol, 0.5% bromophenol blue
RB100 buffer	25 mM HEPES (pH 7.5), 100 mM KOAc, 10 mM $MgCl_2$, 1 mM dithiothreitol (DTT), 0.05% Triton X-100, 10% glycerol
GSH elution buffer	50 mM Tris, 100 mM NaCl, 40 mM reduced Glutathione (pH 7.5)
Wash buffer	20 mM Hepes-KOH, 150 mM NaCl pH 7.8
Wash buffer (2)	20 mM Hepes-KOH, 1 M NaCl pH 7.8
Binding buffer	Wash buffer, 0.5% Triton X-100
Crosslinker	100 mM disuccinimidyl suberate (DSS) in dimethyl sulfoxide (DMSO) (37mg/ml)
Crosslinking solution	12.5% crosslinker, 87.5% wash buffer
Elution buffer	0.1 M Glycine (pH 2.5)
Lysis buffer	80 mM K-PIPES (pH 6.8), 1 mM EDTA, 1mM $MgCl_2$, 1% NP40, 150 mM NaCl, 10 mM NaF, 1 mM Na_2VO_4, 10 mM β-Glycerophosphate, 5 mM $Na_4P_2O_7$ with 1X Halt Protease Inhibitor Cocktail (ThermoScientific)
Resolving Gel (7.5%)	7.5% acrylamide, 375 mM Tris HCl (pH 8.8), 0.1% SDS, 0.1% ammonium persulfate (APS), 0.01% tetramethylethylenediamine (TEMED)
Stacking Gel (4%)	4% acrylamide, 125 mM Tris HCl (pH 6.8), 1% SDS, 0.06% APS, 0.003% TEMED
Running buffer	25 mM Tris, 192 mM glycine, 0.1% SDS
Transfer buffer	25mM Tris, 192 mM glycine, 20% methanol
Blocking buffer (WB)	5% non-fat dry milk in TBST
0.1 M Sodium phosphate	20 ml of 0.2M NaH_2PO_4, 80ml of 0.2M Na_2HPO_4,100 ml ddH2O for pH 7.4

buffer	
Fish fix	0.1 M Sodium phosphate buffer, 12 mM $CaCl_2$, 4% paraformaldehyde (PFA), 4% sucrose
Bleaching solution	3% H_20_2, 1% KOH in PBS
PBT	1X PBS, 0.1% Triton X-100
PBDT	1X PBS, 2% bovine serum albumin (BSA), 1% DMSO, 0.1% Triton X-100
Blocking solution (IF)	PBDT + 2% sheep serum
PTW	1X diethyl pyrocarbonate (DEPC)-treated PBS, 0.1% Tween 20
Incomplete hybridisation solution	50% formamide, 5X saline-sodium citrate (SSC), 0.1% Tween 20, 9.2 mM citric acid
Complete hybridisation solution	50% formamide, 5X SSC, 0.1% Tween 20, 9.2 mM citric acid, heparin (5 ng/ml), tRNA (200 ng/ml)
Blocking solution (*in situ*)	PTW, 2% sheep serum, 2% BSA
Staining buffer	0.1 M Tris pH 9.5, 0.5M $MgCl_2$, 1 mM NaCl, 0.1% Tween 20
Staining solution	Staining buffer, nitro-blue tetrazolium chloride (NBT) (4.5 µl/ml), 5-bromo-4-chloro-3'-indolyphosphate p-toluidine salt (BCIP) (3.5 µl/ml)
LB agar	10 g/l agar, 10 g/l tryptone, 5 g/l NaCl, 5 g/l yeast extract
LB broth	10 g/l tryptone, 5 g/l NaCl, 5 g/l yeast extract
Terrific Broth (TB)	24 g/l yeast extract, 12 g/l casein peptone, potassium phosphate (monobasic) 2.2 g/l, potassium phosphate (dibasic) 9.4 g/l, 0.4% glycerol
Alkaline Lysis buffer	25 mM NaOH, 0.2 mM ethylenediaminetetraacetic acid (EDTA)
Neutralisation buffer	40 mM Tris-HCl (pH 8)
Paramecia water	0.3 mg/ml Instant Ocean, pH 7 with $NaHCO_3$

2.2 Ethics Statement

Animal models were handled following standard practices and guidelines from the UK Home Office under the Animals Act (1986) and were approved by the University of Sheffield Ethical Review Committee. In Singapore, ethical approval was issued by the Institutional Animal Care and Use Committee (IACUC) from the Biological Resource Centre (BRC/ IACUC/003/F5).

2.3 Zebrafish Husbandry

Wild type *Danio rerio* were maintained in the Zebrafish Core Facility in the Bateson Centre, Sheffield (TL) and Institute of Molecular and Cell Biology, Singapore (AB). Adult zebrafish were kept at 28.5°C with a light/ dark cycle of 14 hours/10 hours. Both pair-mating and group mating (using the marbling method) were used to obtain embryos. Embryos were sorted from unfertilised eggs and left to develop in E3 containing methylene blue at 28°C. For larvae used in behavioural assays, embryos were transferred to E3 at 24 hpf and placed in an incubator with a light/ dark cycle of 14 hours/10 hours and fed once a day with live paramecia from 5 dpf. Tricaine Mesylate (50 mg/ml) was used for anaesthesia and euthanasia for fish older than 5 dpf.

2.4 Bacterial Cultures

For both LB-antibiotic plates and LB Broth, throughout these methods, final concentrations of antibiotics were 100 µg/ml for carbenicillin/ ampicillin, 50 µg/ml for kanamycin.

2.5 Purification of zDisc1 polyclonal antibody serum

A previously purified zDisc1 (*N*)-GB1 fusion protein (A. Zarkesh MSc thesis, University of Sheffield, 2016) was used to raise a new rabbit polyclonal antibody (Eurogentec). In order to purify the serum from non-specific antibodies and antibodies selective to GB1 tag, we used GST-tagged zDisc1 (*N*).

2.6 Expression and purification of GST-tagged zDisc1 (*N*)

A GST-tagged zDisc1 (*N*) plasmid was synthesised using *pGEX-6b1* (kind gift of Dr G. Hautbergue). Primer pairs were designed with BamHI and XhoI restriction sites to ensure directionality. A 600 bp product was amplified using Herculase II (Agilent) proofreading polymerase. Adenosines were added and the polymerase chain reaction (PCR) product was subcloned into pCR-II TOPO vector. Following sequencing, a double digest was performed on the subcloning vector pCR-II-*disc1* and pGEX-6b1 using BamHI and XhoI. The linearized vector was dephosphorylated using recombinant Shrimp Alkaline Phosphatase (rSAP). Vector and insert were purified and a 10 µl ligation reaction was set up using T4 Ligase (BioLabs):

Reagent	**Volume (µl)**
Insert	1.5
Linearized vector	4.5
10 X T4 Ligase buffer	1
Sterile water	2.5
T4 Ligase enzyme	0.5

This reaction was incubated overnight (O/N) at 16°C and 2 µl was transformed into library efficiency TOP10 cells which were spread and grown in LB + Carbenicillin. Plasmid DNA was extracted and purified using a Miniprep kit (QIAGEN). Sequencing was performed to confirm the reading frame.

One hundred ng of *pGEX6b1-disc1* plasmid was transformed into Rosetta cells and large-scale protein expression was induced using IPTG (3 mM). Briefly, the bacterial cell pellet was lysed in 25 ml of RB100 buffer (+ 150 µl Protease Inhibitor Cocktail (PIC) + 0.6 mM PMSF). The solution was sonicated for 2.5 minutes (min) and centrifuged for 20 min at 48,000 g at 4°C. The supernatant was then added to 150 µl of washed GSH sepharose beads 4B (GE Healthcare) and left to bind via rotation for 30 min at room temperature (RT). Bound protein and the beads were washed twice in RB100 buffer and eluted in GSH elution buffer.

2.6.1 GST-fusion protein crosslinking

Eight mg of purified Disc1 (*N*)-GST was dialysed in 100X the volume of wash buffer O/N at 4°C to remove amine groups that can react with DSS. Binding of Disc1 (*N*)-GST with 1.5 ml of GSH beads was performed for 1 hour at 4°C. Bead complexes were washed 1X in binding buffer and 3X in wash buffer. The wash buffer was removed, and the beads were incubated in a crosslinking solution for 30 min at RT. The unreacted DSS was quenched by adding 100 µl of 1 M Tris (pH 7.4).

2.6.2 Antibody binding

Serum was centrifuged at 20,000 g for 20 min at 4°C. Five ml of supernatant was incubated with the crosslinked protein-bead complex O/N at 4°C on via rotation. Keeping the temperature at 4°C, the solution was poured through a column and beads were allowed to settle. The tap was opened to drain off the supernatant and unbound antibodies. Twenty ml of wash buffer (1) was poured through and, subsequently, 20 ml of binding buffer. Then, 20 ml of wash buffer (2) was poured through and, again, 20 ml of binding buffer. Beads were soaked in 2.5 ml of elution buffer for 15 min. The eluate was collected and neutralised using 50 µl of 1 M Tris (non-pHed). This was then dialysed in wash buffer for 3 hours and a final dialysis step was performed in wash buffer with 40% glycerol. The contents of the dialysis tubing, with apore size of 12-14 kilodaltons (kDa) were transferred to a microcentrifuge tube and stored at -20°C.

2.7 Mammalian cell culture and transfection

Full length PCS2+*disc1*-FL was transfected into HEK293 cells (ATCC) at 70-80% confluency, using polyethyleinimine (PEI) transfection reagent. Two µg of plasmid DNA was first mixed with 6 µl PEI (28.8 ng/µl) in 200 µl of OptiMEM media (Invitrogen) and left 20 min at RT. Transfection was performed by

pipetting the mixture onto the cells which were incubated 20 min at RT and then transferred to an incubator (37°C, 5% CO2). After 6 hours, the media was replaced with fresh DMEM.

2.8 Protein extraction from mammalian cells

Protein was extracted 24 hours post-transfection. Cells were washed in PBS, scraped into ice cold lysis buffer and lysed on ice for 30 min. Protein was separated from cell debris by centrifugation for 1 min at 14,000 rpm at 4°C. Protein concentrations were calculated from a standard curve of BSA using a Bradford assay. Samples were diluted at a 1:1 ratio in 2X Laemmli buffer and stored at -80°C.

2.9 Protein extraction from zebrafish larvae

Protein was extracted from 26 and 52 hpf zebrafish head lysates. Extracts were prepared by homogenising 40 decapitated heads in 100 µl of 1X Laemmli sample buffer then heating at 95°C for 5 min. Protein extracts were stored at -80°C.

2.10 Western Blotting

Protein extracts were thawed, heated for 5 min at 95°C and centrifuged for 1 min at 14,000 rpm. Glass plates were washed and cleaned with 100% ethanol, then assembled, fixed upright, and checked for leaks. Five ml of 7.5 % resolving gel was loaded between the plates. Once set, 1 ml of 4% stacking gel was loaded and left to set with a gel comb to form wells. Fifteen µl of protein in Laemmli buffer (equivalent to 3 or 6 embryo heads) or 20 µl of mammalian cell lysate in Laemmli buffer (1 ug/ µl) was loaded into each well and resolved by SDS-PAGE for 75 min at 150 V in running buffer. A wet transfer to methanol activated PVDF membranes was performed for 1 hour at 120V or O/N at 30V in transfer buffer. Membranes were then incubated in blocking buffer (WB) for 1 hour at RT and probed with anti-zDisc1 antibody (1:1000) O/N at 4°C. Membranes were then washed for 3 x 10 min in TBST before a 1-hour incubation with goat-anti-rabbit HRP-conjugated secondary antibody (1:5000) at RT. Membranes were washed for 3 x 10 min in TBST again before detection using enhanced chemiluminescence (ECL) (Geneflow), using a 1:1 ratio of reagents. Protein bands were detected using ECL hyperfilm (GE healthcare) and developing solution or imaged using a G-BOX (Intellichem) and analysed with FIJI software.

2.11 Tissue fixation

Embryos were dechorionated, anaesthetised and transferred to microcentrifuge tubes prior to fixation. They were washed 3 times in PBS and fixed in Fish fix O/N at 4°C. Skin pigmentation was

removed by incubating the samples in bleaching solution for 20 min. Samples were washed 3 times in PBT. These were then dehydrated via a series of washes with 25, 50 and 75% methanol: PBS and stored in 100% methanol at -20°C.

2.12 Immunofluorescence

Fixed embryos were rehydrated to PBS via a series of 75%, 50% and 25% methanol in PBS then washed in PBT. Embryos were cracked using prechilled acetone for 6 min (24-72 hpf) at -20°C or permeabilised with 0.125% of Trypsin-EDTA in PBS for 30 min (5 dpf and above) on ice. They were then washed for 3 x 5 min in PBT followed by 3 x 10 min in PBDT. Then, they were blocked in blocking solution for 3 hours. Embryos were incubated in primary antibodies diluted in Blocking solution (IF) O/N at 4°C. On the second day, embryos were washed for 6 x 15 min in PBDT at RT and incubated in secondary antibodies. For α-Disc1, Alexa Fluor 488 anti-rabbit (1) was used (Table 2.1). For anti-pERK and anti-tERK, a combination of Alexa Fluor 488 anti-rabbit (2) and Alexa Fluor 647 anti-mouse were used (Table 2.1). Incubations were left O/N at 4°C. To minimise exposure to ultraviolet (UV) light, tubes were kept in foil. On the third day, secondary antibodies were removed and embryos were co-stained with DAPI (1:1000) for 30 min. Embryos were washed for 6 x 15 min in PBT, transferred through a series of 10%, 25% and 50% to 75% glycerol and mounted on microscope slides. Alternatively, larvae were washed for 6 x 15 min in PBT and mounted in 2% low-melting point agarose (LMA) in PBS, ventral side up, in 15 µl, 2-well glass-bottomed slides (Ibidi) for large-scale analysis.

Table 2.1. Antibody specifications

Antibody	Epitope	Host	Dilution	Company
i) Primary				
pERK		rabbit	1:500	Cell Signalling Technology #4370
tERK		mouse	1:500	Cell Signalling Technology #4696
zDisc1		rabbit	1:200 (IF) 1:1000 (WB)	Dr Jon Wood lab
α-tubulin		mouse	1:1000	Sigma #T6557
β-actin		mouse	1:1000	Abcam #8226
ii) Secondary				

HRP α-mouse	Mouse IgG	goat	1:5000	Dako
HRP α-rabbit	Rabbit IgG	goat	1:5000	Dako
Alexa Fluor 488 α-rabbit (1)	Rabbit IgG	donkey	1:1000	ThermoFisher
Alexa Fluor 488 α-rabbit (2)	Rabbit IgG	goat	1:500	ThermoFisher
Alexa Fluor 647 α-mouse	Mouse IgG	goat	1:500	ThermoFisher

2.13 Z-brain registration and brain-mapping

Samples were imaged on an LSM-700 inverted microscope (Zeiss) and acquired with ZenBlue software using a 20X air objective. Full-brain stacks (z=137) and image tiling (2x1) was performed to capture the entire brain at 7 dpf and stitching was performed post-acquisition. Analysis was performed using FIJI and MATLAB (Mathworks), as published in Randlett *et al*. (2015). The Computational Morphometry Toolkit (https://www.nitrc.org/projects/cmtk) was used for image registration as previously described by Randlett et al. (2015). Calculation of brain activity was done using the MakeTHEMAPMap.m function in MATLAB. Another MATLAB function called ZBrainAnalysisOfMAPMaps.m was used to identify regions of interest (ROIs).

2.14 Digoxigenin (DIG) labelled probe synthesis

Antisense probes against *steroidogenic factor 1* (*ff1b*), *retinal homeobox 3* (*rx3*), and *tyrosine hydroxylase* (*th*) were synthesised from existing plasmids (generously provided by Prof M. Placzek and Dr L. Trollope). Complementary DNA (cDNA) of *orthopedia b* (*otpb*)*, oxytocin* (*oxt*) and *hypocretin* (*hcrt*) was amplified using primers (Table 2.3) and cloned into pCR-II vector. Templates were linearised with the appropriate restriction enzymes (Table 2.2) and purified. A 20 µl *in vitro* transcription reaction was set up using 1 µg of fully linearised template, 2 µl of 10X transcription buffer, 2 µl 10X DIG-UTP labelling mix (Roche Applied Science), 1 µl of murine RNase inhibitor, DEPC-treated water and 2 µl of T7 or SP6 RNA polymerase. This was mixed and incubated at 37°C for 2 hours. The DNA template was eliminated by adding 2.5 µl 10X DNase buffer and 2.5 µl (5U) RNase-free DNase incubated at 37°C for an additional 30 min. The probe was then precipitated by adding 2.5 µl of 4M LiCl, 75 µl of 100% ethanol and placing at -80°C O/N. The following day, the pellet was collected by centrifugation for 20 min at 13,000 rpm at 4°C. The pellet was then washed with 100 µl RNA grade 75% ethanol and

recentrifuged at 13,000 rpm for a further 15 min at 4°C. The supernatant was removed and tubes were left open for 5 min to air dry. RNA was then resuspended in 50 µl DEPC-treated water and allowed to rehydrate for 5 min, then placed on ice. Three 0.5 µl samples were taken after synthesis, digestion and resuspension and were analysed on a gel to check for recovery. Probe concentrations were assayed using a UV spectrophotometer (Nanodrop) and stored at -80°C after the addition of 50 µl of deionized formamide.

Table 2.2. RNA *in situ* hybridisation plasmid information

Probe	Enzyme to linearise at 5' end	RNA polymerase
ff1b	EcoRV	T7
hcrt	XhoI	SP6
otpb	XhoI	SP6
oxt	XhoI	SP6
rx3	XbaI	T7
th1	XhoI	T3

2.15 Wholemount *in situ* hybridisation

Wholemount *in situ* hybridisation (WISH) was used to detect mRNA expression in fixed tissue (Thisse and Thisse, 2008). On the first day, fixed embryos were rehydrated via a series of 75%, 50% and 25% methanol: PBS washes. Embryos were washed 4 x 5 min each in PTW. Tissue was permeabilised using Proteinase-K (10 µg/ml) treatment for differential times according to embryonic stage. To stop the reaction, fish were refixed in Fish fix for 20 min at RT and washed 5 x 5 min each in 1 ml of PTW. Embryos were then rinsed in 250 µl of incomplete hybridisation solution and then prehybridised in full hybridisation solution for 3 hours at 68°C. Hybridisation with the preheated (68°C) riboprobes mix (1:200) diluted in full hybridisation solution was performed O/N at 68°C. On the second day, the diluted riboprobes were removed and kept at -20°C for reuse. Embryos were washed in preheated (68°C) solutions: 50:50 2X SSC: incomplete hybridisation solution for 20 min, in 2X SSC for 20 min, and twice in 0.2X SSC for 60 min each at 68°C. Next, they were washed in 50:50 0.2X SSC: PTWS and blocking buffer (*in situ*) for 10 min at RT. Non-specific binding was inhibited by a 3-hour blocking step at RT in blocking buffer (*in situ*) prior to an O/N incubation in DIG-AP antibody (1:2000) in blocking buffer (*in situ*) at 4°C. On the final day, samples were washed in PTW for 6 x 20 min at RT. Embryos were equilibrated by 3 x 10 min washes of staining buffer. Alkaline phosphatase activity was detected using staining solution and left to develop for 90-180 min (probe-dependent) in the dark. Staining was stopped by washing for 3 x 5 min in PTW and fixing the embryos O/N in Fish fix at 4°C. Embryos were

further washed and transferred through a series 25%, 50% and 75% glycerol solutions prior to mounting on microscope slides for imaging.

2.16 Generation of a *disc1* mutant

2.16.1 Design and synthesis of *disc1* guide RNA

The CRISPR/Cas9 gene editing technique was used to create a *disc1* mutation. A single guide RNA (gRNA) targeting exon 6 (AGATGCAGGGACCCGTCCTC **AGG)** was designed by R. Lucas (MSc thesis, University of Sheffield, 2014) using the online CRISPR design tool (Zhang lab, MIT; http://crispr.mit.edu/). This gRNA also contained the T7 promoter and sequences to recruit Cas9. The target site was designed with an internal restriction enzyme site for binding and cleavage by DdeI. The following oligonucleotide was ordered from IDT (Integrated DNA Technologies):

(5'-GAAATTAATACGACTCACTATAAGATGCAGGGACCCGTCCTCGTTTTAGAGCTAGAAATAGC-3').

To ensure DNA cleavage, the antisense oligonucleotide was amplified, and *in vitro* validation of gRNA was performed by R. Lucas (MSc thesis, University of Sheffield, 2014). In Singapore, the antisense oligonucleotide was amplified using Phusion polymerase mix (ThermoScientific) in a 100 µL reaction with the following cycling conditions:

Reagent	**Volume (µl)**
Custom Oligonucleotide (100 µM)	2.5
Reverse primer (50 nM)	2.5
dNTPs (10 µM)	2.5
DMSO	2.5
5X Phusion Buffer	20
Phusion polymerase	1
Sterile water	69

	Steps	**Temperature (°C)**	**Time**
	Initial denaturation	98	30 s
35 cycles of	Denaturation	98	10 s
	Annealing	60	30 s
	Extension	72	15 s
	Final extension	72	10 min

Subsequently, the PCR product was purified (QIAGEN kit) and transcribed using T7 MEGAshortscript kit (Life Technologies) in a 20 µl reaction and incubated at 37°C for 4 hours.

Reagent	**Volume (µl)**
Purified PCR product (1 µg)	8

dUTPs (10µM)	8
10X T7 buffer	2
T7 enzyme mix	2

To remove the template, 2 µl of TurboDNAase was added and incubation was continued for an additional 30 min. The transcribed RNA was precipitated at -20°C O/N by addition of 15 µl ammonium acetate, 300 µl of 100% ethanol and 115 µl of nuclease-free water.

2.16.2 Microinjection of gRNA into zebrafish embryos

Needles were pulled using a micropipette puller (P2000 - Sutter instrument Co.). Tips were carefully removed using forceps. Needles were loaded with a 1:1 ratio of gRNA (1.5 µg/µl) and *Cas9* (1.5 µg/µl). The injection volume was calibrated to 0.75 nl. The needle was inserted through the yolk sac and the mixture was injected into the 1-cell stage zebrafish embryos. Injected embryos were incubated at 28°C and dead embryos were removed at the end of the day. Uninjected controls were kept for later comparative analyses. All of this work was performed by Yan Ling Chong prior to my arrival in Singapore.

2.17 Genomic DNA extraction

In adults, genomic DNA (gDNA) was extracted from fin-clips performed at 2 months post fertilisation (mpf). In embryos, extraction was performed at both 24 hpf and at 7 dpf dependent on the genotyping needs. Samples were placed in strip-tubes containing 100 µl PBS. PBS was then removed and replaced with alkaline lysis buffer and incubated at 95°C for 30 min:

Tissue	**Alkaline Buffer volume (µl)**
Fin (2 mpf)	40
Whole embryo (24 hpf)	10
Whole larva (7-8 dpf)	25

Post-lysis, neutralisation buffer was added to the strip tubes at a 1:1 ratio. For PCR set-up, 1 µl of gDNA was used as template DNA.

2.18 *In vivo* validation of gRNA

To determine the efficiency of *disc1* gRNA, gDNA was extracted from 8 injected and 8 uninjected controls and amplification of the target site in exon 6 was performed by PCR in a 10 µl reaction:

Reagent	**Volume (µl)**
gDNA (100 ng)	1
disc1 exon 6 Forward (500 nM)	2.5

disc1 exon 6 Reverse (500 nM)	2.5
MiFy mix	4

	Steps	**Temperature (°C)**	**Time**
	Initial denaturation	95	60 s
39 cycles of	Denaturation	95	20 s
	Annealing	57	30 s
	Extension	72	40 s
	Final extension	72	60 s

Efficiency was determined based on digestion of the locus-specific amplicon by DdeI in a 25 µl reaction:

Reagent	**Volume (µl)**
PCR product (500 ng)	8.5
Cutsmart buffer (NEB)	2.5
DdeI (NEB)	0.5
Sterile water	13.5

Embryos were raised to sexual maturity. F0s were outcrossed to AB wild types and F1 embryos were checked for transmission rates. *disc1* exon6-specific amplicons were amplified as described above and cloned into pCR-II using the TOPO TA cloning kit (Invitrogen). Briefly, a ligation reaction of 3:1 (insert: vector) ratio was set-up and then transformed into chemically competent DHα cells. These were grown O/N at 37°C on LB agar plates containing carbenicillin (33 µg/ml). Fives clones from each ligation reaction were picked and grown in LB broth containing carbenicillin. Cultures were miniprepped using QIAGEN Miniprep kit and the pCR-II vector containing the insert was sequenced using MI3R primer (Table 2.3) to discover the nature of the insertion-deletions (indels).

Table 2.3. Primer sequences

Primer Name	**Primer sequence**
disc1-GST primer Forward	5’ -- GGATCCATGATGTTCGCAGGAATGGTCAGG -- 3’
disc1-GST primer Reverse	5’ -- CTCGAGTCAGCTGGTTTCTGATTGGCTCA -- 3’
otpb primer Forward	5’ -- AACTCCGGTCTTCAACTCCAC -- 3’
otpb primer Reverse	5’ -- AGACGGGAACTGAGGCAAAC -- 3’
oxt primer Forward	5’ --CTCCGCAAGCTCTCGGTGTC -- 3’
oxt primer Reverse	5’ -- CTGCACTAATGTACAGTCAAGC -- 3’
hcrt primer Forward	5’ --CTGCACAGCTAAGAAGCTCCA -- 3’
hcrt primer Reverse	5’ --GCGACAAGTGTCATCGTTTTTC -- 3’
disc1 genotyping exon 6 Forward	5’ -- ACCATTGCTGCATGGGGAAT -- 3’
disc1 genotyping exon 6 Reverse	5’ -- AAAGTGGGACTGGGTCTACA -- 3’

disc1 F3 CRISPR mRNA Forward	5’ – CGAGAGACGCTGTTAGAGGAG -- 3’
disc1 F3 CRISPR mRNA Reverse	5’ – CCCAGCTGTCACTGAAGTAGT -- 3’
disc1 qPCR CRISPR Forward	5’ -- ACCATTGCTGCATGGGGA -- 3’
disc1 qPCR CRISPR Reverse	5’ -- CTGAGACAGCATCGCCTGAAG -- 3’
hprt1 qPCR CRISPR Forward	5’ -- TCATCGAGCCCGTGTGTCGT -- 3’
hprt1 qPCR CRISPR Reverse	5’ -- ACCCGCTCTAAGTCAGCCGCAT -- 3’
disc1 GST tag Forward	5’ -- GGATCCATGATGTTCGCAGGAATGGTCAGG -- 3’
disc1 GST tag Reverse	5’ -- CTCGAGTCAGCTGGTTTCTGATTGGCTCA -- 3’

2.19 RNA extraction

Forty embryos were collected and washed once in PBS and once in dH_2O. As much liquid as possible was removed as possible and 600 µl of TRIZOL (Ambion) was added to the microcentrifuge tube. Tissue was homogenised using a needle (23G 1¼TW -0.6 mmx32 mm) by 10 times upwards and downward suctions. Homogenate was left to sit for 5 min at RT. Subsequently, 120 µl of chloroform was added and tubes were inverted vigorously for 15 seconds (s). Tubes were left to sit for 3 min at RT and then centrifuged at 14,000 rpm for 15 min at 4°C. All of the subsequent steps were done on ice. The clear aqueous layer was transferred into a fresh tube containing 216 µl of isopropanol. Flicking was used to mix, and the solution was left to sit for 10 min at RT. Tubes were centrifuged at 12,000 rpm for 10 min at 4°C. The supernatant was removed to reveal a white RNA pellet. Molecular grade 75% ethanol was added to wash the pellet. This was vortexed and centrifuged on the same settings. The supernatant was removed and tubes were air-dried for 5 min. The pellet was resuspended in 20 µl of DEPC-treated water and RNA was stored at -80°C.

2.20 First-strand synthesis of cDNA

Two µg of RNA was used for first-strand cDNA synthesis. The following 10 µl reaction was incubated for 5 min at 65°C:

Reagent	**Volume (µl)**
RNA (1000 ng/µL)	2
Olig (dT) 20 (50 µM)	1
dNTPs mix (10 mM)	1
DEPC-treated ddH2O	6

This reaction was placed on ice and to each tube was added:

Reagent	Volume (µl)
10X RT buffer	2
MgCl 2 (25 mM)	4
DTT (0.1 M)	2
RNAase OUT (40 U/µL)	1
Superscript III Reverse Transcriptase	1

This reaction was incubated for 1 hour at 50°C and terminated by a 5 min incubation at 85°C. Tubes were then placed on ice and 1 µl of RNAase H was added to digest RNA. Tubes were incubated for 20 min at 37°C and stored at -20°C.

2.21 Quantitative Polymerase Chain Reaction (qPCR)

qPCR was performed to measure levels of *disc1* mRNA in CRISPR-generated mutants. Wild type and mutant embryos were collected at 55 hpf for RNA extraction. Two µg of total RNA was used for First Strand cDNA synthesis using the Superscript III kit (Invitrogen, #18080-051). Primers (Table 2.3) were designed downstream of the target site and flanking intron-exon boundaries to eliminate the possibility of gDNA contamination. Primers against the reference gene *hprt1* (Table 2.3) were used internal controls. The qPCR reaction was assembled using Ultrafast SYBR green Master mix (Invitrogen, 11780200) in 20 µl reactions with the following cycling conditions:

Reagent	Volume (µl)
cDNA (2 ng/µL)	6
SYBR green	10
Forward primer (5 µM)	2
Sterile water (5 µM)	2

	Steps	Temperature (°C)	Time
	Initial denaturation	95	20 s
40 cycles of	Denaturation	95	1 s
	Annealing/ Extension	60	20 s

Reactions were carried out in experimental and technical triplicates in MicroAmp Fast 96-well reaction plate (Applied Biosystems) using Fast 7900HT Real Time machine (Applied Biosystems). 2^{-ddC^t} was used to calculate fold changes between samples.

2.22 Behavioural assays in larval zebrafish

2.22.1 Hunting assay

At 7 dpf, zebrafish larvae received their daily live feed (*Paramecia*) at 9 AM. Subsequently, *Paramecia* were flushed, individual larvae were transferred to a 24-well plate devoid of food and starved for 3 hours. Meanwhile, *Paramecia* were dyed with Neutral Red (5 µg/ml, Abcam #14635) for 30 min on the rocker to facilitate their visualisation. The plate was positioned on the behaviour rig with bottom LED lighting for 30 min for habituation, following which 100 µl of dyed *Paramecia* was added to each well and left for 5 min prior to video recording. Hunting behaviour was recorded for t=10 min at 30 frames.s^{-1}. Hunting bouts and strikes were manually counted *post-hoc*. Data was plotted using GraphPad (Prism 8).

2.22.2 Feeding assay

At 7 dpf, zebrafish larvae received their daily feed at 9AM. Subsequently, *Paramecia* were flushed, and larvae were starved for 3 hours. Meanwhile, harvested *Paramecia* were centrifuged in 50 ml plastic tubes at 2,750 rpm for 5 min. The supernatant was removed and 5 ml pellets were pooled and aliquoted into microcentrifuge tubes. DiD dye (2.5 mg/ml in ethanol, D7757; 5 µl dye/ml of concentrated paramecia) was used to dye the *Paramecia* for 2 hours (covered with foil, gentle rotation). After 2 hours, dyed *Paramecia* were centrifuged at 2,750 rpm for 5 min and the supernatant was replaced with 1ml of E3. After two washes, the contents of all tubes were pooled and the volume of dyed *Paramecia* was adjusted to 1 ml per dish of larvae. One ml of dyed *Paramecia* was added to habituated zebrafish larvae (n=30 per plate), ensuring dyed *Paramecia* were distributed evenly around the dish. Larvae were left to feed for 15 min. After this period, the zebrafish were poured through tubed sieves, washed with E3 and submerged in ice cold 4% paraformaldehyde (PFA) in PBS. These were left to shake O/N at 4°C. Gut fluorescence (Fig. 2.1) was quantified the next day, using a stereoscope (Leica) under far red Cy5 LED illumination. Images were analysed in FIJI (ImageJ) using a macro (written by Dr. Caroline Wee, available on www.github.com/carolinewee) for automation.

Figure 2.1. Zebrafish larvae (7dpf) post-ingestion of fluorescently labelled *Paramecia*

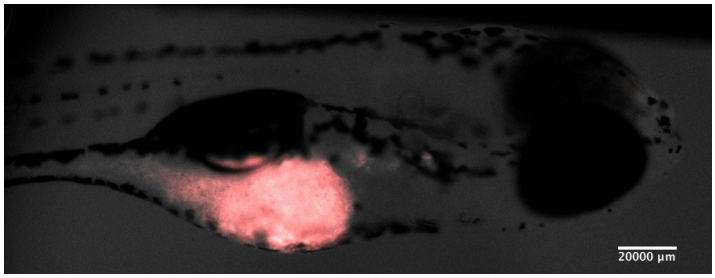

2.22.3 Locomotion and Dark-Flash test

At 7 dpf, zebrafish larvae received their daily feed at 9 AM. Subsequently, *Paramecia* were flushed and individual larvae were transferred to a 48-well plate. The plate was placed in an incubator (28.5°C) with bottom illumination (LED or infrared lighting) with a Basler acA2040-90u mNIR camera (30 frames.s^{-1}) placed above. Recordings were performed over 2 days. On day 1, larvae were habituated and then exposed to a series of 6 dark-cycles (40 min) intercalated with light-cycles (20 min). The final light OFF (infrared) was continuous for 10 hours and considered "night-time". On day 2, locomotion was recorded for a further 6 hours. Tracking of X:Y coordinates was performed by custom PyCharm (Python) software (by Dr. R. Cheng) and raw data was collected as signatures in Excel (Microsoft). Seconds of activity per min (active s.min^{-1}) was plotted using GraphPad (Prism 8).

2.22.4 Night-time arousal test

The same setup was used for measuring sensory-motor gating in 11 dpf larvae. To assess arousal during sleep, different intensities of sound were emitted through an audio speaker controlled by a modified version of the activity-tracking code in Python. Locomotion was recorded over 2 nights, starting at 1 AM every night, where eighteen stimuli of nine different intensities, were delivered for 200 ms at a rate of 1 sound.min^{-1}. Intensities started at 0% and increased 12.5% every minute to reach a maximal value (100%) of 72 decibels (dB). At odd hours (1 AM, 3 AM, 5 AM), the stimulus intensities were descending from 0-9min and ascending from 10-19 min. At even hours (2 AM, 4 AM, 6 AM), the stimulus intensities were ascending from 0-9 min and descending from 10-19 min (Fig. 2.2). A total of (19x6) 114 sounds were delivered each night. Tracking of X: Y coordinates was performed by PyCharm (Python) and raw data was collected as excel files. Percentage of fish responding was averaged over the 2 nights of recordings and plotted using GraphPad (Prism 8). We corrected measurements for variations in basal locomotor activity using the equation (Woods et al., 2014):

$$\text{corrected P (response)} = \text{observed value} \times \frac{(\text{observed value} - \text{background offset})}{(\text{max observed value} - \text{background offset})}$$

Figure 2.2 Scheme of Night-time Arousal (NTA) test

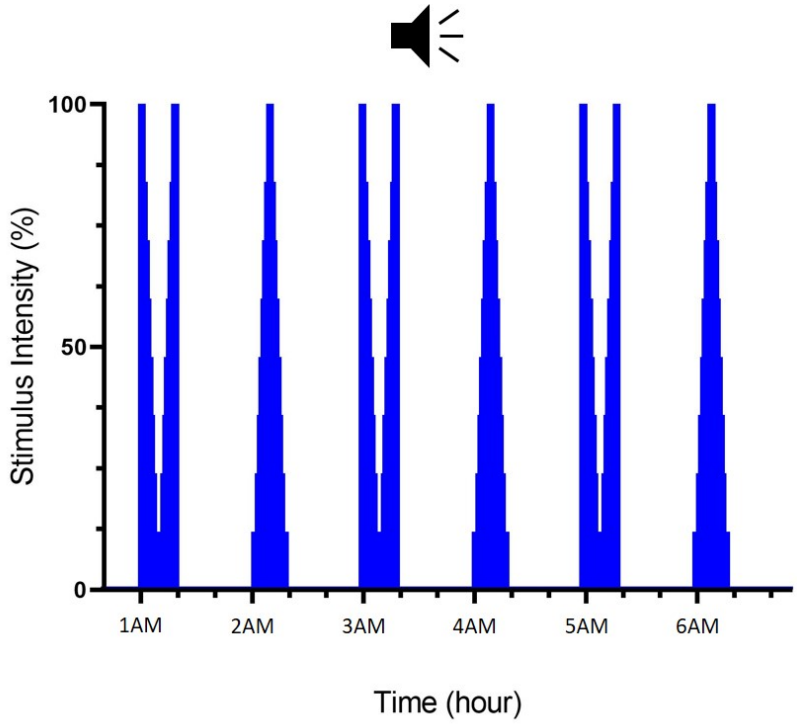

2.23 Drug treatment

2.23.1 Developmental CHIR99021 treatment

GSK-3 activity was inhibited using 2, 4-dibenzyl-5-oxothiadiazolidine-3-thione (CHIR99021) (MedChemExpress #05974). Aliquots of stock solution (50 mM) were made up in DMSO and stored at -20°C. Embryos were dechorionated and treated with 50 µM CHIR99021 from 24-48 hpf. The drug was washed-off by transferring embryos through E3 and placing them in fresh E3. They were left to develop at 28.5°C until fixation for *in situ* hybridisation at 55 hpf or for feeding assays at 7 dpf. DMSO (0.5%) was used as negative control.

2.23.2 Acute CHIR99021 treatment

Larval zebrafish were treated acutely with CHIR99021 prior to addition of the dyed *Paramecia*. Briefly, 30 µl of stock solution was diluted in 30 ml of E3. Larvae were transferred from their habituated/ starved state to either DMSO (0.5%) or CHIR99021 (50 µM). After 30 min of exposure, dyed *Paramecia* were added to petri dishes and the feeding assay was continued as per usual.

2.23.3 Acute larval stress

Larval zebrafish were treated acutely with varying concentrations of sodium chloride (NaCl) prior to the addition of the dyed *Paramecia*. Briefly, a volume of 500 µl stock NaCl stock solution was added to 30 ml of E3 to get a final concentration of 100 mM or 250 mM and larvae were exposed for 10 min. This was washed off and larvae were left to habituate for 5 min before dyed Paramecia were added and the feeding assay was continued as per usual.

2.24 *Paramecia* propagation and harvest

Propagation was performed once a week. Briefly, a week-old *Paramecium* culture was used to propagate 8 subcultures. One hundred ml of *Paramecia* culture was transferred to new subcultures in glass bottles (1 l) containing 500 ml of *Paramecia* water and 100 ml of wheat pellets (Carolina), 3.75 mg/ml. Five drops of RotigrowPlus were added and *Paramecia* were grown at 28 °C. *Paramecia* cultures were fed twice a week with RotigrowPlus. To harvest *Paramecia*, the culture was first filtered through a large-pored (120 µM) sieve. The collected through-flow was then filtered through a second small-pored (25 µM) sieve. The second through-flow was discarded and 30 ml of *Paramecia* water was used to rinse the collected *Paramecia*. The harvested *Paramecia* were transferred to a 50 ml plastic tube, left to sediment O/N and subsequently used to feed the fish.

2.25 Novel Tank Diving (NTD) Assay

Adult zebrafish were tested consistently from 1-4 PM to account for circadian cortisol fluctuations. Tall and narrow one litre tanks (20 cm x 10 cm x 5 cm) were filled with filtered facility water. Top light illumination at low intensity (1.5 µW/mm^2) was used. Videos were recorded using a Basler Ace (acA1300–200 µm; 1,280 × 1,024) camera placed ~40 cm in front of the tanks. Locomotion was recorded for 10 min at 20 frames.s^{-1}. Tracking of X: Y coordinates was performed using PyCharm (Python) and raw data was collected as signatures in excel files and automated analysis scripts were applied (Haghani et al., 2019). Bottom dwell was quantified by the percentage of time spent in the bottom third (red line, Fig. 2.3) of the tank at every 2 min interval. Thigmotaxic behaviour was quantified by measuring the percentage of time spend near the walls of the tank (maroon zone, Fig. 2.3). The script enabled calculation of the number of freezing episodes (>1 s of immobility) and the number of darting episodes (8 standard deviations away from mean swimming velocity) (Schirmer et al., 2013).

Figure 2.3 Adult behavioural setup

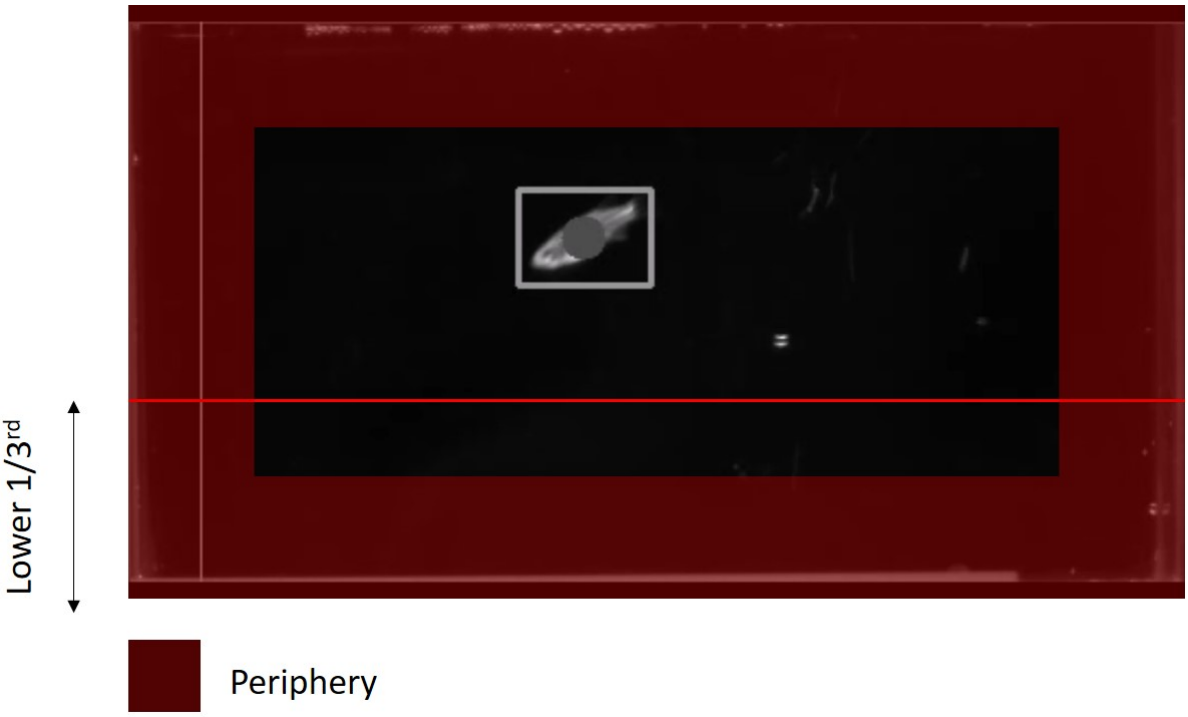

2.26 Statistical Analysis

Data are presented as mean ± standard error of mean (SEM) or mean ± standard deviation (SD) when appropriate, with N indicating the sample size (number of larvae). The Shapiro-Wilks test was performed to assess if data sets followed a normal distribution. If data passed the normality test, statistical analysis of two groups was measured using Student t-test (unpaired). Statistical analysis of more than two groups was performed using a one or two-way analysis of variance (ANOVA), followed by Tukey *post-hoc* analysis, to account for multiple comparisons. For data that did not pass the normality test, the Mann-Whitney test was used to compare two groups and the Kruskal-Wallis for more than 2 groups, with pairwise comparison. For behavioural measures comparing the same samples at multiple timepoints or exposed to different stimuli, factorial ANOVA with repeated measures were used. The threshold for statistical significance was set to P value ≤0.05.

Chapter 3: Tools for elucidating disc1 function in zebrafish

3.1 Introduction

3.1.1 Expression of *disrupted-in-schizophrenia 1* (*disc1*) in zebrafish

The genetic tractability and optical transparency of the zebrafish enables an in-depth investigation into the specific function of genes and proteins of interest. The developmental expression of the genetic risk factor *disc1* has previously been characterised. In the zebrafish embryos, maternal contribution of *disc1* appears as early as 3 hpf and levels gradually decrease before another round of zygotic *disc1* expression occurs around 10 hpf (De Rienzo et al., 2011) coinciding with the maternal to zygotic transition. Expression of *disc1* occurs predominantly between 1 and 3 dpf and peaks at 52 hpf, a timepoint when most of organogenesis has already occurred. *disc1* is expressed in the muscle trunk and in the developing brain and is particularly enriched in the ventral diencephalon (Eachus et al., 2017). Expression in the larval zebrafish is thought to decrease over time but has not been thoroughly investigated at later stages due to lack of a zebrafish-specific antibody.

3.1.2 The challenge of immunohistochemistry in zebrafish research

Tens of thousands of commercially available antibodies exist against various proteins and they remain an essential component of the backbone of the molecular biology toolkit. They have significantly contributed to our understanding of basic cellular biology thanks to methods such as immunohistochemistry, immunoprecipitation, and SDS-PAGE. Two main types of commercially synthesised antibodies exist. Polyclonal antibodies consist of heterogeneous immunoglobulin (Ig) molecules which can bind to several different epitopes from a single antigen. These are usually purified from the serum of immunised rabbits, donkeys, or goats. Monoclonal antibodies, as the name suggests, bind to a single epitope within a target antigen, composed of homogenously cloned immunoglobulin molecules. These single specificity antibodies are made by fusing antibody-producing cells from the immunised animal to an immortalised cell line.

Due to the early divergence from humans over 450 million years ago, protein conservation between mammals and zebrafish is limited. These differences mean that many commercial antibodies do not cross react with most zebrafish orthologs, but this ultimately depends on the degree of homology between the two specific proteins and whether the antibody binds to common epitopes. Commercially available antibodies for non-mammalian model organisms are underrepresented compared with mammalian models. This lack of zebrafish antibodies could be attributed to less

funding in the field. Nevertheless, polyclonal antibodies are often made “in-house” and shared amongst research groups.

The lack of zebrafish-specific zDisc1 antibody can hinder research progress, particularly when investigating its mechanisms in cellular biology. It was therefore important to synthesise a high affinity antibody against zDisc1, as an essential research tool for this project. The estimated molecular mass of the endogenous zebrafish Disc1 protein (zDisc1) is 112 kDa (expasy.org/compute_pi) but the protein has not been fully characterised in zebrafish. Cross-species sequence conservation between zebrafish, mice and humans is largely restricted to the *C*-terminus (Porteous and Millar, 2006). Due to the differences in the sequence of the *N*-terminus between species, we decided to use a zDisc1 *N*-terminal polypeptide for raising a polyclonal antibody. The reason being that most commercially available antibodies raised against the *C*-terminus will react with mammalian Disc1 isoforms, however, they do not react with zDisc1.

3.1.3 Generating *disc1* zebrafish models

Morpholino studies, carried out by microinjection of antisense oligonucleotides targeting *disc1,* contributed to the initial characterisation of *disc1*’s function in zebrafish. In these studies, different MO targeted different parts of the *disc1* locus. MO targeting the start codon (AUG) resulted in gross developmental abnormalities and oligodendrocyte mislocalisation by 5 dpf. This was also the case for another MO targeting the exon 2/intron 2 splice boundary (Wood et al., 2009). MO targeting the intron 2/exon 3 splice-acceptor site altered *disc1* pre-mRNA splicing and introduced a premature stop site, leading to deletion of exon 3. This resulted in abnormalities in craniofacial development and delayed neural crest migration at 5 dpf in a high proportion of *disc1* morphants (Drerup et al., 2009). The same phenotypes were also observed in morphants using another MO targeting the exon 8/ intron 8 boundary. Another study used MO targeting the splice donor site between exon 1 and intron 1/2, ablating all *disc1* mRNA. Two groups of morphants emerged, divided into strong and mild phenotypes. Strong phenotype morphants had abnormal brain morphogenesis and lack of tail. Mild phenotype morphants had less defined, smaller brain ventricles and defects in somitogenesis at 24 hpf. Axon outgrowth and organisation was also affected to a corresponding extent between strong and mild morphants (Brandon et al., 2009). The same group used another MO targeting the intron between exons 8 and 9, recapitulating the human equivalent breakpoint. These morphants had much less severe phenotypes with no severe morphological differences in neurodevelopment. The reduction in ventricle size was restricted to midbrain and hindbrain ventricles only. These morphants also had smaller and more bent tails.

In zebrafish, evidence suggest that in 15-20% of cases, MOs can cause off-target effects. In most cases, off-target effects result from p53 activation from 1-2 dpf leading to apoptosis (Robu et al., 2007); Simultaneous morpholino knockdown of p53 can rescue this apoptosis and is now used to control for gene-specific phenotypes. In other cases, off-target toxicity can occur through interaction with other mRNA sequences unrelated to the gene of interest. To ascertain whether these *disc1* phenotypes are a consequence of *disc1* knockdown or due to off-target effects, it was necessary to use stable *disc1* knockout models.

ENU (N-ethyl-N-nitrosourea) mutagenesis has been used in TILLING (Targeting Induced Local Lesions in Genomes) screens to induce and identify point mutations in protein-coding regions. Two *disc1* ENU mutants were identified with two different nonsense mutations in exon 2: *disc1*^{L115X} and *disc1*^{Y472X} (Draper et al., 2004). Homozygous mutants had defects in brain connectivity and morphological phenotypes at 24 hpf (De Rienzo et al., 2011). Since then, though, these results have not been successfully reproduced by other groups. After multiple generations (≥ than 3) of alternating outcrossing to TL wild types and incrossing, homozygous *disc1*$^{L115X/L115X}$ and *disc1*$^{Y472X/Y472X}$ mutant embryos appear to develop relatively normally and only very mild phenotypes have been reported (Eachus et al., 2017). Contradictions in phenotypes between *disc1* knockdown using MOs and *disc1* homozygous knockout mutants raise questions over the true loss of function phenotype. A new approach using targeted genome editing is therefore necessary to resolve these discrepancies.

3.1.4 Targeted genome editing

Since the introduction of precise genome editing methods to create stable mutant lines, the use of MOs has fallen from favour in the zebrafish community. Creating targeted mutations has become accessible, thanks to the development of tools such as zinc finger nucleases (ZFNs) and transcription activator-like effector nucleases (TALENs). Both techniques function through precise protein-induced genome cleavage, creating DSB. This causes changes in the genetic sequence of the target site through error-prone repair mechanisms such as non-homologous end joining. However, both techniques come with their limitations: TALENs are very large and require laborious cloning steps to obtain the numerous repeat sequences required for their function. On the other hand, ZFN are much smaller, enabling their incorporation into viral vectors, the delivery method used in mammalian models. Unfortunately, they are more difficult to design, more expensive and harbour a lower mutagenesis rate compared with TALENs (Joung and Sander, 2013). Multiple attempts to generate a *disc1* TALEN knockout and knock in mutants have been made by our group but with no success, due to a low frequency (10%) of *in vivo* cleavage (P. Boyd PhD thesis, University of Sheffield, 2014).

3.1.5 The CRISPR/ Cas9 system

CRISPR (Clustered Regularly Interspaced Short Palindromic Repeats)/ Cas (CRISPR-associated system) has recently revolutionised targeted genome editing. In zebrafish, it has been widely used to generate stable mutants via site-specific mutagenesis or transgenic lines by the subsequent insertion of reporter tags. This system utilises the adaptive immune response endogenous to prokaryotes and *archea*. As a defence mechanism, most bacteria can store genomic sequences from viruses by splicing them into the host's genome near CRISPR sites. Upon viral infection, these regions are then transcribed into gRNAs which function to direct Cas endonucleases to the foreign DNA which is subsequently degraded (Deltcheva et al., 2011; Wiedenheft et al., 2012). This system has been reported to be more precise than the aforementioned ZFN and TALEN system due to the stronger bond formation between RNA and DNA as opposed to protein/ DNA (Gaj et al., 2013). The type II CRISPR/ Cas9 system from *Streptococcus pyogenes* has been engineered and is applied in various *in vitro* and *in vivo* models for genetic engineering. A 20 bp gRNA can be designed to complement any target site, provided that a protospacer adjacent motif (PAM) is present immediately upstream of the binding site, to enable DNA cleavage by Cas9 (Jinek et al., 2012). gRNAs are injected along with *Cas9* mRNA or protein into one-cell stage embryos. This leads to the generation of DSB in the organism's DNA causing the formation of indels at the target site. In zebrafish, the efficiency of mutagenesis is relatively high with studies reporting ~85% (Hruscha et al., 2013). While the CRISPR/Cas9 system is the preferred method for targeted genome editing, off-target mutagenesis can still occur due to base mismatches. This is especially evident in human cell lines (Fu et al., 2013; Rayner et al., 2019; Zhang et al., 2015). Importantly though, occurrences of off-target mutations in zebrafish remain relatively low (Hruscha et al., 2013). Another drawback of the CRISPR/Cas9 system in zebrafish research emerged after a lack of phenotype was observed in many loss of function CRISPR/ Cas9 mutants. This has been attributed to the phenomenon of genetic compensation (Rossi et al., 2015).

There was a need to generate a CRISPR/ Cas9 *disc1* mutant due to the discrepancy in results from the ENU-generated *disc1* mutants. Additionally, the zebrafish community has moved away from using morpholinos for genetic characterisation, as mentioned above. The simplicity of the CRISPR/ Cas9 system as well as the relatively short zebrafish life cycle meant it was perfectly reasonable to design, generate and characterise a novel *disc1* mutant within the scope of this project.

3.2 Results

3.2.1 Anti-zDisc1 serum recognises epitope in wild type zebrafish embryos

To investigate the expression profile and location of the zebrafish zDisc1, a novel zebrafish-specific antibody was raised against an *N*-terminus zDisc1 polypeptide (~20 kDa). A construct previously synthesised was used to express a fusion protein of zDisc1 (*N*) fused to the GB1 tag: zDisc1 (*N*)-GB1 (A. Zarkesh MSc thesis, University of Sheffield, 2016). The GB1 tag was used as it increases the solubility of the recombinant protein facilitating its purification. Purified zDisc1 (*N*)-GB1 was sent for rabbit immunisation and antiserum was generated.

To determine if there was a need to purify the antiserum to enrich for polyclonal antibodies, we first tested the serum. Protein was extracted from zebrafish heads at 52 hpf, a timepoint where *disc1* is highly expressed (Boyd et al., 2015; Eachus et al., 2017; Wood et al., 2009). We performed western blotting using two different concentrations of heads lysates and blotted with antiserum from pre-immune and zDisc1 (*N*)-GB1-immunised bleeds from rabbits (Fig. 3.1). A weak band was detected at 40 kDa on blots using the pre-immune antiserum. A much stronger band was detected at 70 kDa on blots using antiserum from zDisc1 immunised antiserum. The intensity of the signal increased proportionally to the amount of protein loaded and was absent in pre-immune samples. Four weaker and smaller bands were observed in the most concentrated samples. Antibodies from the zDisc1 (*N*)-GB1-immunised antiserum also cross reacted with the molecular weight standards. Such cross reactions are common as crude serum contains a mixture of antibodies.

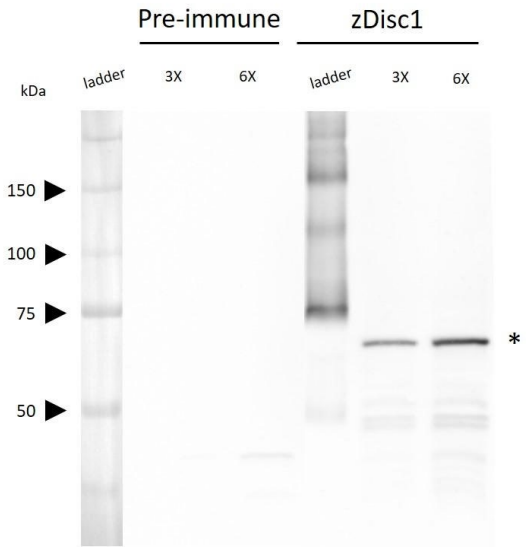

Figure 3.1. Western blots of zebrafish embryo head lysates with pre-immune and zDisc1 antiserum

Western blot protein extracted from wild type zebrafish heads at 52 hpf. Two different concentrations (3X and 6X heads per well) were loaded and using pre-immune antiserum (left) and zDisc1-immunised antiserum (right). A strong 70 kDa band, marked with an asterisk (*) was detected using zDisc1 (*N*)-GB1-immunised antiserum.

3.2.2 Two-step purification of zDisc1 antiserum

After establishing that the antiserum did not recognise the expected size of zDisc1 (112 kDa), we decided to deplete the serum of antibodies specific to the GB1 tag. This small tag (~12 kDa) is a modified version of protein G expressed by *Streptococci* and specifically binds the F_c arm of IgG (Akerstrom et al., 1985). GB1-specific antibodies were depleted by column purification and collection of the eluate: GB1-depleted zDisc1 antiserum (see section 2.5.2).

Next, zDisc1-specific antibodies were enriched by using an affinity column. Briefly, a zDisc1 (*N*)-GST protein was synthesised by cloning the same *disc1 (5')* sequence used for zDisc1 (*N*)-GB1 synthesis into *pGEX-6b1* (kind gift of Dr G. Hautbergue). After confirming the reading frame by sequencing, *pGEX-6b1-disc1* was transformed into competent cells, expressed and purified (see section 2.5.1). zDisc1 (*N*)-GST and GSH sepharose bead complexes were crosslinked and incubated with the GB1-depleted zDisc1 antiserum. The beads were packed into a column for antibody purification. The through-flow was made up of non-specific antibodies and serum proteins. After multiple washes, an acid glycine elution was performed to release zDisc1-specific antibodies from the zDisc1 (*N*)-GST antigen. The eluate was immediately neutralised and dialysed against wash buffer (see section 2.6.2). The yield was estimated at ~1-2 mg of specific antibodies.

To confirm GB1-specific antibody depletion and that the remaining antibodies still retained specificity to zDisc1, we resolved recombinant protein by SDS-PAGE, blotted and immunostained with the three stages of sera: i. crude zDisc1 antiserum, ii. GB1-depleted antiserum, iii. Purified zDisc1 antibody (Fig. 3.2). zDisc1 (*N*)-GB1 was detected at ~32 kDa [zDisc1 (*N*) (20 kDa) fused to GB1 (12 kDa)] while zDisc1 (*N*)-GST ran at ~48 kDa [zDisc1 (*N*) (20 kDa) fused to GST (~28 kDa)]. The antiserum recognised zDisc1 (*N*)-GB1, zDisc1 (*N*)-GST and the GB1 tag alone (12 kDa). After GBI-specific antibody depletion, detection of the GB1 tag decreased considerably but did not totally disappear. Blots from GB1-depleted antiserum and zDisc1 antibody were more specific for zDisc1 recombinant proteins. The bands observed below these proteins correspond to partially degraded zDisc1 protein, explaining why they retained immunopositivity.

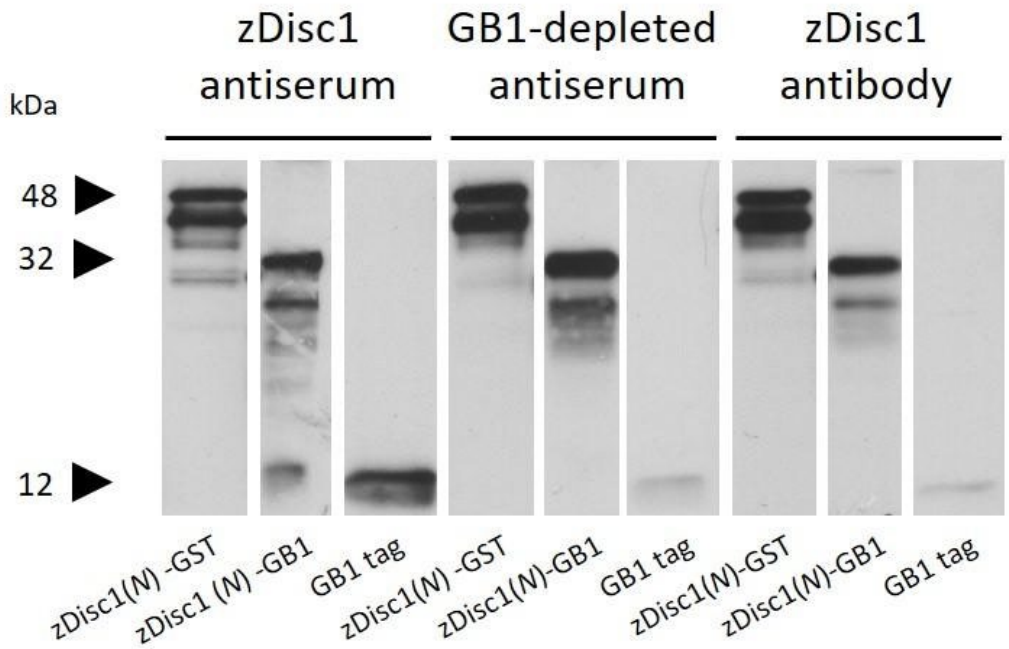

Figure 3.2. Western blots of purified zDisc1-GST, zDisc1-GB1 and GB1 protein
Western blot using protein purified from bacterial cultures blotted using zDisc1 antiserum (left), GB1-depleted antiserum (middle) and zDisc1 antibody (right).

To test the specificity of the purified antibody to endogenous zebrafish zDisc1, we performed western blotting on embryo head lysates (Fig. 3.3). The same strong 70 kDa band was detected using all 3 stages of antisera and antibody purifications.

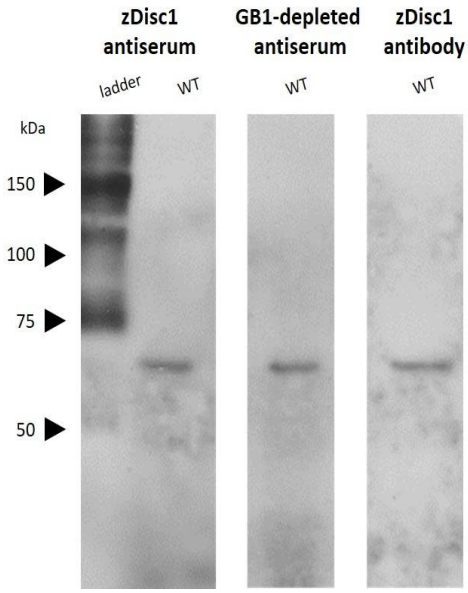

Figure 3.3. Western blots of zebrafish embryo head lysates after a 2-step purification
Western blot using protein extracted from 52 hpf wild type (WT) zebrafish heads blotted using zDisc1 antiserum (left), GB1-depleted antiserum (middle) and zDisc1 antibody (right).

To determine the apparent molecular weight of zebrafish Disc1, we turned to a mammalian cell culture system and overexpressed full length zDisc1 (zDisc1-FL) in HEK 293 cells (Fig. 3.4). The zDisc1 antibody was able to recognise overexpressed zDisc1-FL, which ran close to its expected molecular weight, as shown by the presence of a 112 kDa band in transfected cells (right lane), which was absent in un-transfected cells (left lane).

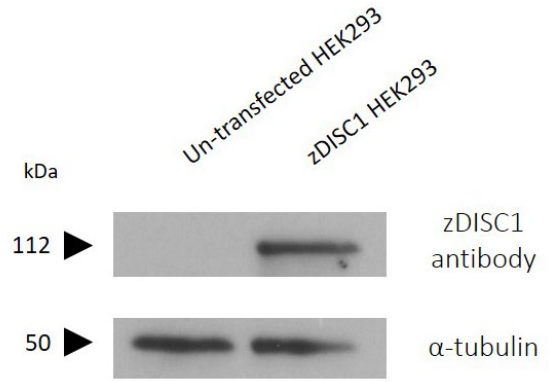

Figure 3.4. zDisc1 antibody can recognise overexpressed full-length zebrafish zDisc1
Western blot using protein extracted from and HEK 293 cells expressing full-length zebrafish Disc1 (zDisc1 F-L) and blotted using purified zDisc1 antibody. The antibody recognises a band corresponding to the zDisc1 size. Tubulin was used as a loading control.

Finally, to establish whether the 70 kDa ban present wild types was a previously uncharacterised zDisc1 isoform, we extracted protein from *disc1*$^{Y472X/Y472XX}$ homozygous mutants at 52 hpf and immunoblotted them alongside extracts from *disc1*$^{+/+}$ controls using the purified antibody (Fig. 3.5). The *disc1*^{Y472X} nonsense mutation codes for a PTC in exon 2 of *disc1* and leads to 0.6-fold decrease in *disc1* mRNA (Eachus et al., 2017). The functional effect at the polypeptide level remains uncharacterised. We would expect to see a decrease in protein levels or the possibility of a truncated protein (around 51 kDa) containing the *N*-terminal domain of the polypeptide or a complete lack of protein due to nonsense-mediated decay (NMD) of the shortened mRNA transcript. The presence of the same 70 kDa band in the *disc1*$^{Y472X/Y472X}$ homozygous mutant lysates indicates that the purified antibody does not recognise endogenously expressed zDisc1 in zebrafish embryo extracts and that the strong band is not a newly identified zDisc1 isoform.

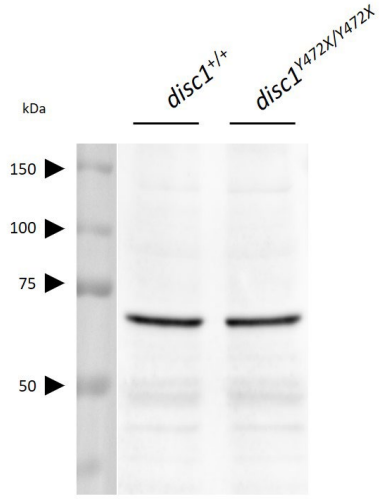

Figure 3.5. zDisc1 antibody does not recognise endogenous levels of zDisc1
Western blot of protein extracted from *disc1*$^{+/+}$ and *disc1*$^{Y472X/Y472X}$ mutants at 52 hpf, immunoblotted with purified zDisc1 antibody. The antibody recognises a band at 70 kDa in both from *disc1*$^{+/+}$ and *disc1*$^{Y472X/Y472X}$ samples.

To ensure that the lack of specificity to endogenous zebrafish protein was not a result of the protein denaturation step performed prior to polyacrylamide gel electrophoresis (PAGE), we sectioned the heads of wild type zebrafish at 52 hpf and performed immunohistochemistry (Fig. 3.6). Staining appears disperse throughout the section and non-specific to the expected expression of zDisc1.

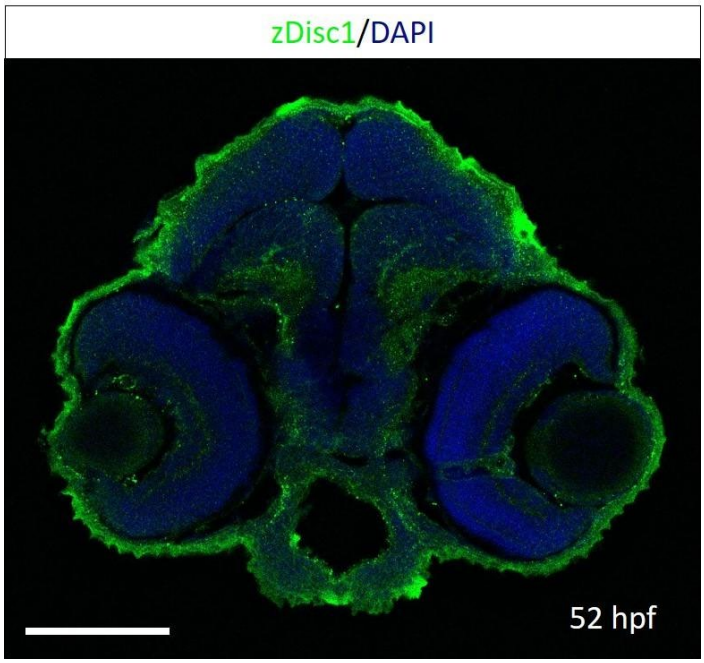

Figure 3.6. Immunofluorescence *in vivo* using purified antibody
Coronal section through the anterior diencephalon. Fluorescence showing DAPI nuclear staining (in blue) and purified antibody staining (in green). Staining appears disperse with a considerable edge effect. Scale bar indicates 200 µm.

3.2.3 Generation of a *disc1* mutant zebrafish using CRISPR/ Cas9 genetic editing

Another tool commonly used to investigate the function of genes is loss of function (LOF) mutants. In mice, a multitude of different strains of transgenic mice containing partial loss and/or inducible *Disc1* gene mutations have been generated and studied (Clapcote et al., 2007; Hikida et al., 2007; Koike et al., 2006; Pletnikov et al., 2008; Shen et al., 2008) with very few groups having studied the effect of a complete lack of *Disc1*. A *Disc1* model lacking exons 2 and 3 of the *Disc1* gene was generated and developed no gross abnormality. As in other mutants, defects in long-term potentiation (LTP) were reported. Behaviourally, $Disc1^{\Delta 2\text{-}3/\Delta 2\text{-}3}$ were less anxious and displayed higher impulsivity compared to wild type littermates (Kuroda et al., 2011). In zebrafish, two *disc1* nonsense mutants have previously been identified following a TILLING screen (Draper et al., 2004). In recent years, the zebrafish community has moved towards creating stable genetic mutants using the CRISPR/ *Cas9* system. The reasons for creating a *disc1* CRISPR/ *Cas9* mutant for my project were four-fold: i. there was a possibility of additional closely linked mutations in ENU mutants, ii. no previously CRISPR *disc1* mutant had been generated, iii. a line with an indel mutation would enable faster and cheaper genotyping, iv. a mutation much closer to the human equivalent translocation site was desired. The need for a

definitive LOF model to investigate the role of *disc1* was therefore addressed by using CRISPR/Cas9 technology.

A single gRNA was designed and validated for *in vitro* cleavage (R. Lucas MSc thesis, University of Sheffield, 2014) resulting in indels at the target site in exon 6. We then injected this gRNA and *Cas9* mRNA into 1-cell stage zebrafish embryos. Mosaic F0s were screened for on-target *in vivo* cuts at 24 hpf. Targeting of *disc1* exon6 was efficient with mutations occurring in 70-80% surviving embryos. Eight injected embryos were pooled together for gDNA extraction and screening was carried out by amplifying a 438 bp PCR product around the target site (Fig. 3.7A). There was no difference in band size observed between un-injected and injected embryos. Bands were gel extracted and inserted into the pCR-II vector via TOPO cloning for sequencing. Colonies were picked and the target site of injected embryos showed a 4 bp deletion (Fig. 3.7B), validating the initial efficiency of *disc1*^{exon6} gRNA *in vivo***.** The lack of difference in band size can be explained by the small size of the deletion.

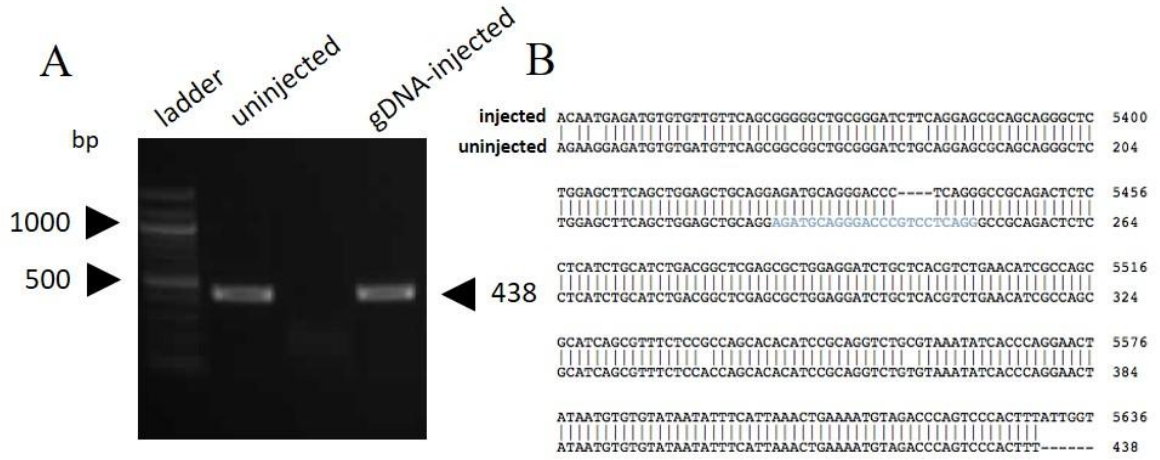

Figure 3.7. Validating efficiency of *disc1* exon6 gRNA *in vivo*

(A) gRNA and Cas9 mRNA were injected into 1-cell stage zebrafish embryos. Injected and un-injected controls were pooled respectively and gDNA was extracted. Primers were used to amplify the region spanning the gRNA target site. PCR products from both injected and un-injected controls show similar sizes.

(B) Products were gel extracted, cloned into pR-II TOPO and sequenced. Alignment shows gDNA-injected sequence (above) aligned with un-injected sequence (below). Sequence targeted by the gRNA is highlighted in blue. Initial screening showed a 4 bp deletion.

F0s were grown-up to sexual maturity and genotyped. To identify founders harbouring germline mutations, they were crossed with AB wild types and gDNA was extracted from individual progeny to look for transmission of mutant alleles. Various lengths of indels ranging from 2 bp to 30 bp were identified near the target region by sequencing. We selected an indel (16 bp deletion) that we had identified in numerous F1 genotyped fish and one which caused a PTC close (7 amino acids) to the

disc1^{exon6} target sequence (Fig. 3.8A). A frameshift mutation occurring at residue G625P resulted in scrambled amino acids after this position until a truncation at residue S633X due to a PTC. Heterozygote F1s were subsequently incrossed to produce a genotypically homogenous F2 generation. Genotyping was carried out on F2 adults using PCR and *DdeI* digestion (Fig. 3.8B). Genotypes followed Mendelian ratios: wild type +/+ (25%), heterozygote +/- (50%) and mutant -/- (25%). Finally, because of the previously reported maternal contribution of *disc1* mRNA (De Rienzo et al., 2011; Drerup et al., 2009), *disc1*$^{exon6/exon6}$ homozygous mutants from the F2 generation were incrossed once more to produce F3 *disc1*^{exon6} maternal zygotic (MZ) mutants. *disc1*^{exon6} maternal zygotic mutants (*disc1*^{exon6} MZ) showed no gross morphological abnormalities compared to wild types.

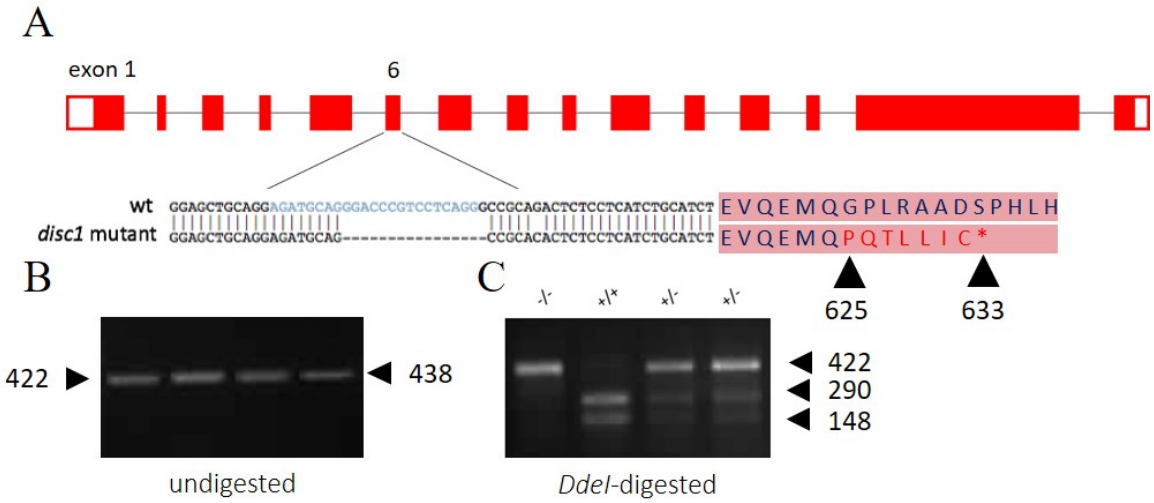

Figure 3.8. Generation of a stable CRISPR/Cas9 *disc1* zebrafish mutant

(A) Schematic of the *disc1* gene with untranslated regions (white boxes), exons (red boxes) and introns (black connecting lines). The gRNA was designed complementary to target sequence (blue) in wild types (wt) at exon 6. When translated (pink boxes), the 16-bp deletion in the *disc1* mutant sequence causes a frameshift mutation at residue G625P leading to a premature stop codon at residue S633*.

(B) Gel electrophoresis of *disc1* amplicons from gDNA isolated from adult F2 fin-clips.

(C) *DdeI* digestion of amplicons: wild type (+/+) generates 2 bands (290 bp and 148 bp). Loss of the restriction site due to on target mutagenesis gives undigested products in mutants (422bp: 16bp smaller than 438bp wild type band). Heterozygotes (+/-) have all 3 bands (422 bp, 290 bp and 148 bp).

3.2.4 Validation of the *disc1*^{exon6} mutant line

We next wanted to investigate if the effect of the CRISPR-generated deletion in gDNA of *disc1*$^{exon6/exon6}$ was transcribed to mRNA. Recent studies in zebrafish have shown cases of exon-skipping whereby the endogenous transcription machinery bypassed mutations generated by CRISPR/ *Cas9* editing, causing a truncated but functional protein (Anderson et al., 2017). We pooled 52 hpf F3 homozygous mutant embryos together, extracted RNA and performed cDNA synthesis. Primers spanning exon-exon

junctions were designed and used to specifically amplify *disc1* transcripts (Fig. 3.9A). A PCR product was observed in *disc1*^{exon6} MZ mutants (right lane). The band was gel extracted, inserted into pCR-II via TOPO cloning and sequenced. Sequence alignment showed the 16 bp deletion was conserved in *disc1* mRNA transcripts (Fig. 3.9B) with no evidence of exon-skipping. Next, qPCR was performed on RNA extracted from these samples. There was a significant decrease (0.7-fold) of *disc1* expression in *disc1*^{exon6} MZ mutants compared to wild types (Fig. 3.9C).

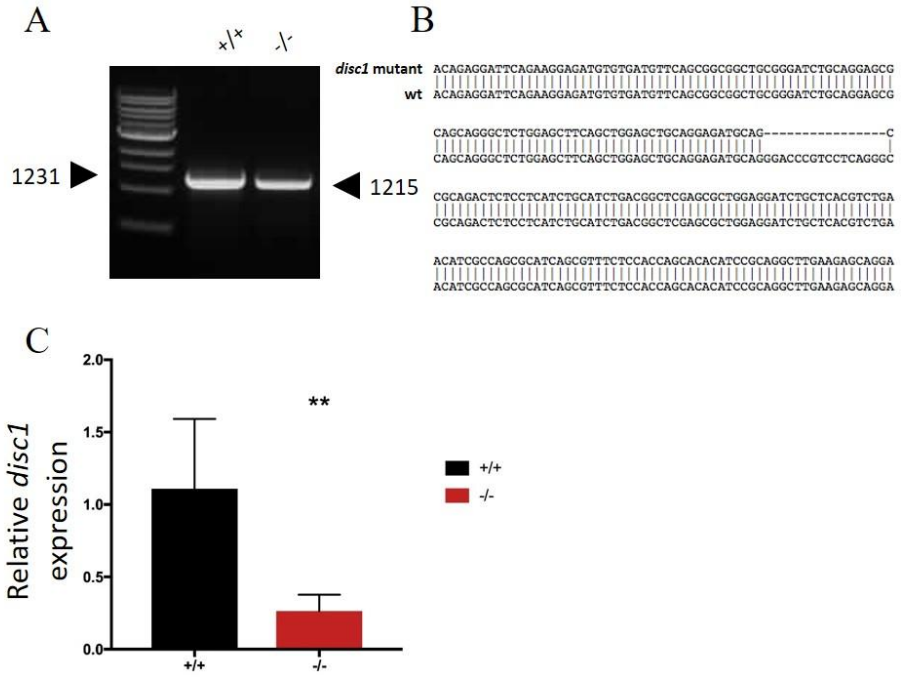

Figure 3.9. Validation of 16 bp deletion in *disc1* transcripts from maternal zygotic mutants and qPCR analysis of *disc1* expression

RNA was extracted from *disc1* maternal zygotic mutants and controls at 52 hpf. First strand cDNA synthesis was performed.

(A) Primers were used to amplify a region spanning the target site *disc1* transcripts. There were no apparent differences in transcripts between *disc1*^{exon6} MZ mutants and *disc1*$^{+/+}$ controls.

(B) Products were gel extracted, cloned into pCR-II TOPO and sequenced. Alignment shows the 16 bp deletion in the *disc1* transcripts from mutants (above) wild type sequence (below).

(C) Primers were designed and validated for qPCR. 3 technical replicates and 3 experimental replicates were performed. Bars indicate mean ± SD. Data distribution passed the Shapiro-Wilk normality test, unpaired Student t-test, p value < 0.01 (**).

To obtain conclusive evidence of the ineffectiveness of the zDisc1 zebrafish-specific antibody previously synthesised, protein from 52 hpf *disc1*$^{exon6/exon6}$ mutants was extracted and western blotting was performed (Fig. 3.10). Again, the 70 kDa band was still present in the *disc1*$^{exon6/exon6}$ mutant samples (right lane) similar to results observed from *disc1*$^{Y472X/Y472X}$ western blots (Fig. 3.5). Therefore, we concluded that the synthesised antibody was unable to recognise endogenous zDisc1.

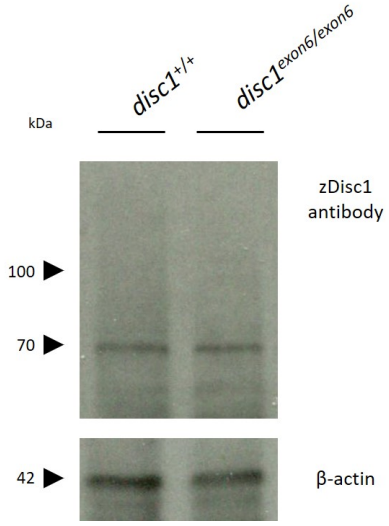

Figure 3.10. zDisc1 antibody does not detect endogenous levels of zDisc1 at 52 hpf

Western blot using protein extracted from *disc1*$^{+/+}$ and *disc1*$^{exon6/exon6}$ mutants at 52 hpf, blotted using purified zDisc1 antibody. The antibody recognises a band at 70 kDa which does not correspond to zDisc1 as it is size and present in *disc1*$^{exon6/exon6}$ mutants. There is no band detected at 112 kDa. β-actin was used as a loading control.

3.3 Discussion

3.3.1 Novel zDisc1 antibody detects overexpressed but not endogenous zDisc1

The polyclonal antibody can recognise overexpressed zDisc1 protein (Fig. 3.4), which is estimated to have a molecular mass of 112 kDa (expasy.org/compute_pi). However, this same antibody was incapable of recognising the endogenous protein from zebrafish head extracts (Figs. 3.1, 3.3, 3.5 and 3.10), despite studies in zebrafish finding that *disc1* is most highly expressed at 2-3 dpf (De Rienzo et al., 2011; Drerup et al., 2009; Eachus et al., 2017; Wood et al., 2009). Antibody specificity can depend on several factors such as purity of the antigen used to immunise, purity of the serum returned, immunogenicity of the protein and conditions of purification. For example, the final acid elution step may not have caused enough change in conditions to permit release of all bound antibodies which could lead to low yields in the final dialysed product (Devanaboyina et al., 2013). However, in this case, this scenario is unlikely as similar strong bands were observed when using purified antibodies compared to antiserum to recognise recombinant zDisc1 proteins (Fig. 3.2). The most prominent protein detected was at a lower molecular mass than predicted. This protein was also present *in disc1*$^{Y472X/Y472X}$ (Fig. 3.5) and *disc1*$^{exon6/exon6}$ (Fig. 3.10) which indicates non-specific binding of the zDisc1 antibody to an irrelevant protein. In hindsight, antibody purification may not have been worthwhile as when comparing crude antiserum to purified zDisc1 antibody, the laborious process does not seem to have significantly increased specificity or sensitivity (Fig. 3.2).

Protein extraction from zebrafish embryos is not a common laboratory technique and some groups report its ineffectiveness. This is often due to the presence of yolk lipids or proteases present in vast

quantities in the gut that are used to break down nutrients into single amino acids (Link et al., 2006). In our experiments, we avoided this by decapitating heads prior to protein extraction. Moreover, the 42 kDa bands corresponding to β-actin used as loading controls, clearly show a good yield of intact protein (Fig. 3.10).

Another possibility is that endogenous protein detection was not successful due to an endogenous low abundance of zDisc1. The expression of DISC1 appears to be extremely low in both transcriptomic and mass spectrometry data (Kuroda et al., 2011). This was also noted in iPSCs, where Wilkinson et al. (2019) were unable to detect endogenous levels of DISC1. They used CRISPR/ VP64-p65-Rta activation to upregulate *DISC1* expression by 2-fold and detected the DISC1 at centrosomes and the perinuclear region. This inherent low abundance is not aided by the fact that DISC1 undergoes rapid degradation. Its half-life is estimated between 3-6 hours in mammalian cells. This is very short for a scaffold protein, the average for structural proteins being usually 20-24 hours (Barodia et al., 2015; Yalla et al., 2018). Protein stability is reportedly affected by subcellular localisation; for example, multiple proteins in the cytosol, Golgi and transmembrane proteins have shorter half-lives compared to nuclear or mitochondrial proteins (Toyama and Hetzer, 2013). Therefore, differential cellular compartmentalisation of DISC1 may affect its half-life. Recently, synaptic activity was also found to have an influence of the half-life of specific neuronal proteins (Fornasiero et al., 2018).

Immunohistochemistry was also performed to determine if the purified antibody could recognise zDisc1 in its tertiary structure. Protein expression pattern was examined and compared to previously published *disc1 in situ* hybridisation figures (De Rienzo et al., 2011; Eachus et al., 2017; Wood et al., 2009). Immunofluorescence staining was dispersed and did not mirror results from RNA *in situ* hybridisation at 52 hpf, indicating non-specific binding of the purified antibody (Fig. 3.6). In future work, antigen-retrieval could be used before immunostaining to optimise epitope availability (Inoue and Wittbrodt, 2011). In addition, *disc1* expression could be upregulated by activating known upstream regulators such as the Sonic hedgehog pathway (Boyd et al., 2015). The lack of a high quality antibody could be addressed by raising zebrafish-specific zDisc1 monoclonal antibodies through hybridoma banks; however, this technique is notoriously expensive.

3.3.2 Uses and application of the new *disc1*^{exon6} mutant line

The decision to target exon 6 arose because of the high degree of conservation between the *C*-terminal part of zDisc1 and human DISC1. This coiled-coil region is evolutionarily conserved in vertebrates and is essential for protein folding and protein interactions. Inhibiting interactions at the *C*-terminus but potentially retaining those at the N-terminal end could hypothetically provide a better

model of the human t (1; 11). However, the gRNA does not target the human equivalent breakpoint, located in exon 8 of *disc1*. The mutant is therefore not designed to mimic the human *DISC1* translocation but aims to generate a novel tool for investigating *disc1* biology. Previous work by our group indicated the high efficiency of a specific gRNA by both *in vitro* and *in vivo* validation (R. Lucas MSc thesis, University of Sheffield, 2014). This was also the case in my hands. Promisingly, the 16 bp deletion is predicted to cause a frameshift mutation which would result in a severely altered protein with a non-functional *C*-terminal domain. Compared to point mutations, this type of disruption is much more likely to affect zDisc1 expression and function. Precise targeting of this locus also meant we could choose to delete a restriction enzyme binding site (*DdeI*), to facilitate genotyping through restriction fragment length polymorphism (RFLP). This enables genotyping to be performed through restriction analysis only, rather than sequencing, used for genotyping the *disc1*^{Y472X} line. This significantly accelerated and lowered the cost of genotyping which was invaluable during characterisation stages and for high throughput assays. To our knowledge, this was the first CRISPR-generated *disc1* zebrafish mutant and we predict that this new mutant will help to resolve phenotypic discrepancies observed between *disc1* MO and ENU-generated homozygous mutant zebrafish. However, during the course of this study, another group reported the generation of a CRISPR *disc1* mutant using a gRNA targeting exon 2 (Tang et al., 2020). Social interaction phenotypes including an enhanced cohesion and reduced dispersion were observed in *disc1* adult zebrafish mutants. This highlights the necessity of such mutant lines and the ongoing relevance to the neuropsychiatric field.

The CRISPR/Cas9 system can also be used to knock in donor DNA sequences via homology directed repair (HDR). By using this method or Bacterial Artificial Chromosome (BAC) recombineering, we could tag the *disc1* gene or zDisc1 protein with small epitopes (ie. FLAG, Myc, HA) or larger fluorescent proteins (GFP, mCherry, Cerulean) to study the dynamics and localisation *in vivo.* To overcome the current lack of reliable or commercially available antibodies against zDisc1, we attempted to generate a zDisc1-GFP BAC transgenic however attempts were unsuccessful and are not presented in this thesis. The novel line presented in this chapter will be used to study the behaviours relevant to the diverse hypothalamic functions. Homeostatic behaviours relating to sleep and feeding as well as stimulus-induced responses at the larval stage and finally innate fear in adults will subsequently be assayed. Hypothalamic cellular phenotypes will then be probed in the developing *disc1* mutants and these results will be compared to those obtained from previous studies.

Chapter 4: Homeostatic behaviours in disc1 mutants

4.1 Introduction

Homeostasis is the dynamic state of equilibrium maintained by living systems. An animal's behaviour is strongly influenced by homeostatic drives that are crucial for survival and reproduction, such as the drive to eat, sleep or escape from aversive stimuli. The impact of "threatened homeostasis" is involved in many disease processes.

4.1.1 Feeding and hunting

Foraging for external food sources is a key behaviour in the animal kingdom and dominates our time spent in wakefulness. Meeting the metabolic needs to match energy expenditure is key to survival. When this balance is disrupted, it can lead to malnutrition, starvation, weight gain and obesity at an individual level, and at a larger scale, can cause the extinction or expansion of an entire species. Our relationship with food becomes more complex in humans. This can be attributed to an over-supply of nutrients with high calorific content and the transition to a sedentary lifestyle. The constant social pressure of attaining happiness through aesthetic beauty and health also adds to this complexity.

Eating disorders such as obesity, anorexia nervosa and bulimia nervosa are often reported as comorbidities in patients with neuropsychiatric disorders. For example, in a cohort of major depressive disorders, 40% were overweight (Faulconbridge et al., 2011). Anorexia nervosa is often co-diagnosed in patients with schizoaffective disorders and often precedes psychosis. Some of these reports have been documented in medicated patients who are administered antidepressant and/ or antipsychotics. Adverse metabolic side effects are well-known from both atypical and typical antipsychotics but eating disorders are also present in medication-naive cases. In Bleuler's first report of schizophrenia, anorexia was even considered one of the negative symptoms (Hoff, 2012). Lifestyle choices could explain the link between eating disorders and mental illness. Many patients report binge eating disorder which can be classified as a "coping" mechanism (Troop et al., 1998). Notably, the stress axis and metabolism are intimately linked. Weight gain and/or loss is commonly observed in people under high stress and a loss of appetite is a key sign of anxiety and stress (Epel et al., 2000). In mice, acute stress inhibits feeding behaviours, whilst chronic stress leads to an overall increase in weight and body fat. The appetite-suppressing effects of stress in zebrafish have been linked to levels crf. In goldfish, central injections of crf elicit a dose-dependent decrease in food intake which was reversed by pretreatment with helical $crf_{(9–41)}$, a crf-receptor antagonist (dePedro et al., 1997).

Hyperosmotic conditions causing the activation of the HPI axis and downstream expression of *crf* can also lead to a decrease in food intake in zebrafish larvae (De Marco et al., 2014).

Many gene regions that have been linked to schizophrenia overlap with regions linked to type II diabetes (Gough and O'Donovan, 2005). Specifically, copy number variations (CNV) in the human chromosome 16 (16p11.2) increase the risk of developing schizophrenia by 16-fold (Maillard et al., 2015). Duplications in 16p11.2 are associated with decreased body mass whereas microdeletions are associated with obesity (D'Angelo et al., 2016). A recent GWAS elucidated the similarities in genetic architectures between risk factors for schizophrenia and anorexia (Duncan et al., 2017; Warrier et al., 2018). Animal models expressing genetic risk factors for affective disorders have alterations in weight and feeding behaviour (Thyme et al., 2019). In *Disc1* mutant mice, consumption of sugar is decreased in homozygote mutants. While this was interpreted as a sign of anhedonia, where mutants did not perceive the reward as "strongly" as their siblings linking caloric intake to the dopaminergic reward pathway (Clapcote et al., 2007), the neural circuitry of appetite could also be involved.

A major centre involved in the control of feeding and appetite is the hypothalamus, though many other brain regions are also involved. The hypothalamus integrates peripheral signals from the gastrointestinal tract, liver and adipose tissues, including nutrient levels sensed by vagal afferents and the nutrient-sensing neurons lining the ventricular system, as well as endocrine signals sensed through the neuroendocrine system. A range of neuropeptides and hormones play a role in appetite control. These can be grossly divided into orexigenic, which induce feeding, and anorexigenic, which inhibit appetite and food consumption. Orexigenic peptides conserved in teleosts include neuropeptide Y (NPY), orexin A/B, Agouti-Related protein (AgRP) and ghrelin. The most potent and conserved anorexigenic peptides include cocaine- and amphetamine-regulated transcript (CART), proopiomelanocortin (POMC) and corticotropin-releasing factor (CRF) (Volkoff et al., 2005). In zebrafish, *pomc* is expressed from 32 hpf in the corticotropic cells of the pituitary gland and in the hypothalamus (Hansen et al., 2003). Acute stress (vortex) in adult zebrafish was followed by an upregulation of *pomc* expression (Fuzzen et al., 2010). It was recently shown that stress-induced decreases in food intake are associated with increased levels of central *pomc* (Cortes et al., 2018), linking this neuronal circuit to stress-induced anorexia. At 5 dpf, *pomc*$^{+}$ neurons appear disorganised in *disc1*^{Y472X} mutants, and were not detected in the characteristic horseshoe pattern found in the wild type controls (Eachus et al., 2017).

Steroidogenic factor 1^{+} (Sf-1) neurons are also involved in feeding. Their activation through optogenetic manipulation in the ventral medial hypothalamus of mice suppresses feeding (Viskaitis et al., 2017). Prenatal ablation of these neurons leads to diet-induced obesity in adult mice (Cheung et al., 2015). It was shown that these neurons directly synapse and inhibit $Pomc^{+}$ neurons (Sternson et al., 2005) and therefore, would alter feeding through direct changes in appetite. Interestingly, Sf-1 neurons also play a prominent role in stress and anxiety, and their activation also increases anxiety-like phenotypes (Viskaitis et al., 2017). The observed alteration in food intake could also arise from a secondary effect from glucocorticoid (GC) activation. The expression of the zebrafish orthologue of *Sf-1*, *ff1b*, is increased in developing hypothalamus and unchanged in the interrenal gland of $disc1^{Y472X}$mutants (Eachus et al., 2017). This, in turn, was linked to a maladaptive response to stress. We therefore predict that these mutants would also exhibit changes in their feeding behaviour. Non-homeostatic mechanisms regulating food intake have also been uncovered. Monoaminergic systems, particularly serotonergic and dopaminergic, mediate the effect of hedonic feeding (Bojanowska and Ciosek, 2016). Based on sensory perception or pleasure, circuitry is thought to be tightly linked to the brain reward system (Rossi and Stuber, 2018). Drugs targeting serotonin (5HT2c) and dopamine (D2 and D3) receptors have been shown to increase appetite effect on feeding behaviour (Lett et al., 2012). In teleosts, the lateral tuberal nucleus (NTL) or PVN, the homologue of the mammalian arcuate nucleus, is believed to be an important feeding centre. The NTL contains $pomc^{+}$, $agrp^{+}$ and the *leptin receptor*$^{+}$ neurons. Neural activity signatures in hunting zebrafish larvae show increases in this area during consumption (Muto et al., 2017). Zebrafish embryos develop around and feed from their yolk until 5 dpf. When this internal source of food depletes, larvae instinctively start to forage for external sources of food. Many laboratories use *Paramecia* to study feeding behaviour in larvae. *Paramecia* are freely swimming, unicellular organisms that propel themselves via ciliary movement. From 6 dpf, zebrafish display a stereotypical hunting behaviour characterised by J turns, approach, and decision to ingest prey. Each step has been fully characterised, and machine learning software is available to automatically track such behaviour. Feeding networks and systems are highly conserved in zebrafish, in which drug library screens revealed similar effects on consumption in rodents (Jordi et al., 2018).

4.1.2 Regulation of sleep

Another key behaviour vital for physical and mental health in animals is sleep. It is controlled by both a homeostatic process, which increases sleep “pressure” relative to duration of wakefulness, and the circadian rhythm, which is responsible for physiological fluctuations of neuropeptides throughout the day. Sleep is a body wide phenomenon, common to all animals, however its duration, frequency and

time of onset vary between animals. Human electroencephalogram (EEG) recordings, measured from the neocortex, reveal different neural signatures known as “waves” which differentiate the different stages of sleep. Despite it being a well-studied behaviour, the function of sleep is still highly contentious. Memory consolidation, brain and peripheral tissue repair are all processes which occur during sleep. It is believed that being in wakeful state causes the build-up of "by-products" such as reactive oxidative species which are cleared during sleep. Sleep disorders are reported in 30-80% of patients with psychiatric disorders and are characterised by an increase in sleep onset latency and reductions in total sleep time, sleep efficiency, rapid eye movement (REM) and slow wave sleep in schizophrenic and depressive patients (Monti et al., 2013; Nutt et al., 2008). For bipolar disorder, sleep disturbances can evolve with the various stages of illness. For example, in the manic stages, 70-99% of individuals report a lessened need for sleep, whereas in the depressive stages, hypersomnia is reported in 40-80% of cases (Kaplan et al., 2015; Robillard et al., 2013). Sleep disruptions could be viewed as originating from medication as most antipsychotic medication, if taken at high doses, has severe sedative effects. However, in a recent study, schizophrenia patients treated with typical antipsychotics showed an increase in their sleep efficiency and duration, reporting improvements in their sleep quality compared to their sleep during premedication stages. Moreover, sleep disturbances, in many cases, are reported in newly diagnosed, medication-naive patients. Therefore, a common mechanistic origin is more likely to account for this comorbidity as common neurotransmitter systems and regulatory pathways are involved (Wulff et al., 2010).

Transgenic *αCaMKII-Disc1* mice display wild type-like intrinsic circadian periods in constant darkness, however, spent more time awake and less time asleep compared to wild types during both light and dark periods (Jaaro-Peled et al., 2016). In addition, overexpression of wild type human DISC1, disturbed sleep homeostasis in *Drosophila* (Sawamura et al., 2008). Testing a LOF animal model would provide additional insight into the role of Disc1 in sleep regulation. In another schizophrenia-relevant *Drosophila* model, a reduction in AKT signalling shortened the circadian period (Zheng and Sehgal, 2010). Deficits in working memory and in prepulse inhibition (PPI) are observed in some *Disc1* mouse models (Clapcote et al., 2007; Hikida et al., 2007; Niwa et al., 2010; Pletnikov et al., 2008; Wang et al., 2011). Because of the role played by sleep in memory, one might speculate these memory deficits arise, partly, due to lack of sleep or decrease in quality of sleep, however few of these mouse studies concurrently tested for sleeping behaviour.

Sleep regulation is mediated via the histamine, GABAergic and acetylcholine neurotransmitter systems (Baghdoyan et al., 1989; Sitaram et al., 1976). This is particularly evident in studies using

hypnotic drugs, a class of psychoactive drugs which induce sleep. Commonly used compounds are H1-receptor antihistamines (mepyramine and promethazine), a $GABA_A$-receptor agonist (Gaboxadol) and an acetylcholine esterase inhibitor (Eserine). In mammals, precise neural networks responsible for sleep-wake states have been mapped to the pontomedullary neuronal network, the lateral hypothalamus (LH) and preoptic area (PO). Two important peptidergic systems in the LH are hypocretin (HCRT) and melanin-concentrating hormone (MCH)-positive neurons. HCRT neuronal firing is most active during wakefulness and knocking out of these neurons causes excessive sleepiness (narcolepsy) in mice (Chemelli et al., 1999). MCH neurons are involved primarily in REM sleep (Jego et al., 2013). The PO also contains sleep-active neurons. Lesions in the PO have been shown to cause up to a 40% loss of sleep in rats. Both optogenetic and chemogenetic activation of the ventrolateral PO increases sleep (Kroeger et al., 2018).

Teleost models have been used to study sleep, because like humans they exhibit a diurnal sleep rhythm, as opposed to rodents which tend to be nocturnal. Due to their decrease in swimming during the night, it is simple to monitor and determine their state. Moreover, subcortical regions and neurotransmitter systems involved in sleep (discussed above) are well conserved throughout vertebrates. An exception is HCRT which in mammals is expressed in monoaminergic regions in both developing and mature brain areas, whereas in zebrafish, hcrt does not colocalise with dopaminergic or serotonergic neurons (Yokogawa et al., 2007). Nevertheless, this neuropeptide still plays a role in sleep and arousal in zebrafish, as hcrt overexpression causes an increase in sleep episodes (Prober et al., 2006). Until recently, because of their lack of neocortex (the area from which EEG recordings are made), it was unknown whether sleep architecture and the presence of non-REM and REM sleep were conserved in lower vertebrates. Due to the optical transparency of larvae, Leung et al. (2019) were able to observe different brain activities, muscle tones and heart rates analogous to those observed during different sleep states in humans, confirming the conservation of this sleep feature in zebrafish larvae.

4.2 Results

4.2.1 Food intake is reduced in disc1 mutant zebrafish larvae

We measured food intake in 7 dpf larval zebrafish. In normal laboratory conditions, at 5 dpf, larvae would be transferred to a nursery and are fed powdered food. Although hunting is an instinctive behaviour, we trained larvae to hunt and feed on the *Paramecia* by exposing them from 5 dpf.

Paramecia used for feeding at 7 dpf were labelled with DiI dye which emits fluorescence under far red light. Fixation was performed after 15 min to precede gut-emptying/digestion mechanisms. Gut fluorescence was used as a measure of food intake. There was a significant decrease in gut fluorescence between *disc1*$^{-/-}$ mutants and their respective *disc1*$^{+/+}$ controls in both *disc1*^{Y472X} (Fig. 4.1A) and *disc1*^{exon6} lines (Fig. 4.1B).

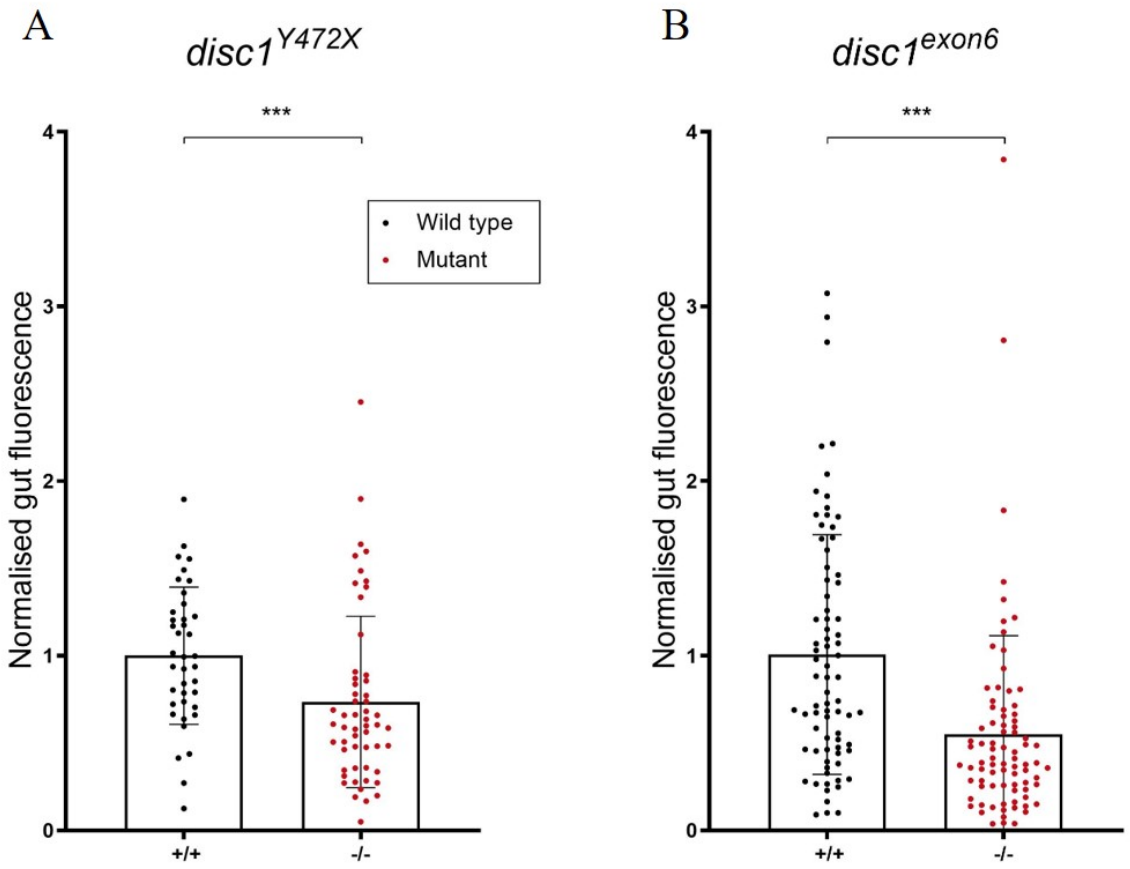

Figure 4.1. Food intake in *disc1* maternal zygotic mutants at 7 dpf
Points represent individual larvae, bars indicate mean ± SD. Wild type (+/+), wild type in-cross larvae (non-sibling); Mutant (-/-), homozygous mutant in-cross larvae. Data pooled from 3 independent clutches of embryos for each genotype.

(A) For *disc1*^{Y472X}, N= 94. Data distribution did not pass the Shapiro-Wilk normality test. Mann-Whitney test, *** = $p < 0.001$.
(B) For *disc1*^{exon6}, N= 159. Data distribution did not pass the Shapiro-Wilk normality test. Mann-Whitney test, *** = $p < 0.001$.

Food intake was also measured in progeny from a *disc1*^{exon6} heterozygote incrosses, and larvae were genotyped *post-hoc*. This was done to avoid any environmental contributions from differences in rearing conditions (number of larvae, food source, experience, etc.). Again, we found a significant

decrease in gut fluorescence in *disc1*^{exon6} homozygous mutants compared to heterozygotes and wild types (Fig. 4.2, Table 4.1).

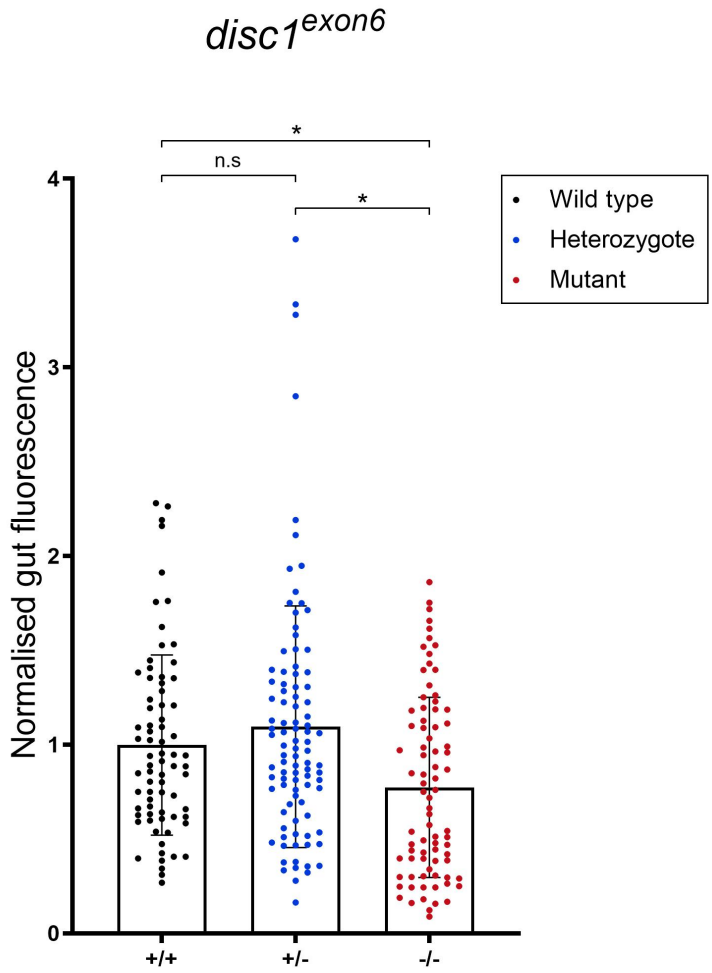

Figure 4.2. Food intake in progeny from a *disc1*^{exon6} heterozygote incross at 7 dpf

Points represent individual larvae, bars indicate mean ± SD. Wild type (+/+), heterozygote in-cross larvae (sibling); Heterozygote (+/-), heterozygote in-cross larvae (sibling); Mutant (-/-), homozygous mutant in-cross larvae. Data pooled from 4 independent clutches of embryos. N = 250. Data distribution passed the Shapiro-Wilk normality test, one-way ANOVA, F (2, 206) = 5.396, * = p < 0.05. See Table 4.1 for statistics.

Table 4.1. Tukey's *post hoc* multiple comparison

Tukey Multiple Comparison	**P value**	**Sig.**
Wild type: Heterozygote	0.999	n.s
Wild type: Mutant	0.011	*
Heterozygote: Mutant	0.023	*

4.2.2 Hunting behaviour is reduced in *disc1* mutant zebrafish larvae

The decrease in gut fluorescence observed in *disc1* mutant larvae could arise from abnormal hunting behaviour. We manually quantified hunting by recording 10-min videos, 5 min after addition of *Paramecia* at 7dpf. There was a significant decrease in hunting bouts between *disc1*$^{-/-}$ mutants and their respective *disc1*$^{+/+}$ controls in both *disc1*^{Y472X} (Fig. 4.3A) and *disc1*^{exon6} lines (Fig. 4.3B).

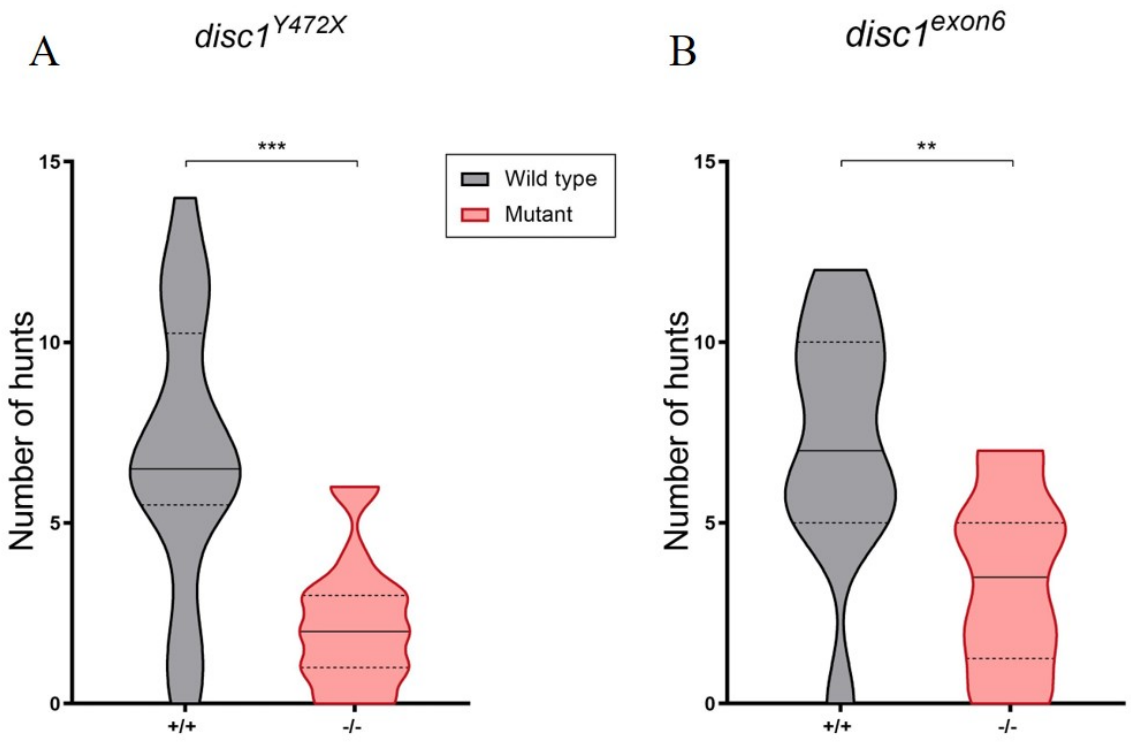

Figure 4.3. Hunting behaviour in *disc1* maternal zygotic mutants at 7 dpf

Violin plots represent sample distribution, full lines indicate median, and dotted lines indicate first quartile (below) and third quartile (top). Wild type (+/+), wild type in-cross larvae (non-sibling); Mutant (-/-), homozygous mutant in-cross larvae. Data pooled from 2 independent clutches of embryos for each genotype.

(A) For *disc1*^{Y472X}, N= 36, data distribution passed the Shapiro-Wilk normality test. Student's t-test, *** = $p < 0.001$.

(B) For *disc1*^{exon6,} N= 23, data distribution passed the Shapiro-Wilk normality test. Student's t-test, ** = $p < 0.005$.

4.2.3 Stress-induced anorexic behaviour is attenuated in *disc1* mutant zebrafish larvae

It was previously shown that hyperosmotic conditions cause activation of stress response in teleosts (Yeh et al., 2013). Zebrafish exposed to hyperosmotic conditions display a difference in lateral displacement toward *Paramecia* (De Marco et al., 2014). Recently, it was shown than *disc1* mutants have an altered response to stress (Eachus et al., 2017). Considering *disc1* mutants also have an altered feeding behaviour (Fig. 4.1, 4.2), we decided to investigate the effect of stress on food intake in *disc1* mutants. We applied sodium chloride (NaCl), an osmotic stressor, to the larvae 10 min prior to the feeding assay. This delay was chosen as cortisol peak occurs 10-15 min after exposure to a stressful stimulus (Yeh et al., 2013). We observed different effects between *disc1*$^{+/+}$ and *disc1*$^{Y472X/Y472X}$ in response to varying concentrations of NaCl. As expected, acute stress causes a decrease in food intake in a dose-dependent manner in wild type larvae (Fig. 4.4). In *disc1*$^{Y472X/Y472X}$ mutants, acute stress had

no effect on gut fluorescence at lower NaCl concentrations (100 mM) whereas the effect was comparable with wild types at higher NaCl concentrations (250 mM).

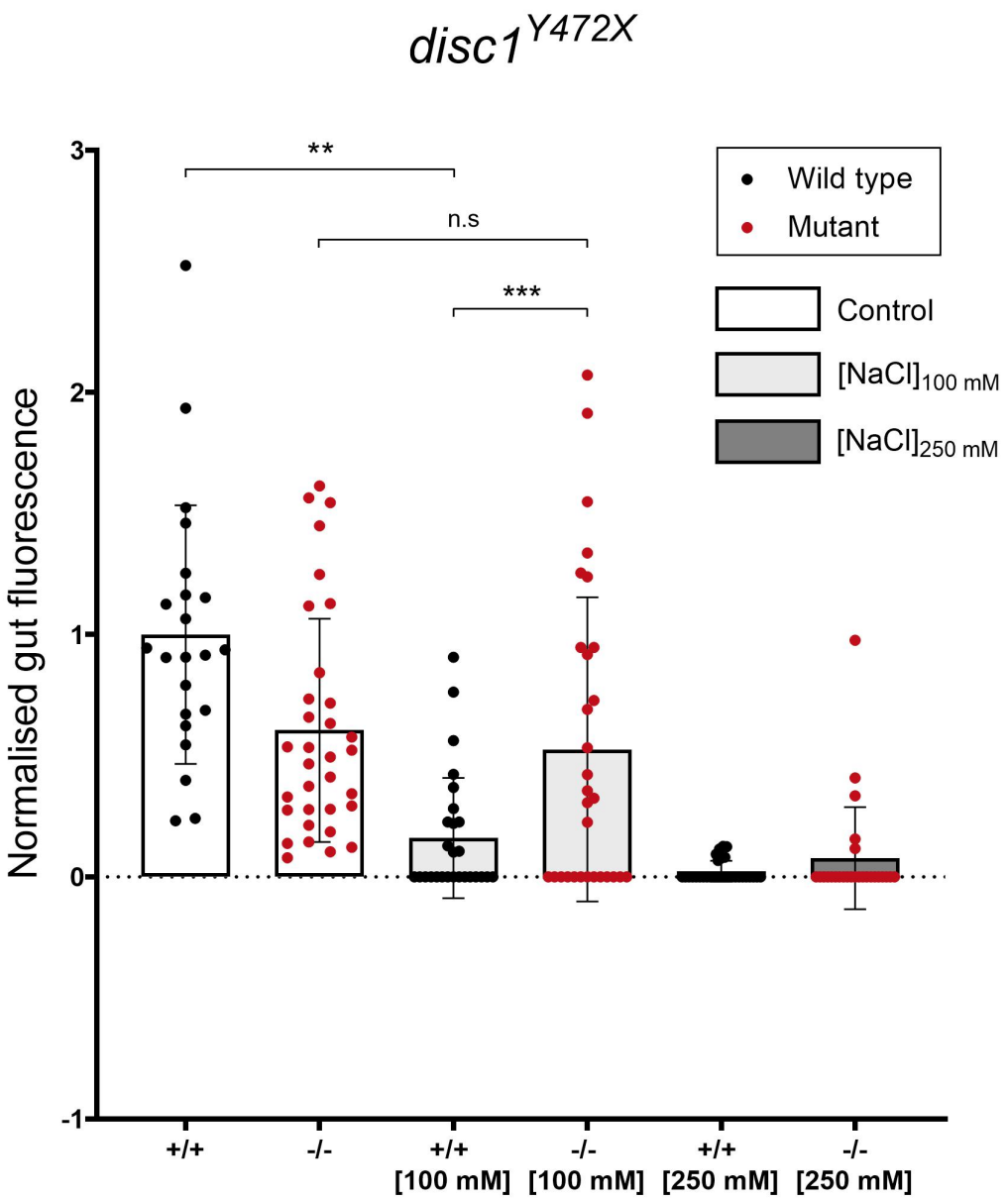

Figure 4.4. Stress-induced anorexia in *disc1*^{Y472X} maternal zygotic mutants
Points represent individual larvae, bars indicate mean ± SD. Wild type (+/+), wild type in-cross larvae (non-sibling); Mutant (-/-), homozygous mutant in-cross larvae. Data from a single clutch of embryos. $N_{+/+}$= 22, $N_{-/-}$= 33, $N_{+/+\ [100\ mM]}$= 27, $N_{-/-\ [100\ mM]}$= 30, $N_{+/+\ [250\ mM]}$= 30, $N_{-/-\ [250\ mM]}$= 26, data distribution did not pass the Shapiro-Wilk normality test. Two-way ANOVA and Tukey's multiple comparison ** = $p < 0.01$, *** = $p < 0.001$). See Table 4.2 for statistics.

Table 4.2. Tukey's *post hoc* multiple comparison for gut fluorescence in *disc1*^{Y472X} after exposure to varying concentrations of sodium chloride

Two -way ANOVA				
Factor	**F value**	**d.f**	**P value**	**Sig.**
Treatment	46.631	2	> 0.001	***
Genotype	0.016	1	0.9	n.s
Treatment : Genotype	11.975	2	> 0.001	***
Tukey Multiple Comparison				
WT Control: Mut Control			0.001	**
WT Low Salt : Mut Low Salt			0.001	**
WT High Salt: Mut High Salt			0.624	n.s
WT Control: WT Low Salt			> 0.001	***
WT Control: WT High Salt			> 0.001	***
WT Low Salt : WT High Salt			0.241	n.s
Mut Control: Mut Low Salt			0.525	n.s
Mut Control: Mut High Salt			> 0.001	***
Mut Low Salt : Mut High Salt			0.002	**

4.2.4 Sleep is decreased in *disc1* mutant zebrafish larvae

In zebrafish, the circadian rhythm can be measured through locomotor activity as early as 5 dpf (Hastings et al., 2003). As in all diurnal animals, activity is greatly reduced during night-time. This state can be simulated by exposure to a 14hr: 10hr light: dark cycle. Larvae were placed in individual wells and activity was measured over 3 consecutive nights (6-9 dpf) and averaged. *disc1*^{Y472X} mutants showed an increased activity during the night-time and a decrease in activity during the daytime compared with *disc1*$^{+/+}$ controls (Fig. 4.5A,B,C). To investigate sleeping behaviour, we quantified the

number of sleep episodes, defined by ≥1 min of inactivity. *disc1*^{Y472X} mutants slept significantly less during the night compared to controls (Fig. 4.5D). During the day, there were no differences in number of sleep episodes between *disc1*^{Y472X} mutants and controls (Fig. 4.5E). *disc1*^{exon6} mutants exhibited wild type-like locomotor activity and number of sleep episodes during the night (Fig. 4.6A,B,D), however, showed a significantly increase locomotor activity during the day (Fig. 4.6C). There was no difference between *disc1*^{exon6} mutants and controls in number of sleep episodes during the day (Fig. 4.6E).

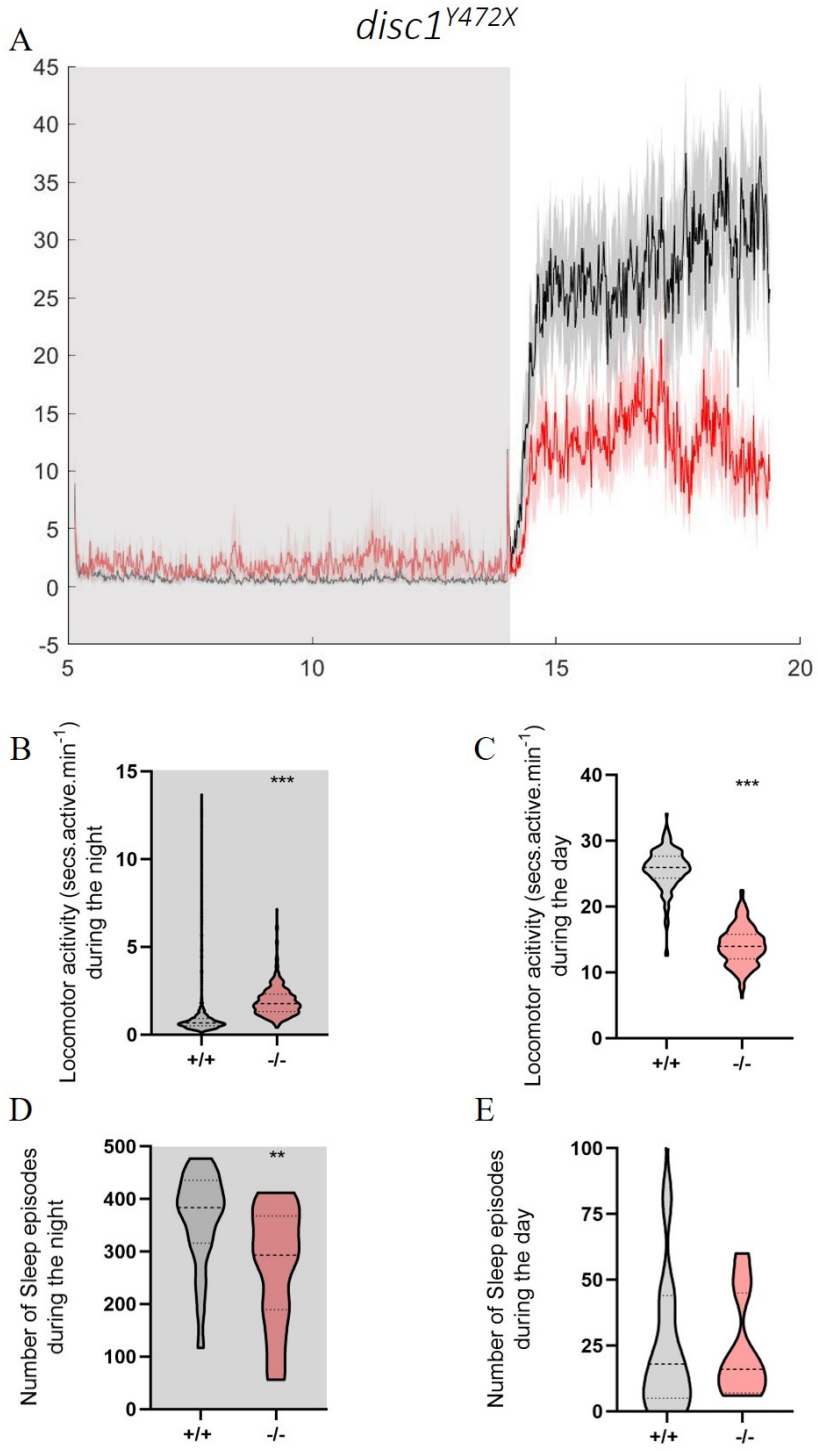

Figure 4.5. Locomotor activity and sleep episodes in *disc1*^{Y472X} maternal zygotic mutants

Activity traces over 15 hours. +/+, wild type in-cross larvae (non-sibling); -/-, homozygous mutant in-cross larvae. Data pooled from 2 independent clutches of embryos. N=48, 3 experimental replicates. White and grey boxes indicate lights ON (day) and lights OFF (night), respectively. The same data points were used for quantification in (B) and (C).

(A) Lines and shaded areas represent means ± SD. Night-time activity is increased in *disc1*^{Y472X} mutants compared wild types. Daytime activity is decreased in *disc1*^{Y472X} mutants compared wild types.

(B) Box and violin plots of locomotor activity during the night (grey box). Dashed lines indicate median (middle), first (lower) and third (higher) quartile. Data distribution did not pass the Shapiro-Wilk normality test., Mann-Whitney test, *** = $p < 0.001$.

(C) Box and violin plots of locomotor activity during the day. Dashed lines indicate median (middle), first (lower) and third (higher) quartile. Data distribution did not pass the Shapiro-Wilk normality test., Mann-Whitney test, *** = $p < 0.001$.

(D) Box and violin plots of sleep episodes during the night (grey box). Dashed lines indicate median (middle), first (lower) and third (higher) quartile. Data distribution passed the Shapiro-Wilk normality test., unpaired Student's t-test, ** = $p < 0.01$.

(E) Box and violin plots of sleep episodes during the day. Dashed lines indicate median (middle), first (lower) and third (higher) quartile. Data distribution passed the Shapiro-Wilk normality test, unpaired Student's t-test, n.s = $p > 0.05$.

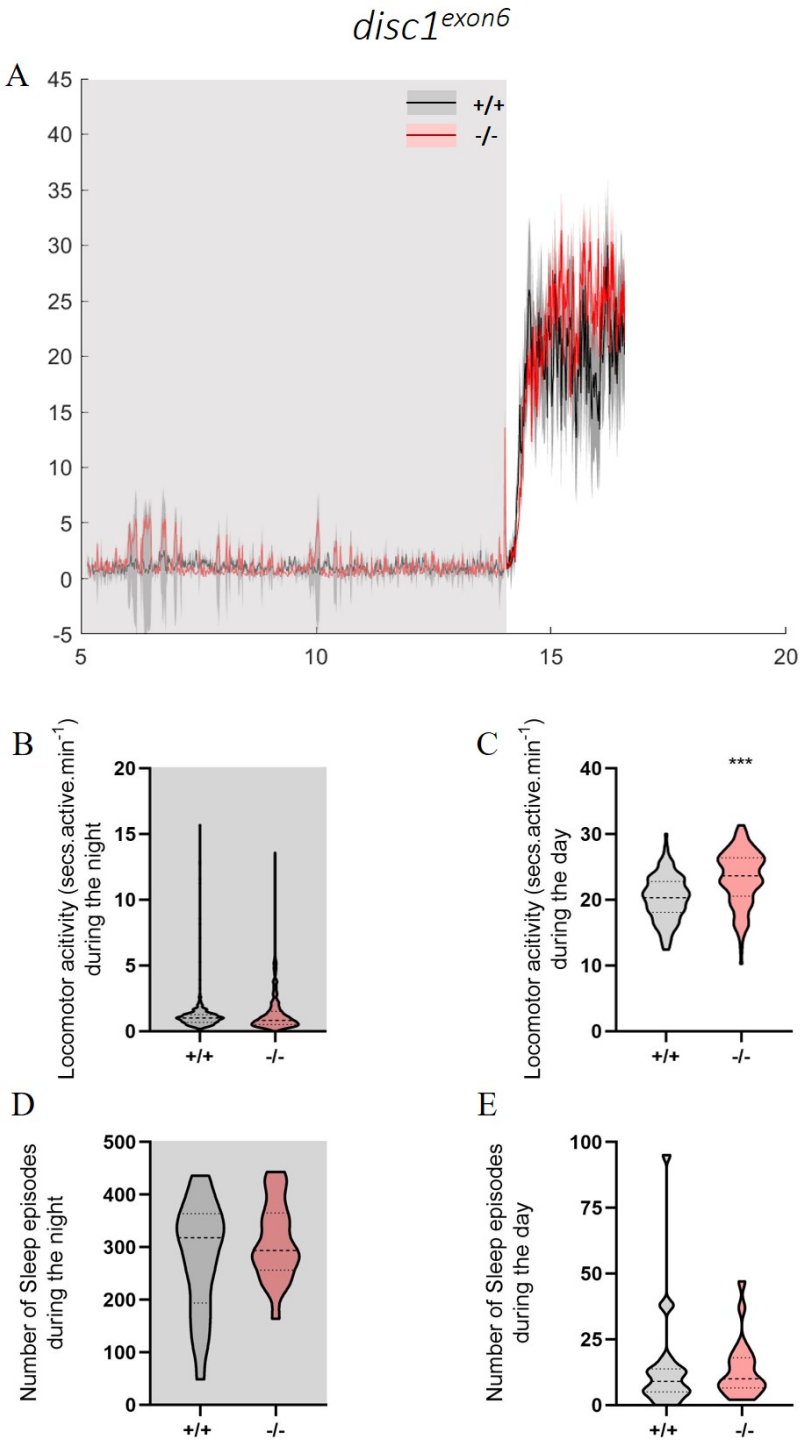
disc1exon6
A
+/+
-/-
B
Locomotor acitivity (secs.active.min-1) during the night
C
Locomotor acitivity (secs.active.min-1) during the day
***
D
Number of Sleep episodes during the night
E
Number of Sleep episodes during the day

Figure 4.6. Locomotor activity and sleep episodes in in *disc1*^{exon6} maternal zygotic mutants

Activity traces over 12 hours. +/+, wild type incross larvae (non-sibling); -/-, homozygous mutant incross larvae. Data pooled from 2 independent clutches of embryos. N=48, 3 experimental replicates. White and grey boxes indicate lights ON (day) and lights OFF (night), respectively. The same data pointed were used for quantification in (B) and (C).

(A) Lines and shaded areas represent means ± SD. Night-time activity is increased in *disc1*^{exon6} mutants compared wild types. Daytime activity is similar between *disc1*^{exon6} mutants and wild types.

(B) Box and violin plots of locomotor activity during the night (grey box). Dashed lines indicate median (middle), first (lower) and third (higher) quartile. Data distribution did not pass the Shapiro-Wilk normality test., Mann-Whitney test, n.s = $p > 0.05$.

(C) Box and violin plots of locomotor activity during the day. Dashed lines indicate median (middle), first (lower) and third (higher) quartile. Data distribution did not pass the Shapiro-Wilk normality test., Mann-Whitney test, *** = $p < 0.001$.

(D) Box and violin plots of sleep episodes during the night (grey box). Dashed lines indicate median (middle), first (lower) and third (higher) quartile. Data distribution passed the Shapiro-Wilk normality test, unpaired Student's t-test, n.s = $p > 0.05$.

(E) Box and violin plots of sleep episodes during the day (white box). Dashed lines indicate median (middle), first (lower) and third (higher) quartile. Data distribution passed the Shapiro-Wilk normality test, unpaired Student's t-test, n.s = $p > 0.05$.

For the same reasons as aforementioned in the feeding assay, we measured locomotor activity in progeny from *disc1*^{exon6} heterozygote incrosses and performed genotyping *post hoc*. There was a significant increase in night-time locomotor activity in both *disc1*$^{exon6/+}$ and *disc1*$^{exon6/exon6}$ (Fig. 4.7A,B). There was also a significant increase in daytime locomotor activity in *disc1*$^{exon6/exon6}$ compared to *disc1*$^{+/+}$ siblings; however, *disc1*$^{exon6/+}$ exhibited a significantly decreased locomotor activity during the day compared to *disc1*$^{+/+}$ siblings and *disc1*$^{exon6/exon6}$ (Fig. 4.7C). There was no difference in number of sleep episodes during neither the day or night between all genotypes (Fig. 4.7D,E).

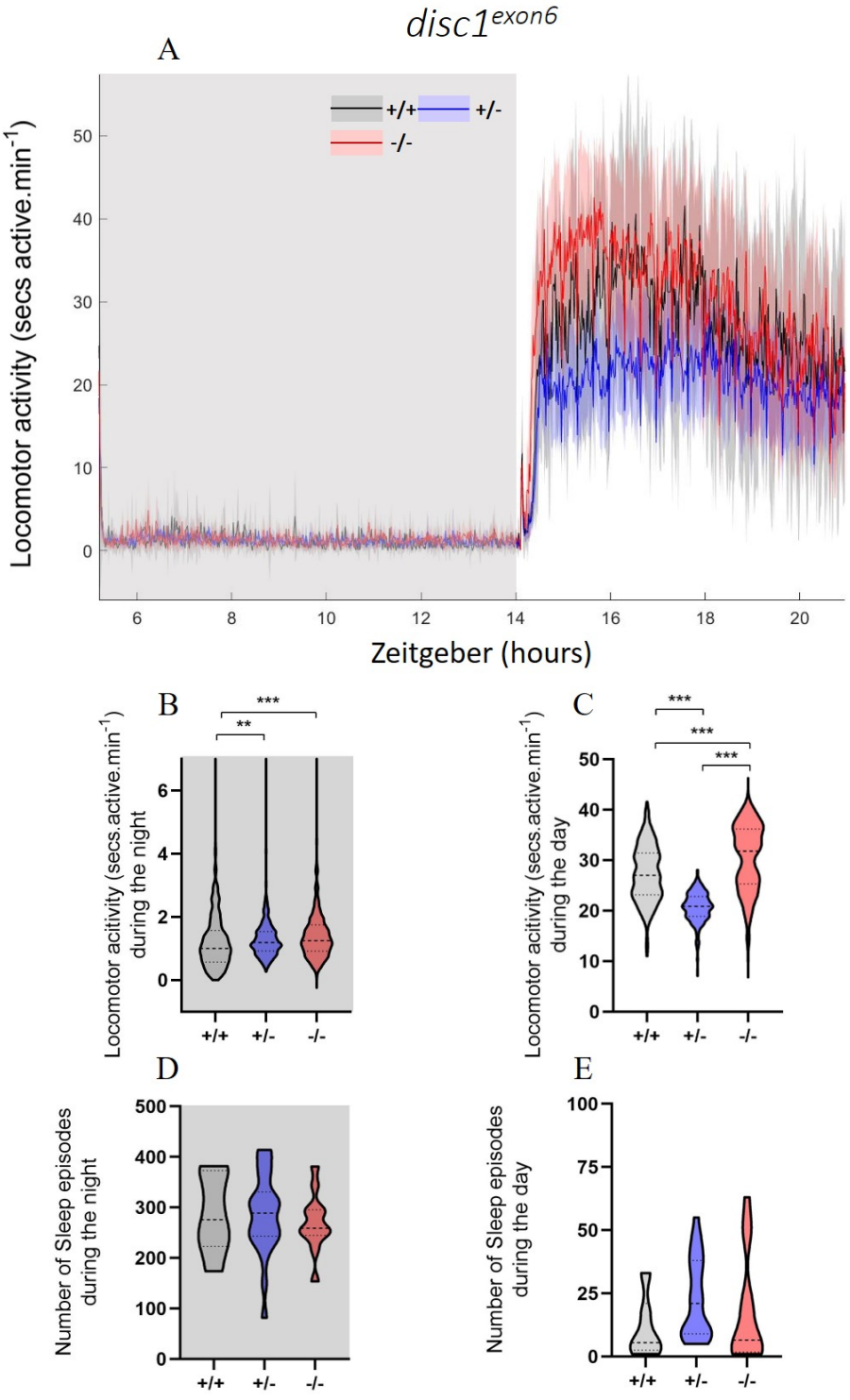
disc1exon6
A
+/+
+/-
-/-
Locomotor activity (secs active.min-1)
Zeitgeber (hours)
B
Locomotor acitivity (secs.active.min-1) during the night
C
Locomotor acitivity (secs.active.min-1) during the day
D
Number of Sleep episodes during the night
E
Number of Sleep episodes during the day
+/+
+/-
-/-

Figure 4.7. Locomotor activity and sleep episodes in progeny from a *disc1*^{exon6} heterozygote incross
Activity traces over 15 hours. +/+, homozygous sibling; +/-, heterozygous mutant; -/-, homozygous mutant. Data pooled from 2 independent clutches of embryos. N=96, 2 experimental replicates. White and grey boxes indicate lights ON (day) and lights OFF (night), respectively. The same data points were used for quantification in (B) and (C).

(A) Lines and shaded areas represent means ± SD. Night-time and daytime activity is similar between *disc1*^{exon6} mutants, heterozygotes, and wild types.
(B) Box and violin plots of locomotor activity during the night (grey box). Dashed lines indicate median (middle), first (lower) and third (higher) quartile. Data did not pass the Shapiro-Wilks test. Kruskal-Wallis test with pairwise comparison was significant, P<0.01 = **, P<0.001 = ***.
(C) Box and violin plots of locomotor activity during the day (white box). Dashed lines indicate median (middle), first (lower) and third (higher) quartile. Data did not pass the Shapiro-Wilks test. Kruskal-Wallis test with pairwise comparison was significant, P<0.01 = **, P<0.001 = ***.
(D) Box and violin plots of sleep episodes during the night (grey box). Dashed lines indicate median (middle), first (lower) and third (higher) quartile. Data distribution passed the Shapiro-Wilk normality test, one-way ANOVA, F (2,44) = 0.696, n.s = p > 0.05.
(E) Box and violin plots of sleep episodes during the day (white box). Dashed lines indicate median (middle), first (lower) and third (higher) quartile. Data distribution passed the Shapiro-Wilk normality test, one-way ANOVA, F (2,44) = 1.316, n.s = p > 0.05.

4.3 Discussion

4.3.1 Analysis of feeding and hunting behaviour in *disc1* larvae

We report a decrease in feeding which could indicate either a deficit in metabolic needs or a decrease in appetite. *Disc1* mouse models have a decrease in sucrose consumption which was linked to anhedonia; however, no differences in size or weight was ever reported. No differences in size in body length or head width were also reported in *disc1*^{Y472X} mutant zebrafish (H. Eachus PhD thesis, University of Sheffield, 2015). This suggests that the decrease in hunting and food intake is due to a decrease in appetite or motivation rather than difference in metabolic need. The consistency of this phenotype between *disc1*^{Y472X}and *disc1*^{exon6} indicates that this reduction in appetite is a gene-specific effect. The consistency of the phenotype in homozygous mutants derived from heterozygote incrosses which were raised in identical conditions, rules out the contribution of environmental/ rearing conditions. Loss of appetite and anorexia is commonly comorbid with medication-naïve neuropsychiatric disorders. Of note, other zebrafish models harbouring mutations in schizophrenia-associated genes have decreases in both hunting and feeding (Thyme et al., 2019). These results seem to suggest that functionally diverse genetic risk factors for psychiatric disease, including *disc1*, converge at the behavioural level.

4.3.2 The relation between stress and food consumption

The response to stress is mediated, in part, by the HPA axis, which causes an increase in plasma glucocorticoids that feed back into the brain. In rats, daily injections of the synthetic glucocorticoid

dexamethasone can suppress food intake (Jahng et al., 2008). In zebrafish larvae, hyperosmotic conditions which increases cortisol secretion, will also suppress food intake. When cortisol returns to basal levels, normal feeding is re-established (De Marco et al., 2014). In rainbow trout, the growth suppressing effects of cortisol administration were linked to an increase in *crf* in the preoptic area (Madison et al., 2015). In contrast, chronic stress in goldfish and sea bass (by daily intraperitoneal cortisol injections), increases food intake (Bernier et al., 2004; Leal et al., 2011). These differences could be due to the effect of chronic vs acute stress, the dose administered or species selectivity. Our group previously found that, unlike wild type controls, *disc1*^{Y472X} mutant larvae do not upregulate cortisol in response to acute stress at 5 dpf (Eachus et al., 2017). We report here, that *disc1*^{Y472X} mutant larvae do not decrease food consumption in response to acute stress (Fig. 4.4). The lack of downregulation of food intake after NaCl $_{[100\ mM]}$ treatment (mild acute stress) in *disc1* mutants could be explained by a lack of cortisol upregulation, however, the necessary repeats and rescue experiments to demonstrate this have not been performed yet.

4.3.3 Analysis of locomotion in *disc1* mutant larvae

Baseline swimming activity during the day appeared decreased in *disc1*^{Y472X} mutants compared to *disc1*$^{+/+}$ (Fig. 4.5A,C). This observation is in direct contrast from the 'normal' baseline swimming activity previously reported in *disc1*$^{Y472X/Y472X}$ at 5 dpf (H. Eachus PhD thesis, University of Sheffield, 2015). Interestingly, *disc1*^{exon6} mutants, originating from both homozygous (Fig. 4.6A,C) and heterozygous crosses (Fig. 4.7A,C), were hyperactive during the day. Daytime hypoactivity has not been reported in other *Disc1* animal models. In fact, the most widely reported locomotor phenotype in mice is hyperactivity (Clapcote et al., 2007; Hikida et al., 2007) or no change in locomotor activity (Koike et al., 2006; Pletnikov et al., 2008). Hyperactivity is an endophenotypes of schizophrenia and linked to stereotypical behaviour of schizoaffective models (lion pacing a cage/obsessive compulsion behaviour, anxiety). On the other hand, hypolocomotion is an endophenotype commonly observed in animal models of depression (de Abreu et al., 2018). It has been linked to alterations in dopaminergic ascending neurons and alterations to brain areas associated with motivation and initiation of locomotion

We found that *disc1*^{Y472X} mutants have an increased locomotor activity during the night and a decrease in number of sleep episodes (Fig. 4.5A,B,D). *disc1*^{exon6} mutants originating from homozygous crosses, showed no differences in their night-time activity or sleep behaviour (Fig. 4.6B,D,E); however, *disc1*^{exon6} mutants originating from heterozygous crosses, also exhibited night-time hyperactivity (Fig. 4.7A,B). The number of sleep episodes during the night also appeared decreased in *disc1*^{exon6} mutants, however this was not statistically significant (Fig. 4.7D). Night-time hyperactivity has also been

reported in *Disc1* transgenic *Drosophila* and mice models (see section 4.1.2). In other zebrafish mutants modelling neurodevelopmental disorders such as *cntnap2,* a risk factor for autism, night-time hyperactivity is also a prominent phenotype and even used as a readout for determining drug efficacy (Hoffman et al., 2016). This work is the first study suggesting that *disc1* mutant larvae sleep less than wild type larvae. This finding could be related to the insomnia comorbidities often reported in neuropsychiatric disorders. Of note, in human carriers of the *DISC1* translocation and in *Disc1* mice models, memory and learning deficits have been reported (Cannon et al., 2005; Koike et al., 2006; Thomson et al., 2016). As previously discussed, sleep quality and length significantly impact on memory and neuroplasticity. Therefore, sleep disturbances could play a secondary role in some of these deficits. A more thorough analysis of sleep architecture on *disc1* mutant zebrafish larvae is needed and could include comparing slow wave sleep (SWS) and propagating wave sleep (PWS) episodes to pinpoint precise differences. Such techniques were recently developed for examining sleep architecture in larvae and reinforces the validity of larval zebrafish for modelling human sleep (Leung et al., 2019).

4.3.4 Phenotypical differences between genotypes and crosses

While the feeding phenotype was consistent between genotypes and crosses, the sleep phenotype showed more disparities. With regards to daytime locomotion, *disc1*^{Y472X} mutants were hypoactive (Fig. 4.5C), whereas *disc1*^{exon6} mutants (Fig. 4.6C, 4.7C) were hyperactive. As both mutant lines have premature stop codons (PTC) and a significant decrease in *disc1* expression (Fig. 3.9C; Eachus et al., 2017), it is unlikely that differences observed between *disc1*^{Y472X} and *disc1*^{exon6} are due to differential levels of zDisc1 protein. Phenotypical differences could arise due to differences in allele functionality between in *disc1*^{Y472X} and *disc1*^{exon6} (see section 8.6.1, for detailed discussion).

Differences were also observed in locomotor activity between mutants from *disc1*^{exon6} heterozygote incrosses versus *disc1*^{exon6} homozygote incrosses. While *disc1*^{exon6} maternal zygotic mutants were found to show no differences in night-time activity (Fig. 4.6B), *disc1*$^{exon6/exon6}$ and *disc1*$^{exon6/+}$ mutants from heterozygotes incrosses had an increase in night-time activity compared to *disc1*$^{+/+}$ siblings (Fig. 4.7B). Differences in these results could be explained by the large variability of the locomotor activity data in the *disc1*^{exon6} homozygous incrosses (Fig. 4.6B). To conclude, loss of *disc1* causes a decrease in food consumption and hunting behaviour and in some cases, may affect sleep regulation. Given that *disc1* mutant lines show opposite daytime locomotor phenotypes yet still have a decrease in *Paramecia* consumption, we concluded this phenotype is not secondary effect of hypolocomotion. Considering the role of *disc1* in the development of the hypothalamus, these new results could implicate hypothalamic-driven alterations in motivation and arousal.

Chapter 5: Stimulus-evoked behaviours in *disc1* mutants

5.1 Introduction

5.1.1 Stimulus-evoked behaviours and arousal

In contrast to homeostatic behaviours, stimulus-evoked behaviours are initiated in response to external cues. The correct responsiveness to the external environment is key to an animal's survival and heavily involved in predator evasion. Even the most primitive invertebrates possess the ability to respond to their external environment. In a pioneering piece of work, Eric Kandel and colleagues demonstrated that a tactile stimulus elicited a withdrawal response in the sea snail, *Aplysia californica* (Kandel et al., 1967). Measuring arousal is a way of quantifying responses to external stimuli. These stimuli are diverse (auditory, visual, chemical, mechanical), unexpected and most often aversive. Whereas sleep and wake are relatively simple behaviours to characterise, an animal's arousal state is more ambiguous but is well defined. Arousal is characterised by an increase in motor activation, sensory responsiveness and emotional reactivity (Pfaff, 2006). Therefore, an animal in an elevated state of arousal exhibits both increased spontaneous activity (endogenous arousal) and increased responsiveness to sensory stimuli (exogenous arousal) (Pfaff et al., 2008). At least five major neurotransmitter systems (dopamine, noradrenaline, serotonin, acetylcholine, and histamine) work collectively to increase arousal. In more complex animals, such responses modulated by external cues are termed startle responses and appear relatively early in development. The relationship between stress and arousal is uneven; there is clear possibility to have arousal without stress but the inverse, stress without arousal, is not true (Pfaff et al., 2007). Functionally, arousal is crucial for motivating behaviours such as locomotion, escape, reward- seeking (e.g. pursuit of prey) and courtship activity.

5.1.2 Modelling stimulus-evoked behaviours in zebrafish

Zebrafish express a rich repertoire of stimulus-evoked behaviours with striking similarities to mammals. Larval zebrafish are useful vertebrate models for defensive behaviours because of their relatively simple nervous system. Escape reflexes to a variety of threats (visual, tactile or vibrational-acoustic) elicit a fast, robust, high angle and stereotypical behaviour (the C bend) (O'Malley et al., 1996). Vibrational-acoustic startle are detected through sensory hair cells of the lateral line and otic vesicle which project to large escape-promoting Mauthner neurons in the hindbrain (reticulospinal circuit) (Eaton et al., 1977; Liu and Fetcho, 1999).

Other visually evoked behaviours include the visual startle response, elicited by a looming stimulus and which is also Mauthner-medicated (Dunn et al., 2016). These protective startle responses are

characterised by upregulation of activity and a change in direction to escape potential predators. Changes in illumination cause different light-induced locomotor responses (LLR) such as an acute response termed visual motor responses (VMR) which appears seconds after the change (Burgess and Granato, 2007). More long-term LLRs occur minutes after the change of light (Gao et al., 2014). LLRs can temporarily override endogenous activity levels set by the circadian clock, a phenomenon homologous to masking in mammals (Mrosovsky et al., 2005). Negative masking is an acute effect of light exposure which causes a downregulation of locomotion in nocturnal species (Aschoff, 1999). Arousal behaviours are modality specific. This signifies that the responsiveness to different sensory modalities (light, sound, pain) are dissociable. For example, transient overexpression of *hcrt* at 5 dpf selectively increases the larvae's response to a dark flash but not to acoustic stimuli (Woods et al., 2014). This highlights the importance of measuring responses to multiple modalities when investigating behavioural phenotypes.

Escapes are energetically costly movements and additional modulation is provided from the dopaminergic (DA) and serotoninergic (5-HT) systems (Yao et al., 2016). Evidence for the involvement of dopaminergic neurons in exogenous arousal has primarily come from *Drosophila* studies (Lebestky et al., 2009; Van Swinderen and Andretic, 2011). Genetic variation in startle-induced locomotion is thought to be associated with differences in DA levels (Carbone et al., 2006; Kume et al., 2005). In zebrafish, changes to LLRs are often reported in models of Parkinson's disease where the loss of DA neurons in ventral diencephalon causes abnormal responses to light (da Fonseca et al., 2013; Stednitz et al., 2015; Xi et al., 2010).

The behavioural repertoire in adult zebrafish is far richer than at larval stages, even though social behaviours emerge as early as 3 weeks post-fertilisation (wpf). Response to a novel environment is widely used to examine risk-taking behaviour and anxiety in adult fish (Gerlai et al., 2000; Maximino et al., 2010). When placed in a novel environment or when exposed to a stressor (NaCl or alarm substance), adult zebrafish spend more time at the bottom of the tank termed bottom dwelling behaviour (Mathuru et al., 2012; Speedie and Gerlai, 2008; Waldman, 1982). Freezing and erratic swimming episodes increase, disrupting the baseline continuous swimming pattern (Blechinger et al., 2007). Importantly, alterations can be reversed by acute treatment of anxiolytics (Egan et al., 2009). Another anxiety paradigm is the open-field test. Similarly to rodents, response to stress, zebrafish display avoidance of the centre of the tank (Champagne et al., 2010; Hall and Ballachey, 1932). This behaviour termed thigmotaxis, is abnormal in DN-*Disc1*, *Disc1*^{L100P} *and Disc1*^{Q31L} missense mutant mice following immunological challenge (Abazyan et al., 2010; Lipina et al., 2013). In addition, drug

screening assays in adult zebrafish have shown anxiogenic drugs generally increase startle responses; while anxiolytic drugs generally decrease startle responses (Hale, 2000; Pittman and Lott, 2014). These findings suggest that stimulus-induced behaviours can become abnormal after genetic and environmental insult and are sensitive to relevant compounds.

5.1.3 Neuronal gating dysfunctions in neuropsychiatric disorders

Startle assays are commonly used in psychopharmacology studies. Arousal states and sensorimotor information processing are dysregulated across a subset of neuropsychiatric disorders. An imbalance between excitatory and inhibitory circuits could affect the dynamic of arousal circuits causing alterations in cognitive function. In schizophrenia, post-traumatic stress disorder (PTSD) and anxiety, hyperarousal is often reported whereas hypoarousal is often associated with attention deficit hyperactivity disorder (ADHD) and depression (Carlsson et al., 1999; de Lecea et al., 2012; Haller et al., 2005; Miano et al., 2006). Recently, startle-evoked responses were able to reliably predict the severity and breadth of psychopathology in human patients (Lang et al., 2018).

Sensorimotor gating (SMG) is the selective transmission of indispensable sensory signals to the motor system as dispensable signals are ignored. Sensorimotor gating defects are a fundamental feature in schizophrenia and ASD, leading to heightened perception of sensory information (McGhie and Chapman, 1961). A measure of SMG is prepulse inhibition (PPI) of the startle response. PPI is a form of SMG where the startle response is markedly attenuated when a weaker stimulus is presented immediately before the startling stimulus (Braff et al., 1995). PPI is diminished in individuals with a range of neuropsychiatric disorders including schizophrenia and bipolar disorder (Geyer, 2006; Perry et al., 2001). Neural circuits governing PPI are incompletely understood although dopamine agonists (e.g. apomorphine), NMDA antagonists (e.g. ketamine) and some antipsychotic compounds can rescue PPI defects in both schizophrenic patients and animal models (Schwabe and Krauss, 2018; Swerdlow et al., 2001). Many *Disc1* mutant mouse models have deficits in PPI (Clapcote et al., 2007; Kakuda et al., 2019; Shen et al., 2008); however, other groups using transgenic *Disc1* mice with ectopic promoters or missense mutations find wild type PPI responses (Dachtler et al., 2016; Hikida et al., 2007; Pletnikov et al., 2008). The presence of startle modulation and its similar pharmacological sensitivity to antipsychotics, make larval zebrafish a pertinent tool for studying neuropsychiatric disorders, however we decided not to assay PPI in zebrafish *disc1* mutants as results previous results indicated a lack of PPI phenotype (personal communication with Dr Summer Thyme, Harvard University). The experiments described in the following Chapter utilised two mutant strains *(disc1*^{Y472X} and *disc1*^{exon6}) at different developmental stages 11 dpf (auditory), 6 dpf (visual) and 2 mpf (novel environment) depending on the stimulus used.

5.2 Results

5.2.1 Startle responses to auditory stimuli in *disc1* mutant larvae

We first investigated responses of zebrafish *disc1* mutants to auditory stimuli administered during the night. We decided to assay the acoustic startle during the night from 1 AM to 6:20 AM (see section 2.22.4) in order to perform the analysis at the lowest state of arousal (during sleep). We optimised the testing age of larvae to reduce inter-individual variability of behaviour and selected at 11-13 dpf. Larvae were placed in individual wells of a 48-well plate and exposed to 8 varying intensities of auditory stimuli. We measured the percentage of fish that were responsive at each stimulus. Larvae were considered responsive if a displacement of >10 pixels in the 5 s following the auditory stimulus was detected. Of note, we decided to test progeny from heterozygote crosses first to avoid environmental contributions towards observed phenotypes. All larvae were raised together until the day of assay and larvae were genotyped *post hoc*. There were no differences in percentages of fish responding to auditory stimuli between *disc1*$^{Y472X/Y472X}$ homozygous mutants, *disc1*$^{Y472X/+}$ heterozygotes and *disc1*$^{+/+}$ homozygous wild type siblings during the night-time arousal (NTA) test (Fig. 5.1, Table 5.1).

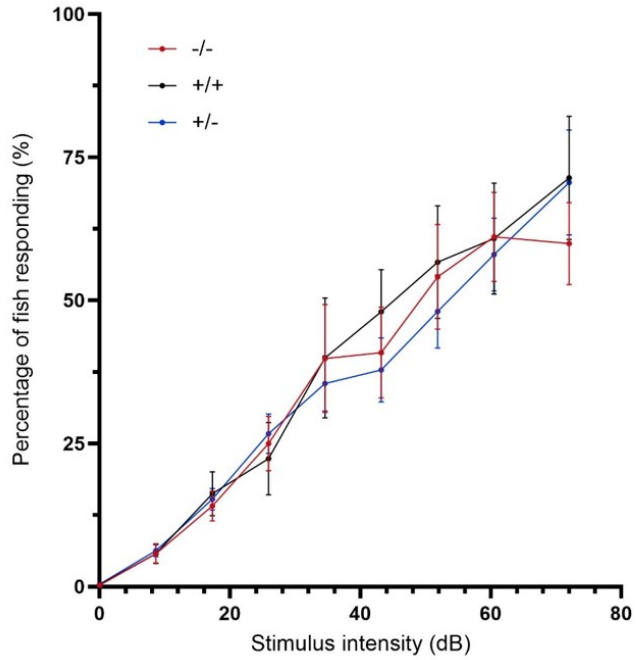

Figure 5.1. Responses of *disc1*^{Y472X} larvae during the night-time arousal test

Percentage of larvae responding to varying intensity of auditory stimuli. +/+, *disc1*$^{+/+}$ homozygous siblings; +/-, *disc1*$^{Y472X/+}$ heterozygotes; -/-, *disc1*$^{Y472X/Y472X}$ homozygous mutants. N=48 per clutch. Responses averaged over 6 hours and then over 2 nights, data pooled from 2 independent experiments. Bars indicate mean ± SEM. Data distribution passed the Shapiro-Wilk normality test. See Table 5.1 for statistical analysis.

Percentage of larvae, responsive to auditory stimuli				
Factor	**F value**	**d.f**	**P value**	**Sig.**
Genotype	1.209	2	0.308	n.s
Stimulus	82.203	7	< 0.0001	****
Genotype: Stimulus	0.897	14	0.563	n.s

Table 5.1. Statistical analysis of night-time arousal test in *disc1*^{Y472X} line
The results of a factorial ANOVA with repeated measures for time and genotype are shown. There is no significant effect of genotype on the percentage of larvae responding. There is a significant effect of stimulus on response. There is no significant interaction between genotype and stimulus. P > 0.05 = n.s, P < 0.0001 = ****. See Figure 5.1 for graphical representation of data.

We performed the NTA test in the other *disc1* line (Fig. 5.2). Overlapping error bars at low sound intensities (8 dB, 17 dB, 26 dB) and high sound intensities (52 dB, 60 dB, 72 dB) suggested there were no differences in auditory startle response between *disc1*$^{exon6/exon6}$ homozygous mutants, *disc1*$^{exon6/+}$ heterozygotes and *disc1*$^{+/+}$ homozygous wild type siblings. Non-overlapping error bars at medium intensities (35 dB, 43 dB) suggested there were differences in auditory startle between *disc1*$^{exon6/exon6}$ mutants and *disc1*$^{+/+}$ with a gene dosage effect for *disc1*$^{exon6/+}$. We performed a one-way ANOVA for each stimulus intensity and results showed a significant difference at intensity 35 dB ($F(3, 68) = 3.171$, $p = 0.030$) and 43 dB ($F(2, 69) = 2.703$, $p = 0.046$). This upwards shift of the -/- and +/- lines indicates an increased responsiveness of *disc1*$^{exon6/exon6}$ homozygous mutants and *disc1*$^{exon6/+}$ heterozygotes respectively. As expected, the results from a factorial ANOVA with repeated measures revealed there was a strong effect of stimulus and weak effect of genotype (Table 5.2). We hypothesise that there is the interaction between genotype and stimulus is not statistically significant because, at most stimuli (6 out of the 8), error bars overlap and there are no significant differences between *disc1*$^{exon6/exon6}$, *disc1*$^{exon6/+}$ and *disc1*$^{+/+}$.

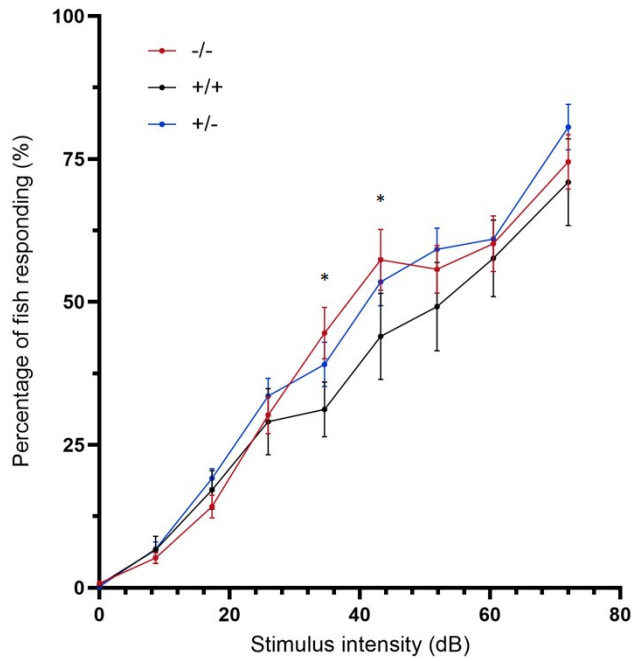

Figure 5.2. Responses of *disc1*^{exon6} larvae during the night-time arousal test

Percentage of larvae responding to varying intensity of auditory stimuli. +/+, *disc1*$^{+/+}$ homozygous siblings; +/-, *disc1*$^{exon6/+}$ heterozygotes; -/-, *disc1*$^{exon6/exon6}$ homozygous mutants. N=48. Responses averaged over 6 hours and then over 2 nights, data pooled from 2 independent experiments. Bars indicate mean ± SEM. Data distribution passed the Shapiro-Wilk normality test. One-way ANOVA was performed at individual intensities. P < 0.05 = *. See Table 5.2 for statistics.

Percentage of larvae, responsive to auditory stimuli				
Factor	**F value**	**d.f**	**P value**	**Sig.**
Genotype	3.356	2	0.044	*
Stimulus	149.805	7	< 0.0001	****
Genotype*Stimulus	1.558	14	0.090	n.s

Table 5.2. Statistical analysis of night-time arousal test in *disc1*^{exon6} line

The results of a factorial ANOVA with repeated measures for time and genotype are shown. There is a nominally significant effect of genotype on the percentage of larvae responding. There is a significant effect of stimulus on response. There is no significant interaction between genotype and stimulus. P > 0.05 = n.s, P < 0.05 = *, P < 0.0001 = ****. See Figure 5.2 for plot.

After observing a weak effect of genotype in the *disc1*^{exon6} line and statistically significant differences at some stimulus intensities, we decided to perform the NTA test on *disc1*$^{exon6/exon6}$ MZ mutants. The possible gene dosage effect led us to hypothesise that *disc1*$^{exon6/exon6}$ MZ mutants, which lack maternal contribution of *disc1*, would have a more severe auditory startle phenotype. We performed the NTA test on *disc1*^{exon6} MZ mutants and compared them to *disc1*$^{+/+}$ controls (Fig. 5.3). There was a significant difference in percentages of larvae responding to auditory stimuli between *disc1*^{exon6} MZ (red line) and *disc1*$^{+/+}$ (black line) (Table 5.3). The upwards shift of the red line (*disc1*^{exon6} MZ) compared to the black line (*disc1*$^{+/+}$) indicates that *disc1*^{exon6} MZ mutants are hyper-responsive to auditory stimuli during the

night. We were unable to examine the *disc1*$^{Y472X/Y472X}$ maternal zygotes (*disc1*^{Y472X} MZ) due to time and breeding constraints (homozygous incrosses stopped yielding embryos).

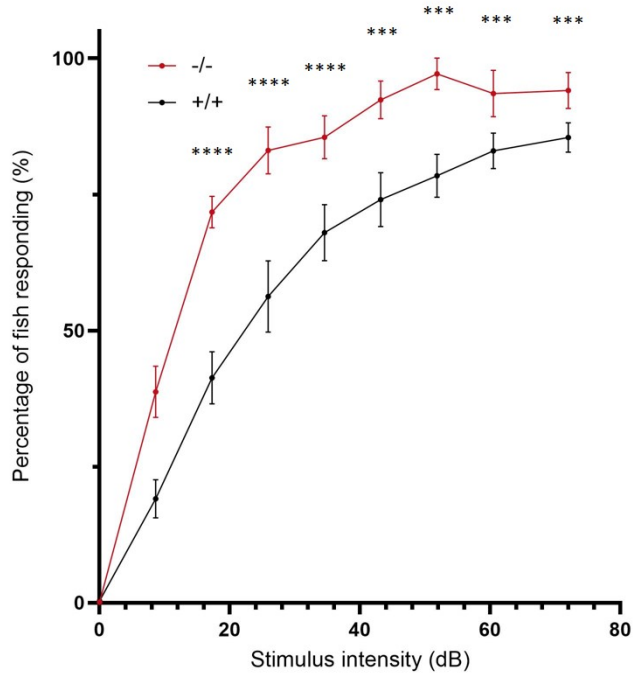

Figure 5.3. Responses of *disc1*^{exon6} maternal zygotes during the night-time arousal test

Percentage of larvae responding to varying intensity of auditory stimulus+/+, *disc1*$^{+/+}$ wild type in-cross larvae (non-sibling); -/-, *disc1*$^{exon6/exon6}$ homozygous mutant in-cross larvae. N=24. Responses averaged over 6 hours and then over 2 nights, data pooled from 2 independent experiments. Bars indicate mean ± SEM. Non-overlapping error bars at all intensities suggested there are differences in auditory startle between *disc1*^{exon6} maternal zygotic mutants and controls. Data distribution passed the Shapiro-Wilk normality test, unpaired Student t-test was performed at individual intensities. P < 0.001 = ***, P < 0.0001 = ****. See Table 5.3 for statistics.

Percentage of larvae, responsive to auditory stimuli				
Factor	**F value**	**d.f**	**P value**	**Sig.**
Genotype	401.556	1	< 0.0001	****
Stimulus	168.197	7	< 0.0001	****
Genotype*Stimulus	9.022	7	< 0.0001	****

Table 5.3. Statistical analysis of night-time arousal test in *disc1*^{exon6} maternal zygotes

The results of a factorial ANOVA with repeated measures for time and genotype are shown. There is a significant effect of genotype and stimulus on the percentage of larvae responding. There is a significant interaction between genotype and stimulus. P < 0.0001 = ****. See Figure 5.3 for plot.

5.2.2 Startle responses to visual stimuli in *disc1* mutant larvae

To investigate another modality of arousal, we turned to the visual system. We used highly reproducible patterns of activity induced by changes in illumination as a measure for LLR. These responses have been extensively studied in larval zebrafish. After a transition from light to dark, swimming activity spikes to a maximum, 15 min after the dark onset and then decreases to reach a

stable low level, 10 min after the peak. After a transition from dark to light, activity initially decreases (for the first 5 min), preceding a gradual increase to a stable high level, approximately 20 min after light onset (Burgess and Granato, 2007; MacPhail et al., 2009; Prober et al., 2006). Therefore, we used 6 alternating cycles of dark (40 min) and light (20 min).

We observed no differences in the decrease in activity during the transitions from dark to light between *disc1*^{Y472X} MZ mutants and disc1$^{+/+}$ sibling controls (Fig. 5.4B, point **a.**). The increase in activity during extended exposure to light appeared slower was delayed in *disc1*^{Y472X} MZ compared with disc1$^{+/+}$ (Fig. 5.4B, point **b.**). Locomotion during this period was lower in *disc1*^{Y472X} MZ compared to controls and this difference persisted after the dark flash (Fig. 5.4B, point **c.**). There was no difference between *disc1*^{Y472X} MZ and controls in the onset time (15 min after dark-flash) of the dark-induced increase in activity, however *disc1*^{Y472X} MZ exhibited consistently lower peaks in activity (Fig. 5.4B, point **d.**). There was no difference in the latency of the decline of activity during the extended period of darkness between the 2 groups (Fig. 5.4B, point **e.**). Interestingly, when activity returned to baseline in the dark (Fig. 5.4B, point **f.**), *disc1*^{Y472X} MZ mutants were more active as previously reported (Fig. 4.5A). The results of a factorial ANOVA show there is no significant effect of genotype and no significant interaction between genotype and either time or light on locomotor activity (Table 5.4). We averaged locomotor activity during the dark phases and light phases and compared *disc1*^{Y472X} MZ mutants and *disc1*$^{+/+}$. Over both dark and light phases, *disc1*^{Y472X} MZ mutants had a significantly lower swimming activity compared to *disc1*$^{+/+}$ (Fig. 5.4C, D), indicating *disc1*^{Y472X} MZ mutants are hyporesponsive to changes in illumination compared to *disc1*$^{+/+}$.

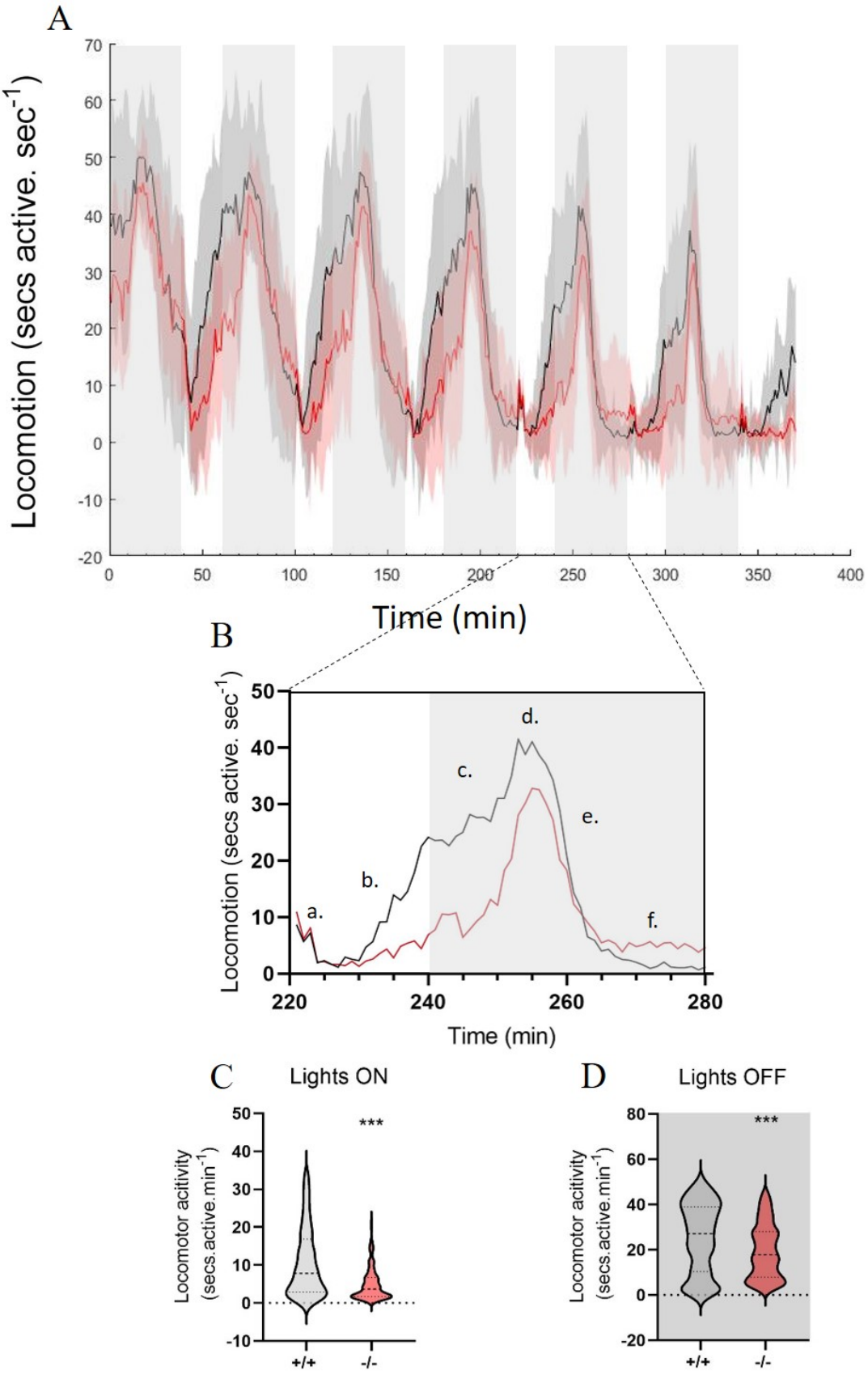
A
Locomotion (secs active. sec-1)
70
60
50
40
30
20
10
0
-10
-20
0
50
100
150
200
250
300
350
400
Time (min)
B
Locomotion (secs active. sec-1)
50
40
30
20
10
0
a.
b.
c.
d.
e.
f.
220
240
260
280
Time (min)
C
Lights ON
Locomotor acitivity (secs.active.min-1)
50
40
30
20
10
0
-10
***
+/+
-/-
D
Lights OFF
Locomotor acitivity (secs.active.min-1)
80
60
40
20
0
-20
***
+/+
-/-

Figure 5.4. Visual motor response of *disc1*^{Y472X} mutants in response to dark/ light flashes

(A) Activity traces over 6 hours. +/+, homozygous wild type control; -/-, *disc1*^{Y472X} maternal zygotic mutant. N=24, data pooled from 2 independent experiments. Lines and shaded areas represent means ± SD White and grey boxes indicate lights ON and lights OFF, respectively.

(B) Activity traces over 1 hour, representative of mean activity. Zoom in from 220 to 280 min of recording with a., b., c., d., e., f. corresponding to defined changes in locomotor activity

(C) Box and violin plots of locomotor activity during light transitions day (white box). Dashed lines indicate median (middle), first (lower) and third (higher) quartile. Data did not pass the Shapiro-Wilks test. Mann-Whitney test was significant, P<0.001 = ***. Box and violin plots of locomotor activity during dark transitions day (grey box). Dashed lines indicate median (middle), first (lower) and third (higher) quartile. Data did not pass the Shapiro-Wilks test. Mann-Whitney test was significant, P<0.001 = ***.

(D) Box and violin plots of locomotor activity during dark transitions day (grey box). Dashed lines indicate median (middle), first (lower) and third (higher) quartile. Data did not pass the Shapiro-Wilks test. Mann-Whitney test was significant, P<0.001 = ***.

Locomotion in response to dark/ light flashes				
Factor	**F value**	**d.f**	**P value**	**Sig.**
Genotype	0.378	1	0.545	n.s
Time	123.615	5	< 0.0001	****
Light	102.360	1	< 0.0001	****
Genotype: Time	0.705	5	0.621	n.s
Genotype: Light	0.001	1	0.616	n.s

Table 5.4. Statistical analysis of dark/ light flash test in *disc1*^{Y472X} line

The results of a three-way factorial ANOVA with repeated measures for time, genotype and light are shown. There is a significant effect of time and light on locomotion in larvae. There are no significant interactions between genotype and time or genotype and light. P > 0.05 = n.s, P < 0.0001 = ****. See Figure 5.4 for plot of data.

Similar to *disc1*^{Y472X} MZ, we observed no differences in the decrease in activity during transitions from dark to light between *disc1*^{exon6} MZ and controls (Fig. 5.5B, point **a.**). The increase in activity to extended exposure to light was heightened in *disc1*^{exon6} MZ compared with controls (Fig. 5.5B, point **b.**). This upregulation persisted during the rapid increase in activity after the transition from light to dark (Fig. 5.5B, point **c.**). There was no difference in onset time or peak of activity between *disc1*^{exon6} MZ and controls (Fig. 5.5B, point **d.**). We observed a rightwards shift in the response of *disc1*^{exon6} MZ (red line) over the decline of activity during the extended period of darkness (Fig. 5.5B, point **e.**). Baseline activity in the dark was similar between *disc1*^{exon6} MZ and controls (Fig. 5.5B, point **f.**) as previously reported (Fig. 4.6A). The results of a factorial ANOVA show there is a significant effect of

genotype and a significant interaction between genotype and time (Table 5.5). We averaged locomotor activity during the dark phases and light phases and compared *disc1*^{exon6} MZ mutants and *disc1*$^{+/+}$. Over both dark and light phases, *disc1*^{exon6} MZ mutants had a significantly increased swimming activity compared to *disc1*$^{+/+}$ (Fig. 5.5C, D), indicating that, as opposed to *disc1*^{Y472X}, *disc1*^{exon6} MZ mutants are hyperresponsive to changes in illumination compared to *disc1*$^{+/+}$.

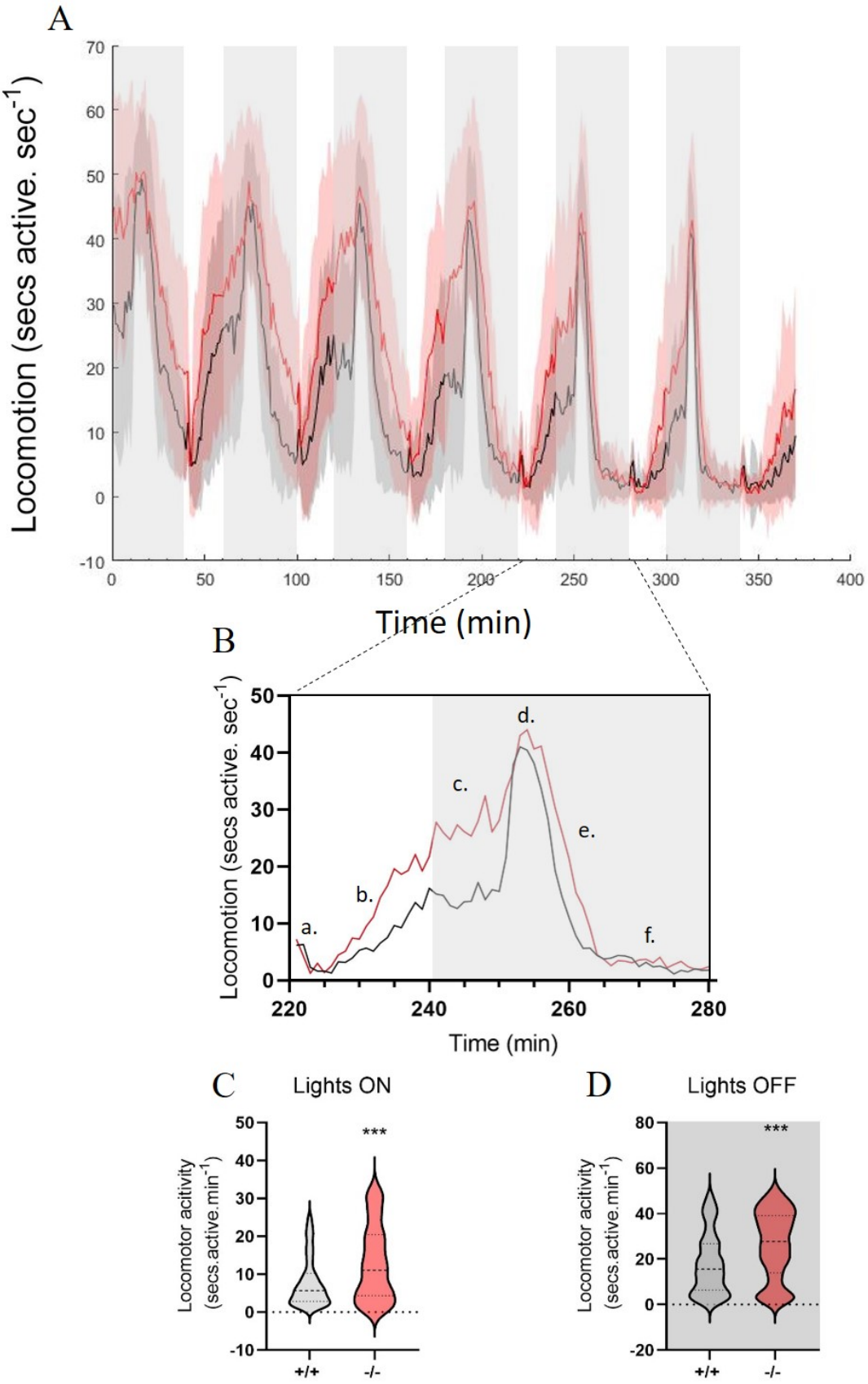
A
Locomotion (secs active. sec-1)
Time (min)
B
Locomotion (secs active. sec-1)
Time (min)
a.
b.
c.
d.
e.
f.
C
Lights ON
Locomotor acitivity (secs.active.min-1)
***
+/+
-/-
D
Lights OFF
Locomotor acitivity (secs.active.min-1)
***
+/+
-/-

Figure 5.5. Visual motor response of *disc1*^{exon6} mutants in response to dark/ light flashes

(A) Activity traces over 6 hours. +/+, homozygous wild type control; -/-, disc1exon6 maternal zygotic mutant. N=24, data pooled from 2 independent experiments. Lines and shaded areas represent means ± SD. White and grey boxes indicate lights ON and lights OFF, respectively.

(B) Activity traces over 1 hour, representative of mean activity. Zoom in from 220 to 280 min of recording with a., b., c., d., e., f. corresponding to defined changes in locomotor activity.

(C) Box and violin plots of locomotor activity during light transitions day (white box). Dashed lines indicate median (middle), first (lower) and third (higher) quartile. Data did not pass the Shapiro-Wilks test. Mann-Whitney test was significant, P<0.001 = ***.

(D) Box and violin plots of locomotor activity during dark transitions day (grey box). Dashed lines indicate median (middle), first (lower) and third (higher) quartile. Data did not pass the Shapiro-Wilks test. Mann-Whitney test was significant, P<0.001 = ***.

Locomotion in response to dark/ light flashes				
Factor	**F value**	**d.f**	**P value**	**Sig.**
Genotype	9.759	1	0.005	**
Time	140.03	5	< 0.0001	****
Light	49.516	1	< 0.0001	****
Genotype: Time	2.837	5	0.019	*
Genotype: Light	0.259	1	0.616	n.s

Table 5.5. Statistical analysis of dark/ light flash test in *disc1*^{exon6} line

The results of a three-way factorial ANOVA with repeated measures for time, genotype and light are shown. There is a significant effect of genotype, time and light on locomotion in larvae. There is a significant interaction between genotype and time but not between genotype and light. P < 0.05 = *, P < 0.01 = **, P < 0.0001 = ****. See Figure 5.5 for plot of data.

5.2.3 Novel tank diving in *disc1* adult zebrafish

Following, characterisation of stimulus-evoked behaviours in larval zebrafish, we moved onto investigate behavioural parameters in the adults. We performed the novel tank diving (NTD) test, an extensively used assay to measure novelty stress/innate fear in adult zebrafish (Bencan et al., 2009; Grossman et al., 2010; Mathuru et al., 2012). When placed in a novel environment, adult zebrafish show a place preference for the bottom third of the tank, particularly in the first 2 min of the assay. After the first 2 min, zebrafish enter the top two thirds of the tank and gradually display more exploratory swimming behaviour. After 8 to 10 min adult zebrafish become fully acclimated to their environment. NTD was previously performed on the *disc1*$^{Y472X/Y472X}$ mutants on a small scale (N= 10

per group) (H. Eachus PhD thesis, University of Sheffield, 2015); however, the results obtained with controls did not show the characteristic decline in percentage of time spent in the bottom third over time (acclimation) and it was concluded that no significant differences emerged between *disc1*$^{Y472X/Y472X}$ homozygous mutants, *disc1*$^{Y472X/+}$ heterozygotes and *disc1*$^{+/+}$ siblings.

We decided to repeat the NTD assay using the behavioural rig at IMCB, Singapore (custom-made by Dr R. Cheng and Dr A. Mathuru), with larger sample sizes (N ≥ 24 per group) on both *disc1*^{Y472X} and *disc1*^{exon6} lines. We observed acclimation after 6 min, as previously reported in wild type adults (Egan et al., 2009; Levin, 2011). In the *disc1*^{Y472X} line, there was a significant effect of time on the percentage of time spent in the bottom third (Fig. 5.6, Table 5.6) due to the shift in place preference. There was no significant effect of genotype and lines mapping place preference of *disc1*$^{Y472X/Y472X}$ (red), *disc1*$^{Y472X/+}$ (blue) and *disc1*$^{+/+}$ (black) overlapped. Of note, there was a small yet significant interaction between time and genotype and we hypothesise that this is due to downwards shift of *disc1*$^{Y472X/+}$ group in the first 3 min of recording, as error bars do not overlap.

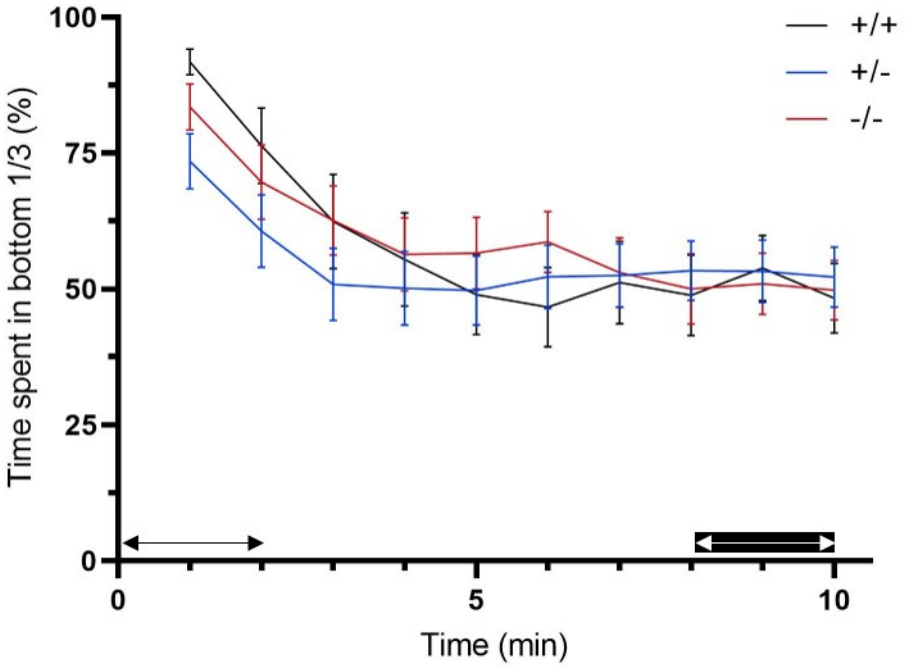

Figure 5.6. Bottom Dwell behaviour in response to NTD test in *disc1^{Y472X}* line

Percentage of time spent in the bottom third of the tank over time. +/+, *disc1$^{+/+}$* homozygous siblings; +/-, *disc1$^{Y472X/+}$* heterozygotes; -/-, *disc1$^{Y472X/Y472X}$* homozygous mutants. . $N_{+/+}$= 26, $N_{+/-}$= 24 and $N_{-/-}$= 25. Bars indicate mean ± SEM. Black arrows indicate data from the first 2 min of recording and white arrows indicate data from the last 2 min of recording. Overlapping error bars suggest there are no differences in NTD test between +/+, +/- and -/-. Data distribution passed the Shapiro-Wilk normality test. See Table 5.6 for statistical analysis.

Factorial ANOVA, repeated measures (*disc1^{Y472X}*)				
Factor	**F value**	**d.f**	**P value**	**Sig.**
Genotype	2.236	2	0.118	n.s
Time	20.258	3.484	< 0.0001	****
Time: Genotype	2.412	8.509	0.014	*

Table 5.6. Statistical analysis of NTD in *disc1^{Y472X}* line

The results of a factorial ANOVA with repeated measures for time and genotype are shown. There is no significant effect of genotype and a significant effect of time spent in bottom third. There is a significant interaction between genotype and time. P > 0.05 = n.s, P < 0.05 = *, P < 0.0001 = ****. See Figure 5.6 for plot of data.

We repeated the same assay in the *disc1^{exon6}* line and observed a significant effect of time and genotype on the percentage of time spent in the bottom third (Fig. 5.7, Table 5.7). Interestingly, *disc1$^{exon6/exon6}$* mutants (red line) spent significantly less time in the bottom third, throughout the 10 min of recording, particularly in the first 4 min of the assay compared to *disc1$^{exon6/+}$* heterozygotes and *disc1$^{+/+}$* controls (Fig. 5.7) suggesting more "explorative" swimming behaviour and an impaired response to a novel environment.

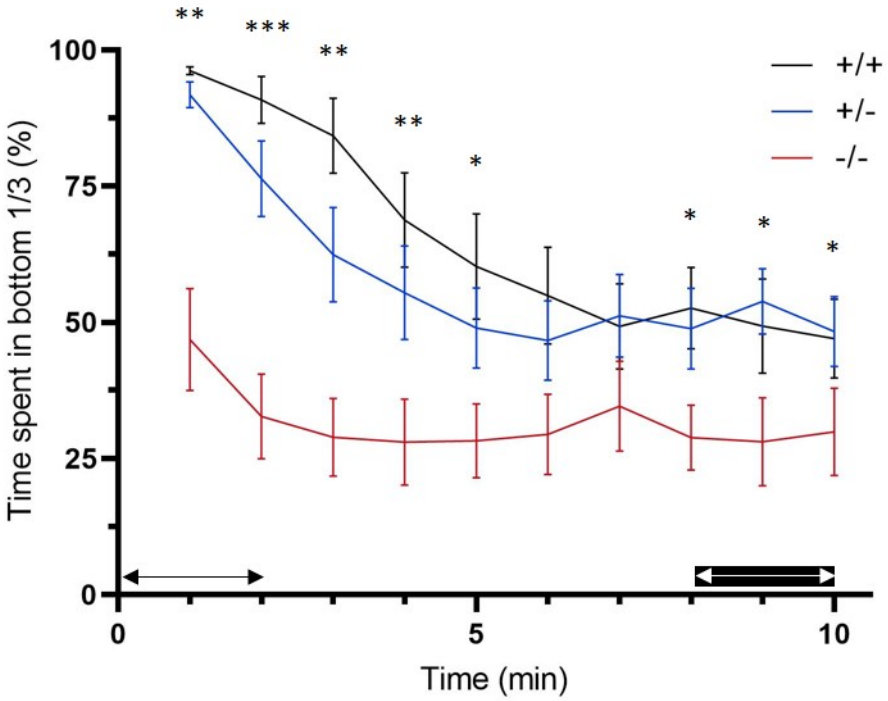

Figure 5.7. Bottom Dwell behaviour in response to NTD test in *disc1*^{exon6} line

Percentage of time spent in the bottom third of the tank over time. +/+, *disc1*$^{+/+}$ homozygous siblings; +/-, *disc1*$^{exon6/+}$ heterozygotes; -/-, *disc1*$^{exon6/exon6}$ homozygous mutants. Bottom dwell behaviour over a 10 min recording. $N_{+/+}$= 26, $N_{+/-}$= 30 and $N_{-/-}$= 29. Bars indicate mean ± SEM. Black arrows indicate data from the first 2 min of recording and white arrows indicate data from the last 2 min of recording. Non-overlapping error bars suggests there are differences in NTD test between +/+, +/- and -/-. Data distribution passed the Shapiro-Wilk normality test. One-way ANOVA was used to compare individual means are each timepoint. P < 0.05 = *, P < 0.01 = **, P < 0.001 = ***. See Table 5.7 for statistical analysis.

Factorial ANOVA, repeated measures (*disc1*^{exon6})				
Factor	**F value**	**d.f**	**P value**	**Sig.**
Genotype	11.882	2	< 0.0001	****
Time	19.782	5.226	< 0.0001	****
Time: Genotype	3.015	10.073	0.001	**

Table 5.7. Statistical analysis of NTD in *disc1*^{exon6} line

The results of a factorial ANOVA with repeated measures for time and genotype are shown. There is a significant effect of genotype and a significant effect on time spent in the bottom third. There is a significant interaction between genotype and time. P < 0.01 = **, P < 0.0001 = ****. See Figure 5.7 for plot.

To determine if the effect described above was due to differences in baseline swimming, we measured total distance and average velocity of swimming during 10 min of recording in both lines. There were no significant differences between *disc1*$^{Y47X2/Y472X}$ mutants and *disc1*$^{+/+}$ controls in total distance (Fig. 5.8A) or in average velocity (Fig. 5.8C). Similarly, there were no significant differences between *disc1*$^{exon6/exon6}$ mutants and *disc1*$^{+/+}$ controls in total distance (Fig. 5.8B) or in average velocity (Fig. 5.8D). These results indicate that adult *disc1* mutants have a wild type-like baseline locomotor activity under LED lighting. Of note, it appeared that *disc1*^{exon6} fish raised on an AB background swam longer distances than the *disc1*^{Y472X} line raised on the TL background. We ensured measures and respective controls were always compared within lines to exclude any possible contribution of interstrain differences.

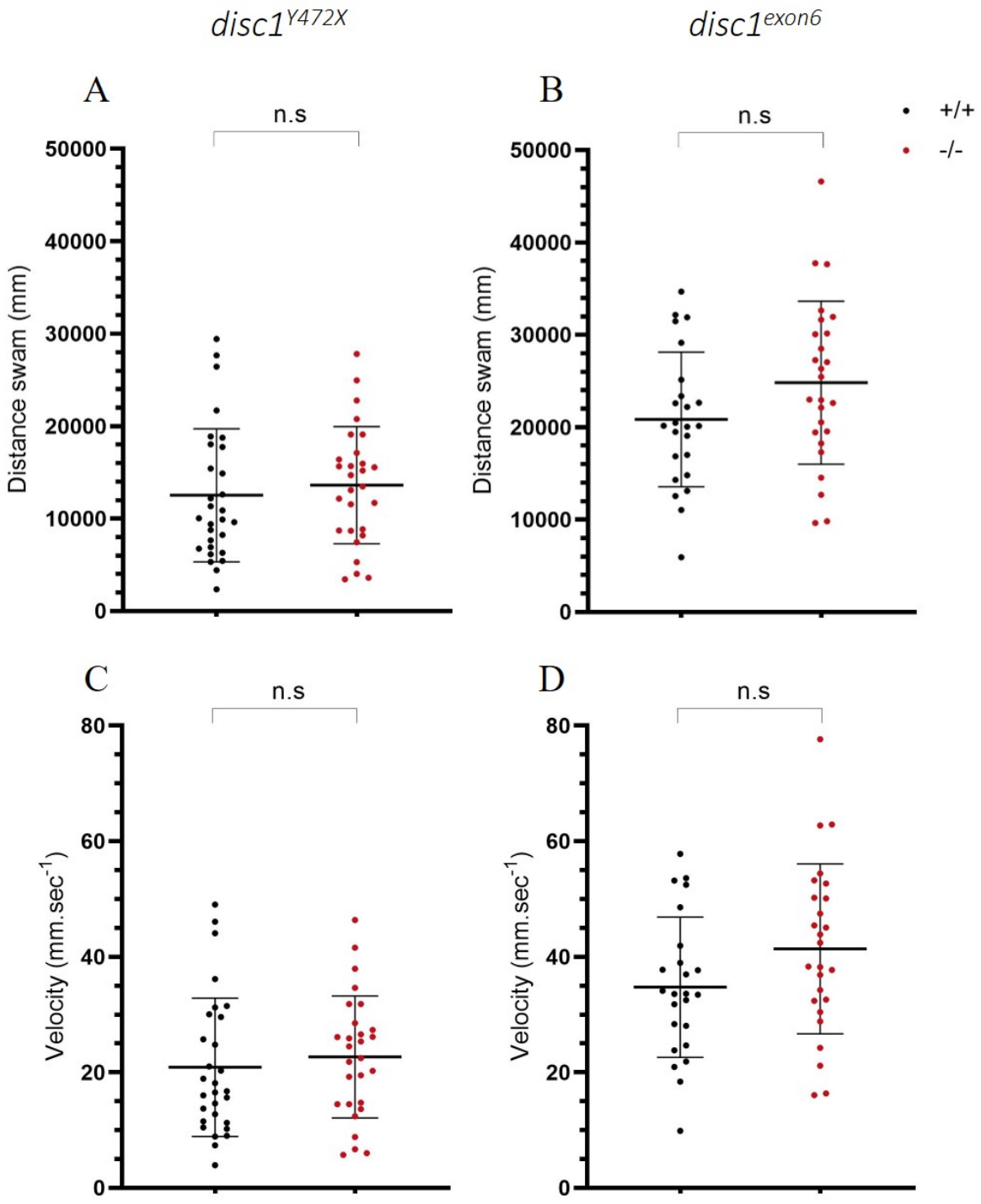

Figure 5.8. Swimming behaviour in adult *disc1* zebrafish

Baseline swimming behaviour. +/+, *disc1*$^{+/+}$ controls; -/-, *disc1*$^{-/-}$ homozygous mutants. (A) and (C), *disc1*^{Y472X}, $N_{+/+}$= 24 and $N_{-/-}$= 25. (B) and (D), *disc1*^{exon6}, $N_{+/+}$= 30 and $N_{-/-}$= 29. Bars indicate mean ± SD. (A) and (B) indicate total distance covered during 10 min of recording. (C) and (D) indicate average velocity during 10 min of recording. Data points followed a normal distribution. Individual groups were compared with unpaired t-test, p value > 0.05 (n.s).

We next sought to investigate place preference in response to NTD in the first 2 min (stressed) and last 2 min (acclimated) of recording. Following exposure to a novel environment, adult zebrafish show a clear preference for the bottom third of the tank (bottom dwelling) and periphery/ walls of the tank (thigmotaxis) (see section 5.1.2). There was no significant difference in bottom dwell behaviour between *disc1*$^{Y472X/Y472X}$ mutants compared to *disc1*$^{+/+}$ controls in the first 2 min (black arrow) and last 2 min (white arrow) of recording (Fig. 5.9A, Table 9.1, Appendix). *disc1*$^{exon6/exon6}$ mutants spent significantly less time in the bottom third in the first 2 and in the last 2 min of recording compared to *disc1*$^{+/+}$ controls (Fig. 5.9B, Table 9.2, Appendix). Both *disc1*^{Y472X} and *disc1*^{exon6} lines spent significantly less time in the bottom third in the last 2 min compared to the first 2 min of recording, as expected after a period of acclimation. Thigmotaxis was measured by defining adult zebrafish swimming in the periphery as "wall-hugging" (see section 2.25; Fig. 2.3). There was no significant difference in thigmotaxis between *disc1*$^{Y472X/Y472X}$ mutants and *disc1*$^{+/+}$ controls in either the first 2 or the last 2 min of recording (Fig. 5.9C, Table 9.3, Appendix). In the other line, during the first 2 min, *disc1*$^{exon6/exon6}$ mutants spent significantly less time near the wall compared to *disc1*$^{+/+}$ controls. There was no significant difference between *disc1*$^{exon6/exon6}$ mutants and *disc1*$^{+/+}$ controls during the last 2 min of recording (Fig. 5.9D, Table 9.4, Appendix). There were significant differences between the first 2 min and the last 2 min of recording in the *disc1*$^{+/+}$ controls but not *disc1*$^{exon6/exon6}$ mutants. These results suggest that adult *disc1*$^{exon6/exon6}$ mutants do not display a thigmotaxic response or bottom dwell behaviour upon exposure to a novel environment.

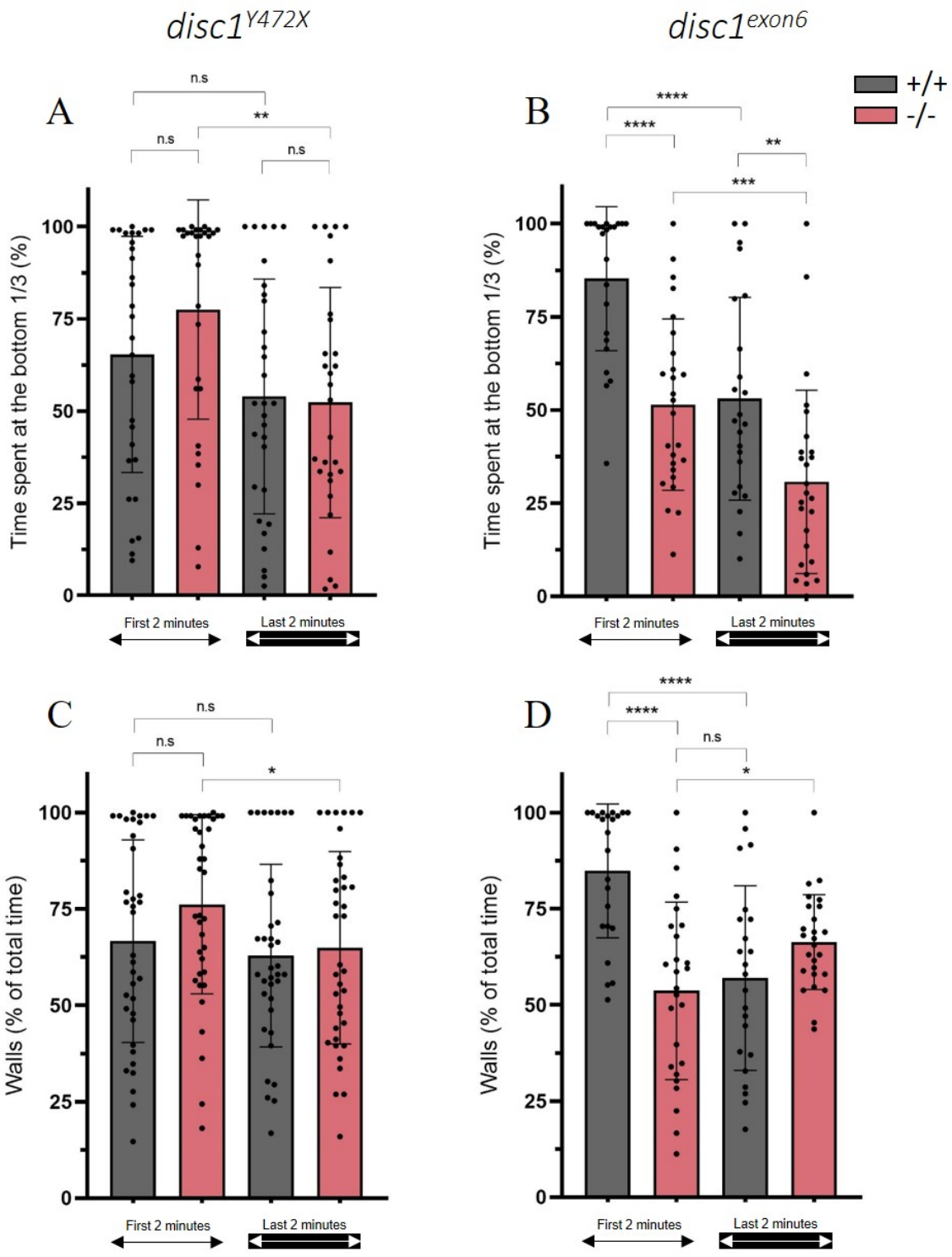

Figure 5.9. Place preference in response to NTD in adult *disc1* zebrafish

+/+, *disc1*$^{+/+}$ controls; -/-, *disc1*$^{-/-}$ homozygous mutants. (A) and (C), *disc1*^{Y472X}, $N_{+/+}$= 24 and $N_{-/-}$= 25. (B) and (D), *disc1*^{exon6}, $N_{+/+}$= 30 and $N_{-/-}$= 29. Bars indicate mean ± SD. Black arrows indicate data from the first 2 min of recording and white arrows indicate data from the last 2 min of recording. (A) and (B) indicate percentage of time spent in the bottom third of the tank (bottom dwell). (C) and (D) indicate percentage of time spent near the walls (thigmotaxis). Data points do not follow a normal distribution, two-way ANOVA with pairwise comparisons was performed. P value > 0.05 (n.s), p value < 0.01 (**), p value < 0.001 (***), p value < 0.0001 (****). See table 9.1 & 9.2 (Appendix) for statistical analysis.

Other behavioural indications of anxiety in zebrafish include erratic swimming episodes (darting) alternating with periods of inactivity (freezing). There was no significant difference in number of darting episodes between *disc1*$^{Y7472X/Y472X}$ mutants and *disc1*$^{+/+}$ controls in either the first 2 min or last 2 min of recording (Fig. 5.10A). There is a significant difference between the first 2 min and last 2 min in both *disc1*$^{Y7472X/Y472X}$ mutants and *disc1*$^{+/+}$ controls, showing time but not genotype has an effect on darting (Table 9.5, Appendix). Similarly, there was no significant difference between *disc1*$^{exon6/exon6}$ mutants and *disc1*$^{+/+}$ controls in either the first 2 min or last 2 min of recording (Fig. 5.10B). There was a significant difference between the first 2 min and last 2 min in both *disc1*$^{exon6/exon6}$ mutants and *disc1*$^{+/+}$ controls, again, showing time but not genotype has a significant effect on darting (Table 9.6, Appendix).

Next, we quantified freezing episodes in adult zebrafish. There was no significant difference between *disc1*$^{Y7472X/Y472X}$ mutants and *disc1*$^{+/+}$ controls in either the first 2 min or last 2 min of recording (Fig. 5.10C, Table 9.7, Appendix). Similar to darting, we observed a decrease in freezing, as zebrafish became acclimated, even though this was not statistically significant in *disc1*$^{+/+}$ controls. Importantly, *disc1*$^{exon6/exon6}$ mutants froze significantly less during the first 2 min of recording compared to *disc1*$^{+/+}$ controls (Fig. 5.10D, Table 9.8, Appendix). There was no difference in number of freezing episodes during the last 2 min of recording between *disc1*$^{exon6/exon6}$ mutants and *disc1*$^{+/+}$ controls. These results suggest that freezing episodes but not darting episodes are decreased in *disc1*$^{exon6/exon6}$ mutants upon exposure to a novel environment and support the hypothesis of an abnormal swimming response to stress.

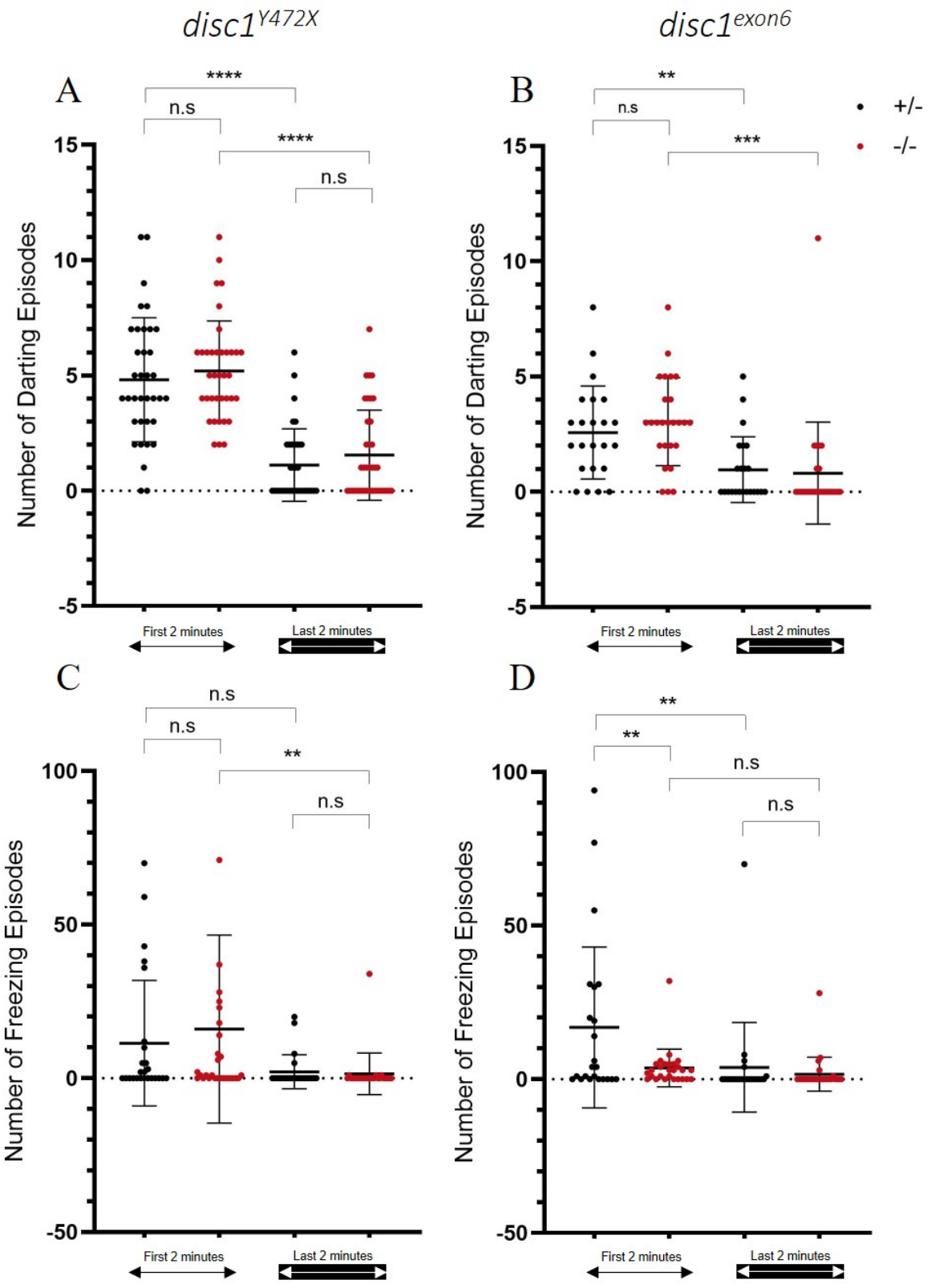
disc1Y472X
disc1exon6
A
B
C
D
+/-
-/-
Number of Darting Episodes
Number of Freezing Episodes
First 2 minutes
Last 2 minutes
n.s
****
**
***

Figure 5.10. Darting and freezing episodes in adult *disc1* zebrafish
+/+, *disc1*$^{+/+}$ controls; -/-, *disc1*$^{-/-}$ homozygous mutants. (A) and (C), *disc1*^{Y472X}, $N_{+/+}$= 24 and $N_{-/-}$= 25. (B) and (D), *disc1*^{exon6}, $N_{+/}$= 30 and $N_{-/-}$= 29. Bars indicate mean ± SD. Black arrows indicate data from the first 2 min of recording and white arrows indicate data from the last 2 min of recording. (A) and (B) indicate the number of erratic swim episodes (darting). (C) and (D) indicate the number of inactivity episodes (freezing). Data points do not follow a normal distribution, a two-way ANOVA with pairwise comparisons was performed. P value > 0.05 (n.s), p value < 0.01 (**), p value < 0.001 (***), p value < 0.0001 (****). See Table 9.5-9.8 (Appendix) for statistics.

5.3 Discussion

5.3.1 Analysis of auditory startle response

We used a quantitative behavioural assay for salient acoustic stimuli to induce startle responses in zebrafish larvae (designed by Dr R. Cheng). Because we previously observed changes in homeostatic locomotor activity during the night in *disc1* mutants (Fig. 4. 5A, Fig 4.6A), we corrected acoustic responsiveness for background differences in locomotor activity (see section 2.22.4). In the night-time arousal (NTA) test, we observed no differences in the percentage of larvae responding between *disc1*$^{Y472X/Y472X}$ mutants, *disc1*$^{Y472X/+}$ heterozygotes and *disc1*$^{+/+}$ siblings (Fig. 5.1). In *disc1*$^{exon6/exon6}$ mutants, we observed a subtle difference in the auditory startle responses, particularly prominent at medium intensities when compared to *disc1*$^{exon6/+}$ heterozygotes and *disc1*$^{+/+}$ siblings (Fig. 5.2). This auditory hypersensitivity becomes more evident when comparing *disc1*$^{exon6/exon6}$ maternal zygotic mutants to *disc1*$^{+/+}$ controls (Fig. 5.3). The upwards shift in response shows *disc1*$^{exon6/exon6}$ mutants have a decreased auditory arousal threshold (Fig. 5.3). Of note, it is of high importance to replicate this assay at least one more time to confirm the strength of this observation.

Importantly, because *disc1*$^{Y472X/Y472X}$ mutants were hyperactive at night (Fig. 4.5) but had wild type-like acoustic startle responses (Fig. 5.1), we can deduce that changes leading to this hypersensitisation are independent from changes in spontaneous arousal. Conversely, *disc1*$^{exon6/exon6}$ mutants which showed a no night-time hyperactivity (Fig. 4.6), are hyper-responsive to acoustic stimuli during the NTA test (Fig. 5.3). Moreover, the optimal (*disc1*^{Y472X}) and larger than optimal (*disc1*^{exon6}) responses to acoustic stimuli in the NTA test demonstrate that *disc1* mutants do have defects in their peripheral auditory system and that development of the mechanosensory hair cells is not disrupted. This is important because *disc1* is expressed in the developing ear (otic vesicle) at 24 hpf (Drerup et al., 2009).

In contrast to *disc1* zebrafish larvae, *Disc1* locus impairment (LI) adult mice, in which the majority of *Disc1* isoforms are supressed, exhibit a blunted startle reflex to high intensity sounds (Jaaro-Peled et al., PREPRINT). Neuronal firing in the dorsomedial striatum (DMS) was significantly decreased in response to acoustic stimuli in the *Disc1* LI mutants compared to wild type littermates. This discrepancy between the *disc1* zebrafish and the *Disc1* mouse phenotype could arise due to inherent divergences between zebrafish and mammalian brain architecture. Although many brain regions involved in the control of affective behaviours in zebrafish larvae show structural and functional homology to mammals (Kalueff et al., 2014), the teleost's CNS is more primitive (Cheng et al., 2014). For example, the true homologue of the mammalian amygdala has been mapped to the dorsomedial portion of the pallium (Maximino et al., 2013). The subpallium is homologous to the basal ganglia (Mueller et al., 2008), which includes the striatum. An area that is lacking in the teleost brain is the neocortex and therefore the corticostriatal circuits remain somewhat elusive in zebrafish. Despite the lack of this structure, lower vertebrates retain the ability of higher order processing with neuropeptidergic signalling playing a major role in these pathway (Jarvis et al., 2005).

In humans, hyperacusis, a form of auditory hypersensitivity, is highly prevalent in patients with anxiety, schizophrenia, autism spectrum disorders and other neurodevelopmental disorders (Cutting and Dunne, 1986; Dubal and Viaud-Delmon, 2008). This pronounced intolerance to ordinary environmental sound can lead to social withdrawal and isolation. It has been attributed to neural hyper excitability of central auditory processing. fMRI studies reveal that limbic structures (particularly the amygdala) show an over-activation in response to sound (Viaud-Delmon et al., 2011). Moreover, a prominent positive symptom often described in schizophrenic disorders is auditory hallucinations. Spontaneous activation of the auditory cortex and areas related to the acoustic processing of external cues underlies such phenomena (Hunter et al., 2006). It is challenging to assess such affective traits in lower vertebrates, although alterations in auditory perception and gating could offer clues of analogous dysfunction. Transgenic overexpression of the conserved neuropeptides *adcyap1* and *cgrp* causes an upwards shift in auditory responsiveness in zebrafish larvae (Woods et al., 2014) similar to results observed in *disc1*^{exon6} mutants (Fig. 5.3). In rodents too, infusion of Adcyap1 or Cgrp into the brain enhances acoustic startle responses and increases anxiety-like phenotypes (Hammack et al., 2009; Hashimoto et al., 2001; Kovacs et al., 1999; Sink et al., 2011), suggesting neural circuits are conserved throughout vertebrates and intimately linked to affective disorders.

5.3.2 Analysis of swimming modulation in response to changes in illumination

We used a well-established larval behavioural assay to investigate LLRs in *disc1* mutant larvae. When *disc1*^{Y472X} MZ and *disc1*^{exon6} MZ mutants were exposed to light, larvae downregulated their locomotion

accordingly, in a similar manner to respective controls (Fig. 5.4B, 5.5B, point **a.**). We observed differences between *disc1*^{Y472X} MZ and controls and between *disc1*^{exon6} MZ and controls in the visuomotor response to dark onset, however we can attribute these differences to locomotor differences preceding the onset of darkness (Fig. 5.4B, 5.5B, point **b.**). As previously reported in wild type larvae (Prober et al., 2006), our results suggest that if locomotion is lower immediately before dark onset, as in *disc1*^{Y472X} MZ (red line, Fig. 5.4B, point **b.**) or *disc1*^{exon6} MZ (black line, Fig. 5.5B, point **b.**), the arousal threshold to dark onset becomes increased (red line and black line, Fig. 5.4B, 5.5B, point **c.**). Ultimately, both *disc1*^{Y472X} MZ and *disc1*^{exon6} MZ mutants were able to up-regulate their locomotor activity in response to dark onset (Fig. 5.4B, 5.5B, point **c.**) indicating that there were no defects in the VMR of *disc1* mutant zebrafish. These results suggest that *disc1* mutants have functional retinal photoreceptors and can detect light (Liu et al., 2015). Our findings replicate previous behavioural light/dark assays performed on *disc1*^{Y472X} and *disc1*^{L115X} mutant lines (H. Eachus PhD thesis, University of Sheffield, 2015).

We extended our experimental design to measure the LLR to sustained light or dark. Previous tests aforementioned were performed with short periods of alternating light: dark (1: 4 min). Our tests used longer intervals (20: 40 min) on (see section 2.22.3) to measure the biphasic LLR in response to light (apparent after 5 min) and the biphasic LLR in response to dark (apparent after 15 min) (Gao et al., 2014; Prober et al., 2006). This assay revealed opposite effects of the different *disc1* alleles on swimming adaptation to sustained periods of light/dark. Consistent with auditory arousal results, *disc1*^{exon6} larvae were hyperresponsive to both light and dark changes (Fig. 5.5C, D). Interestingly, *disc1*^{Y472X} mutants were hyporesponsive to both light and dark changes (Fig. 5.4C, D). In *disc1*^{Y472X} MZ mutants, there was a delay and a milder upregulation of activity in response to sustained light (Fig. 5.4B, point **b.**). In contrast, *disc1*^{exon6} MZ mutants had the opposite phenotype, displaying hyperactive swimming in response to extended periods of light (Fig. 5.5B, point **b.**). This *disc1*^{exon6} MZ hyperarousal are consistent with findings from the NTA test (Fig. 5.3). In response to extended periods of darkness, *disc1*^{Y472X} MZ mutants exhibited a wild type-like downregulation of locomotion (Fig. 5.4B, point **e.**). In contrast, *disc1*^{exon6} MZ mutants showed a delay in response to extended periods of dark (Fig. 5.5B, point **e.**). These differences in swimming modulation, albeit in opposite directions highlight that arousal and long-term LLR are altered by loss of *disc1.*

These responses are mediated by both retinal and non-retinal photoreceptors. Long-term LLRs do not require the visual system and act via deep brain melanopsin-expressing photoreceptors. Despite their lack of eyes and VMR, *chokh* mutants retain long-term LLR in responses to dark onset. Non-retinal

opn4a^{+} photoreceptors located in the preoptic area (PO) of the hypothalamus, a structure homologous to the mammalian PVN, are instrumental in this "slow light-OFF" response (Fernandes et al., 2012). Furthermore, exposure to light after a period of dark acclimation, elevates whole body cortisol in larval zebrafish (De Marco et al., 2013). Interestingly, cortisol levels return to baseline after 20 min, which coincides, with the return to baseline of swimming activity in both light and dark paradigms. In addition, changes in illumination evoke bursting activity in the dopaminergic neurons of the caudal hypothalamus (cH) in larval zebrafish (Mu et al., 2012). By blocking the glucocorticoid system using genetic and pharmacologic interventions, Lee et al. (2019) showed that the function of HPI is required for LLRs in larval zebrafish. Yet, our group previously showed that HPI function in *disc1*^{Y472X} mutant zebrafish larvae is affected (Eachus et al., 2017). Therefore, we hypothesise that these differences in *disc1* LLRs could arise due to hypothalamic defects.

When comparing LLRs from the *disc1*^{Y472X} line (Fig. 5.4A) and from the *disc1*^{exon6} line (Fig. 5.5A), we identified striking differences in locomotor activity of *disc1*$^{+/+}$ control. Locomotion of *disc1*^{Y472X} controls in response to light increased much more rapidly (reaching 25 secs of activity/ min at 240 min) (Fig. 5.4B, point **b.**) than that of *disc1*^{exon6} controls (17 secs of activity/ min at 240 min) (Fig. 5.5B, point **b.**). Furthermore, locomotion of *disc1*^{exon6} controls, in the first 10 min after dark onset, remained constant (Fig. 5.5B, point **c.**), whereas locomotion of *disc1*^{Y472X} controls steadily increases (Fig. 5.4, point **c.** on inset panel). At first, results between *disc1*^{Y472X} and the *disc1*^{exon6} lines were so inverse, we considered we had mixed up genotyping results. However, after experimental repeats, this emerged as the true phenotype. Different wild type strains differ in their genetics and behaviours (Coe et al., 2009). Our results agree with previously identified interstrain differences in LLRs between ABs and TLs (Liu et al., 2015; van den Bos et al., 2017). ABs (which *disc1*^{exon6} were raised on) exhibit a lower activity in both light and dark as larvae compared to TLs (de Esch et al., 2012) (which *disc1*^{Y472X} were raised on). This difference could indirectly reflect differences in the baseline activity of the HPI. Recently, a study determined that TL larvae have a lower HPI axis activity and are more sensitive to anxiogenic stimuli compared to AB larvae (van den Bos et al., 2019). This could explain why we observed a steady increase in locomotion after dark onset in the *disc1*^{Y472X} line (TLs) (Fig. 5.4B, point **c.**) whereas the locomotion of *disc1*^{exon6} (AB) initially remains constant (Fig. 5.5B, point **c.**).

Overall, we see a gradual dissipation of the response over the repetitive cycles of dark: light in both lines of *disc1* mutants and controls (Fig. 5.4A, Fig. 5.5A). This represents habituation, an ancestral form of non-associative learning which reflects cognitive function and can easily be assessed in larval zebrafish (Best et al., 2008). Both *disc1*^{Y472X} MZ and *disc1*^{exon6} MZ mutants downregulate their innate

response to changes in illumination over time. Interestingly, we also observe habituation of the rightwards shift in the *disc1*^{exon6} MZ mutants' (red line) and mutants were able to downregulate their swimming activity at a comparable rate to *disc1*^{exon6} controls after 5 cycles (Fig. 5.5). This highlights that the loss of *disc1* does not affect the ability of zebrafish to habituate their response to change in illumination at larval stages.

5.3.3 Analysis of adult behavioural swimming

Distance travelled and average velocity was measured repeatedly between 1PM and 4PM in the day, to account for fluctuations in cortisol levels which can affect swimming behaviours (Schreck, 2010). Adults were assayed in isolation, to avoid any contribution from potential differences in social interaction associated with a loss of *disc1* (Tang et al., 2020). We observed no differences in baseline locomotion between *disc1* mutants and controls (Fig. 5.8), suggesting that differences in baseline locomotion identified in *disc1*$^{Y472X/Y472X}$ (Fig. 4.5A), become less pronounced as larvae mature into adults.

We decided to repeat the NTD assay in adult zebrafish even though this had previously been performed in Sheffield with the *disc1*^{Y472X} line. First, we wanted to recapitulate findings from *disc1*$^{Y472X/Y472X}$ (H. Eachus PhD thesis, University of Sheffield, 2015) on the behavioural apparatus in Singapore. Secondly, we wanted to characterise NTD behaviour in the *disc1*^{exon6} line. The validity of our NTD assay is demonstrated by the expected decrease of bottom dwell behaviour over time in the *disc1*$^{+/+}$ control line (Fig. 5.6). There were no differences in the response to NTD between *disc1*$^{Y472X/Y472X}$ mutants, *disc1*$^{Y472X/+}$ heterozygotes and *disc1*$^{+/+}$ controls (Fig. 5.6, 5.8A, 5.8C), as previously reported (H. Eachus PhD thesis, University of Sheffield, 2015). We did, however, observe differences when NTD was performed on the *disc1*^{exon6} line. There was a significant decrease in bottom dwell in *disc1*$^{exon6/exon6}$ mutants compared to *disc1*$^{exon6/+}$ heterozygotes and *disc1*$^{+/+}$ siblings (Fig. 5.7, 5.8B). There was also a loss of thigmotaxis in *disc1*$^{exon6/exon6}$ mutants upon exposure to a novel environment (Fig. 5.8D).

Freezing and darting were also assayed as measures of anxiety. Again, we observed no differences between *disc1*$^{Y472X/Y472X}$ mutants and *disc1*$^{+/+}$ controls (Fig. 5.9A, Fig. 5.9C). Although *disc1*$^{exon6/exon6}$ mutants froze significantly less than *disc1*$^{+/+}$ controls (Fig, 5.9D), they performed the same number of darting episodes (Fig. 5.9B). This adult behavioural study reinforces the notion that *disc1*$^{exon6/exon6}$ mutants have loss of innate fear in the NTD test. In the initial 2 min after exposure to a novel environment, they spent less time in the bottom third, more time in the centre of the tank and froze less. We did not detect any abnormal responses to stress in the *disc1*$^{Y7472X/Y472X}$ mutants, perhaps because the stimulus (novel environment) was too mild. In our previous experimental design, the

alarm substance was used to elicit a stress response and *disc1*$^{Y7472X/Y472X}$ mutants were hyporesponsive (Eachus et al., 2017). Therefore, the direction of change is consistent between the two *disc1* lines even though the emergence of a quantifiable phenotype in the *disc1*^{Y472X} mutants may require a stronger stressful stimulus. Many groups have investigated various anxiety-related behaviours in *Disc1* mouse models. Female *Disc1*^{D453G} mice show elevated novelty-induced exploration (Dachtler et al., 2016). A *Disc1* BAC transgenic mouse model, expressing 2 copies of truncated *Disc1*, also showed a blunted response to stress freeze less than wild type littermates when presented with a tone or shock, and emit less vocal communication (squeaks) under stressful conditions (Shen et al., 2008).

Practical limitations of the zebrafish thigmotaxis assay were highlighted here and contention about whether this is an anxiety-related measure has emerged (Blaser et al., 2010; Grossman et al., 2010; Ziv et al., 2013). Interestingly, in the first 2 min of recording, the *disc1*^{Y7472X} line performs more darting episodes ($\bar{x}_{disc1}{}^{Y472X}$ =5) compared to the *disc1*^{exon6} line ($\bar{x}_{disc1}{}^{exon6}$ =2.8). Adult zebrafish measure around 3 cm in body length. This increased darting (requiring more space) could explain the reason why we report less "wall-hugging" behaviour in the *disc1*^{Y7472X} line (Fig. 5.8C) compared to *disc1*^{exon6} line (Fig. 5.8D) in the first 2 min of recording. To conclude, *disc1*$^{Y472X/Y472X}$ mutants have very subtle stimulus-evoked phenotypes at both larval and adult stages. On the other hand, *disc1*$^{exon6/exon6}$ mutants have much stronger stimulus-evoked phenotypes such as hypersensitivity to sound and long-term modulation to light flashes at larval stages. Adult *disc1*$^{exon6/exon6}$ mutants are also hyporesponsive to novelty-induced stress.

Chapter 6: Neuronal basis of *disc1* mutant phenotypes

6.1 Introduction

Neuropsychiatric disorders are diagnosed based on behavioural criteria scores and, as is the case in many neurological or neurodegenerative diseases, biomarkers remain elusive. Thanks to the advancement of non-invasive techniques, functional brain imaging provides a window into the brain activity of diagnosed patients. fMRI in both resting and task-related studies has uncovered widespread brain pathology in schizophrenia, bipolar disorder, and depression. Abnormal fMRI signals in the dorsolateral prefrontal cortex (DLPFC), anterior cingulate, basal ganglia, hippocampus, parahippocampal gyrus and amygdala are widely reported in schizophrenia and depression. The aberrant activity in these regions is observed in task-related experiments and has been correlated to sensory processing, motor regulation, working memory performance and fear processing (Fletcher et al., 2010; Hirjak et al., 2015; Schlosser, 2010). In the absence of task-oriented behaviour, the resting brain still exhibits spontaneous slow neuronal firing. Task-independent regions (more active at rest than during cognitive tasks) are referred to as the "default network" (DN) and include the medial prefrontal cortex, the precuneus, the lateral parietal cortex, and the anterior and posterior cingulate cortex (Raichle et al., 2001). The DN plays a role in self-referential thought and higher cognition (Buckner et al., 2008). In patients with schizophrenia and depression, a hyperactivation of the hippocampus at rest and an inability to suppress DN activity upon task-initiation has been reported (Guo et al., 2014; Schneider et al., 2017; Whitfield-Gabrieli et al., 2008) and could contribute to the core cognitive symptoms of such neuropsychiatric disorders (Hill et al., 2004; Liu et al., 2006a).

In zebrafish, live brain imaging capitalises on their transparency and genetic manipulability. As aforementioned (see section 1.1.4), neuroanatomical regions are highly conserved. Genetically encoded calcium indicators (GECIs) such as GCaMP, enable the visualisation of calcium influx into cells upon neuronal depolarisation (Muto et al., 2011). A drawback of calcium imaging in zebrafish, is that the head must be immobilised to restrict its movement and therefore larvae cannot behave freely. Another method uses the endogenous expression IEGs to detect neuronal activity in fixed samples. The expression of *Fos* and *Arc* increases in active neurons and is widely used in mammals to identify key nuclei involved in certain behaviours. However, such markers exhibit slow transcriptional time courses (Okuyama et al., 2011) and *c-fos* and *arc* are expressed with a low baseline in the teleost brain (Baraban et al., 2005), making them inadequate for zebrafish research. Recently, extracellular signal-regulated kinase (ERK) and more particularly its phosphorylation upon calcium influx into cells, has been successfully used to localise active neurons in zebrafish larvae (Hussain et al., 2013; Randlett et al., 2015; Thyme et al., 2019; Wee et al., 2019b). This procedure uses whole brain imaging and

mapping to specific nuclei is made possible by the creation and annotation of larval brain atlases (Randlett et al., 2015).

In neuropsychiatric disease modelling, whole brain imaging provides a non-bias approach, eliminating the possibility of *a priori* assumptions about known dysfunctional circuitry. A study investigating the effect of schizophrenia-associated genes on whole brain activity was published during the course of my project. One hundred and thirty-two CRISPR-generated mutants harbouring mutations in GWAS-identified genetic risk factors were characterised (Thyme et al., 2019). Over half of the mutants had substantial brain activity differences at baseline. As previously discussed, *DISC1* was not identified in the most recent schizophrenia GWAS cohort (Ripke et al., 2014), despite its clear link to the disease, and therefore *disc1* was not part of the mutated genes. Both increased and decreased activity differences emerged in common regions across different mutants. Overlapping signals were mostly reported in the tectum, pallium, hypothalamus, and olfactory bulb. Mutants for *tcf4*$^{-/-}$, a transcription factor involved in neurodevelopment and associated with neuropsychiatric disorders had simultaneous decreases in activity in hypothalamic neurons and the retinal arborisation field 7 (AF7), both regions known to specifically activate upon prey hunting (Muto et al., 2017; Semmelhack et al., 2014). Based on the role of *disc1* in neurodevelopment, differences observed in hypothalamic cell markers at 5 dpf and decreases in food intake and hunting behaviour in *disc1* mutant larvae, we hypothesised to also observe activity differences in hypothalamic regions and AF7, among other regions.

6.2 Results

6.2.1 Brain activity mapping

To investigate brain activity in zebrafish larvae, we performed immunofluorescence at 7 dpf using antibodies against total Erk1/2 (tERK) (background staining) and phosphorylated Erk1/2 (pERK) to label active neurons. Western blot analysis show pERK1/2 antibodies detect only a single protein of 44 kDa in zebrafish larvae (Ng et al., 2012). To determine staining validity, we first imaged wild type larvae (Fig. 6.1). We imaged Z=137 stacks (dorsal to ventral) and performed stitching to capture whole brain views (Fig. 6.1A). tERK expression was homogenous, labelling all anatomical regions of the larval brain. In contrast, pERK expression was not pan-neuronal and mostly found in the telencephalon (Fig. 6.1, white box) as well as in periventricular cells (Fig. 6.1, white asterisk). Spontaneous activity of these neurons has previously been reported and our staining reproduced published results (Randlett et al., 2015). A higher magnification of a single slice (Z=1) of the telencephalon (Fig. 6.1, white box) shows that tERK is

concentrated around the cell membrane whilst pERK is expressed in the cytosol (Fig. 6.1B). These differences in subcellular localisation of active vs. inactive Erk1/2 are consistent with previous findings (Harding et al., 2005). Initial results, therefore, indicate epitope specificity of Erk1/2 and pErk1/2 antibodies in zebrafish larvae and strong enough cellular resolution for whole brain activity mapping of individual neurons.

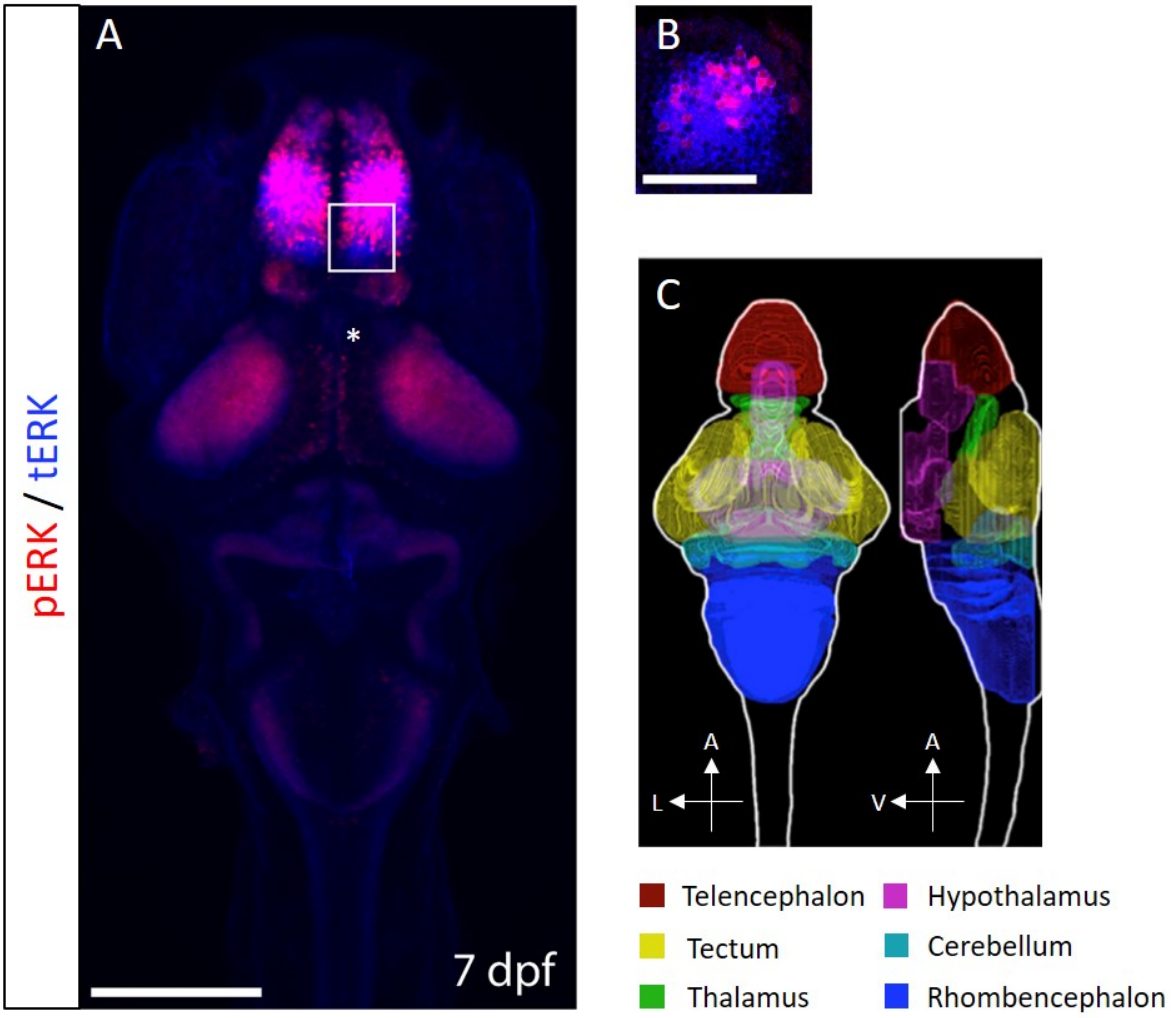

Figure 6.1. Immunofluorescence in wild type 7 dpf zebrafish larvae using pERK and tERK

(A) Wholemount dorsal view of Z-projection (Z=137). tERK staining (in blue) is pan-neuronal and pERK staining (in red) localises mainly to the telencephalon (white box) and periventricular mesencephalic cells (white asterisk). Scale bar indicates 200 µm

(B) Higher magnification of the telencephalon (Z=1). tERK staining (in blue) localises close to the cell-membrane, pERK staining (in red) is cytosolic. Scale bar indicates 50 µm

(C) Schematic adapted from Thyme et *al.* (2019). Neuroanatomical landmarks of the larval zebrafish brain, dorsal view (left), transverse view (right) and legend below. A: anterior, L: lateral, V: ventral.

After establishing the specificity of staining and optimising imaging to ensure the best compromise between high resolution and whole brain view, we scaled up the experiment. We investigated differences in brain activity between *disc1* mutants and controls. Larvae were raised until 7 dpf and fixed rapidly to ensure brain activity remained intact (see section 2.5). Immunofluorescence was performed, stained larvae were imbedded in agarose and whole brain images were acquired. Imaging data was aligned using morphing algorithms from the Computational Morphometry Toolkit for registration and to correct for rotation (see section 2.13). Significant changes of activity were measured between mutants and wild types. Anatomical areas were then localised by overlapping our brain-activity maps with the annotated Z-brain atlas, containing 29 labels of 294 segmented regions (http://stackjoint.com/zbrain/). Data are presented visually using Z-projections (Z=137) of significant differences in activity (Fig.6.2, 6.3), where purple indicates a relative significant decrease in activity, green indicates a relative significant increase in activity and black indicates similar activities between *disc1* mutants and controls. Maps were overlaid with Z-projections from the pan-neuronal Vmat2::GFP maker (grey) to specify neuroanatomical landmarks (Fig. 6.2, 6.3, left panels). Dorsal and lateral views of Z-projections were then displayed over a black background for contrast enhancement (Fig. 6.2, 6.3, right panels).

In *disc1*^{Y472X} mutants, differences in brain activity emerged in broad patterns across the brain (Fig. 6.2). We observed decreased activities (purple) in hypothalamus, thalamus, and the posterior tuberculum (Fig. 6.2). Neuronal populations exhibiting a decrease in activity in *disc1*^{Y472X} mutants included Orthopedia b (Otpb) and Oxytocin (Oxt) clusters in the diencephalon, DA clusters in posterior tuberculum and hypothalamus (Table 6.1). We observed increased activities (green) in the olfactory epithelium, pallium, subpallium, cerebellum and rhombencephalon (Fig. 6.2, Table 6.1).

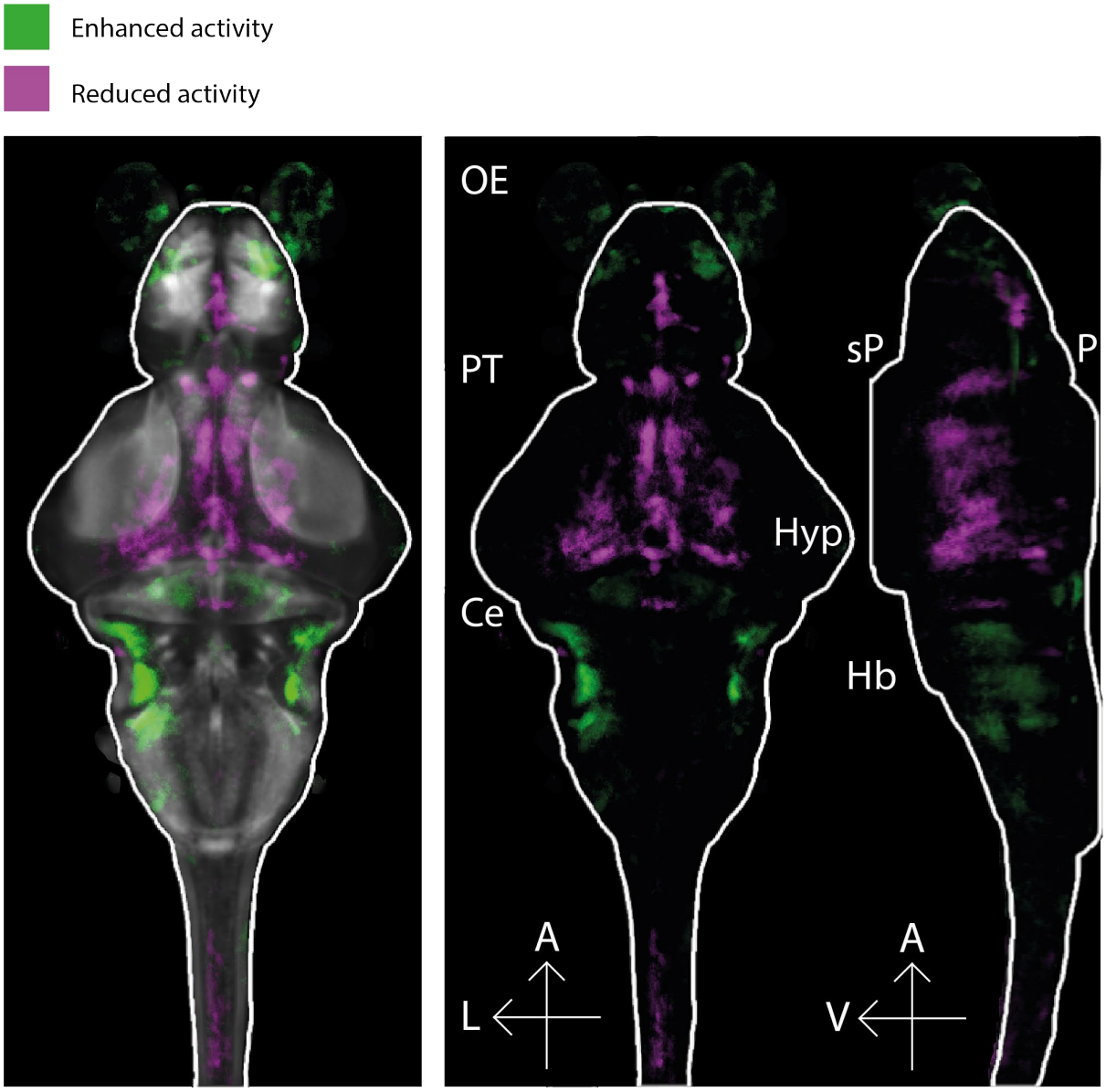

Figure 6.2. Brain activity maps from *disc1*^{Y472X} mutants

Wholemount dorsal view of Z-projection (Z=137). $N_{+/+}$= 76, $N_{-/-}$= 88, image representative of 2 experimental repeats. Activity increases are indicated in green and localise to the olfactory epithelium (OE), pallium (P), subpallium (sP), cerebellum (Ce) and hindbrain (Hb). Activity decreases are indicated in purple and localise to posterior tuberculum (PT) and hypothalamus (Hyp). Orientation shown by arrows at the bottom right. A: anterior, L: lateral, V: ventral.

Decrease in Activity	Increase in Activity
Telencephalon - Subpallial Otpb strip	Olfactory Epithelium
Diencephalon - Otpb Cluster 1, 2, 4	Subpallium
Preoptic Area - Oxt Cluster 1	Pallium
Diencephalon - Oxt Cluster 3, 2, 5	Rhombencephalon – HcrtR Stripe 2, cluster 3
Hypothalamus - Oxt Cluster 4	Rhombencephalon - Rhombomere 7
Periventricular PT - Dopaminergic Cluster 1	Cerebellum - Vglut2 enriched areas
PT - Dopaminergic Cluster 2	Ganglia - Lateral Line Neuromast OC1
PT and hypothalamus - Dopaminergic Cluster 4/5	
Hypothalamus - Dopaminergic Cluster 3, 6	
Hypothalamus - Hcrt cluster 1, 2	
Rhombencephalon - Superior Raphe	

Table 6.1. Identified ROIs with differences in brain activity in *disc1*^{Y472X} line
Neuronal populations were identified using ZBrainAnalysisOfMAPMaps.m (MATLAB) which generates output as an excel table. The ROIs displayed above satisfy the criteria of i. signal in ROI ≥ 100 and ii. validated in ≥ 2 experimental repeats. Organised by anatomical location from anterior most (top) to posterior (bottom). Populations underlined highlight common hits with *disc1*^{exon6} line (Table 6.2).

Next, we performed the same analysis on the immunofluorescence data from the *disc1*^{exon6} line. As opposed to *disc1*^{Y472X} mutants, *disc1*^{exon6} brain activity maps revealed differences in a more restricted pattern across the brain (Fig. 6. 3). Furthermore, increases and decreases were less pronounced in *disc1*^{exon6} brain activity maps (Fig. 6.3) compared to in *disc1*^{Y472X} brain activity maps (Fig. 6.2) suggesting that *disc1*^{exon6} mutants have a less severe brain activity phenotype. Similar hits identified between *disc1*^{exon6} mutants and *disc1*^{Y472X} mutants were underlined (Table 6.2). Common neuronal populations exhibiting a decrease in activity included subpallial Otpb strip, Otpb cluster 4 in the diencephalon, Oxt cluster 1 in the PO, DA cluster 2 in the PT, and Hcrt clusters 1 and 2 in the hypothalamus. Common neuronal populations exhibiting an increase in activity include the olfactory epithelium, the subpallium, pallium, neuromast OC1 cells of the lateral line (Table 6.3). These brain activity maps reveal the diversity of phenotypes caused by mutations in *disc1* but also uncover common populations with altered neuronal activity.

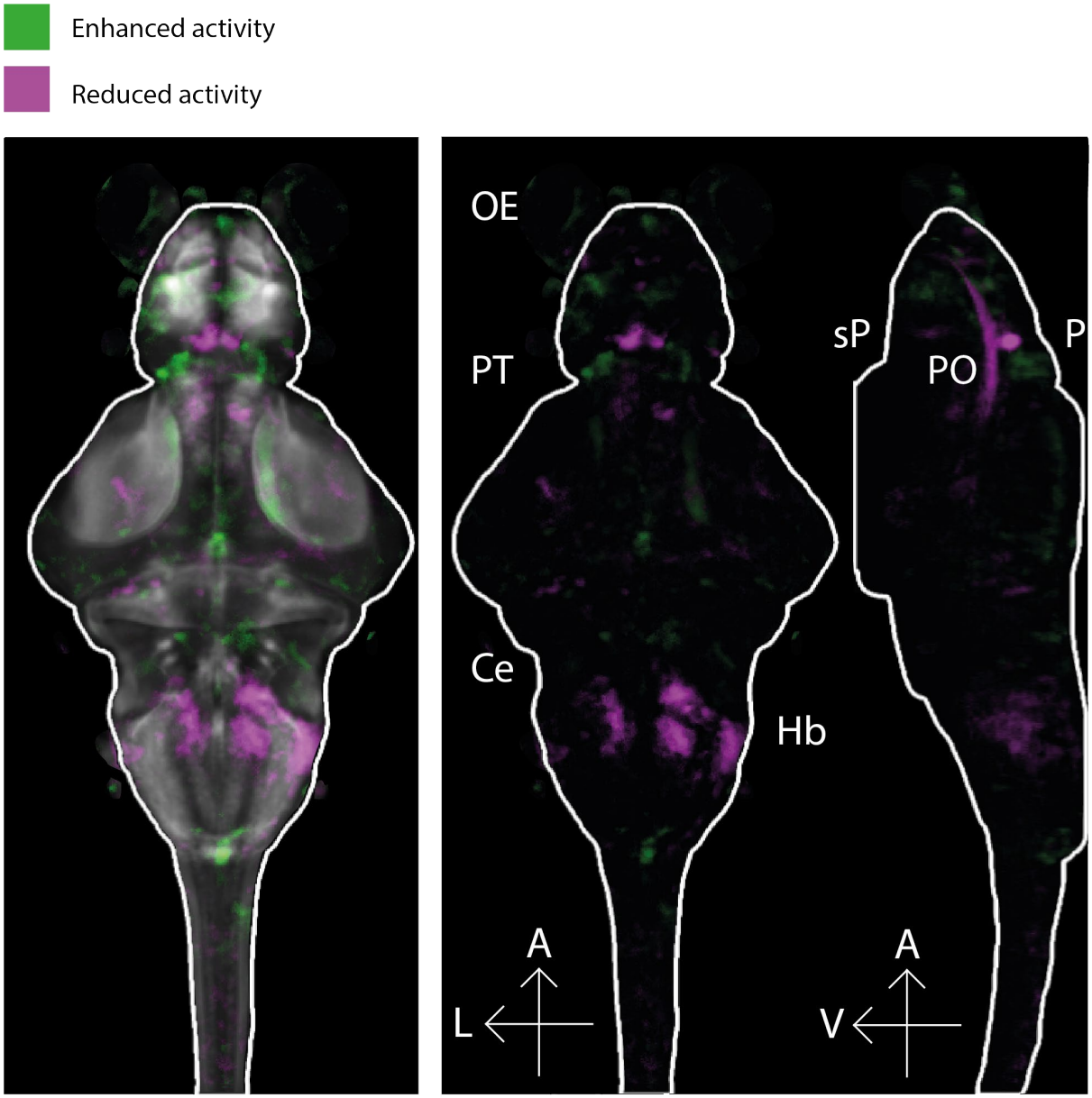

Figure 6.3. Brain activity maps from *disc1*^{exon6} mutants

Wholemount dorsal view of Z-projection (Z=137). $N_{+/+}$= 40, $N_{-/-}$= 35, image representative of 2 experimental repeats. Activity increases are indicated in green and localise to the olfactory epithelium (OE), pallium (P), subpallium (sP) and hindbrain (Hb). Activity decreases are indicated in purple and localise to the preoptic area (PO), posterior tuberculum (PT) and hypothalamus (Hyp), cerebellum (Ce). Orientation shown by arrows at the bottom right. A: anterior, L: lateral, V: ventral.

Decrease in Activity	Increase in Activity
Telencephalon - Subpallial Otpb strip, DA cluster	Olfactory Epithelium & Bulb
Diencephalon - Otpb Cluster 4	Subpallium
Preoptic Area - Oxt Cluster 1	Pallium
PT - Dopaminergic Cluster 2	Diencephalon - Otpb Cluster 3
Hypothalamus - Hcrt cluster 1, 2	Rhombencephalon - HcrtR Stripe 3,
Cerebellum - Olig2 enriched areas	Ganglia - Lateral Line Neuromast OC1, SO2
Rhombencephalon - Otpb Cluster 6	
Rhombencephalon - HcrtR cluster 1, 3, 5	

Table 6.2. Identified ROIs with differences in brain activity in *disc1*^{exon6} line
Neuronal populations were identified using ZBrainAnalysisOfMAPMaps.m (MATLAB) which generates output as an excel table. The ROIs displayed above satisfy the criteria of i. signal in ROI ≥ 100 and ii. validated in ≥ 2 experimental repeats. Organised by anatomical location from anterior most (top) to posterior (bottom). Populations underlined highlight common hits with *disc1*^{Y472X} line (Table 6.1).

6.2.2 Developmental expression of identified neuronal populations

After establishing common and reproducible ROIs with differences in neuronal activity, we decided to investigate the developmental expression of the neuronal populations identified with differences common to both *disc1* mutant lines. RNA *in situ* hybridisation is a common technique used in zebrafish research and circumvents the immediate need for zebrafish-specific antibodies. We designed and synthesised probes against *orthopedia B (otpb)* and *oxcytocin (oxt).* We synthesised a previously designed probe (template kind gift from Dr L. Trollope) against *tyrosine hydroxylase (th)* and performed wholemount *in situ* hybridisation (WISH). Tyrosine hydroxylase (TH) is the rate-limiting enzyme in the dopamine synthesis pathway and is often used as a marker for DA neurons (Molinoff and Axelrod, 1971).

disc1 is highly expressed at 2-3 dpf (De Rienzo et al., 2011; Wood et al., 2009) and differences in hypothalamic cell markers were previously identified in *disc1*^{Y472X} mutants at 3 dpf (Eachus et al., 2017). In addition, WISH and the visualisation of ventral neuronal populations are problematic after 5 dpf due to limited cell permeability and formation of the jaw cartilage. Therefore, we assessed the expression of *oxt, otpb* and *th* at 3 dpf. Bilateral nuclei of *oxt*-expressing neurons appear as early as 36 hpf in the developing zebrafish embryo and by 3 dpf are localised to the PO (Unger and Glasgow, 2003). There was a significant increase in *oxt*$^{+}$ neurons in both *disc1*^{Y472X} mutants and *disc1*^{exon6} mutants at 3 dpf (Fig. 6.4).

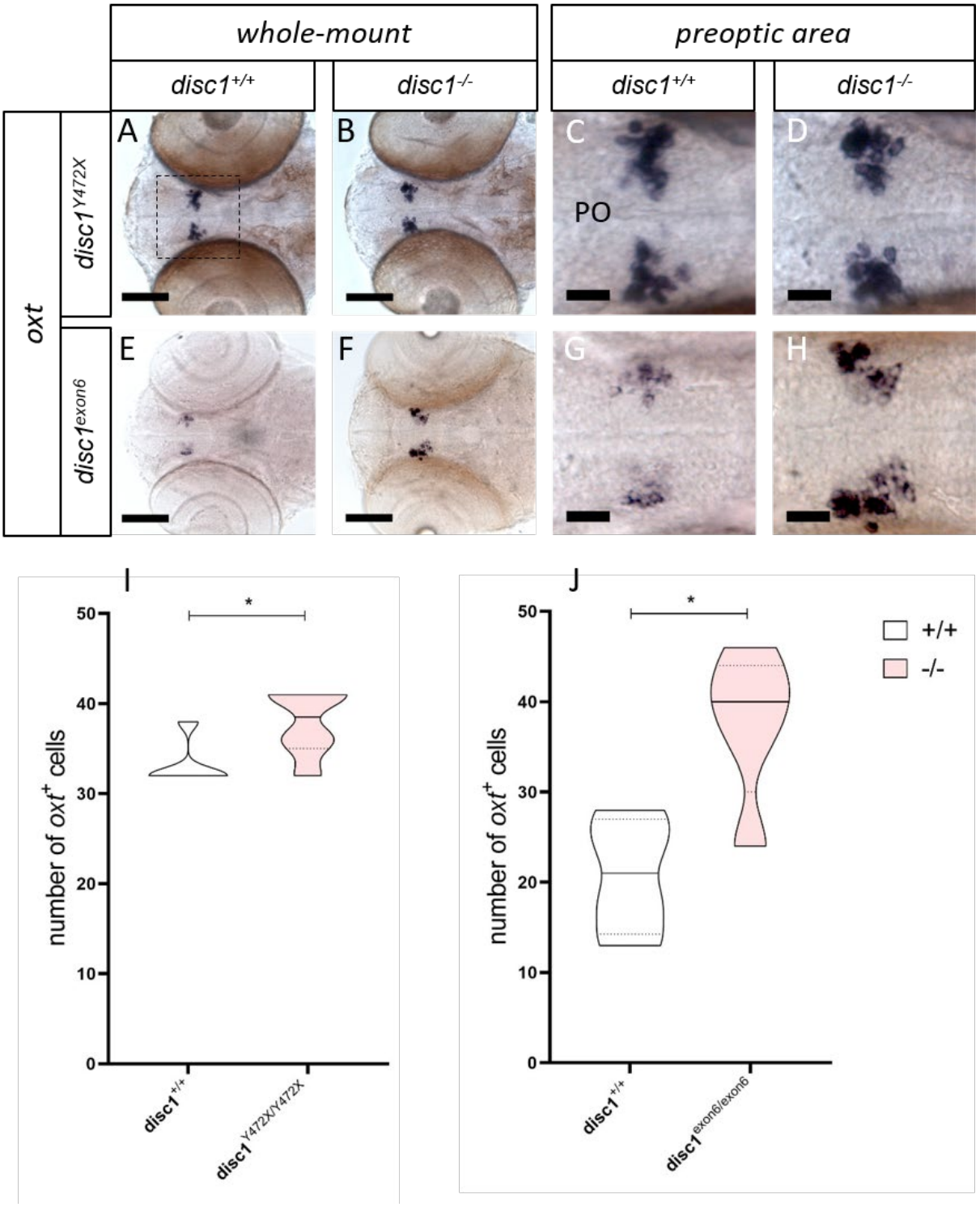

Figure 6.4 Wholemount *in situ* hybridisation (WISH) and cell counts of *oxytocin*-expressing neurons in *disc1* mutants at 3 dpf

Wholemount ventral view (A, B, E, and F) and preoptic area (dashed box, C, D, G, and H). Purple signal indicates spatial expression of *oxytocin* (*oxt*). Large scale bar (left) indicates 100 µm and smaller scale bar (right) indicates 25 µm. Quantification of *oxt*+ cells in *disc1*^{Y472X} (I) and *disc1*^{exon6} (J). PO: preoptic area. Box and violin plots represent sample distribution, full lines indicate median, and dotted lines indicate first quartile (below) and third quartile (top). N = 6 per group, 3 experimental replicates. Data distribution passed the Shapiro-Wilk normality test, unpaired Student's t-test, * = $p < 0.05$.

Next, we performed WISH using a probe against *optb*. At 3 dpf, *optb* is expressed in the preoptic area (PO), posterior tuberculum (PT), caudal hypothalamus (cH) and hindbrain (Hb) (Fernandes et al., 2013). We observed an apparent overall increase in the intensity of *optb* expression in *disc1*^{Y472X} and *disc1*^{exon6} mutants compared to controls (Fig. 6.5). We quantified *otpb*$^{+}$ cells in the cH of the *disc1*^{Y472X} line only, as cellular resolution of *otpb*$^{+}$ cells in the PO, PT and Hb as well as in the cH of *disc1*^{exon6} line was limited (Fig. 6.5). While there was an increase in the number of *otpb*$^{+}$ cells counted in the cH of *disc1*^{Y472X} mutants, this difference was not statistically significant (Fig. 6.5I).

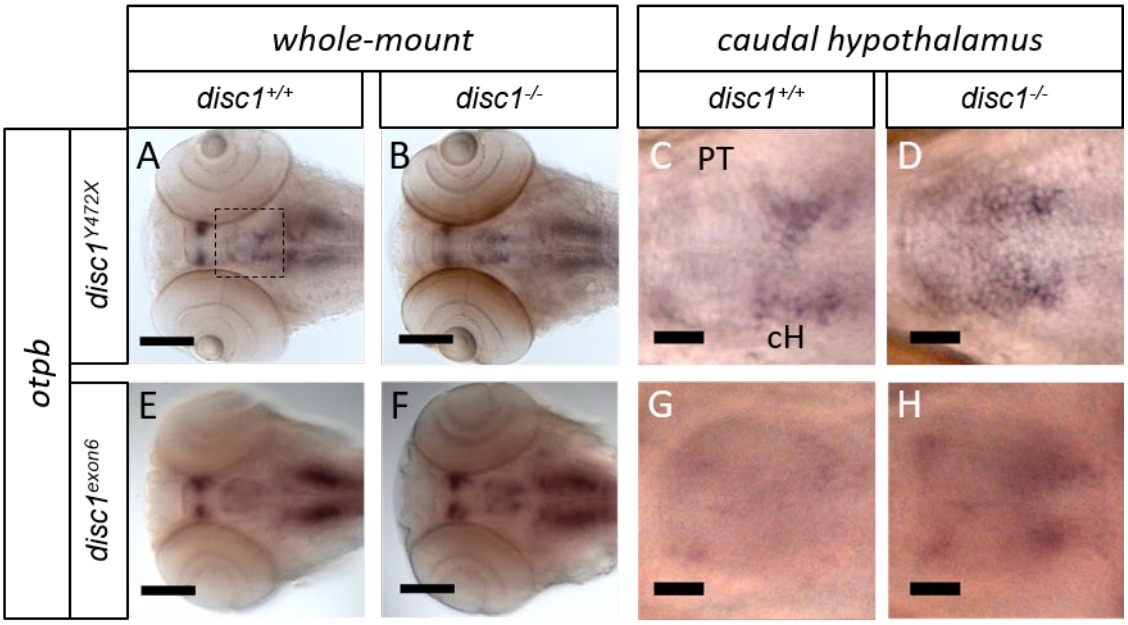

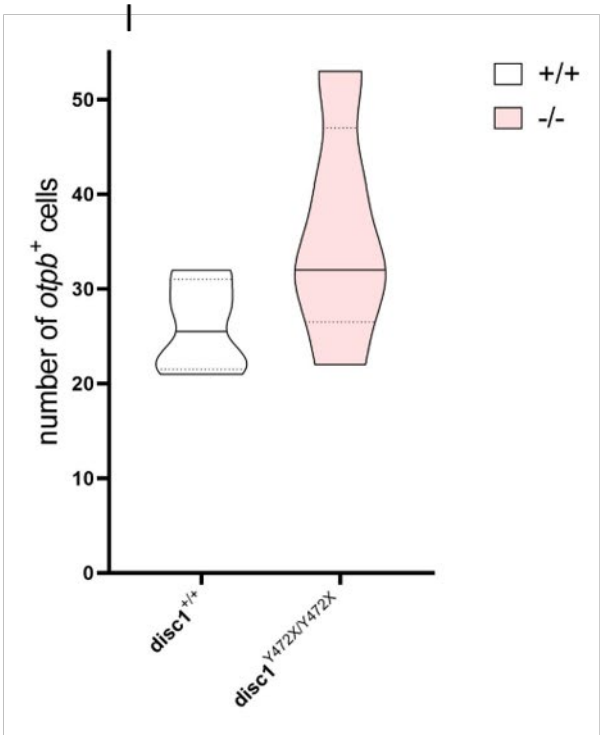

Figure 6.5 Wholemount *in situ* hybridisation (WISH) and cell counts of *orthopedia b*-expressing neurons in *disc1* mutants at 3 dpf

Wholemount ventral view (A, B, E, and F) and caudal hypothalamus (dashed box, C, D, G, and H). Purple signal indicates spatial expression of *orthopedia b* (*otpb*). Large Scale bar (left) indicates 100 µm and small scale bar (right) indicates 25 µm. PT: posterior tuberculum, cH: caudal hypothalamus. Quantification of $otpb^{+}$ cells in $disc1^{Y472X}$ (I). Box and violin plots represent sample distribution, full lines indicate median, and dotted lines indicate first quartile (below) and third quartile (top). N = 6 per group, 3 experimental replicates. Data distribution passed the Shapiro-Wilk normality test, unpaired Student's t-test, n.s = $p > 0.05$.

Finally, we performed WISH using a *th1* probe, to identify DA cell populations at 3 dpf (Fig. 6.6). Zebrafish express two homologues of the *tyrosine hydroxylase* (*th*) gene: *th1* and *th2* (Candy and Collet, 2005; Rink and Wullimann, 2002). *th1* is expressed in the telencephalon and diencephalon whereas *th2* is preferentially expressed in the latter and also labels cH populations. $th1^{+}$ clusters (2-6) located in the PT and hypothalamus were unaffected in $disc1^{exon6}$ mutants compared to controls (Fig. 6.6B, 6.6D, 6.6E). Similar $th1^{+}$ cluster analysis was also performed in the $disc1^{Y472X}$ line (A. Malkowska BSc thesis, University of Sheffield, 2018), and no differences were detected in $disc1^{Y472X}$ mutants.

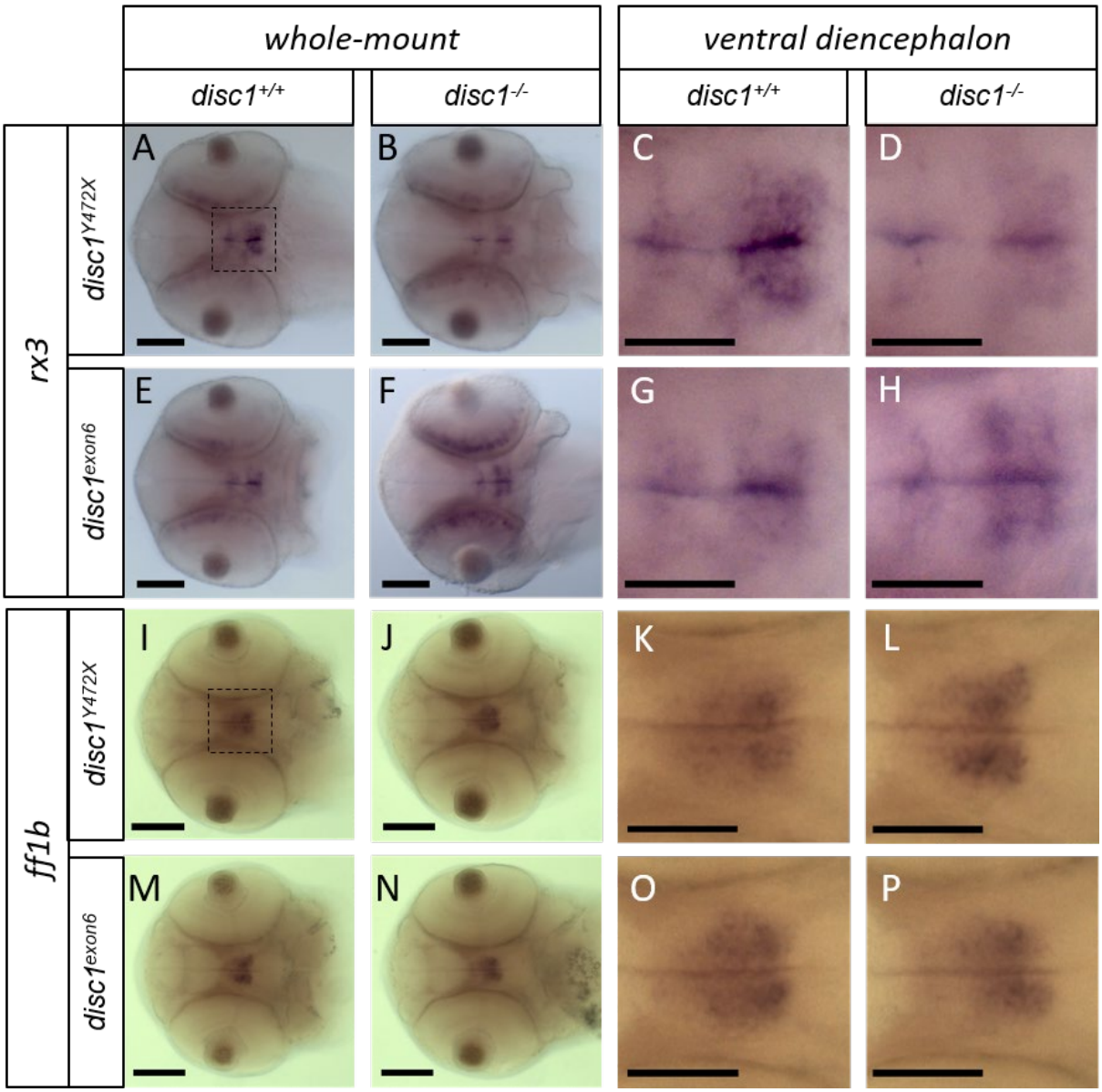

Figure 6.7 Wholemount *in situ* hybridisation (WISH) of *retinal homeobox 3* and *steroidogenic factor 1* in *disc1* mutants at 52 hpf

Wholemount ventral view (A, B, E, F, I, J, M, N) and ventral diencephalon (dashed box, C, D, G, H, K, L, O, P). Purple signal indicates spatial expression of *rx3* and *ff1b*. Small scale bar (left) indicates 100 µm and large scale bar (right) indicates 25 µm. Image representative of N = 6 per group.

Finally, we investigated the expression of *pomc* in both *disc1* mutant lines. We observed no differences in *pomc*$^{+}$ cell number at 52 hpf in either *disc1*^{Y472X} mutants or in *disc1*^{exon6} mutants, compared to their respective controls (Fig. 6.8), as previously reported by our group (Eachus et al., 2017).

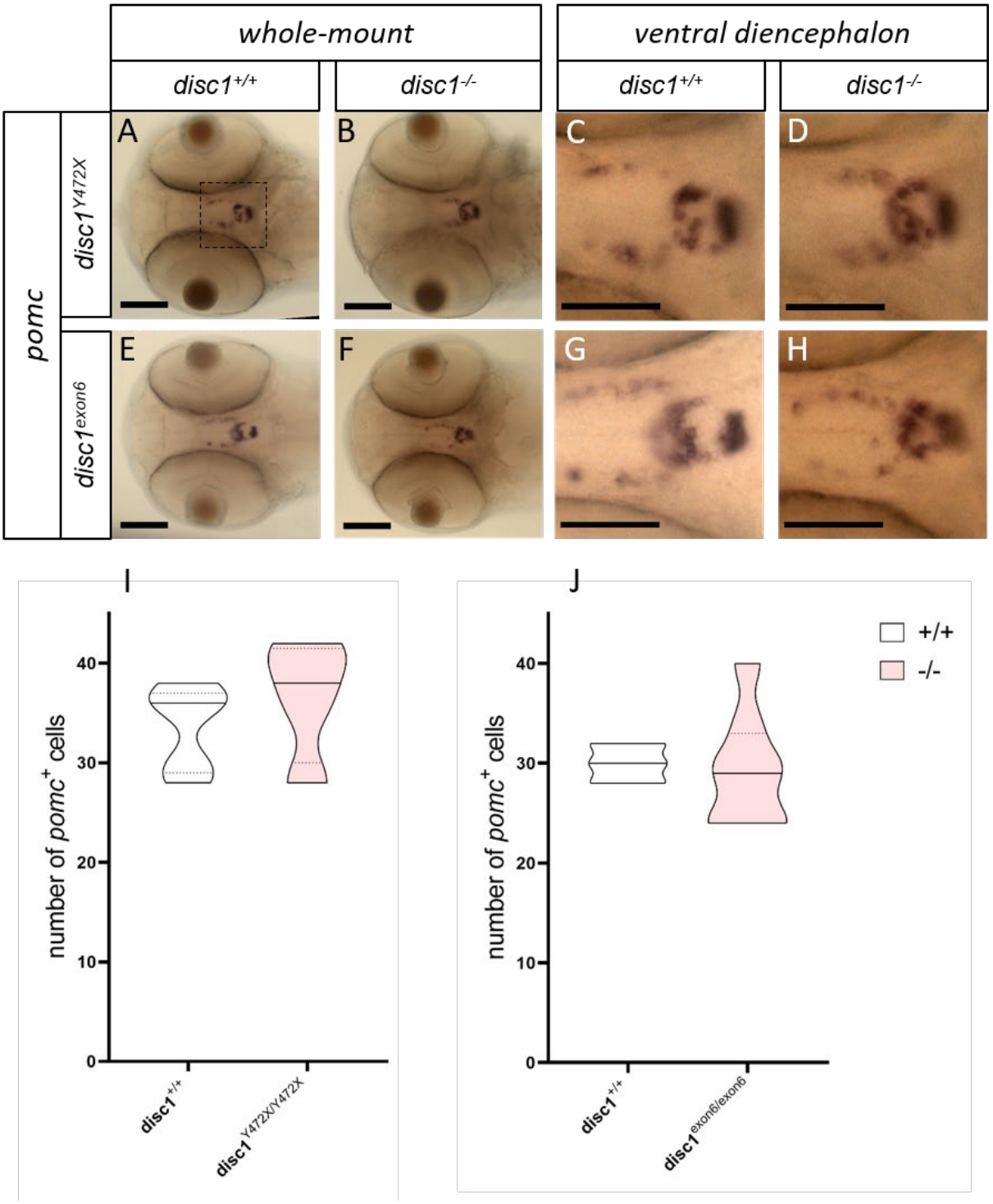

Figure 6.8 Wholemount *in situ* hybridisation (WISH) and cell counts of *proopiomelanocortin*-expressing neurons in *disc1* mutants at 52 hpf

Wholemount ventral view (A, B, E, and F) and ventral diencephalon (dashed box, C, D, G, and H). Purple signal indicates spatial expression of *pomc*. Small scale bar (left) indicates 100 µm and large scale bar (right) indicates 25 µm. N = 6 per group, 3 experimental replicates. Data distribution passed the Shapiro-Wilk normality test, unpaired Student's t-test, n.s = $p > 0.05$.

6.3 Discussion

Using a non-biased approach, we identified altered neuronal activity in the larval hypothalamus of *disc1* mutants supporting the role of *disc1* in hypothalamic development and function. Importantly, there was a strong decrease in activity from oxytocinergic, dopaminergic, Orthopedia b^+ and Hypocretin$^+$ neuronal populations in the ventral diencephalon (Fig. 6.2, Table 6.1, Fig. 6.3, Table 6.2).

6.3.1 Interpretation of oxytocinergic deficits in *disc1* mutants

We investigated *oxytocin* (*oxt*) expression at 3 dpf in *disc1* mutants and observed a significant increase in the number of *oxt*$^+$ cells (Fig. 6.4). At first, this result appeared counterintuitive, as neuronal activity in the preoptic Otx cluster 1 (part of the same lineage) is decreased in mutants (Table 6.1, 6.2). Neuronal circuits are complex and upstream neurotransmitter systems (which govern neuronal activity) are multiplex. It is also important to note that relationships between cell number and activity are not linear. Furthermore, interpretation becomes more ambiguous because of the differences in developmental stages analysed in the different experiments (3 vs. 7 dpf). For example in humans, the expression of *OXT* and its receptor (*OXTR1*) changes dynamically with age (Gimpl and Fahrenholz, 2001). Nevertheless, a loss of *disc1* causes a significant difference in preoptic *oxt* cell number and activity (Fig. 6.2, Table 6.1, Fig. 6.3, Table 6.2, Fig. 6.4). In *Disc1*^{L100P} male adult mice, hypothalamic *Oxt* expression was also significantly affected (O'Tuathaigh et al., 2017). In accordance with these results, the oxytocinergic system has been linked to the pathophysiology of neurodevelopmental disorders. Specific genetic polymorphisms in *OXTR* are associated with schizophrenia and autism (Jacob et al., 2007; Wu et al., 2005). In individuals with major depression, the number of OXT-producing neurons is increased in the PVN (Meynen et al., 2007). Interestingly, oxytocinergic abnormalities extend beyond the hypothalamus, evidenced by an increased expression of OXTR in the dorsolateral prefrontal cortex (DLPFC) of depressive and bipolar disorder patients (Lee et al., 2018). In addition, peripheral *OXT* and *OXTR* expression was increased and OXT neuropeptide levels in the CSF and blood were reduced in individuals with schizophrenia (Yang et al., 2017). Additional links of OXT to mental illness are provided by studies investigating the therapeutic use OXT. Both intravenous injections (Bakharev et al., 1986) and more recently, intranasal administration of oxytocin (Lee et al., 2013) led to an improvement of negative symptoms in schizophrenia and depression. Thus, our observations in *disc1* mutant larvae are consistent with the wealth of literature implicating OXT in mental illness.

6.3.2 Interpretation of dopaminergic deficit in *disc1* mutants

After observing a decrease in activity in dopaminergic neurons of the PT in *disc1* mutants (Table 6.1, 6.2), we wanted to investigate the expression of *tyrosine hydroxylase* (*th*) expression at 3 dpf in *disc1*

mutants. Expression of *th1* was investigated in the *disc1*^{Y472X} line in Sheffield. There was no significant difference in the number of *th1*$^{+}$ cells in *disc1*^{Y472X} mutants compared to controls at 3 dpf (A. Malkowska BSc thesis, University of Sheffield, 2018). We performed the same experiment on the *disc1*^{exon6} line in Singapore and also observed no significant differences in *th1*$^{+}$ cells between *disc1*^{exon6} mutants and controls (Fig. 6.6). These results suggest that the altered activity in dopaminergic populations is not because of an early developmental mispatterning of *th1*$^{+}$ clusters.

A large body of results indicate a link between Disc1 and the dopaminergic system in the mature brain. The expression of TH in the frontal cortex is significantly decreased in a transient *Disc1* knockdown mouse model (Niwa et al., 2010). In another mouse model, overexpressing *DISC1*, a decrease in dopaminergic neurons in the striatum has been reported (Hamburg et al., 2016). Moreover, Disc1 directly interacts with the dopamine receptor D2 (D2R) (Lipina et al., 2010). The same group investigated levels of this receptor in the striatum and found a significant increase in *Disc1*^{L100P} mice (Lipina et al., 2012). Furthermore, uncoupling of this Disc1-D2R interaction in mutant mice ameliorated behavioural phenotypes (Su et al., 2014) and administration of intranasal dopamine in a transgenic DISC1 rat model, can reverse memory and attention deficits (Wang et al., 2017). The dopamine hypothesis posits that excessive dopamine at rest and release in the ventral striatal projections from the midbrain play a central role in the symptoms of schizophrenia (Kegeles et al., 2010) and compounds that raise dopamine levels at the synapse cause psychosis (Davis et al., 1991). The periventricular dopaminergic neurons identified in our studies with cell bodies in the posterior tuberculum have projections to the subpallium in the teleost brain, the mammalian equivalent of the mesostriatal pathway (Rink and Wullimann, 2001; Tay et al., 2011). Therefore, the increase in activity in the subpallium in *disc1* mutant activity maps could mirror the hyperactive striatal connections reported in mammals.

A limitation of the use of zebrafish larvae in modelling dopaminergic abnormalities in the CNS is the lack of a midbrain dopaminergic population in zebrafish analogous to ventral tegmental area (VTA) (Rink and Wullimann, 2002), which play an important role in the mammalian mesolimbic reward pathway. However, projectome and developmental analysis suggests that the aforementioned ventral diencephalic-subpallial dopamine system, forms part of reward network in zebrafish and therefore comparative analysis can still be made (Lohr et al., 2009). Another pitfall in the experimental design could be the use of *th1* as a marker for specific dopaminergic neuronal populations. *Tyrosine hydroxylase* is expressed in both dopaminergic and noradrenergic neurons. Therefore, the lack of difference in *th1*$^{+}$ cell numbers in *disc1*^{exon6} mutants could arise due to masking by a concurrent

decrease in noradrenergic populations. An alternative and more specific marker for dopaminergic populations that could be used in future experiments is *dopamine transporter* (*dat*) (Meng et al., 2008).

6.3.3 Interpretation of *orthopedia b* deficits in *disc1* mutants

The activity of subpallial neurons and cluster 4 Otpb neurons was significantly decreased in *disc1* mutants at 7 dpf (Table 6.1, 6.2). Expression of *otpb* appeared increased in *disc1* mutants at 3 dpf (Fig. 6.5). Due to poor cellular resolution of *otpb* WISH staining, quantification was only performed on *otpb*$^{+}$ cells of the cauddal hypothalamus and no significant difference was noted. It is however important to note that *otpb* expression in the PO, PT and lateral hindbrain strips appeared increased, particularly in *disc1*^{exon6} mutants compared to controls (Fig. 6.5E-H). Two *otp* paralogs exist in the zebrafish genome (*otpa* and *otpb*), display some functional redundancy. The function of OTP is highly conserved throughout vertebrates, acting as a transcription factor involved in the differentiation of a subset of dopaminergic and oxytocinergic neurons cell types involved in hypothalamic neuroendocrine function (Blechman et al., 2007). This is the first report of altered activity in Otpb populations in *disc1* or any animal model recapitulating features of schizophrenia or depression. Considering the role of *otp* in neuroendocrine cell lineages and the fact that *otpb* colocalises with *rx3*+ cells (Muthu et al., 2016) and with DA clusters 3 and 4 in zebrafish at 3 dpf (S. Brown PhD thesis, University of Sheffield, 2016), its dysregulation is not unexpected. Further investigation into this cell type could provide important insights. The next steps could include quantification of *otpb* mRNA levels using qPCR or using a previously synthesised zebrafish-specific OTP (by Prof. G. Levkowitz). In addition, we could perform WISH against *neurod4,* a marker for newly determined neuronal cells (Mueller and Wullimann, 2002) and often used in combination with *otpb* to investigate dopaminergic neuronal differentiation (Thompson et al., 2017).

6.3.4 Other identified populations in *disc1* mutants

Other cell populations with altered neuronal activity in the hypothalamus are Hcrt clusters 1 and 2. Hypocretin (aka. Orexin) is a critical sleep neuromodulator and loss of these neurons in mammals leads to narcolepsy (excessive sleeping during the day and disturbed sleep at night) (Lin et al., 1999). The function of HCRT in sleep regulation and arousal is conserved in zebrafish larvae and neuronal activity of these neurons drives wakefulness (Adamantidis et al., 2007; Prober et al., 2006; Yokogawa et al., 2007). Although sleep disturbances have been reported in *DISC1* animal models, no group has investigated the expression or activity of HCRT^{+} neurons. Moreover, multiple lines of evidence link this system to neuropsychiatric disorders. The orexin 1 receptor (HCRTR1) was identified as a susceptibility factor for schizophrenia and major depression (Cengiz et al., 2019; Fukunaka et al., 2007). Another

study found that plasma orexin-A levels were significantly reduced in patients with bipolar disorder (Tsuchimine et al., 2019). Thus, our observations in *disc1* mutant larvae are in line with clinical observations of HCRT defects in neuropsychiatric disorders. Hyperactivity in the pallium was observed in both *disc1* mutant brain activity maps. The teleost pallium functions in spatial and emotional learning and memory and contains the functional homolog of the mammalian amygdala and hippocampus (Portavella et al., 2002; Riedel, 1997). The identification of altered activity in this region of *disc1* mutants is consistent with previous results reporting hyperactivation of the hippocampus, parahippocampal gyrus and amygdala in schizophrenia patients discussed above (see section 6.1).

Odour-evoked activity in the olfactory bulb (OB) can be seen as early as 3 dpf in zebrafish (Hussain et al., 2013). An interesting result from the brain maps is the increased neuronal activity in the olfactory bulb of *disc1* mutants compared to controls (Fig. 6.2, Table 6.1, Fig. 6.3, Table 6.2). This result was unexpected due to the previous observation of a decrease in food intake, which one could hypothesise would be due to a decrease in nutrient detection. MRI scans from patients with schizophrenia revealed structural deficits in the olfactory bulbs (Turetsky et al., 2000). A subset of individuals with major depression also have decreased olfactory bulb volume and olfactory sensitivity (Negoias et al., 2010). OB abnormalities are commonly reported in such disorders and this feature is used in the olfactory bulbectomy model of depression in rats (Kelly et al., 1997). Importantly, depressive-like phenotypes following the removal of OBs are reversible following chronic administration of antidepressants. Another observation we made, was the widespread increase in activity in more caudal areas of the larval brain. Notably, the activity of the cerebellum and hindbrain was affected by a loss of *disc1*. The cerebellum is an area of the brain involved in motor function and coordination. Disc1 is strongly expressed in the cerebellum, in all cell types (Goudarzi et al., 2013). The role of DISC1 in cerebellar physiology, has been investigated using a mouse model of inducible expression of human mutant DISC1 in the cerebellum. *T*he frequency and amplitude of Purkinje cell firing was significantly increased in mutant *Disc1* samples (Ayhan et al., 2011). To our surprise, there was no difference in activity in AF7, despite the strength of the feeding phenotype (Fig. 4.1, 4.2, 4.3) in *disc1* mutants. AF7 neuronal activity is directly correlated with hunting and was dysregulated in other larval zebrafish mutants modelling schizophrenia and autism (Thyme et al., 2019). These results point to a convergence of behavioural phenotypes despite the diversity of risk gene function and brain activity phenotypes.

6.3.5 The expression of previously characterised neuroendocrine hypothalamic cell fates

After creating the *disc1*^{exon6} line, we decided to characterise previously investigated cell types, identified as being altered in the *disc1*^{Y472X} line (Eachus et al., 2017). At 52 hpf, both *disc1* and *rx3* are

coexpressed in the lateral recesses and cells lining the 3rd ventricle of the zebrafish hypothalamus (H. Eachus PhD thesis, University of Sheffield, 2015). Disc1 expression is also detected in hypothalamic cells in embryonic and adult mice (Austin et al., 2003; James et al., 2004). In mice, *Rax*$^{+}$ cells label hypothalamic progenitor cells and are required for the development of Sf-1^{+} and Pomc^{+} cells (Lu et al., 2013). The expression of *rx3* and *ff1b* in *disc1*^{exon6} mutants was also altered, albeit in different directions to the *disc1*^{Y472X} mutants (Fig. 6.7), indicating that the hypothalamic progenitor pool and neuronal differentiation is altered in *disc1* mutants. *pomc* which is expressed in the arcuate nucleus and in the pituitary gland at 3 dpf was also investigated (Fig. 6.8). No differences in expression or cell number were observed in *disc1*^{exon6} mutants and *disc1*^{Y472X} mutants compared to respective controls as previously found (H. Eachus PhD thesis, University of Sheffield, 2015). Our analysis of *rx3, ff1b* and *pomc* expression in the *disc1*^{exon6} line offers less depth of analysis compared to the previous characterisation in *disc1*^{Y472X} as we did not perform a longitudinal expression analysis (from 24 hpf to 5 dpf), and only focussed on 52 hpf (H. Eachus PhD thesis, University of Sheffield, 2015). Furthermore, we did not perform any sectioning to compare differences along the rostro-caudal axis, due to time constraints. At 5 dpf, there were significantly fewer *pomc*$^{+}$ cells in the hypothalamus and pituitary in *disc1*^{Y472X} mutants compared to controls (H. Eachus PhD thesis, University of Sheffield, 2015). We hypothesise that performing *pomc* WISH at a later developmental stage in *disc1*^{exon6} larvae, may also reveal significant differences between mutants and controls. Our findings suggest an imbalance in hypothalamic cell fates caused by *disc1*-driven proliferative and/ or cell migration defects. This early cellular mispatterning could lead to a broad dysregulation of behaviour, consistent with the role of the hypothalamus in homeostasis.

Chapter 7: Early inhibition of GSK-3β as a therapy for *disc1*-related phenotypes

7.1 Introduction

Glycogen synthase kinase 3 (GSK-3) is a serine/ threonine protein kinase expressed as two isoenzymes (GSK-3α and GSK-3β) which are encoded by distinct genes. Expression is ubiquitous and these kinases are active under basal conditions (Woodgett, 1994). The canonical Wnt signalling pathway involves Wnt proteins, which are involved in morphogenesis and neural progenitor proliferation. In the absence of extracellular Wnt ligand, the transmembrane Frizzled (Fz) receptor is inactive. GSK-3β is a member of the destruction complex and phosphorylates β-catenin, causing its degradation. When Wnt ligands bind Fz receptors, GSK-3β is phosphorylated and becomes inactive. Stable β-catenin can then translocate into the nucleus and form a complex with T cell factor/ lymphoid enhancer factor (TCF/ LEF). This allows for transcription of Wnt target genes (Moon et al., 1997).

Alterations in Wnt signalling have been shown to cause shifts in neuronal fates and could contribute to psychiatric disease aetiology. Elevated WNT1 expression and low β-catenin levels were reported in post-mortem tissue from the hippocampus of schizophrenia patients (Cotter et al., 1998; Miyaoka et al., 1999). GSK-3β protein levels were 41% lower in prefrontal cortex (PFC) samples of schizophrenia patients compared with normal controls (Kozlovsky et al., 2000). Moreover, levels of phosphorylated (at Ser9) GSK-3β (pGSK-3β) were also significantly decreased in the PFC tissue and lymphocytes of individuals with schizophrenia (Emamian et al., 2004; Nadri et al., 2002). In a rat model of schizophrenia, generated through prenatal exposure to methylazoxymethanol acetate (MAM), a significant difference in the pGSK-3β/ GSK-3β ratio in juveniles was reported (Xing et al., 2016).

Modulation of GSK-3β may also play a pivotal role in alleviating symptoms in neuropsychiatric disorders. Lithium, one of the most effective mood stabilisers functions through multiple mechanisms of action. Most relevant to this study, is its ability to selectively inhibit GSK-3β activity at a far higher potency compared to other protein kinases (Bain et al., 2007). Indeed, mice lacking one GSK-3β allele, phenocopied behaviours of mice treated with lithium (O'Brien et al., 2004). Other antipsychotics such as clozapine and haloperidol have also been found to stimulate GSK-3β phosphorylation, reducing its activity (Emamian et al., 2004; Kang et al., 2004). In addition, a newly synthesised, more potent GSK-3β inhibitors conferred antidepressant and antimanic properties in rodent studies (Khan et al., 2016; Kozikowski et al., 2011).

DISC1 is a critical regulator of canonical Wnt signalling. Human lymphoblast cell lines (LCLs) from bipolar disorder patients, homozygous for *DISC1*$^{RR264/RR264}$ and healthy controls were infected with a TCF/LEF luciferase reporter gene to determine the level of Wnt activity. *DISC1*$^{R264Q/R264Q}$ LCLs had significantly lower TCF/LEF reporter activity compared with controls (Singh et al., 2011). Disruption of exon 2 and/or exon 8 of *DISC1* in human neural cells leads to an increase in canonical Wnt signalling and causes changes in cell fate. Strikingly, the Wnt antagonist XAV939 rescued expression of downstream factors *FoxG1* and *Tbr2*, normalising cell fates (Srikanth et al., 2015). Critically, DISC1 was found to interact directly with and inhibits GSK-3β, thus stabilising β-catenin (Newburn et al., 2011). Two different binding domains were mapped, spanning amino acids (aa) 1–220 and 356–595 in DISC1. Relatively conserved domains are found in mice and zebrafish, and also demonstrate similar binding dynamics. The *N*-terminally located fragment (aa 1-220) possess a stronger inhibitory activity on GSK-3β (Mao et al., 2009). In the absence of GSK-3β-DISC1 interactions, GSK-3β activity increases, leading to an increase in β-catenin degradation and a decrease in Wnt target gene transcription. This in turn affects neural progenitors, reducing their proliferation and causing premature cell cycle exit (Freyberg et al., 2010; Mao et al., 2009). In mice, missense *Disc1*^{Q31L} and *Disc1*^{L100P} both reduce the GSK-3β-Disc1 interaction. Moreover, acute administration of the GSK-3β inhibitor TDZD-8 (TDZD-8) was effective in reversing behavioural deficits in both *Disc1*^{Q31L} and *Disc1*^{L100P} mice models (Lipina et al., 2012; Lipina et al., 2011). Another missense mutation *Disc1*^{D453G}, occurring within the second interacting fragment (aa 356–595), also led to a decrease in GSK-3β-Disc1 interaction and reduced β-catenin abundance. *Disc1*^{D453G} mutant mice showed sex-dependant anxiety-related and social behavioural deficits (Dachtler et al., 2016).

In zebrafish, expression of DN-GSK-3β was able to rescue abnormal brain morphology and axonal tract defects in *disc1* MO embryos (De Rienzo et al., 2011). In cell culture, treatment with CHIR99021 (a GSK-3β antagonist), pushed NPCs to spontaneously differentiate. We hypothesised that treating *disc1* mutants with the same compound during hypothalamic development would rescue cell fate determination and have durable effects on behaviours. We assayed its effect by investigating the strongest and most consistent phenotypes observed in *disc1*^{Y472X} mutants: *ff1b* expression, food intake and brain activity. We decided to perform the following experiments on the *disc1*^{Y472X} line only for two reasons: i. reproducibility of the map-identified ROIs was weak in the *disc1*^{exon6} line and ii. RNA *in situ* hybridisation had already been performed in *disc1*^{Y472X} embryos.

7.2 Results

An initial toxicity assay of CHIR99021 treatment in zebrafish embryos was performed by C. Donaldson (MSc thesis, University of Sheffield, 2017). Previous studies used doses varying from 600 nM to 25 µM (Chen et al., 2014; Veldman et al., 2013). Wild type embryos were treated with 2 µM, 10 µM and 50 µM CHIR99021. Drug treatment did not cause any teratogenic effects (morphological abnormalities) and therefore 50 µM was selected as the most suitable dose to achieve the largest pharmacological effect. Drug treatment was applied between 24-52 hpf of embryonic development to inhibit GSK-3β during hypothalamic patterning. We hypothesised this would normalise the hypothalamus-associated deficits in *disc1*$^{-/-}$ mutants. Following fixation at 52 hpf, *in situ* hybridisation was performed to examine hypothalamic cell phenotypes. Expression of *ff1b* was chosen because of how strong and reproducible this phenotype was in *disc1*^{Y472X} mutants (Fig. 6.7; Eachus et al., 2017). In DMSO-treated embryos, we observed the characteristic increase in *ff1b* staining in *disc1*^{Y472X} mutants compared to controls (Fig. 7.1A, B). Following GSK-3β inhibition, we observed a strong reduction in *ff1b* expression in *disc1*^{Y472X} mutants compared to DMSO-treated *disc1*^{Y472X} mutants (Fig. 7.1B, D). This suggests that GSK-3β inhibition during a specific developmental time window (28 hours of treatment), can normalise *ff1b* expression to wild type levels. Interestingly, GSK-3β inhibition also affected *disc1*$^{+/+}$ controls, in which we observed an increase in *ff1b* expression compared to DMSO-treated controls (Fig. 7.1A, C).

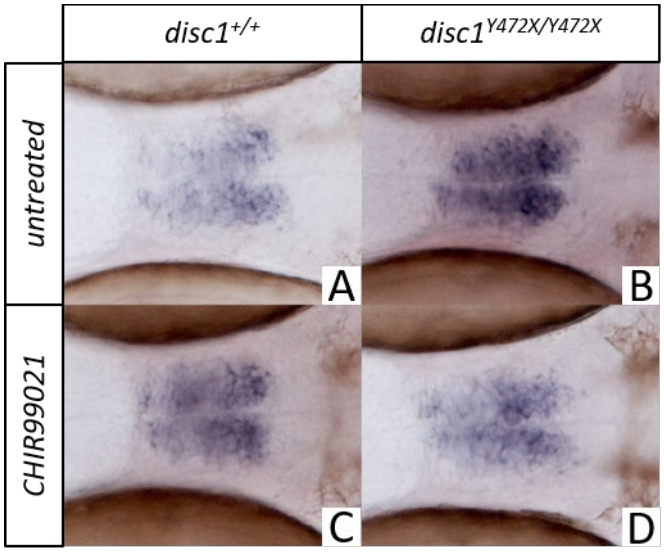

Figure 7.1. Early GSK-3β inhibition can normalise *ff1b* expression in *disc1*^{Y472X} mutants

Experiment performed and imaged by C. Donaldson (MSc thesis, University of Sheffield, 2017). Ventral view of the ventral diencephalon of CHRI99021-treated (C, D) and controls (DMSO) (A, B) *disc1*^{Y472X} controls (A, C) and *disc1*^{Y472X} mutants (B, D). Purple signal indicates spatial expression of *ff1b*. Scale bar. Images representative of N = 5 per group, 2 experimental repeats.

After establishing that GSK-3β inhibition could normalise *ff1b* expression in *disc1*^{Y472X} mutants at 52 hpf, we wanted to determine the effect of drug treatment on behaviour. Again, we selected a highly reproducible behavioural phenotype in *disc1*^{Y472X} mutants: feeding. Drug treatment was applied during a specific embryonic developmental time window as previously described, washed off and embryos were left to develop until 7 dpf. Similar to observations in embryos, larvae did not develop any

downstream teratogenicity from the drug treatment. Subsequently, we performed the feeding assay on DMSO and CHIR99021-treated *disc1*^{Y472X} mutants and *disc1*$^{+/+}$ controls. As previously reported (Fig. 4.1), there was a significant decrease in gut fluorescence in *disc1*^{Y472X} mutants compared to *disc1*$^{+/+}$ controls (Fig. 7.2). Remarkably, early GSK-3β inhibition, significantly increased food intake in *disc1*^{Y472X} mutants to levels comparable with untreated *disc1*$^{+/+}$ controls (Fig. 7.2). Notably, the effect of CHIR99021 treatment was again, not exclusive to the mutants; there was significant decrease in gut fluorescence in *disc1*$^{+/+}$ controls following drug treatment. These observations are consistent with the changes in direction of *ff1b* expression observed in drug-treated *disc1*$^{+/+}$ controls (Fig. 7.1C).

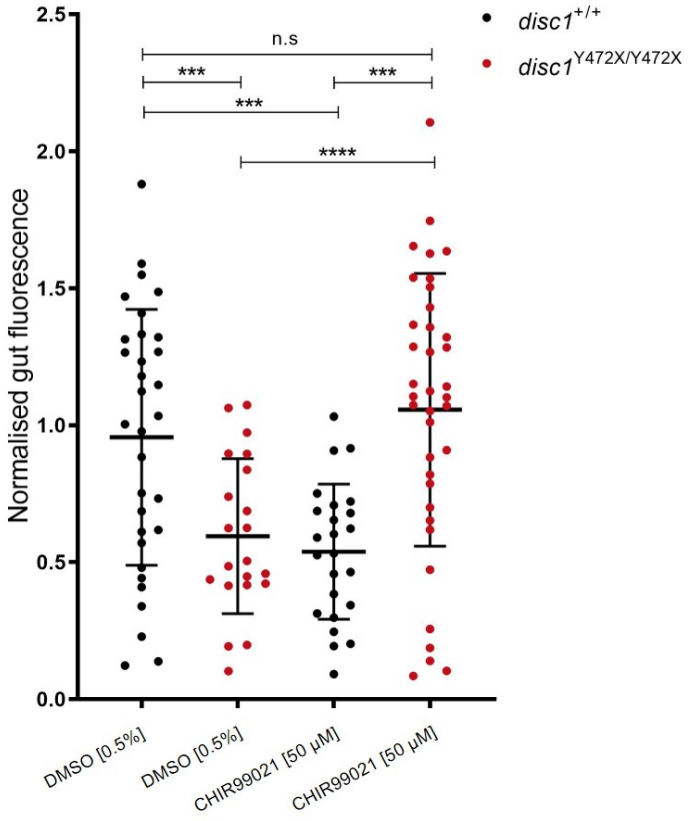

Figure 7.2. Early inhibition of GSK-3β can normalise feeding in *disc1*^{Y472X} mutants

Points represent individual larvae, bars indicate mean ± SD. Wild type (*disc1*$^{+/+}$), wild type in-cross larvae (non-sibling); mutant (*disc1*$^{Y472X/Y472X}$), homozygous mutant in-cross larvae. N= 114. 2 experimental repeats. Early CHIR99021 treatment rescues the feeding phenotype observed in *disc1*^{Y472X} mutant larvae at 7 dpf. See Table 7.1 for statistics.

Table 7.1. Tukey's *post hoc* multiple comparison for gut fluorescence in *disc1*^{Y472X} after exposure to CHIR99021

Two-way ANOVA				
Factor	**F value**	**d.f**	**P value**	**Sig.**
Genotype	0.466	1	0.496	n.s
Treatment	0	1	0.999	n.s
Genotype*Treatment	31.140	1	< 0.0001	****
Tukey Multiple comparison				
Factor			**P value**	**Sig.**
Control DMSO: Mutant DMSO			< 0.001	***
Control DMSO: Control drug			< 0.001	***
Mutant DMSO: Mutant drug			< 0.0001	****
Control drug: Mutant drug			< 0.001	***
Control DMSO: Mutant drug			0.894	n.s

To ensure that larval feeding behaviour at 7 dpf was not affected by residual compound still present in the E3 medium (after washes at 52 hpf), we investigated acute effects of GSK-3β inhibition on feeding behaviour. Wild type larvae were treated 30 min prior to the feeding assay (See Methods, section 2.23.2). We observed no significant effect of acute DMSO or CHIR99021-treatment on gut fluorescence (Fig. 7.3).

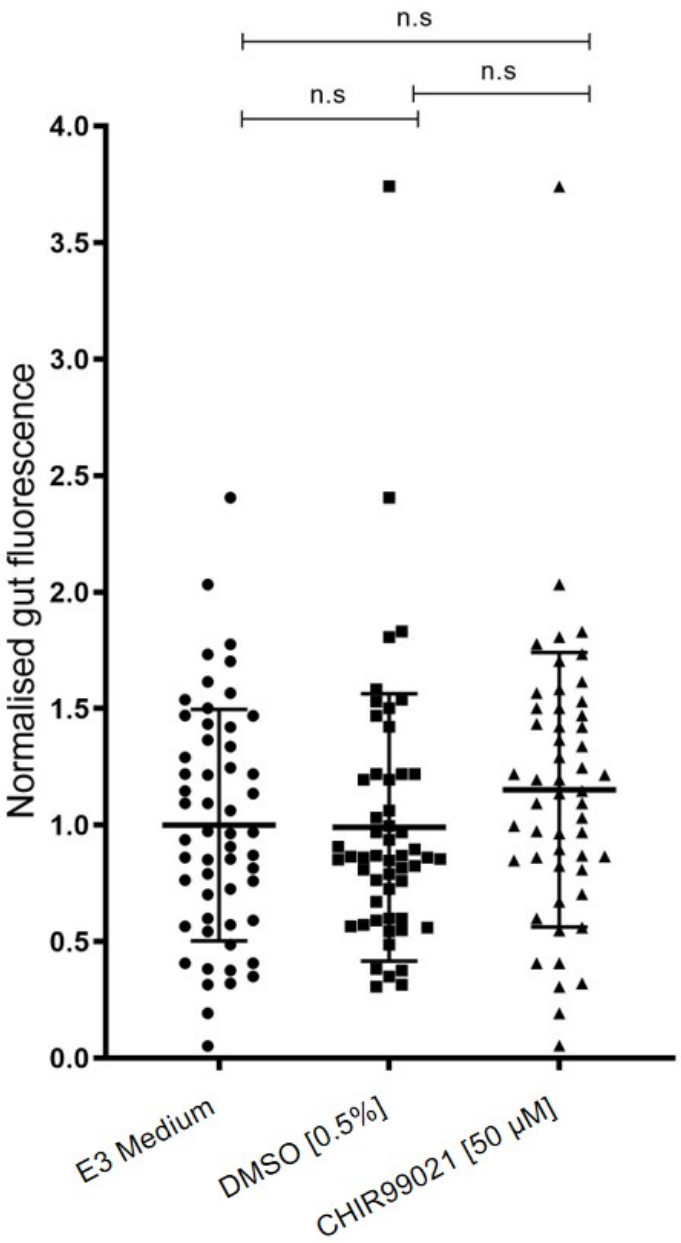

Figure 7.3. Acute inhibition of GSK-3β has no effect on feeding in wild type larvae

Points represent individual larvae, bars indicate mean ± SD. N= 160. 2 experimental repeats. Data distribution passed the Shapiro-Wilk normality test, one-way ANOVA, $F(2, 157) = 1.402$, n.s = $p > 0.05$. Treatment had no effect on food intake in wild type larvae at 7 dpf.

Next, we sought to investigate if the rescue of *ff1b* expression (Fig. 7.1) and feeding phenotype (Fig. 7.2) was underlying a rescue in brain activity. CHIR99021 and DMSO-treated *disc1*^{Y472X} mutants and disc1$^{+/+}$ were fixed at 7 dpf and immunofluorescence against pERK/ tERK was performed. Firstly, brain activity maps were created to compare CHIR99021-treated *disc1*^{Y472X} mutants and untreated *disc1*^{Y472X} mutants (Fig. 7.4). This was to determine if drug treatment could reverse the brain activity in previously identified regions of interest in *disc1*^{Y472X} mutants (Fig. 6.2, Table 6.1). Early GSK-3β inhibition reversed activity (i.e. increase instead of decrease in activity or decrease instead of increase in activity) in three previously identified ROIs (olfactory epithelium, preoptic Otx cluster 1 and Otpb cluster 2 in the diencephalon) (labelled in bold, Table 7.2). Early GSK-3β inhibition also caused changes

in the same direction in some neuronal populations (underlined in Table 7.2) previously identified in *disc1*^{Y472X} mutants (Table 6.1). This suggests that drug treatment exacerbated the increases in activity in the pallium, subpallium and rhombomere 7 of larvae (Fig. 7.4).

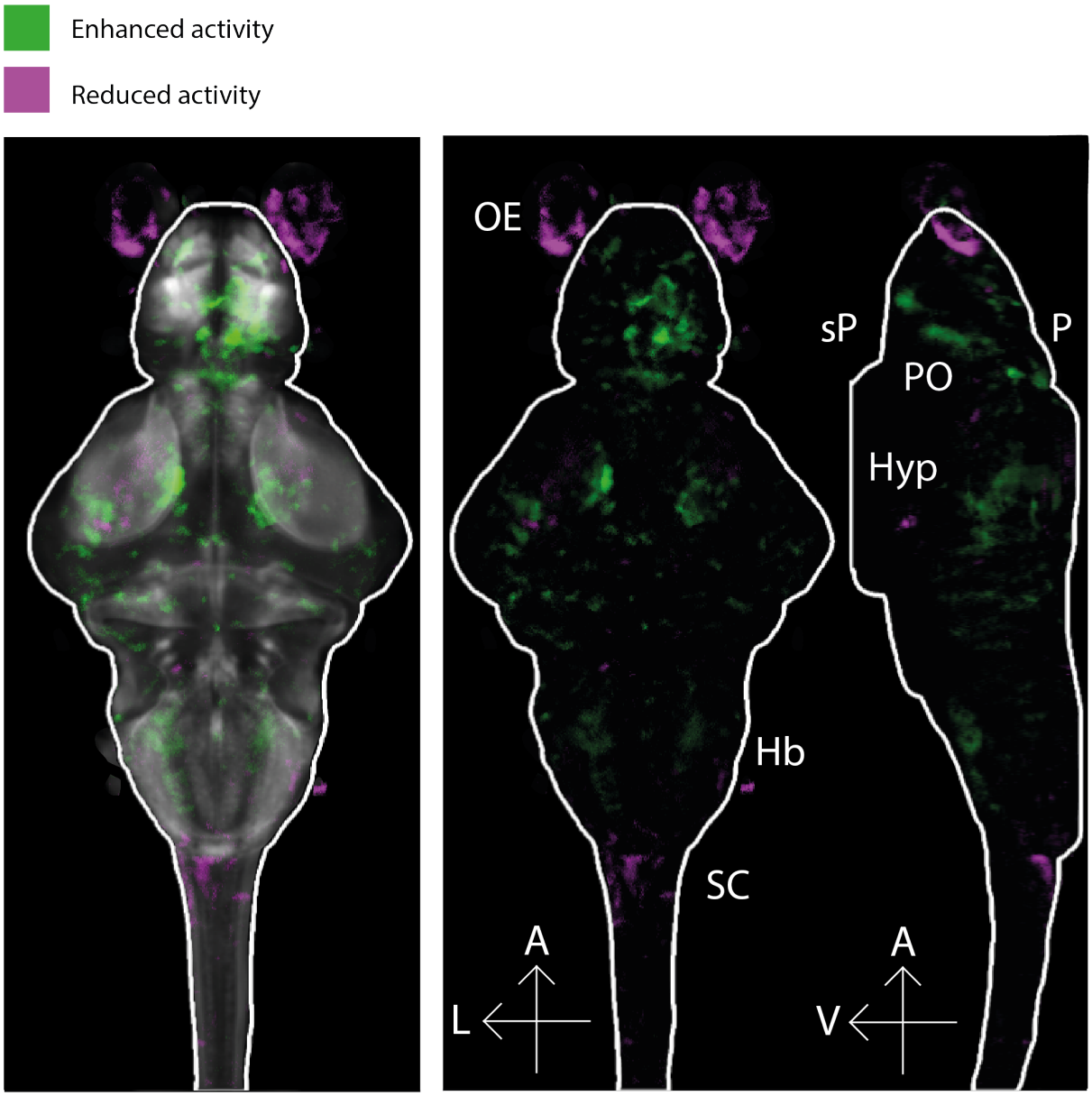

Figure 7.4. Brain activity maps from CHIR99021-treated *disc1*^{Y472X} mutants vs. DMSO-treated *disc1*^{Y472X} mutants

Wholemount dorsal view of Z-projection (Z=137). $N_{-/-DMSO}$= 36, $N_{-/-DRUG}$= 37. Activity increases are indicated in green and localise to the pallium (P) and subpallium (sP), preoptic area (PO) and hindbrain (Hb). Activity decreases are indicated in purple and localise to the olfactory epithelium (OE), hypothalamus (Hyp) and spinal cord (SC). Orientation shown by arrows at the bottom right. A: anterior, L: lateral, V: ventral.

Decrease in Activity	Increase in Activity
Olfactory Epithelium	Subpallium
Hypothalamus Vglut2 cluster 3	Pallium
Ganglia - Lateral Line Neuromast D2, D1, SO1, N, SO2, SO3	Habenula
Spinal cord - Lateral Line Neuromast D2, D1, SO1, N, SO2, SO3	**Preoptic Area - Oxt Cluster 1**, Otpb Cluster
Spinal cord - Vglut2 Stripe 1 and 2, Gad1b Stripe 1, Vmat2 Stripe 1, Glyt2 Stripe	Mesencephalon (Tectum and pretectum)
	Diencephalon - Otpb Cluster 2
	Cerebellum - Gad1b enriched areas
	Rhombencephalon - Otpb Cluster 1
	Rhombencephalon – HcrtR cluster 3, stripe 3
	Rhombencephalon - Rhombomere 7, 6

Table 7.2. Identified ROIs with differences in brain activity in CHIR99021-treated *disc1*^{Y472X} mutants vs. DMSO-treated *disc1*^{Y472X} mutants

Neuronal populations were identified using ZBrainAnalysisOfMAPMaps.m (MATLAB) which generates output as an excel table. The ROIs displayed above satisfy the criteria of i. signal in ROI ≥ 100 and ii. validated in ≥ 2 experimental repeats. Organised by anatomical location from anterior most (top) to posterior (bottom). Populations underlined highlight common ROIs with *disc1*^{Y472X} mutants. Population in bold highlight ROIs with reversal of activity differences compared to *disc1*^{Y472X} mutant (Table 6.1).

Secondly, brain activity differences were compared between CHIR99021-treated *disc1*^{Y472X} mutants and untreated *disc1*$^{+/+}$ controls and brain activity maps were created (Fig. 7.5). This was to assess if the drug treatment could normalise brain activity to a similar level as controls. We reasoned that if this were the case, brain maps would appear black (i.e. no significant differences). Brain activity maps revealed that activity was significantly increased in a widespread pattern throughout CHIR99021-treated *disc1*^{Y472X} mutant brains compared to untreated *disc1*$^{+/+}$ controls, particularly in the tectum and hypothalamus. We also observed a slight decrease in activity in the olfactory epithelium (Fig. 7.5). The combination of both these activity maps (Fig. 7.4 and Fig. 7.5) suggests that, unlike *ff1b* expression (Fig. 7.1) and the feeding phenotype (Fig. 7.2), early CHIR99021 treatment did not normalise specific brain activity patterns.

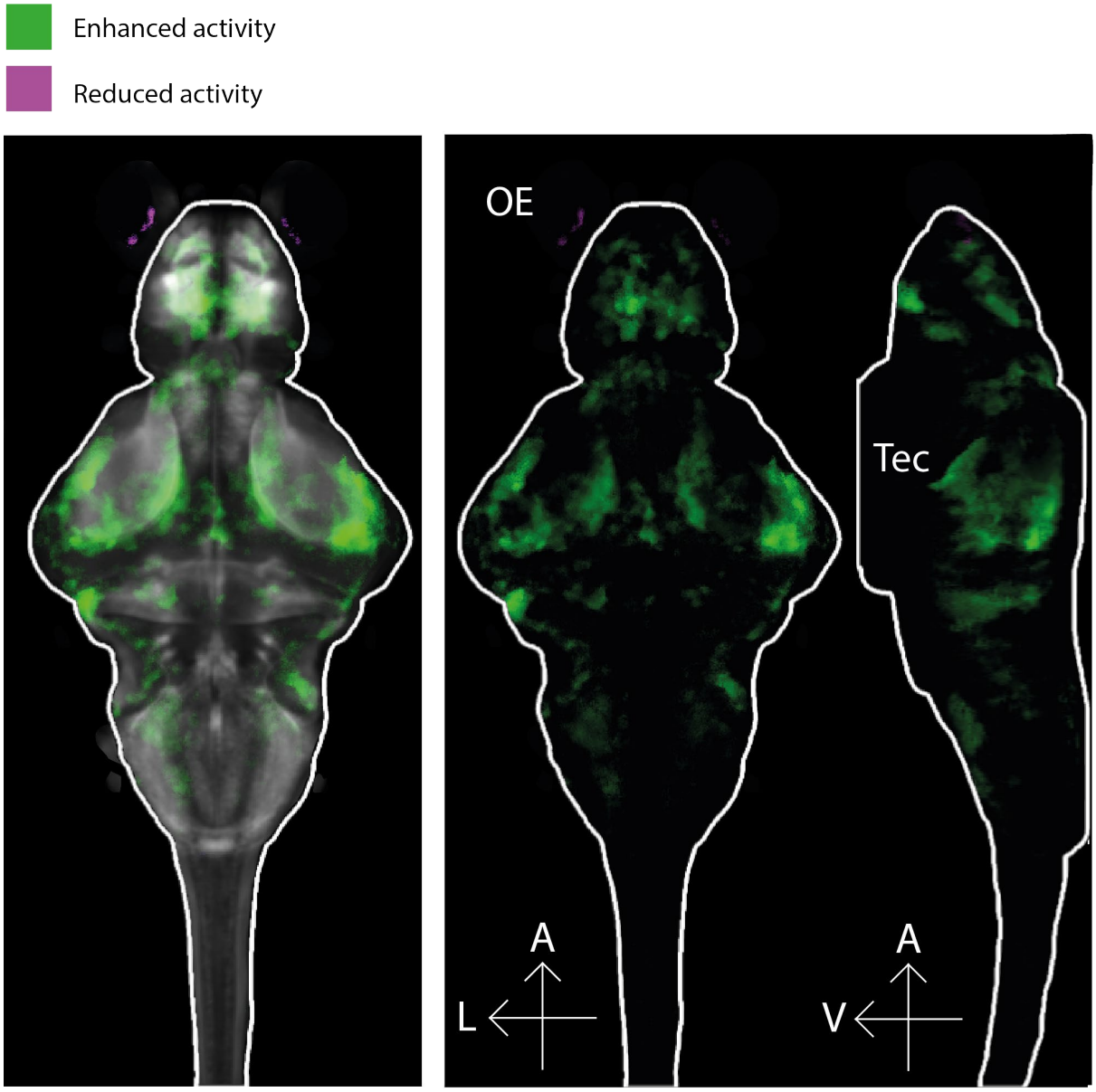

Figure 7.5. Brain activity maps from CHIR99021-treated *disc1*^{Y472X} mutants vs. DMSO-treated *disc1*$^{+/+}$ controls

Wholemount dorsal view of Z-projection (Z=137). $N_{+/+DMSO}$= 40, $N_{-/-DRUG}$= 37. Activity increases are indicated in green and widespread, particularly prominent in the tectum (Tec). Activity decreases are indicated in purple and localise to the olfactory epithelium (OE) only. Orientation shown by arrows at the bottom right. A: anterior, L: lateral, V: ventral.

7.1 Discussion

Transient inhibition of GSK-3β during embryonic development led to altered expression of hypothalamic *ff1b* in zebrafish at 52 hpf (Fig. 7.1). In *disc1*^{Y472X} mutants, cell fate perturbation leads to an excessive production of *ff1b*+ cells (Eachus et al., 2017; Fig. 6.5, Fig.7.1E-F). The dramatic rescue of *ff1b* expression in *disc1*^{Y472X} mutants suggests that alterations in cell fate have been rectified. This experiment was performed before the identification of *oxt* and *otpb* phenotypes in *disc1*^{Y472X} mutants (Fig. 6.4, 6.5) and therefore future experiments analysing the expression of these markers would

provide additional insight. Our results also reflect the effect of Wnt modulation on hypothalamic *ff1b*$^{+}$ cell development. Canonical Wnt signalling is a major signalling pathway required for the patterning and function of the zebrafish hypothalamus (Kapsimali et al., 2004; Lee et al., 2006). Wnt ligands are highly expressed in the developing hypothalamus from 2-3 dpf in zebrafish embryos (Duncan et al., 2016). Future work could also include quantification of CHIR99021-mediated Wnt modulation using a *tcf/ lef* reporter line as a readout.

Given the role of the hypothalamus in regulating appetite and feeding, we set out to investigate if GSK-3β inhibition could normalise food intake in *disc1*^{Y472X} mutants. Extraordinarily, a brief exposure to CHIR99021 in early development, seems to have a lasting effect on behaviour, as *disc1*^{Y472X} mutants increased their food intake to similar levels as controls (Fig. 7.2) more than 4 days after treatment. Xing et al. (2016) also inhibited GSK-3β during pre-symptomatic stages in a rat model of schizophrenia and found long-term effects on spiny neuron deficits and amelioration of cognitive symptoms. Importantly, we found that acute drug treatment had no effect on gut fluorescence (Fig. 7.3). This illustrates that behavioural changes induced by early drug treatment derive from developmental origin and are not a secondary acute effect of residual drug in the E3 medium.

Of relevance to these findings, *Sf-1*/*ff1b*-expressing neurons are nutrient and hormone-responsive and play a role in food intake (Bingham et al., 2008; Dhillon et al., 2006; Tong et al., 2007). *Sf-1* knockout (KO) mice are non-viable due to adrenal agenesis. Nonetheless, *Sf-1* KO mice supplemented with adrenal transplants and glucocorticoid injections were viable and developed obesity (Majdic et al., 2002). Potential secondary metabolic effects from the transplantations and injections could, however, contribute to this weight gain. In a CNS-specific knockout of *Sf-1* using the *Nestin-Cre* system, *Sf-1*$^{Nestin\text{-}Cre}$ mice showed gross abnormalities in the patterning of the ventromedial hypothalamic nucleus (VMH) (Kim et al., 2011). Behaviourally, *Sf-1*$^{Nestin\text{-}Cre}$ mice exhibited hyperphagia and a reduction in locomotion, ultimately leading to obesity (Kinyua et al., 2016). Optogenetic stimulation of *Sf-1* neurons in the VMH suppressed feeding and chemogenic ablation of these neurons increased food intake (Viskaitis et al., 2017). Therefore, *Sf-1*/*ff1b* expression is critical for VMH development and function in satiety. The decrease in *ff1b* expression in response to CHIR99021 (Fig. 7.1) could underlie the changes in feeding behaviour in *disc1*^{Y472X} mutants (Fig. 7.2). Many groups have postulated that activity from *SF-1*$^{+}$ neurons in the VMH increases excitatory input to POMC neurons in the arcuate nucleus, which in turn activates the anorexigenic circuits (Cowley et al., 2001; Sternson et al., 2005). Unexpectedly however, when blocking all *Sf-1* mediated excitatory output from the VMH, *Vglut2*$^{Sf\text{-}1\text{-}Cre}$ mice did not develop obesity (Cheung et al., 2015). Rather, prenatal ablation of *vGlut2*-expressing

neurons from the *Sf-1* lineage led to a sex-dependant reduction in body mass in female mice. Furthermore, CRISPR-generated *ff1b* maternal zygotic knockout zebrafish are viable yet display phenotypes and are smaller at 6 dpf (Wu et al., 2017a). Even though these studies highlight that the circuitry is not as simple as previously believed, there is an indisputable link between Sf-1/ff1b neurons in the VMH and food intake. To contribute to this knowledge and reinforce our hypothesis, we could perform further experiments to silence *ff1b* neurons using nitroreductase (NTR) and then assess hunting/ feeding behaviour. Food intake could also be assessed in larvae overexpressing *ff1b* using heat-shock methods. In order to understand the underlying changes in circuity governing alterations in larval behaviour, we measured brain activity at 7 dpf. Interestingly, exposure to CHIR99021 in early development seemed to also have a lasting effect on brain activity as well (Fig. 7.4, 7.5). We compared ROIs from *disc1*^{Y472X} brain activity maps (Table 6.1) and ROIs from drug-treated *disc1*^{Y472X} brain activity maps (Table 7.2). The extent to which the drug treatment reversed activity patterns was limited and localised to only 3 neuronal populations: olfactory epithelium, Oxt cluster 1 in the PO and Otpb cluster 2 in the diencephalon. Activity in these populations has been linked to nutrient sensing and appetite modulation (Hussain et al., 2013; Muto et al., 2017; Wee et al., 2019b). In addition, Oxt and Otp cell lineages derive from Sf-1 expressing cells in the hypothalamus (Kurrasch et al., 2007).

Using brain activity changes to measure drug effectiveness is at the basis of the rapidly expanding area of pharmacological MRI (phMRI). Studies have revealed *in vivo* drug action in the brains of neuropsychiatric disease patients. For example, the antidepressant venlafaxine, a serotonin and noradrenaline reuptake inhibitor, increased brain activity in the left insula and left anterior cingulate after 2 and 8 weeks of treatment, respectively (Davidson et al., 2003). The antipsychotic olanzapine, normalised functional connections between the cerebellum and PFC in treated patients (Stephan et al., 2001). Oxytocin treatment attenuated amygdala hyperactivity in patients with social anxiety disorder (Labuschagne et al., 2010). In a rodent model of schizophrenia, pretreatment with both lamotrigine and risperidone caused attenuation of ketamine-induced MRI changes (Doyle et al., 2013). The widespread increase in brain activity from maps comparing CHIR99021-treated *disc1*^{Y472X} mutants to DMSO-treated *disc1*$^{+/+}$ (Fig. 7.5) showed that baseline brain activity differed significantly between the 2 groups, despite similarities in feeding behaviour (Fig. 7.2). This begs the question of how important it is to restore the function/activity of all neuronal populations affected in the *disc1* mutants. In other words, if the drug treatment can normalise behavioural phenotypes, then it does not necessarily have to normalise the activity of all ROIs. To answer this, we would need to perform a more comprehensive behavioural profiling of treated *disc1*^{Y472X} mutants, which could include sleep and stimulus-evoked phenotypes that we identified (Chapter 3, Chapter 4, Chapter 5). Relevant to

this, is the role GSK-3β plays in sleep regulation: overexpression of *shaggy* (the GSK-3β ortholog in *Drosophila*), has been shown to affect circadian clock-regulated locomotion (Martinek et al., 2001). In addition, transgenic mice overexpressing GSK-3β exhibited fragmentated sleep-wake cycles during both the light and dark periods (Ahnaou and Drinkenburg, 2011).

Throughout this chapter, in every parameter assayed, we observed an effect of the drug treatment on *disc1*$^{+/+}$ control zebrafish. Hypothalamic expression of *ff1b* was visibly increased in CHIR99021-treated (Fig. 7.1F) compared to DMSO-treated *disc1*$^{+/+}$ embryos (Fig. 7.1E). In addition, CHIR99021-treated *disc1*$^{+/+}$ larvae had significantly reduced gut fluorescence compared to DMSO-treated *disc1*$^{+/+}$ larvae, indicating drug treatment negatively affected food intake in *disc1*$^{+/+}$ larvae (Fig. 7.2). Finally, brain activity maps comparing CHIR99021-treated *disc1*$^{+/+}$ against DMSO-treated *disc1*$^{+/+}$ larvae showed low widespread increases in brain activity (*data not shown*). The adverse effects of GSK-3β inhibition is predictable, as canonical Wnt signalling is a key regulator of hypothalamic patterning and function (Lee et al., 2006) and therefore its modulation could affect normal developmental processes. Similar results were reported in rodents exposed to SB216763, another GSK-3β inhibitor. In a rat model of schizophrenia treatment rescued phenotypes; however, treatment also led to deficits in spine morphology and working memory in wild type littermates (Xing et al., 2016). Therefore, inhibiting GSK-3β in animals without abnormal GSK-3β activity has detrimental effects and should be considered when designing clinical trials. It was recently proposed that combined therapies (e.g. CHIR99021 and lithium) could be administered at lower doses than their respective effective doses to produce synergistic effects, thus avoiding detrimental side effects (Haggarty et al., 2016).

CHIR99021 is a highly selective GSK-3 inhibitor. Despite its selectivity for GSK-3, it potentiates the activity of both GSK-3α and GSK-3β activity, with a slightly higher potency for GSK-3β (Ring et al., 2003). It is not implausible that crosstalk occurs and that the effect of embryonic drug treatment in *disc1*$^{+/+}$ and *disc1*^{Y472X} mutant zebrafish is mediated through Wnt-independent GSK-3α inhibition. Interestingly, Disc1 also interacts with GSK-3α and genetic inhibition of *GSK-3α in Disc1*^{L100P} mice reversed behavioural phenotypes to a similar extent as the GSK-3 inhibitor TDZD-8 (Lipina et al., 2011). To conclude, these results suggest that GSK-3 inhibition during a critical time window of neurodevelopment can alter cell fate, brain activity and behavioural phenotypes in the *disc1*^{Y472X} mutant zebrafish. These results also support the hypothesis that GSK-3 plays an important role in the pathophysiology of neuropsychiatric disorders.

Chapter 8: General discussion

8.1 Key findings

Using two *disc1* zebrafish mutants (Chapter 3), a range of behavioural and developmental phenotypes were characterised. We identified that *disc1* mutants show a specific decrease in hunting, feeding and sleeping (Chapter 4). Arousal also seems to be affected in *disc1* mutants; however, results differed between the two *disc1* lines (Chapter 5). After a comprehensive investigation of behaviours, we investigated brain activity signatures and found abnormal baseline neuronal activity in *disc1*^{Y472X} and *disc1*^{exon6} mutants when compared to their respective controls (Chapter 6). Despite not phenocopying each other, common hits in both mutants manifested as an increase in activity in the pallium and subpallium and decreased activity was reported in hypothalamic nuclei at 7 dpf larval zebrafish. Abnormal expression of the hypothalamic markers *rx3* and *ff1b* in *disc1* mutant embryos was also reported at 2 dpf. Mutations in *disc1* also caused abnormal expression of the hypothalamic markers *otpb* and *oxt* in embryos at 3 dpf (Chapter 6). Most interesting, is the finding that transient inhibition of GSK-3β, rescues the decreased expression of the hypothalamic marker: *ff1b* in embryos and in larvae, normalises feeding behaviour and affects brain activity (Chapter 7).

8.2 *disc1* mutants have subtle neurodevelopmental defects

Loss of function of *disc1* in our study, is not as severe as first observed in zebrafish. Originally, characterisation of *disc1* morphants revealed gross developmental abnormalities between 24 hpf and 5 dpf (Drerup et al., 2009; Wood et al., 2009). *disc1*$^{fh291/fh291}$ mutants demonstrated both brain, muscle segments and convergence/ extension phenotypes as early as 24 hpf. At 5 dpf, *disc1*$^{fh291/fh291}$ mutants had bent tails, abnormal pigmentation and uninflated swim bladders (De Rienzo et al., 2011). In our hands, we did not observe such severe phenotypes and defects appear more subtle (Eachus et al., 2017). It is possible that these originally observed phenotypes were caused by off-target mutations. Consistent with previous findings from our group, we observed altered expression of the hypothalamic markers *rx3* and *ff1b*, with additional characterisation of *otpb* and *oxt* expression and dopaminergic clusters. Interestingly both *disc1*^{Y472X} and *disc1*^{exon6} mutants have altered *rx3* expression, albeit in different directions. While *disc1*^{Y472X} mutants have a decrease, *disc1*^{exon6} have an increase in *rx3* expression in the hypothalamus at 52 hpf (Fig. 6.7). *rx3* is expressed in proliferating progenitors of the hypothalamus and upon differentiation, a fraction of these become *ff1b*$^{+}$. Therefore, abnormal numbers of *rx3*$^{+}$ progenitor cells in the hypothalamus could affect differentiating cells. Indeed, *ff1b* expression is also altered in *disc1*^{Y472X} and *disc1*^{exon6} mutants compared to their respective controls (Fig. 6.7). In essence, *disc1*^{Y472X} mutants have a decrease in *rx3* expression and therefore an increase in *ff1b*

expression compared to controls whereas *disc1*^{exon6} mutants have an increase in *rx3* expression and decreased *ff1b* expression compared to controls. A limitation is that WISH was performed at 52 hpf only, and direction of change in *rx3* and *ff1b* expression is likely to change over time. For example, it was observed that *rx3* expression is reduced in *disc1*^{Y472X} mutants at 52 hpf however is increased relative to controls at 5 dpf (H. Eachus PhD thesis, University of Sheffield, 2015). These results highlight an imbalance in early hypothalamic cells' fate determination. Importantly, we also report a widespread increase in *otpb* expression (Fig. 6.5) and an increase in *oxt* expression in the PO at 3 dpf in both *disc1* mutant lines (Fig. 6.4). *Orthopedia b* is a key transcription factor found to regulate the specification of various hypothalamic cell types including DA, *oxt, crf* and *pomc*. Accordingly, the increase in *oxt*$^{+}$ cells may be a direct consequence of the increase in *otpb* expression.

Subtle alterations in cytoarchitecture in *disc1* mutants could arise from abnormal proliferation during neurogenesis. Indeed, the role of *DISC1* in NPC proliferation is well established. DISC1 is highly expressed in NPCs and both *Disc1* transgenic and shRNA *DISC1* new-born mouse pups, have a significant reduction in BrdU labelling in the cortex (Mao et al., 2009; Shen et al., 2008). This reduction in NPC proliferation leads to premature cell cycle exit and differentiation. At 24 hpf, *disc1*^{Y472X} zebrafish mutants show brain-specific widespread increase in phosphorylated histone H3 (phosH3), an M-phase marker, compared to controls. This is followed by a decrease in phosH3 in *disc1*^{Y472X} mutants at 3 dpf compared to controls, suggesting that *disc1* is also required to maintain NPCs in zebrafish embryos (Eachus et al., 2017). We therefore hypothesise that the increase *oxt* and *optb* expression at 3 dpf is caused by altered cell fate determination, perhaps owning to a decrease in NPC proliferation and premature cell cycle exit. In future experiments, BrdU/EdU pulse chase labelling or immunofluorescence against phosH3 could be performed on both *disc1*^{Y472X} and *disc1*^{exon6} mutants to confirm this.

DISC1 has been shown to act in cell proliferation via the Wnt signalling pathway and more specifically through GSK-3β. Some DISC1 variants which are unable to bind and inhibit GSK-3β (DISC1^{A83V}, DISC1^{R264Q} and DISC1^{L607F}), lose their ability to activate Wnt signalling, causing a decrease in NPC proliferation compared to wild type DISC1 (Singh et al., 2011). Recapitulating the balanced *DISC1* translocation in iPSCs using TALENs, led to altered Wnt activity and a reduced NPC proliferation, changing neuronal cell fates (Srikanth et al., 2015). To increase Wnt signalling and rescue NPC proliferation at 24 hpf, *disc1*^{Y472X} mutants and control embryos were treated with the GSK-3β inhibitor CHIR99021. This reduced the abnormally elevated expression of *ff1b* in the hypothalamus of *disc1*^{Y472X} at 52 hpf and increased the expression of *ff1b* in the hypothalamus of control embryos (C. Donaldson MSc thesis, University of Sheffield, 2017). These findings suggest that altering Wnt signalling in early

development can normalise differentiation of *ff1b* cells in *disc1*^{Y472X} mutants; however, this also affected normal development in control embryos (Fig. 7.1).

Despite the 0.7-fold decrease of *disc1* mRNA in *disc1*^{exon6} mutants compared to controls (Fig. 3.9) and the 0.6-fold decrease of *disc1* mRNA in *disc1*^{Y472X}, we speculated that due to the slightly longer and more stable exon 6 transcripts (containing coiled-coil domains), *disc1*^{exon6} could express more, albeit truncated zDisc1 proteins compared to *disc1*^{Y472X}. As the GSK-3β binding site in zDisc1 is located at the *N*-terminus, *disc1*^{exon6} zDisc1 transcripts could still retain the ability to bind and inhibit GSK-3β. This could explain why *rx3* and *ff1b* expression is not altered as severely and in the same direction as in *disc1*^{Y472X} mutants. To investigate this further, a zDisc1 zebrafish antibody is necessary to first examine whether *disc1* mutants are nulls or express low levels of truncated zDisc1. Secondly, an antibody would also be useful to perform pull-down experiments and investigate interactions between mutant variants and GSK-3β. Unfortunately, efforts to synthesise a high affinity antibody with *in vivo* zDisc1-specificity proved unsuccessful (Fig. 3.5, 3.6, 3.10). We hypothesise that phosH3 may also be dysregulated in *disc1*^{exon6}, but possibly to a lesser extent than in *disc1*^{Y472X} and perhaps again, not in the same direction. Interestingly, a parallel can be drawn from a humanised mouse model study showing that the DISC1^{S704C} variant (*C*-terminus) does not bind and inhibit GSK-3β and therefore has no effect on Wnt signalling and NPC proliferation. Rather, the DISC1^{S704C} variant negatively affects neuronal migration, due to a reduced interaction with Dix domain containing 1 (Dixdc1) (Singh et al., 2011). This study and our results together suggest that due to the multifunctionality of DISC1, different *DISC1* variants cause convergent deleterious effects on brain development, not necessarily arising through the same molecular and cellular mechanisms.

8.3 Behavioural interplay of map-identified neuronal populations

The *rx3* and *ff1b* alterations first identified in *disc1*^{Y472X} mutants, were functionally associated to the hypothalamic neuroendocrine system, and naturally, endocrine function and behavioural responses to stress were investigated. *disc1*^{Y472X} mutants failed to increase cortisol in response to osmotic (NaCl) and organic (alarm substance) stress (Eachus et al., 2017). Baseline cortisol levels and expression of *ff1b* in the interrenal gland of *disc1*^{Y472X} mutants was unaffected (H. Eachus PhD thesis, University of Sheffield, 2015). Moreover, calcium imaging in zebrafish larvae, revealed that *crf*$^{+}$ neurons are highly responsive to osmotic stress (vom Berg-Maurer et al., 2016). We decided to assay whole brain activity using pERK brain-mapping at 7 dpf in zebrafish larvae (Randlett et al., 2015). Brain activity was significantly different between *disc1* mutants and their respective wild type controls (Fig. 6.2, 6.3).

Despite the inter-line variations of brain activity maps, some convergent neuronal populations were characterised and are summarised in Table 8.1. It is crucial to elucidate common phenotypes to inform us about the general disease aetiology and to identify populations to focus therapeutic efforts on. Of note, the decrease in DA neuronal activity in the PT of *disc1* mutant larvae was an unexpected finding given that hyperdopaminergic activity is an established feature of schizophrenia (Seeman et al., 1976). However, results from these brain maps align with the current view of excitatory and inhibitory imbalance underlying these disorders (Lisman, 2012).

Decrease in Activity	Increase in Activity
Telencephalon - Subpallial Otpb strip	Olfactory Epithelium
Diencephalon - Otpb Cluster 4	Subpallium
Preoptic Area - Oxt Cluster 1	Pallium
PT - Dopaminergic Cluster 2	Ganglia - Lateral Line Neuromast OC1
Hypothalamus - Hcrt cluster 1, 2	

Table 8.1. Common neuronal populations with differences in brain activity in *disc1* mutants
Common neuronal populations identified as having altered brain activity in the same direction in *disc1*^{Y472X} (Table 6.2) and *disc1*^{exon6} (Table 6.3) mutants were combined. Organised by anatomical location from anterior most (top) to posterior (bottom). PT = Posterior tuberculum.

Many different processes could be responsible for the observed alterations in brain activity in these neural circuits. For example, intrinsic changes in excitability of different neuronal populations have been reported in the hippocampus (Duan et al., 2007; Kvajo et al., 2011), in the forebrain (Holley et al., 2013; Juan et al., 2014) and in the cerebellum (Shevelkin et al., 2017) of different *Disc1* mouse models. The interaction between DISC1 and different receptors present at the synapse is another possibility for alteration in brain activity. In rat striatal neurons, DISC1 was found to interact with D2R and inhibit its agonist-induced internalisation. This interaction was found to be increased in post-mortem tissue from patients with schizophrenia (Su et al., 2014). Furthermore, DISC1 reduces NRG1-induced ERRB4 activation and thus excitability of cortical interneurons by competing with ERRB4 for the same binding site on PSD95, a major postsynaptic density protein of the glutamatergic synapse (Hayashi-Takagi et al., 2010; Seshadri et al., 2015). However, all these studies relate to the function of DISC1 in the mature brain. Therefore, we do not rule out that brain activity differences in *disc1* larvae could arise from a non-developmental origin. However, our observations, showing that zebrafish embryos have an altered expression of *oxt* and *otpb* at 3 dpf, led us to hypothesise that the decreased activity of the subpallial Optb neurons, Otpb cluster 4 in the diencephalon and Oxt cluster 1 in the PO could be due to developmental abnormalities.

A limitation from the brain maps is that the method can only identify changes in distinct neuronal populations. However, in recent years there has been a hypothesis-shift towards the perspective that impaired connectivity underlies schizoaffective and depressive disorders (Pezawas et al., 2005; Schmitt et al., 2011). Methods have recently been developed in wild type zebrafish larvae to study functional connectivity (Betzel, PREPRINT), but have yet to be used in disease models. We hypothesise that connectivity would be significantly affected in both *disc1* mutant lines. Extending beyond the function of the HPI axis, we decided to assay a more comprehensive repertoire of zebrafish larval behaviours, still tightly linked to the homeostatic and neuromodulatory function of the hypothalamus. Based on the cell populations identified from the brain activity maps (Fig. 6.2, 6.3), one can draw correlations between cell types and the multiple behavioural phenotypes that emerged in *disc1* mutants.

Both *disc1* mutants appeared to have increased *otpb* expression at 3 dpf (Fig. 6.5) and decreased activity of Otpb populations in the subpallium and cluster 4 in the diencephalon (Table 8.1). We also observed differences in light-induced locomotor responses (LLRs) in both *disc1* lines (Fig. 5.4, 5.5). Of note, Otp diencephalic neurons play a role in LLRs. In $otpa^{-/-}$ mutants and/ or following chemogenic ablation of $Otpb^{+}$ neurons, larval zebrafish lose their ability to fully upregulate swimming in response to darkness, (Fernandes et al., 2012). This phenotype resembles the altered LLR in $disc1^{Y472X}$ mutants (Fig. 5.4). The same group showed that deep brain photoreception is independent of dopaminergic clusters and rather, relies of $opn4a^{+}$ neurons in PO and PT. It would therefore be interesting to investigate this opsin population in *disc1* mutants.

Another behavioural phenotype reported in *disc1* mutants is their altered response to stress (Fig. 4.4, 5.7, 5.8, 5.10; Eachus et al., 2017). As was observed in $disc1^{exon6}$ mutants (Fig. 5.8), $otpa^{-/-}$ adult mutant zebrafish spend less time in the bottom third of the tank during the NTD assay (Amir-Zilberstein et al., 2012). Interestingly, $otpa^{-/-}$ mutants do not display the characteristic increase in *crf* levels in response to osmotic stress at 6 dpf. ChIP sequencing revealed that, upon stressful stimuli, Otp is recruited to the *crf* promoter, increasing transcription of *crf* in fish and mammals. At baseline, hypothalamic *crf* expression is slightly decreased in $disc1^{Y472X}$ mutants (Eachus et al., 2017). In future experiments, *crf* expression could be measured in *disc1* mutant lines before and after osmotic stress. Considering the loss of stress-induced cortisol increase (Eachus et al., 2017), the loss of stress-induced anorexia in $disc1^{Y472X}$ larvae (Fig. 4.4) and the loss of innate fear in $disc1^{exon6}$ adults (Fig. 5.8), we hypothesise that similar to $otpa^{-/-}$ mutants, larvae would fail to upregulate *crf* expression in response to stress.

OTP, appetite, and neuropsychiatric disorders are tightly linked. In humans, rare LOF mutations in *OTP* are associated with hyperphagic obesity as well as ADHD In mice, missense $Otp^{R108W/+}$ mutants display

increased anxiety in response to a novel environment as well as increases in food intake leading to weight gain (Moir et al., 2017). The most reproducible behavioural phenotype, in our study, was the decrease in food intake observed in both *disc1*^{Y472X} and *disc1*^{exon6} mutants compared to their respective controls (Fig. 4.1). Again, this could relate to altered expression of *otpb* causing developmental mispatterning of key hypothalamic populations involved in appetite. Indeed, the previously mentioned mouse study found a striking reduction in Oxt^{+} neurons in the PVN, thought to be driving hyperphagia. The number of Avp^{+} neurons in the PVN was also reduced in the *Otp*$^{R108W/+}$ mutant mice. *Avp*-expressing neurons are structurally and functionally linked to the Oxt system, under the transcriptional control of Otp and are involved in neuropsychiatric disorders (Bernstein et al., 2019). Our group also performed WISH for *avp* in the *disc1*^{Y472X} line; however, there was no significant difference at 2-3 dpf (*data not shown*).

The strongest cellular phenotype reported in both *disc1* mutant lines is the increase of *oxt*$^{+}$ cells in PO (Fig. 6.4). In addition, baseline activity of these Oxt neurons is significantly decreased in *disc1* mutants compared to controls (Table 6.1, 6.2). In zebrafish larvae, this neuronal population plays an important role in driving the behavioural response to aversive stimuli (electric shock, mustard oil, heat) (Wee et al., 2019a). Indeed, aversive stimuli increased brain activity in Oxt clusters in the PO and optogenetic activation of Oxt neurons induced large-angle tail bends, similar to the escape response. In humans, OXT can increase defensive responses to unpredictable acoustic startle (Striepens et al., 2012). *disc1*^{Y472X} mutants showed no differences in acoustic startle responses during the NTA (Fig. 5.1). Conversely, *disc1*^{exon6} mutants display significantly increased acoustic startle responses, which were more pronounced in maternal zygotics (Fig. 5.2, 5.3). These results can be juxtaposed with sleep results, whereby *disc1*^{Y472X} mutants and *disc1*^{exon6} mutants slept significantly less than their respective controls (Fig. 4.5, 4.6). One neuropeptide associated with sleep and arousal is hypocretin (Hcrt) and hypothalamic Hcrt neurons showed decreased activity in *disc1* mutants (Table 8.1). The role of HCRT plays in sleep is conserved throughout vertebrates. Overexpression via *hcrt*:heat-shock (hs:hcrt) stimulates locomotor activity during the night and decreases sleep episodes in zebrafish larvae (Prober et al., 2006). Tg(*hs:hcrt_Dr*) show a leftward shift in LLR traces suggesting hypersensitivity to dark-induced locomotion similar to *disc1*^{exon6} mutants (Fig. 5.5). HCRT is also involved in appetite regulation. Indeed, a psychopharmacology study found that, of all antipsychotics tested in rats, only those with an ability to modulate the activity of hypothalamic hypocretinergic neurons (e.g. clozapine, olanzapine, risperidone and chlorpromazine) induced weight gain (Fadel et al., 2002). Therefore, the decreased activity of Hcrt clusters 1 and 2 in *disc1* mutant larvae could not only play a role in the differences reported in sleep and arousal but also have an effect on appetite in disc1 mutants. Curiously, the direction of change in activity (i.e. decrease) is again opposite to what we would expect

to observe behaviourally. Our aim was to eventually investigate the developmental expression of *hcrt*, and an mRNA probe was designed and synthesised, however, time restrictions did not allow for these experiments to be performed. Despite the wealth of data involving *DISC1* in sleep regulation (Jaaro-Peled et al., 2016; Sawamura et al., 2008), not all *DISC1* mutations affect sleep. Evidence comes from the observation that some inbred mouse strains have a naturally occurring deletion in *Disc1* (Clapcote and Roder, 2006). When sleep behaviour was assessed in these mice, no sleep phenotype was detected (Dittrich et al., 2017).

8.4 Neuronal interplay of identified behaviours

We have addressed the fact that disruptions in single cell types can have consequences on multiple behavioural parameters and that sleep, appetite and stress regulation are all interlinked. If we consider this in the inverse direction, there is no single neuronal population that is responsive to precise sensory modalities (e.g. light, acoustic, pain). In reality, multiple cell types are recruited and fire in a concerted manner to efferent pathways. We postulate that these populations are affected by a loss of *disc1* and that these in turn, drive alterations in zebrafish behaviours. In a recent extraordinary effort to study sensory perception of osmotic stress in the hypothalamus, Lovett-Barron et al. (PREPRINT) reported that stress is encoded in the majority of the preoptic hypothalamic population and recruits multiple types of peptidergic cells (*oxt, crf, npy, avp*). Therefore, we suggest that any disruption in the expression of these markers could have downstream effects on the response to osmotic stress and most likely other behaviours as well. Interestingly, ablation of *pomc*$^{+}$ pituitary cells had no effect on the fast response to osmotic stress, indicating that the fast motor response to salt is independent of the slow endocrine system. This could explain why, even though we did not find any differences in *pomc*$^{+}$ at 52 hpf cell numbers (Fig. 6.8), significant differences in stimulus-evoked behaviours were reported in *disc1*^{exon6} mutants.

The anatomical diversity of the various cell populations identified in the brain maps is not unexpected given the wealth of data supporting the role of DISC1 in various brain areas. Some of these populations may be affected due to their afferent connections to the preoptic and tuberal hypothalamus. For example, afferents projecting from the pallium, subpallium and efferents projecting to brainstem spinal-projecting neurons have been mapped in larval zebrafish. In mammals, the hypothalamus is interconnected with itself and mutual communication between PVN, VMH and arcuate nucleus has been mapped (van-Hover and Li, 2015).

8.5 Early CHIR99021 treatment has later functional and behavioural effects

In our experimental design, we decided to treat embryos with CHIR99021 between 24 and 52 hpf, when primary neurogenesis rates are the highest (Kinch et al., 2015). This is unusual in the field, as most groups investigating the use of GSK-3 inhibitors as a therapy for neuropsychiatric disorders, administer it acutely or chronically at adult stages. The concept of brain plasticity postulates that during the early stages of neurodevelopment, whilst new neurons are being born and migrating, early life events can affect neural circuitry formation and consequently behaviour. We found that brief embryonic inhibition of GSK-3, had long-term effects in zebrafish larvae, and was able to rescue feeding deficits in *disc1* mutants and partially ameliorate brain activity (Fig. 7.2, 7.4). Developmental antagonism of GSK-3 during a postnatal time window (P7-P28) normalised neural synchrony and memory in the *Df(16A)*$^{+/-}$ mouse model of the schizophrenia-associated microdeletion in 22q11.2 (Tamura et al., 2016). Twenty-four hpf in zebrafish and P7 in mice are analogous to the second and third trimester in human embryonic development, respectively (Hill, 2020; Workman et al., 2013). In another rodent model of schizophrenia, treatment with a GSK-3 inhibitor between P21-P28 (corresponding to adolescence), normalised spine deficits and cognitive symptoms (Xing et al., 2016). These findings suggest that developmental antagonism of GSK-3 can have lasting effects on neuronal morphology, brain activity and behaviour. Some groups found that drug treatment has beneficial effects only if applied early enough. A mouse model of Tuberous Sclerosis Complex (TSC) was used to investigate comorbid ASD. Exposure to rapamycin (an mTOR inhibitor) at P7, prevented cerebellar deficits and ameliorated defects in social behaviours (Tsai et al., 2012). Remarkably, when *Tsc1*$^{-/-}$ mutant mice were exposed to rapamycin at 10 weeks, this had no therapeutic effect (Tsai et al., 2018). Acute CHIR99021 treatment at 7 dpf in zebrafish larvae, equally, had no effect on behaviour (Fig. 7.3). These results suggest, that in order to rescue deficits, exposure must be administered during a sensitive/ neuroplastic window. Rapamycin treatment also holds potential for *disc1* mutant zebrafish, as therapeutic benefits have been demonstrated in *Disc1* shRNA knockdown mice (Zhou et al., 2013)

In zebrafish research, many groups focus on studying the detrimental effects of early exposure to neurotoxicants. For example, prenatal exposure to low doses of ethanol caused abnormal social behaviour in larval and adult zebrafish, relating to abnormal development of the dopaminergic system (Fernandes and Gerlai, 2009; Mahabir et al., 2014). Valproate exposure from 0-2 dpf, led to hypersensitivity and hyperactivity in response to dark flashes in 6 dpf larvae (Zellner et al., 2011). Exposure to bisphenol A (BPA), caused precocious hypothalamic neurogenesis and led to anxiety-like hyperactive swimming bursts in zebrafish larvae (Kinch et al., 2015). We hypothesise that CHIR99021 also alters hypothalamic neurogenesis in *disc1* mutants via an increase in Wnt signalling, and that this may be driving the alterations in feeding behaviour (Fig. 7.2). Indeed, ample evidence suggests

hypothalamic neurogenesis in both the embryonic and mature brain can affect feeding and satiety pathways (Baoji and Xiangyang, 2016; Pierce and Xu, 2010; Xu et al., 2005). For example, intracerebral infusion of ciliary neurotrophic factor (CNTF), which increases hypothalamic cell proliferation, suppressed food intake in adult mice (Kokoeva et al., 2005).

These findings provide crucial evidence that cellular, functional, and behavioural phenotypes are pharmacologically reversible. Pursuing such early (pre/postnatal) treatments in humans poses a challenge, as up until now, no prodromal biomarkers can reliably provide early diagnoses of neuropsychiatric disorders (Debbané et al., 2015). However, this remains a critical goal in the field and would significantly advance the development of preventative therapies. As opposed to neurodevelopmental disorders such as ASD, neuropsychiatric disorders are late onset, and thus, the time window for potential intervention is much longer.

8.6 Project limitations and future directions

Linking behavioural changes to molecular and neural circuits alterations is challenging, even in a simple model system like the larval zebrafish. One difficulty with these studies is that most cellular/ molecular observations relating to the function of *disc1* are qualitative, and therefore the exact mechanism by which *disc1* alters proliferation and cell fate in zebrafish embryos is still unknown. Other potential drawbacks are described below.

8.6.1 Phenotypic variations between *disc1*^{Y472X} and *disc1*^{exon6} mutants

While some phenotypes (e.g. feeding, *optb* expression, *oxt* expression) were consistent between the *disc1* mutant lines and crosses, others (e.g. sleep, acoustic startle, LLR, brain activity, *ff1*b expression, *rx3* expression) showed discrepancies. As both mutant lines have PTC and significant decreases in *disc1* expression (Fig. 3.9; Eachus et al., 2017), it is unlikely that differences observed between *disc1*^{Y472X} and *disc1*^{exon6} mutants result from differential levels of zDisc1 protein; although, a modest expression of truncated zDisc1 in *disc1*^{exon6} mutants cannot be excluded. Observed differences could arise due to allele functionality differences as PTC in *disc1*^{Y472X} occurs in exon 2 whereas the stop codon in *disc1*^{exon6} occurs in exon 6. Importantly, major components of the Disc1 interactome have been shown to bind to the *C*-terminus of Disc1 (Morris et al., 2003).

A difference in background is also a possible source of discrepancy, as *disc1*^{Y472X} were raised on wild type Tüpfel long fin (TL) and *disc1*^{exon6} were raised on wild type AB. Interstrain variability exists for locomotor activity, sleep and HPI in zebrafish larvae (de Esch et al., 2012; Liu et al., 2015; van den Bos et al., 2017); however, corrections for this should be ensured by comparing mutants to their respective

siblings. Another possibility is that differences are due to effects of mutagenesis techniques: ENU mutagenesis was used to generate *disc1*^{Y472X} mutants. Chemical mutagens can induce hundreds of mutations in the organism and this high mutational load may affect behaviour. As multiple rounds of outcrossing have been performed prior to and during this study, off-target mutations generated by ENU mutagenesis in *disc1*^{Y472X} mutants should have been eliminated. Although unlikely, it could be possible that mutants have retained additional closely linked, recessive mutations (near the *disc1* locus). The more precise CRISPR/ Cas9 system was used to generate *disc1*^{exon6} mutants. This genome editing technique has proven an effective way of eliminating specific gene function with a decreased incidence of off-target events, however a lack of phenotype is commonly observed and, in some cases, has been linked to genetic compensation (Rossi et al., 2015).

To resolve genotypic differences, we could incross *disc1*$^{Y472X/+}$ heterozygotes to *disc1*$^{exon6/+}$ heterozygotes to obtain a *disc1*$^{Y472X/exon6}$ trans-heterozygotes through heteroallelic combination (Yue et al., 1999). We could also generate a second CRISPR/ Cas9 mutant using a single gRNA targeting exon 2, upstream of the Y472X locus. This would elucidate if differences are a consequence of allelic function or due to different genome editing techniques. Of note, another variation we observed in our larval behavioural experiments was intrinsic inter-individual variability. This has been reported in many larval behavioural studies and can only be overcome by increasing sample sizes and experimental repeat numbers to strengthen the power of significance (Hoffman et al., 2016; Thyme et al., 2019)

8.6.2 Limitations of brain activity mapping

A limitation of using pERK to measure neuronal activity in this study is the fact that the DISC1 scaffold protein may function in a pathway directly related to the former protein kinase. In primary neuronal culture, *DISC1* knockdown by siRNA resulted in ERK inactivation (Hashimoto et al., 2006). In astrocytes, DISC1 regulates the ERK signalling pathway by associating with RASSF7 (Wang et al., 2016). In iPSCs derived from patients harbouring a 4 bp deletion in *DISC1*, kinome analysis uncovered dysregulation of multiple kinases, including ERK (Bentea et al., 2019). However, until now, no differences in ERK signalling have been investigated in *disc1* mutant zebrafish. This protein kinase cascade orchestrates neuronal proliferation, differentiation, survival and plasticity (Cowan and Storey, 2003). An impairment in ERK signalling could underlie structural abnormalities in major depression. Indeed, a significant decrease in both tERK and pERK expression was measured in post-mortem brains from depressive-suicidal individuals (Dwivedi et al., 2001). To consolidate the brain activity maps, we would suggest crossing the *disc1* mutants to a line expressing a pan-neuronal GCaMP line to investigate live neuronal activity independent of ERK/ pERK expression.

A limitation of using the Z-brain atlas for aligning the areas with significant differences in brain activity with pre-annotated ROIs is that, because the atlas was constructed based on available transgenic lines, the results do not take into account the overlap between the different molecular markers. For example, in T*g(otpba:Gal4)* larvae, signal is present in *oxt*, *avp*, and *crf*-expressing PO neurons. Furthermore, we investigated expression of the identified cell populations at 3 dpf, whereas activity differences were detected at 7 dpf. It is more than likely that some neurons identified at 7 dpf do not correspond to those expressing the markers at 3 dpf. Therefore, the list of ROIs provides important information about the neuroanatomical locations of altered activity, however, it is restrictive in the list of markers to be studied. An alternative method could be to combine live calcium imaging with fluorescent *in situ* hybridisation (FISH) at the same stage, a method recently optimised (Lovett-Barron et al., 2017). FISH can increase the cellular resolution, detect much lower levels of mRNA expression and enable the combination of 3-4 probes in the same experiment. This, coupled with upstream task-related behaviour, such as neuronal activity in response to prey, acoustic stimuli or osmotic stress could enable a more precise mapping of specific cell types (Lovett-Barron et al., PREPRINT). Engaging the task-related neural circuits rather than measuring the default network (see section 6.1), would perhaps increase homogeneity between the maps of the *disc1*^{Y472X} and *disc1*^{exon6} lines, as well as potentially decreasing inter-individual variability.

8.7 Conclusion

In conclusion, the results in this thesis provide evidence that mutations in the genetic risk factor for neuropsychiatric disorders, *disc1*, confer subtle developmental phenotypes in zebrafish. This gene plays a key role in cell fate determination in both the preoptic and tuberal hypothalamus of zebrafish embryos and in particular, can disrupt the expression profiles of *retinal homeobox 3*, *steroidogenic factor 1*, *orthopedia b* and *oxytocin* at 2-3 dpf. Whether this imbalance in hypothalamic cell fates is driven by proliferative and/ or cell migration defects is yet to be determined. Mutations in *disc1* do not affect baseline locomotion, however they do affect food consumption and hunting behaviour at 7 dpf. They also affect responses to changes in illumination and in response to stressful stimuli. Imaging of brain activity demonstrates that neural circuits are affected at 7 dpf in *disc1* mutants and dysregulation is not solely restricted to hypothalamic populations. Depending on the *disc1* mutant line or even the type of cross, we found inconclusive behavioural results relating to sleep behaviours and acoustic startle. The genetic and environmental interplay governing the emergence of different human disorders (schizophrenia, bipolar disorder, major depression) in genetically similar carriers in the *DISC1* Scottish pedigree (Millar et al., 2000) is still poorly understood, however our results suggest

a complex relationship between genotype and phenotypes. Finally, GSK-3 inhibition during a critical time window in neurodevelopment, can reverse cellular and behavioural phenotypes and significantly affect brain activity in the *disc1*^{Y472X} mutant zebrafish. These results also support the hypothesis of altered GSK-3 activity in the pathophysiology of neuropsychiatric disorders.

This thesis addresses an important research question since psychiatric illnesses are a major economic and societal burden. This work contributes to the field of neuropsychiatric research as results show that early changes in how the brain is formed and later changes in behaviour are affected by genetic factors and can be pharmacologically reversed. Mutations in *disc1* cause specific changes in neurodevelopment and activity of specific brain regions which in turn, relate to maladaptive animal behaviour. These behavioural defects are analogous to those seen in individuals with mental illness.

Lastly, the robustness of the hypophagic phenotype in both *disc1*$^{Y472X/Y472X}$ and *disc1*$^{exon6/exon6}$ mutants, quantifiable through gut fluorescence and reversable after CHIR99021 treatment, offers a unique opportunity for drug screening. High throughput screens based on robust behavioural defects offer unbiased readouts of drug efficacy in zebrafish and are approximately two orders of magnitude faster than drug screens in rodents (Hoffman et al., 2016). Such techniques produce higher success rates in identifying promising small molecule drug compared to target-driven approaches (Jordi et al., 2015).

Appendix

Two -way ANOVA (bottom dwell, *disc1*^{Y472X})						
Factor			**F value**	**d.f**	**P value**	**Sig.**
Genotype			0.836	1	0.362	n.s
Time			10.101	1	0.002	**
Time: Genotype			1.437	1	0.233	n.s
Pairwise comparison (Time: Genotype)						
Time	**A**	**B**	**Mean Difference (A-B)**	**Std. Error**	**P value**	**Sig.**
0-2 min	wt	mutant	12.150	8.132	0.138	n.s
8-10 min	wt	mutant	1.635	8.132	0.841	n.s
Genotype						
het	0-2 min	8-10 min	11.383	8.063	0.161	n.s
mutant	0-2 min	8-10 min	25.167	8.201	0.003	**

Table 9.1. Statistical analysis of bottom dwell in *disc1*^{Y472X} adults

The results of a two-way ANOVA for time and genotype are shown. There is no significant effect of genotype and a significant effect of time on time spent in bottom third. There is no significant interaction between genotype and time. Pairwise comparison reveals no significant differences *disc1*$^{Y472X/Y472X}$ mutants and *disc1*$^{+/+}$ controls in the first 2 min and last 2 min of recording (Time). There was also a significant difference in between the first and last 2 min in *disc1*$^{+/+}$ controls. There is a significant difference in between the first and last 2 min in *disc1*$^{Y472X/Y472X}$ mutants. $P > 0.05$ = n.s, $P < 0.01$ = **. See Figure 5.8A for plot.

Two -way ANOVA (bottom dwell, *disc1*^{exon6})					
Factor			**F value**	**d.f**	**P value**	**Sig.**
Genotype			30.914	1	< 0.0001	****
Time			31.177	1	< 0.0001	****
Time: Genotype			1.013	1	0.317	n.s
Pairwise comparison (Time: Genotype)						
Time	**A**	**B**	**Mean Difference (A-B)**	**Std. Error**	**P value**	**Sig.**
0-2 min	wt	mutant	32.11	6.902	< 0.0001	****
8-10 min	wt	mutant	22.301	6.879	0.002	**
Genotype						
wt	0-2 min	8-10 min	31.995	7.167	< 0.0001	****
mutant	0-2 min	8-10 min	22.186	6.603	0.001	***

Table 9.2. Statistical analysis of bottom dwell in *disc1*^{exon6} adults

The results of a two-way ANOVA for time and genotype are shown. There is a significant effect of genotype and time on time on time spent in bottom third. There is no significant interaction between genotype and time. Pairwise comparison reveals significant differences between *disc1*$^{exon6/exon6}$ mutants and *disc1*$^{+/+}$ controls in the first 2 min and last 2 min of recording (Time). There was also a significant difference in between the first and last 2 min in *disc1*$^{exon6/exon6}$ mutants and *disc1*$^{+/+}$ controls. P > 0.05 = n.s, P < 0.01 = **, P < 0.0001 = ****. See Figure 5.8B for plot.

Two -way ANOVA (Thigmotaxis, *disc1*^{Y472X})						
Factor			**F value**	**d.f**	**P value**	**Sig.**
Time			3.429	1	0.066	n.s
Genotype			2.026	1	0.157	n.s
Time * Genotype			0.844	1	0.360	n.s
Pairwise comparison (Time * Genotype)						
Time	**A**	**B**	**Mean Difference (A-B)**	**Std. Error**	**P value**	**Sig.**
0-2 min	wt	mutant	9.518	5.747	0.100	n.s
8-10 min	wt	mutant	2.050	5.747	0.722	n.s
Genotype						
het	0-2 min	8-10 min	3.792	5.786	0.513	n.s
mutant	0-2 min	8-10 min	11.260	5.708	0.050	n.s

Table 9.3. Statistical analysis of thigmotaxis in *disc1*^{Y472X} adults

The results of a two-way ANOVA for time and genotype are shown. There is no significant effect of genotype on time on time spent in periphery of the tank. There is no significant interaction between genotype and time. Pairwise comparison reveals no significant differences between *disc1*$^{Y472X/Y472X}$ mutants and *disc1*$^{+/+}$ controls in the first 2 min and last 2 min of recording (Time). There was also no significant difference in between the first and last 2 min in *disc1*$^{Y472X/Y472X}$ mutants and *disc1*$^{+/+}$ controls. P > 0.05 = n.s. See Figure 5.8C for plot.

Two -way ANOVA (Darting, *disc1*^{Y472X})						
Factor			**F value**	**d.f**	**P value**	**Sig.**
Time			106.832	1	0	****
Genotype			1.301	1	0.256	n.s
Time * Genotype			0.004	1	0.952	n.s
Pairwise comparison (Time * Genotype)						
Time	**A**	**B**	**Mean Difference (A-B)**	**Std. Error**	**P value**	**Sig.**
0-2 min	het	mutant	0.384	0.500	0.445	n.s
8-10 min	het	mutant	0.426	0.504	0.399	n.s
Genotype						
wt	0-2 min	8-10 min	3.691	0.507	< 0.0001	****
mutant	0-2 min	8-10 min	3.649	0.497	< 0.0001	****

Table 9.4. Statistical analysis of thigmotaxis in *disc1*^{exon6} adults

The results of a two-way ANOVA for time and genotype are shown. There is a significant effect of genotype on time on time spent in periphery of the tank. There is no significant effect of time on time spent in periphery of the tank. There is a significant interaction between genotype and time. Pairwise comparison reveals a significant difference between *disc1*$^{exon6/exon6}$ mutants and *disc1*$^{+/+}$ controls in the first 2 min of recording. There is no significant difference between *disc1*$^{exon6/exon6}$ mutants and *disc1*$^{+/+}$ controls in last 2 min of recording (Time). There was a significant difference in between the first and last 2 min in *disc1*$^{+/+}$ controls and no significant difference between the first and last 2 min in *disc1*^{exon6} mutants. P > 0.05 = n.s. See Figure 5.8D for plot.

Two -way ANOVA (Thigmotaxis, *disc1*^{exon6})						
Factor			**F value**	**d.f**	**P value**	**Sig.**
Time			3.613	1	0.060	n.s
Genotype			7.501	1	0.007	**
Time * Genotype			25.813	1	< 0.0001	****
Pairwise comparison (Time * Genotype)						
Time	**A**	**B**	**Mean Difference (A-B)**	**Std. Error**	**P value**	**Sig.**
0-2 min	wt	mutant	31.195	5.642	< 0.0001	****
8-10 min	wt	mutant	9.342	5.642	0.101	n.s
Genotype						
wt	0-2 min	8-10 min	27.852	5.812	< 0.0001	****
mutant	0-2 min	8-10 min	12.686	5.467	0.022	n.s

Table 9.5. Statistical analysis of darting episodes in *disc1*^{Y472X} adults

The results of a two-way ANOVA for time and genotype are shown. There is a significant effect of time on darting. There is no significant effect of genotype on darting. There is no significant interaction between genotype and time. Pairwise comparison reveals no significant differences between *disc1*$^{Y472X/Y472X}$ mutants and *disc1*$^{+/+}$ controls in the first and last 2 min of recording (Time). There is a significant difference in between the first and last 2 min in *disc1*$^{+/+}$ controls and a significant difference in between the first and last 2 min in *disc1*$^{Y472X/Y472X}$ mutants (Genotype). P > 0.05 = n.s, P < 0.0001 = ****. See Figure 5.10A for plot.

Two -way ANOVA (Darting, *disc1*^{exon6})				
Factor	**F value**	**d.f**	**P value**	**Sig.**
Time	24.325	1	< 0.0001	****
Genotype	0.174	1	0.678	n.s
Time * Genotype	0.639	1	0.426	n.s

Pairwise comparison (Time * Genotype)						
Time	**A**	**B**	**Mean Difference (A-B)**	**Std. Error**	**P value**	**Sig.**
0-2 min	wt	mutant	0.473	0.550	0.392	n.s
8-10 min	wt	mutant	0.149	0.550	0.787	n.s
Genotype						
het	0-2 min	8-10 min	1.609	0.567	0.006	***
mutant	0-2 min	8-10 min	2.231	0.533	< 0.0001	****

Table 9.6. Statistical analysis of darting episodes in *disc1*^{exon6} adults

The results of a two-way ANOVA for time and genotype are shown. There is a significant effect of time on darting. There is no significant effect of genotype on darting. There is no significant interaction between genotype and time. Pairwise comparison reveals no significant differences between *disc1*$^{+/+}$ controls and *disc1*$^{exon6/exon6}$ mutants in the first and last 2 min of recording (Time). There is a significant difference in between the first and last 2 min in *disc1*$^{+/+}$ controls and a significant difference in between the first and last 2 min in *disc1*$^{exon6/exon6}$ mutants (Genotype). P > 0.05 = n.s, P < 0.0001 = ****. See Figure 5.10B for plot.

Two -way ANOVA (Freezing, *disc1*^{Y472X})						
Factor			**F value**	**d.f**	**P value**	**Sig.**
Time			9.436	1	0.003	**
Genotype			0.261	1	0.611	n.s
Time * Genotype			0.458	1	0.500	n.s
Pairwise comparison (Time * Genotype)						
Time	**A**	**B**	**Mean Difference (A-B)**	**Std. Error**	**P value**	**Sig.**
0-2 min	wt	mutant	4.600	5.350	0.392	n.s
8-10 min	wt	mutant	0.645	5.602	0.909	n.s
Genotype						
wt	0-2 min	8-10 min	9.275	5.602	0.101	n.s
mutant	0-2 min	8-10 min	14.520	5.350	0.008	**

Table 9.7. Statistical analysis of freezing episodes in *disc1*^{Y472X} adults

The results of a two-way ANOVA for time and genotype are shown. There is a significant effect of time on freezing. There is no significant effect of genotype on freezing. There is no significant interaction between genotype and time. Pairwise comparison reveals no significant differences between *disc1*$^{Y472X/Y472X}$ mutants and *disc1*$^{+/+}$ controls in the first and last 2 min of recording (Time). There is no significant difference in between the first and last 2 min in *disc1*$^{+/+}$ controls and a significant difference in between the first and last 2 min in *disc1*$^{Y472X/Y472X}$ mutants (Genotype). P > 0.05 = n.s, P < 0.0001 = ****. See Figure 5.10C for plot.

Two -way ANOVA (Freezing, *disc1*^{exon6})						
Factor			**F value**	**d.f**	**P value**	**Sig.**
Time			6.124	1	0.015	*
Genotype			6.541	1	0.012	*
Time * Genotype			3.137	1	0.080	n.s
Pairwise comparison (Time * Genotype)						
Time	**A**	**B**	**Mean Difference (A-B)**	**Std. Error**	**P value**	**Sig.**
0-2 min	wt	mutant	13.254	4.330	0.003	**
8-10 min	wt	mutant	2.408	4.330	0.579	n.s
Genotype						
wt	0-2 min	8-10 min	13.000	4.461	0.004	**
mutant	0-2 min	8-10 min	2.154	4.195	0.609	n.s

Table 9.8. Statistical analysis of freezing episodes in *disc1*^{exon6} adults

The results of a two-way ANOVA for time and genotype are shown. There is a significant effect of time and genotype on freezing. There is no significant interaction between genotype and time. Pairwise comparison reveals a significant difference between *disc1*$^{exon6/exon6}$ mutants and *disc1*$^{+/+}$ controls in the first 2 min of recording. There is no significant difference between *disc1*$^{exon6/exon6}$ mutants and *disc1*$^{+/+}$ controls in last 2 min of recording (Time). There is a significant difference in between the first and last 2 min in *disc1*$^{+/+}$ controls and no significant difference in between the first and last 2 min in *disc1*$^{exon6/exon6}$ mutants (Genotype). P > 0.05 = n.s, P < 0.01 = *, P < 0.001 = **. See Figure 5.10D for plot.

References

Abazyan, B., Nomura, J., Kannan, G., Ishizuka, K., Tamashiro, K.L., Nucifora, F., Pogorelov, V., Ladenheim, B., Yang, C.X., Krasnova, I.N., et al. (2010). Prenatal Interaction of Mutant DISC1 and Immune Activation Produces Adult Psychopathology. Biological Psychiatry 68, 1172-1181.

Adamantidis, A.R., Zhang, F., Aravanis, A.M., Deisseroth, K., and De Lecea, L. (2007). Neural substrates of awakening probed with optogenetic control of hypocretin neurons. Nature 450, 420-429.

Ahnaou, A., and Drinkenburg, W.H.I.M. (2011). Disruption of glycogen synthase kinase-3-beta activity leads to abnormalities in physiological measures in mice. Behavioural Brain Research 221, 246-252.

Akerstrom, B., Brodin, T., Reis, K., and Bjorck, L. (1985). Protein-G – A powerful tool for binding and detection of monoclonal and polyclonal antibodies. Journal of Immunology 135, 2589-2592.

Alsop, D., and Vijayan, M.M. (2009). Molecular programming of the corticosteroid stress axis during zebrafish development. Comparative Biochemistry and Physiology a-Molecular & Integrative Physiology 153, 49-54.

Altschul, A.T. (1988). Symptoms in the mind – An Introduction to descriptive psychopathology – Sims, A. Journal of Advanced Nursing 13, 533-534.

Amir-Zilberstein, L., Blechman, J., Sztainberg, Y., Norton, W.N.J., Reuveny, A., Borodovsky, N., Tahor, M., Bonkowsky, J.L., Bally-Cuif, L., Chen, A., and Levkowitz, G. (2012). Homeodomain Protein Otp and Activity-Dependent Splicing Modulate Neuronal Adaptation to Stress. Neuron 73, 279-291.

Anderson, J.L., Mulligan, T.S., Shen, M.C., Wang, H., Scahill, C.M., Tan, F.J., Du, S.J., Busch-Nentwich, E.M., and Farber, S.A. (2017). mRNA processing in mutant zebrafish lines generated by chemical and CRISPR-mediated mutagenesis produces unexpected transcripts that escape nonsense-mediated decay. Plos Genetics 13, e1007105.

Aschoff, J. (1999). Masking and parametric effects of high-frequency light-dark cycles. Japanese Journal of Physiology 49, 11-18.

Atkin, T.A., Brandon, N.J., and Kittler, J.T. (2012). Disrupted in Schizophrenia 1 forms pathological aggresomes that disrupt its function in intracellular transport. Human Molecular Genetics 21, 2017-2028.

Austin, C.P., Ma, L., Ky, B., Morris, J.A., and Shughrue, P.J. (2003). DISC1 (Disrupted in Schizophrenia-1) is expressed in limbic regions of the primate brain. Neuroreport 14, 951-954.

Ayhan, Y., Abazyan, B., Nomura, J., Kim, R., Ladenheim, B., Krasnova, I.N., Sawa, A., Margolis, R.L., Cadet, J.L., Mori, S., et al. (2011). Differential effects of prenatal and postnatal expressions of mutant human DISC1 on neurobehavioral phenotypes in transgenic mice: evidence for neurodevelopmental origin of major psychiatric disorders. Molecular Psychiatry 16, 293-306.

Baghdoyan, H.A., Lydic, R., Callaway, C.W., and Hobson, J.A. (1989). The carbachol-induced enhancement of desynchronized sleep signs is dose dependent and antagonized by centrally administered atropine. Neuropsychopharmacology 2, 67-79.

Bain, J., Plater, L., Elliott, M., Shpiro, N., Hastie, C.J., McLauchlan, H., Klevernic, I., Arthur, J.S.C., Alessi, D.R., and Cohen, P. (2007). The selectivity of protein kinase inhibitors: a further update. Biochemical Journal 408, 297-315.

Bakharev, V., Tikhomirov, S., and Lozhkina, T. (1986). Psychotropic properties of oxytocin. Neuroscience and Behavioral Physiology 16, 160-164.

Bao, A.M., Hestiantoro, A., Van Someren, E.J.W., Swaab, D.F., and Zhou, J.N. (2005). Colocalization of corticotropin-releasing hormone and oestrogen receptor-alpha in the paraventricular nucleus of the hypothalamus in mood disorders. Brain 128, 1301-1313.

Baoji, X., and Xiangyang, X. (2016). Neurotrophic factor control of satiety and body weight. Nature Reviews Neuroscience 17, 282-292.

Baraban, S.C., Taylor, M.R., Castro, P.A., and Baier, H. (2005). Pentylenetetrazole induced changes in zebrafish behavior, neural activity and c-FoS expression. Neuroscience 131, 759-768.

Barodia, S.K., Park, S.K., Ishizuka, K., Sawa, A., and Kamiya, A. (2015). Half-life of DISC1 protein and its pathological significance under hypoxia stress. Neuroscience Research 97, 1-6.

Bencan, Z., Sledge, D., and Levin, E.D. (2009). Buspirone, chlordiazepoxide and diazepam effects in a zebrafish model of anxiety. Pharmacology Biochemistry and Behavior 94, 75-80.

Bentea, E., Depasquale, E.A.K., O'Donovan, S.M., Sullivan, C.R., Simmons, M., Meador-Woodruff, J.H., Zhou, Y., Xu, C.C., Bai, B., Peng, J.M., et al. (2019). Kinase network dysregulation in a human induced pluripotent stem cell model of DISC1 schizophrenia. Molecular Omics 15, 173-188.

Bernier, N.J., Bedard, N., and Peter, R.E. (2004). Effects of cortisol on food intake, growth, and forebrain neuropeptide Y and corticotropin-releasing factor gene expression in goldfish. General and Comparative Endocrinology 135, 230-240.

Bernier, N.J., and Peter, R.E. (2001). The hypothalamic-pituitary-interrenal axis and the control of food intake in teleost fish. Comparative Biochemistry and Physiology B-Biochemistry & Molecular Biology 129, 639-644.

Bernstein, H.-G., Dobrowolny, H., Bogerts, B., Keilhoff, G., and Steiner, J. (2019). The hypothalamus and neuropsychiatric disorders: psychiatry meets microscopy. Cell and Tissue Research 375, 243-258.

Best, J.D., Berghmans, S., Hunt, J.J., Clarke, S.C., Fleming, A., Goldsmith, P., and Roach, A.G. (2008). Non-associative learning in larval zebrafish. Neuropsychopharmacology 33, 1206-1215.

Betzel, R. (2018). Organizing principles of whole-brain functional connectivity in zebrafish larvae. BioRxiv.

Bingham, N.C., Anderson, K.K., Reuter, A.L., Stallings, N.R., and Parker, K.L. (2008). Selective loss of leptin receptors in the ventromedial hypothalamic nucleus results in increased adiposity and a metabolic syndrome. Endocrinology 149, 2138-2148.

Biran, J., Tahor, M., Wircer, E., and Levkowitz, G. (2015). Role of developmental factors in hypothalamic function. Frontiers in Neuroanatomy 9, 47.

Blackwood, D.H.R., Fordyce, A., Walker, M.T., St Clair, D.M., Porteous, D.J., and Muir, W.J. (2001). Schizophrenia and affective disorders - Cosegregation with a translocation at chromosome 1q42 that

directly disrupts brain-expressed genes: Clinical and P300 findings in a family. American Journal of Human Genetics 69, 428-433.

Blaker-Lee, A.L., Gupta, S., and Sive, H. (2011). Using the zebrafish as a tool for analysis of autism risk gene function. Developmental Biology 356, 121-121.

Blaser, R.E., Chadwick, L., and McGinnis, G.C. (2010). Behavioral measures of anxiety in zebrafish (Danio rerio). Behavioural Brain Research 208, 56-62.

Blechinger, S.R., Kusch, R.C., Haugo, K., Matz, C., Chivers, D.P., and Krone, P.H. (2007). Brief embryonic cadmium exposure induces a stress response and cell death in the developing olfactory system followed by long-term olfactory deficits in juvenile zebrafish. Toxicology and Applied Pharmacology 224, 72-80.

Blechman, J., Borodovsky, N., Eisenberg, M., Nabel-Rosen, H., Grimm, J., and Levkowitz, G. (2007). Specification of hypothalamic neurons by dual regulation of the homeodomain protein Orthopedia. Development 134, 4417-4426.

Bojanowska, E., and Ciosek, J. (2016). Can We Selectively Reduce Appetite for Energy-Dense Foods? An Overview of Pharmacological Strategies for Modification of Food Preference Behavior. Current neuropharmacology 14, 118-142.

Boucher, A.A., Hunt, G.E., Karl, T., Micheau, J., McGregor, I.S., and Arnold, J.C. (2007). Heterozygous neuregulin 1 mice display greater baseline and Δ 9 -tetrahydrocannabinol-induced c-Fos expression. Neuroscience 149, 861-870.

Boyd, P.J., Cunliffe, V.T., Roy, S., and Wood, J.D. (2015). Sonic hedgehog functions upstream of disrupted-in-schizophrenia 1 (disc1): implications for mental illness. Biology Open 4, 1336-1343.

Braff, D.L., Swerdlow, N.R., and Geyer, M.A. (1995). Gating and habituation deficits in the schizophrenia disorders. Clinical Neuroscience 3, 131-139.

Brandon, N.J., Millar, J.K., Korth, C., Sive, H., Singh, K.K., and Sawa, A. (2009). Understanding the Role of DISC1 in Psychiatric Disease and during Normal Development. Journal of Neuroscience 29, 12768-12775.

Brown, D., Samsa, L.A., Ito, C., Ma, H., Batres, K., Arnaout, R., Qian, L., and Liu, J. (2018). Neuregulin-1 is essential for nerve plexus formation during cardiac maturation. Journal of Cellular and Molecular Medicine 22, 2007-2017.

Bruni, G., Rennekamp, A.J., Velenich, A., McCarroll, M., Gendelev, L., Fertsch, E., Taylor, J., Lakhani, P., Lensen, D., Evron, T., et al. (2016). Zebrafish behavioral profiling identifies multitarget antipsychotic-like compounds. Nature Chemical Biology 12, 559–566.

Buckley, P.F. (2005). Neuroimaging of schizophrenia: structural abnormalities and pathophysiological implications. Neuropsychiatric disease and treatment 1, 193-204.

Buckner, R.L., Andrews-Hanna, J.R., and Schacter, D.L. (2008). The brain's default network - Anatomy, function, and relevance to disease. Year in Cognitive Neuroscience 2008 1124, 1-38.

Burgess, H.A., and Granato, M. (2007). Modulation of locomotor activity in larval zebrafish during light adaptation. Journal of Experimental Biology 210, 2526-2539.

Camargo, L.M., Collura, V., Rain, J.C., Mizuguchi, K., Hermjakob, H., Kerrien, S., Bonnert, T.P., Whiting, P.J., and Brandon, N.J. (2007). Disrupted in schizophrenia 1 interactome: evidence for the close connectivity of risk genes and a potential synaptic basis for schizophrenia. Molecular Psychiatry 12, 74-86.

Candy, J., and Collet, C. (2005). Two tyrosine hydroxylase genes in teleosts. Biochimica Et Biophysica Acta-Gene Structure and Expression 1727, 35-44.

Cannon, T.D., Hennah, W., van Erp, T.G.M., Thompson, P.M., Lonnqvist, J., Huttunen, M., Gasperoni, T., Tuulio-Henriksson, A., Pirkola, T., Toga, A.W., et al. (2005). Association of DISC1/TRAX haplotypes with schizophrenia, reduced prefrontal gray matter, and impaired short- and long-term memory. Archives of General Psychiatry 62, 1205-1213.

Carbone, M.A., Jordan, K.W., Lyman, R.F., Harbison, S.T., Leips, J., Morgan, T.J., Deluca, M., Awadalla, P., and Mackay, T.F.C. (2006). Phenotypic Variation and Natural Selection at Catsup, a Pleiotropic Quantitative Trait Gene in Drosophila. Current Biology 16, 912-919.

Carlsson, A., Waters, N., and Carlsson, M.L. (1999). Neurotransmitter interactions in schizophrenia—therapeutic implications. Biological Psychiatry 46, 1388-1395.

Cengiz, M., Karaj, V., Kocabasoglu, N., Gozubatik-Celik, G., Dirican, A., and Bayoglu, B. (2019). Orexin/hypocretin receptor, Orx(1), gene variants are associated with major depressive disorder. International Journal of Psychiatry in Clinical Practice 23, 114-121.

Champagne, D.L., Hoefnagels, C.C.M., de Kloet, R.E., and Richardson, M.K. (2010). Translating rodent behavioral repertoire to zebrafish (Danio rerio): Relevance for stress research. Behavioural Brain Research 214, 332-342.

Chandran, J.S., Kazanis, I., Clapcote, S.J., Ogawa, F., Millar, J.K., Porteous, D.J., and Ffrench-Constant, C. (2014). Disc1 Variation Leads to Specific Alterations in Adult Neurogenesis. Plos One 9, e108088.

Chemelli, R.M., Willie, J.T., Sinton, C.M., Elmquist, J.K., Scammell, T., Lee, C., Richardson, J.A., Williams, S.C., Xiong, Y.M., Kisanuki, Y., et al. (1999). Narcolepsy in orexin knockout mice: Molecular genetics of sleep regulation. Cell 98, 437-451.

Chen, E., Y., Deran, M., T., Ignatius, M., S., Grandinetti, K.B., Clagg, R., Mccarthy, K., M., Lobbardi, R., M., Brockmann, J., Keller, C., Wu, C., and Langenau, D., M. (2014). Glycogen synthase kinase 3 inhibitors induce the canonical WNT/β-catenin pathway to suppress growth and self-renewal in embryonal rhabdomyosarcoma. Proceedings of the National Academy of Sciences 111, 5349.

Chen, S.-Y., Huang, P.-H., and Cheng, H.-J. (2011). Disrupted-in-Schizophrenia 1-mediated axon guidance involves TRIO-RAC-PAK small GTPase pathway signaling. Proceedings of the National Academy of Sciences of the United States of America 108, 5861-5866.

Cheng, R.K., Jesuthasan, S.J., and Penney, T.B. (2014). Zebrafish forebrain and temporal conditioning. Philosophical Transactions of the Royal Society B-Biological Sciences 369, 20120462.

Cheung, C.C., Krause, W.C., Edwards, R.H., Yang, C.F., Shah, N.M., Hnasko, T.S., and Ingraham, H.A. (2015). Sex-dependent changes in metabolism and behavior, as well as reduced anxiety after eliminating ventromedial hypothalamus excitatory output. Molecular Metabolism 4, 857-866.

Chohan, T.W., Boucher, A.A., Spencer, J.R., Kassem, M.S., Hamdi, A.A., Karl, T., Fok, S.Y., Bennett, M.R., and Arnold, J.C. (2014). Partial Genetic Deletion of Neuregulin 1 Modulates the Effects of

Stress on Sensorimotor Gating, Dendritic Morphology, and HPA Axis Activity in Adolescent Mice. Schizophrenia Bulletin 40, 1272-1284.

Chubb, J.E., Bradshaw, N.J., Soares, D.C., Porteous, D.J., and Millar, J.K. (2008). The DISC locus in psychiatric illness. Molecular Psychiatry 13, 36-64.

Clapcote, S.J., Lipina, T.V., Millar, J.K., Mackie, S., Christie, S., Ogawa, F., Lerch, J.P., Trimble, K., Uchiyama, M., Sakuraba, Y., et al. (2007). Behavioral phenotypes of Disc1 missense mutations in mice. Neuron 54, 387-402.

Clapcote, S.J., and Roder, J.C. (2006). Deletion polymorphism of Disc1 is common to all 129 mouse substrains: Implications for gene-targeting studies of brain function. Genetics 173, 2407-2410.

Clark, D.A., Arranz, M.J., Mata, I., Lopez-Ilundain, J., Perez-Nievas, F., and Kerwin, R.W. (2005). Polymorphisms in the promoter region of the alpha1A-adrenoceptor gene are associated with schizophrenia/schizoaffective disorder in a Spanish isolate population. Biological Psychiatry 58, 435-439.

Coe, T.S., Hamilton, P.B., Griffiths, A.M., Hodgson, D.J., Wahab, M.A., and Tyler, C.R. (2009). Genetic variation in strains of zebrafish (Danio rerio) and the implications for ecotoxicology studies. Ecotoxicology 18, 144-150.

Conroy, S., Francis, M., and Hulvershorn, L. (2018). Identifying and Treating the Prodromal Phases of Bipolar Disorder and Schizophrenia. Current Treatment Options in Psychiatry 5, 113-128.

Cortes, R., Teles, M., Oliveira, M., Fierro-Castro, C., Tort, L., and Cerda-Reverter, J.M. (2018). Effects of acute handling stress on short-term central expression of orexigenic/anorexigenic genes in zebrafish. Fish Physiology and Biochemistry 44, 257-272.

Cotter, D., Kerwin, R., Al-Sarraji, S., Brion, J.P., Chadwich, A., Lovestone, S., Anderton, B., and Everall, I. (1998). Abnormalities of Wnt signalling in schizophrenia - evidence for neurodevelopmental abnormality. Neuroreport 9, 1379-1383.

Cowan, K., and Storey, K. (2003). Mitogen-activated protein kinases: new signaling pathways functioning in cellular responses to environmental stress. J Exp Biol 206, 1107-1115.

Cowley, M.A., Smart, J.L., Rubinstein, M., Cordan, M.G., Diano, S., Horvath, T.L., Cone, R.D., and Low, M.J. (2001). Leptin activates anorexigenic POMC neurons through a neural network in the arcuate nucleus. Nature 411, 480-484.

Cutting, J., and Dunne, F. (1986). The Nature of the abnormal perceptual experiences at the onset of schizophrenia. Psychopathology 19, 347-352.

D'Angelo, D., Lebon, S., Chen, Q.X., Martin-Brevet, S., Snyder, L.G., Hippolyte, L., Hanson, E., Maillard, A.M., Faucett, W.A., Mace, A., et al. (2016). Defining the Effect of the 16p11.2 Duplication on Cognition, Behavior, and Medical Comorbidities. Jama Psychiatry 73, 20-30.

da Fonseca, T.L., Correia, A., Hasselaar, W., van der Linde, H.C., Willemsen, R., and Outeiro, T.F. (2013). The zebrafish homologue of Parkinson's disease ATP13A2 is essential for embryonic survival. Brain Research Bulletin 90, 118-126.

Dachtler, J., Elliott, C., Rodgers, R.J., Baillie, G.S., and Clapcote, S.J. (2016). Missense mutation in DISC1 C-terminal coiled-coil has GSK3 beta signaling and sex-dependent behavioral effects in mice. Scientific Reports 6, 18748.

Davidson, R.J., Irwin, W., Anderle, M.J., and Kalin, N.H. (2003). The neural substrates of affective processing in depressed patients treated with venlafaxine. American Journal of Psychiatry 160, 64-75.

Davis, J., Eyre, H., Jacka, F.N., Dodd, S., Dean, O., McEwen, S., Debnath, M., McGrath, J., Maes, M., Amminger, P., et al. (2016). A review of vulnerability and risks for schizophrenia: Beyond the two-hit hypothesis. Neuroscience and Biobehavioral Reviews 65, 185-194.

Davis, K.L., Kahn, R.S., Ko, G., and Davidson, M. (1991). Dopamine in Schizophrenia – A Review and Reconceptualization. American Journal of Psychiatry 148, 1474-1486.

de Abreu, M.S., Friend, A.J., Deming, K.A., Amstislavskaya, T.G., Bao, W.D., and Kalueff, A.V. (2018). Zebrafish models: do we have valid paradigms for depression? Journal of Pharmacological and Toxicological Methods 94, 16-22.

de Esch, C., van der Linde, H., Slieker, R., Willemsen, R., Wolterbeek, A., Woutersen, R., and De Groot, D. (2012). Locomotor activity assay in zebrafish larvae: Influence of age, strain and ethanol. Neurotoxicology and Teratology 34, 425-433.

de Lecea, L., Carter, M.E., and Adamantidis, A. (2012). Shining Light on Wakefulness and Arousal. Biological Psychiatry 71, 1046-1052.

De Marco, R.J., Groneberg, A.H., Yeh, C.-M., Ramirez, L.A.C., and Ryu, S. (2013). Optogenetic elevation of endogenous glucocorticoid level in larval zebrafish. Frontiers in Neural Circuits 7, 82.

De Marco, R.J., Groneberg, A.H., Yeh, C.M., Trevino, M., and Ryu, S. (2014). The behavior of larval zebrafish reveals stressor-mediated anorexia during early vertebrate development. Frontiers in Behavioral Neuroscience 8, 367.

De Rienzo, G., Bishop, J.A., Mao, Y., Pan, L., Ma, T.P., Moens, C.B., Tsai, L.-H., and Sive, H. (2011). Disc1 regulates both beta-catenin-mediated and noncanonical Wnt signaling during vertebrate embryogenesis. Faseb Journal 25, 4184-4197.

Debbané, M., Eliez, S., Badoud, D., Conus, P., Flückiger, R., and Schultze-Lutter, F. (2015). Developing Psychosis and Its Risk States Through the Lens of Schizotypy. Schizophrenia Bulletin 41, 396-407.

Deltcheva, E., Chylinski, K., Sharma, C.M., Gonzales, K., Chao, Y.J., Pirzada, Z.A., Eckert, M.R., Vogel, J., and Charpentier, E. (2011). CRISPR RNA maturation by trans-encoded small RNA and host factor RNase III. Nature 471, 602–607.

dePedro, N., AlonsoGomez, A.L., Gancedo, B., Valenciano, A.I., Delgado, M.J., and AlonsoBedate, M. (1997). Effect of alpha-helical-CRF(9-41) on feeding in goldfish: Involvement of cortisol and catecholamines. Behavioral Neuroscience 111, 398-403.

Devanaboyina, S.C., Lynch, S.M., Ober, R.J., Ram, S., Kim, D., Puig-Canto, A., Breen, S., Kasturirangan, S., Fowler, S., Peng, L., et al. (2013). The effect of pH dependence of antibody-antigen interactions on subcellular trafficking dynamics. Mabs 5, 851-859.

Dhillon, H., Zigman, J.M., Ye, C.P., Lee, C.E., McGovern, R.A., Tang, V.S., Kenny, C.D., Christiansen, L.M., White, R.D., Edelstein, E.A., et al. (2006). Leptin directly activates SF1 neurons in the VMH, and this action by leptin is required for normal body-weight homeostasis. Neuron 49, 191-203.

Dittrich, L., Petese, A., and Jackson, W. (2017). The natural Disc1-deletion present in several inbred mouse strains does not affect sleep. Sci Rep 7, 5665-5665.

Doyle, O.M., De Simoni, S., Schwarz, A.J., Brittain, C., O'Daly, O.G., Williams, S.C.R., and Mehta, M.A. (2013). Quantifying the Attenuation of the Ketamine Pharmacological Magnetic Resonance Imaging Response in Humans: A Validation Using Antipsychotic and Glutamatergic Agents. Journal of Pharmacology and Experimental Therapeutics 345, 151-160.

Draper, B.W., McCallum, C.M., Stout, J.L., Slade, A.J., and Moens, C.B. (2004). A high-throughput method for identifying N-ethyl-N-nitrosourea (ENU)-induced point mutations in zebrafish. Zebrafish:2nd Edition Genetics Genomics and Informatics 77, 91-112.

Drerup, C.M., Wiora, H.M., Topczewski, J., and Morris, J.A. (2009). Disc1 regulates foxd3 and sox10 expression, affecting neural crest migration and differentiation. Development 136, 2623-2632.

Drevets, W., Price, J., and Furey, M. (2008). Brain structural and functional abnormalities in mood disorders: implications for neurocircuitry models of depression. Brain Structure and Function 213, 93-118.

Duan, X., Chang, J.H., Ge, S., Faulkner, R.L., Kim, J.Y., Kitabatake, Y., Liu, X.-b., Yang, C.-H., Jordan, J.D., Ma, D.K., et al. (2007). Disrupted-in-schizophrenia 1 regulates integration of newly generated neurons in the adult brain. Cell 130, 1146-1158.

Dubal, S., and Viaud-Delmon, I. (2008). Magical ideation and hyperacusis. Cortex 44, 1379-1386.

Duncan, L., Yilmaz, Z., Gaspar, H., Walters, R., Goldstein, J., Anttila, V., Bulik-Sullivan, B., Ripke, S., Thornton, L., Daly, M., et al. (2017). Significant Locus and Metabolic Genetic Correlations Revealed in Genome-Wide Association Study of Anorexia Nervosa. American Journal of Psychiatry 174, 850-858.

Duncan, R.N., Xie, Y.Y., McPherson, A.D., Taibi, A.V., Bonkowsky, J.L., Douglass, A.D., and Dorsky, R.I. (2016). Hypothalamic radial glia function as self-renewing neural progenitors in the absence of Wnt/beta-catenin signaling. Development 143, 45-53.

Dunn, Timothy w., Gebhardt, C., Naumann, Eva a., Riegler, C., Ahrens, Misha b., Engert, F., and Del bene, F. (2016). Neural Circuits Underlying Visually Evoked Escapes in Larval Zebrafish. Neuron 89, 613-628.

Dwivedi, Y., Rizavi, H.S., Roberts, R.C., Conley, R.C., Tamminga, C.A., and Pandey, G.N. (2001). Reduced activation and expression of ERK1/2 MAP kinase in the post-mortem brain of depressed suicide subjects. Journal of Neurochemistry 77, 916-928.

Eachus, H., Bright, C., Cunliffe, V.T., Placzek, M., Wood, J.D., and Watt, P.J. (2017). Disrupted-in-Schizophrenia-1 is essential for normal hypothalamic-pituitary-interrenal (HPI) axis function. Human Molecular Genetics 26, 1992-2005.

Eaton, R.C., Bombardieri, R.A., and Meyer, D.L. (1977). The Mauthner-initiated startle response in teleost fish. The Journal of experimental biology 66, 65-81.

Egan, R.J., Bergner, C.L., Hart, P.C., Cachat, J.M., Canavello, P.R., Elegante, M.F., Elkhayat, S.I., Bartels, B.K., Tien, A.K., Tien, D.H., et al. (2009). Understanding behavioral and physiological phenotypes of stress and anxiety in zebrafish. Behavioural Brain Research 205, 38-44.

Ekelund, J., Hennah, W., Hiekkalinna, T., Parker, A., Meyer, J., Lonnqvist, J., and Peltonen, L. (2004). Replication of 1q42 linkage in Finnish schizophrenia pedigrees. Molecular Psychiatry 9, 1037-1041.

Ellis, L.D., and Soanes, K.H. (2012). A larval zebrafish model of bipolar disorder as a screening platform for neuro-therapeutics. Behavioural Brain Research 233, 450-457.

Emamian, E.S., Hall, D., Birnbaum, M.J., Karayiorgou, M., and Gogos, J.A. (2004). Convergent evidence for impaired AKT1-GSK3 beta signaling in schizophrenia. Nature Genetics 36, 131-137.

Epel, E.S., McEwen, B., Seeman, T., Matthews, K., Castellazzo, G., Brownell, K.D., Bell, J., and Ickovics, J.R. (2000). Stress and body shape: Stress-induced cortisol secretion is consistently greater among women with central fat. Psychosomatic Medicine 62, 623-632.

Ettinger, U., Hurlemann, R., and Chan, R.C.K. (2018). Oxytocin and Schizophrenia Spectrum Disorders. Current topics in behavioral neurosciences 35, 515-527.

Fadel, J., Bubser, M., and Deutch, A.Y. (2002). Differential activation of orexin neurons by antipsychotic drugs associated with weight gain. Journal of Neuroscience 22, 6742-6746.

Fatemi, S.H., and Folsom, T.D. (2009). The Neurodevelopmental Hypothesis of Schizophrenia, Revisited. Schizophrenia Bulletin 35, 528-548.

Faulconbridge, L.F., Wadden, T.A., Berkowitz, R.I., Pulcini, M.E., and Treadwell, T. (2011). Treatment of Comorbid Obesity and Major Depressive Disorder: A Prospective Pilot Study for their Combined Treatment. Journal of Obesity, 870385.

Faulkner, R.L., Jang, M.-H., Liu, X.-B., Duan, X., Sailor, K.A., Kim, J.Y., Ge, S., Jones, E.G., Ming, G.-l., Song, H., and Cheng, H.-J. (2008). Development of hippocampal mossy fiber synaptic outputs by new neurons in the adult brain. Proceedings of the National Academy of Sciences of the United States of America 105, 14157-14162.

Fernandes, A.M., Beddows, E., Filippi, A., and Driever, W. (2013). Orthopedia Transcription Factor otpa and otpb Paralogous Genes Function during Dopaminergic and Neuroendocrine Cell Specification in Larval Zebrafish. Plos One 8, e75002.

Fernandes, A.M., Fero, K., Arrenberg, A.B., Bergeron, S.A., Driever, W., and Burgess, H.A. (2012). Deep Brain Photoreceptors Control Light-Seeking Behavior in Zebrafish Larvae. Current Biology 22, 2042-2047.

Fernandes, Y., and Gerlai, R. (2009). Long-Term Behavioral Changes in Response to Early Developmental Exposure to Ethanol in Zebrafish. Alcoholism: Clinical and Experimental Research 33, 601-609.

Fletcher, P.C., Napolitano, A., Skeggs, A., Miller, S.R., Delafont, B., Cambridge, V.C., de Wit, S., Nathan, P.J., Brooke, A., O'Rahilly, S., et al. (2010). Distinct Modulatory Effects of Satiety and Sibutramine on Brain Responses to Food Images in Humans: A Double Dissociation across Hypothalamus, Amygdala, and Ventral Striatum. Journal of Neuroscience 30, 14346-14355.

Fornasiero, E.F., Mandad, S., Wildhagen, H., Alevra, M., Rammner, B., Keihani, S., Opazo, F., Urban, I., Ischebeck, T., Sakib, M.S., et al. (2018). Precisely measured protein lifetimes in the mouse brain reveal differences across tissues and subcellular fractions. Nature Communications 9, 4230.

Freyberg, Z., Ferrando, S.J., and Javitch, J.A. (2010). Roles of the Akt/GSK-3 and Wnt Signaling Pathways in Schizophrenia and Antipsychotic Drug Action. American Journal of Psychiatry 167, 388-396.

Fu, Y., Foden, J.A., Khayter, C., Maeder, M.L., Reyon, D., Joung, J.K., and Sander, J.D. (2013). High-frequency off-target mutagenesis induced by CRISPR-Cas nucleases in human cells. Nature Biotechnology 31, 822–826.

Fukunaka, Y., Shinkai, T., Hwang, R., Hori, H., Utsunomiya, K., Sakata, S., Naoe, Y., Shimizu, K., Matsumoto, C., Ohmori, O., and Nakamura, J. (2007). The orexin 1 receptor (HCRTR1) gene as a susceptibility gene contributing to polydipsia-hyponatremia in schizophrenia. Neuromolecular Medicine 9, 292-297.

Fuzzen, M.L.M., Van Der Kraak, G., and Bernier, N.J. (2010). Stirring Up New Ideas About the Regulation of the Hypothalamic-Pituitary-Interrenal Axis in Zebrafish (Danio rerio). Zebrafish 7, 349-358.

Gaj, T., Gersbach, C.A., and Barbas, C.F. (2013). ZFN, TALEN, and CRISPR/Cas-based methods for genome engineering. Trends in Biotechnology 31, 397-405.

Gao, Y., Chan, R.H.M., Chow, T.W.S., Zhang, L.Y., Bonilla, S., Pang, C.P., Zhang, M.Z., and Leung, Y.F. (2014). A High-Throughput Zebrafish Screening Method for Visual Mutants by Light-Induced Locomotor Response. Ieee-Acm Transactions on Computational Biology and Bioinformatics 11, 693-701.

Gassmann, M., Casagranda, F., Orioli, D., Simon, H., Lai, C., Klein, R., and Lemke, G. (1995). Aberrant Neural and Cardiac Development in Mice lacking the ERBB4 Neuregulin receptor. Nature 378, 390-394.

Geng, Y.J., and Peterson, R.T. (2019). The zebrafish subcortical social brain as a model for studying social behavior disorders. Disease Models & Mechanisms 12.

Gerlai, R., Lahav, M., Guo, S., and Rosenthal, A. (2000). Drinks like a fish: zebra fish (Danio rerio) as a behavior genetic model to study alcohol effects. Pharmacology Biochemistry and Behavior 67, 773-782.

Geyer, M.A. (2006). The family of sensorimotor gating disorders: Comorbidities or diagnostic overlaps? Neurotoxicity Research 10, 211-220.

Gimpl, G., and Fahrenholz, F. (2001). The Oxytocin Receptor System: Structure, function, and regulation. Physiological Reviews 81, 629-683.

Goldstein, J.M., Seidman, L.J., Makris, N., Ahern, T., O'brien, L.M., Caviness, V.S., Kennedy, D.N., Faraone, S.V., and Tsuang, M.T. (2007). Hypothalamic Abnormalities in Schizophrenia: Sex Effects and Genetic Vulnerability. Biological Psychiatry 61, 935-945.

Gottesman, II, and Gould, T.D. (2003). The endophenotype concept in psychiatry: Etymology and strategic intentions. American Journal of Psychiatry 160, 636-645.

Goudarzi, S., Smith, L.J.M., Schutz, S., and Hafizi, S. (2013). Interaction of DISC1 with the PTB domain of Tensin2. Cellular and Molecular Life Sciences 70, 1663-1672.

Gough, S.C.L., and O'Donovan, M.C. (2005). Clustering of metabolic comorbidity in schizophrenia: a genetic contribution? Journal of psychopharmacology (Oxford, England) 19, 47-55.

Green, E.K., Norton, N., Peirce, T., Grozeva, D., Kirov, G., Owen, M.J., O'Donovan, M.C., and Craddock, N. (2006). Evidence that a DISC1 frame-shift deletion associated with psychosis in a single family may not be a pathogenic mutation. Molecular Psychiatry 11, 798-799.

Gregus, A., Wintink, A.J., Davis, A.C., and Kalynchuk, L.E. (2005). Effect of repeated corticosterone injections and restraint stress on anxiety and depression-like behavior in male rats. Behavioural Brain Research 156, 105-114.

Grossman, L., Utterback, E., Stewart, A., Gaikwad, S., Chung, K.M., Suciu, C., Wong, K., Elegante, M., Elkhayat, S., Tan, J., et al. (2010). Characterization of behavioral and endocrine effects of LSD on zebrafish. Behavioural Brain Research 214, 277-284.

Guo, W., Liu, F., Zhang, J., Zhang, Z., Yu, L., Liu, J., Chen, H., and Xiao, C. (2014). Abnormal Default-Mode Network Homogeneity in First-Episode, Drug-Naive Major Depressive Disorder. Plos One 9, e91102

Haggarty, S.J., Fass, D., Pan, J., Ketterman, J., Holson, E., Petryshen, T.L., and Lewis, M.C. (2016). Uses of chemicals to modulate GSK-3 signaling for treatment of bipolar disorder and other brain disorders. Official Gazette of the United States Patent and Trademark Office Patents, US9265764B2.

Haghani, S., Karia, M., Cheng, R.K., and Mathuru, A.S. (2019). An Automated Assay System to Study Novel Tank Induced Anxiety. Frontiers in Behavioral Neuroscience 13, 180.

Hague, F.N., Lipina, T.V., Roder, J.C., and Wong, A.H.C. (2012). Social defeat interacts with Disc1 mutations in the mouse to affect behavior. Behavioural Brain Research 233, 337-344.

Hale, M.E. (2000). Startle responses of fish without Mauthner neurons: Escape behavior of the lumpfish (Cyclopterus lumpus). Biological Bulletin 199, 180-182.

Hall, C., and Ballachey, E.L. (1932). A study of the rat's behavior in a field. A contribution to method in comparative psychology. (University of California Publications in Psychology), pp. 1–12.

Haller, J., Tóth, M., and Halász, J. (2005). The activation of raphe serotonergic neurons in normal and hypoarousal-driven aggression: A double labeling study in rats. Behavioural Brain Research 161, 88-94.

Hamburg, H., Trossbach, S.V., Bader, V., Chwiesko, C., Kipar, A., Sauvage, M., Crum, W.R., Vernon, A.C., Bidmon, H.J., and Korth, C. (2016). Simultaneous effects on parvalbumin-positive interneuron and dopaminergic system development in a transgenic rat model for sporadic schizophrenia. Scientific Reports 6, 34946.

Hammack, S.E., Cheung, J., Rhodes, K.M., Schutz, K.C., Falls, W.A., Braas, K.M., and May, V. (2009). Chronic stress increases pituitary adenylate cyclase-activating peptide (PACAP) and brain-derived neurotrophic factor (BDNF) mRNA expression in the bed nucleus of the stria terminalis (BNST): Roles for PACAP in anxiety-like behavior. Psychoneuroendocrinology 34, 833-843.

Hansen, I.A., To, T.T., Wortmann, S., Burmester, T., Winkler, C., Meyer, S.R., Neuner, C., Fassnacht, M., and Allolio, B. (2003). The pro-opiomelanocortin gene of the zebrafish (Danio rerio). Biochemical and Biophysical Research Communications 303, 1121-1128.

Harding, A., Tian, T.H., Westbury, E., Frische, E., and Hancock, J.F. (2005). Subcellular localization determines MAP kinase signal output. Current Biology 15, 869-873.

Hashimoto, H., Shintani, N., Tanaka, K., Mori, W., Hirose, M., Matsuda, T., Sakaue, M., Miyazaki, J., Niwa, H., Tashiro, F., et al. (2001). Altered psychomotor behaviors in mice lacking pituitary adenylate cyclase-activating polypeptide (PACAP). Proceedings of the National Academy of Sciences of the United States of America 98, 13355-13360.

Hashimoto, R., Numakawa, T., Ohnishi, T., Kumamaru, E., Yagasaki, Y., Ishimoto, T., Mori, T., Nemoto, K., Adachi, N., Izumi, A., et al. (2006). Impact of the DISC1 Ser704Cys polymorphism on risk for major depression, brain morphology and ERK signaling. Human Molecular Genetics 15, 3024-3033.

Hastings, M.H., Reddy, A.B., and Maywood, E.S. (2003). A clockwork web: Circadian timing in brain and periphery, in health and disease. Nature Reviews Neuroscience 4, 649-661.

Hayashi-Takagi, A., Takaki, M., Graziane, N., Seshadri, S., Murdoch, H., Dunlop, A.J., Makino, Y., Seshadri, A.J., Ishizuka, K., Srivastava, D.P., et al. (2010). Disrupted-in-Schizophrenia 1 (DISC1) regulates spines of the glutamate synapse via Rac1. Nature Neuroscience 13, 327-U312.

Heim, C., Newport, D.J., Mletzko, T., Miller, A.H., and Hemeroff, C.B. (2008). The link between childhood trauma and depression: Insights from HPA axis studies in humans. Psychoneuroendocrinology 33, 693-710.

Hennah, W., Thomson, P., Peltonen, L., and Porteous, D. (2006). Beyond schizophrenia: The role of DISC1 in major mental illness. Schizophrenia Bulletin 32, 409-416.

Hensch, T.K. (2005). Critical period plasticity in local cortical circuits. Nature Reviews Neuroscience 6, 877-888.

Hikida, T., Jaaro-Peled, H., Seshadri, S., Oishi, K., Hookway, C., Kong, S., Wu, D., Xue, R., Andrade, M., Tankou, S., et al. (2007). Dominant-negative DISC1 transgenic mice display schizophrenia-associated phenotypes detected by measures translatable to humans. Proceedings of the National Academy of Sciences of the United States of America 104, 14501-14506.

Hill, K., Mann, L., Laws, K.R., Stephenson, C.M.E., Nimmo-Smith, I., and McKenna, P.J. (2004). Hypofrontality in schizophrenia: a meta-analysis of functional imaging studies. Acta Psychiatrica Scandinavica 110, 243-256.

Hirjak, D., Wolf, R.C., Wilder-Smith, E.P., Kubera, K.M., and Thomann, P.A. (2015). Motor Abnormalities and Basal Ganglia in Schizophrenia: Evidence from Structural Magnetic Resonance Imaging. Brain Topography 28, 135-152.

Hoff, P. (2012). Eugen Bleuler's Concept of Schizophrenia and Its Relevance to Present-Day Psychiatry. Neuropsychobiology 66, 6-13.

Hoffman, E.J., Turner, K.J., Fernandez, J.M., Cifuentes, D., Ghosh, M., Ijaz, S., Jain, R.A., Kubo, F., Bill, B.R., Baier, H., et al. (2016). Estrogens Suppress a Behavioral Phenotype in Zebrafish Mutants of the Autism Risk Gene, CNTNAP2. Neuron 89, 725-733.

Holley, S.M., Wang, E.A., Cepeda, C., Jentsch, J.D., Ross, C.A., Pletnikov, M.V., and Levine, M.S. (2013). Frontal cortical synaptic communication is abnormal in Disc1 genetic mouse models of schizophrenia. Schizophrenia Research 146, 264-272.

Holmes, A., le Guisquet, A.M., Vogel, E., Millstein, R.A., Leman, S., and Belzung, C. (2005). Early life genetic, epigenetic and environmental factors shaping emotionality in rodents. Neuroscience and Biobehavioral Reviews 29, 1335-1346.

Holsboer, F. (2000). The corticosteroid receptor hypothesis of depression. Neuropsychopharmacology 23, 477-501.

Howe, K., Clark, M.D., Torroja, C.F., Torrance, J., Berthelot, C., Muffato, M., Collins, J.E., Humphray, S., Mclaren, K., Matthews, L., et al. (2013). The zebrafish reference genome sequence and its relationship to the human genome. Nature 496, 498.

Howes, O.D., McCutcheon, R., Owen, M.J., and Murray, R.M. (2017). The Role of Genes, Stress, and Dopamine in the Development of Schizophrenia. Biological Psychiatry 81, 9-20.

Hruscha, A., Krawitz, P., Rechenberg, A., Heinrich, V., Hecht, J., Haass, C., and Schmid, B. (2013). Efficient CRISPR/Cas9 genome editing with low off-target effects in zebrafish. Development 140, 4982-4987.

Hunter, M.D., Eickhoff, S.B., Miller, T.W.R., Farrow, T.F.D., Wilkinson, I.D., and Woodruff, P.W.R. (2006). Neural activity in speech-sensitive auditory cortex during silence. Proceedings of the National Academy of Sciences of the United States of America 103, 189-194.

Hussain, A., Saraiva, L.R., Ferrero, D.M., Ahuja, G., Krishna, V.S., Liberles, S.D., and Korsching, S.I. (2013). High-affinity olfactory receptor for the death-associated odor cadaverine. Proceedings of the National Academy of Sciences of the United States of America 110, 19579-19584.

Ibi, D., Nagai, T., Koike, H., Kitahara, Y., Mizoguchi, H., Niwa, M., Jaaro-Peled, H., Nitta, A., Yoneda, Y., Nabeshima, T., et al. (2010). Combined effect of neonatal immune activation and mutant DISC1 on phenotypic changes in adulthood. Behavioural Brain Research 206, 32-37.

Inoue, D., and Wittbrodt, J. (2011). One for All-A Highly Efficient and Versatile Method for Fluorescent Immunostaining in Fish Embryos. Plos One 6, e19713.

Insel, T.R. (2010). Rethinking schizophrenia. Nature 468, 187-193.

Iosifescu, D.V. (2012). The relation between mood, cognition and psychosocial functioning in psychiatric disorders. European Neuropsychopharmacology 22, S499-S504.

Iovino, M., Messana, T., De Pergola, G., Iovino, E., Dicuonzo, F., Guastamacchia, E., Giagulli, V.A., and Triggiani, V. (2018). The Role of Neurohypophyseal Hormones Vasopressin and Oxytocin in Neuropsychiatric Disorders. Endocrine Metabolic & Immune Disorders-Drug Targets 18, 341-347.

Ishizuka, K., Kamiya, A., Oh, E.C., Kanki, H., Seshadri, S., Robinson, J.F., Murdoch, H., Dunlop, A.J., Kubo, K., Furukori, K., et al. (2011). DISC1-dependent switch from progenitor proliferation to migration in the developing cortex. Nature 473, 92-U107.

Jaaro-Peled, H., Kumar, S., Hughes, D., Kim, S., Zoubovsky, S., Hirota-Tsuyada, S., Zala, D., Sumitomo, A., Bruyere, J., Katz, B., et al. (2018). The cortico-striatal circuit regulates sensorimotor gating via Disc1/Huntingtin-mediated Bdnf transport. BioRxiv.

Jaaro-Peled, H., Altimus, C., LeGates, T., Cash-Padgett, T., Zoubovsky, S., Hikida, T., Ishizuka, K., Hattar, S., Mongrain, V., and Sawa, A. (2016). Abnormal wake/sleep pattern in a novel gain-of-function model of DISCI. Neuroscience Research 112, 63-69.

Jacob, S., Brune, C.W., Carter, C.S., Leventhal, B.L., Lord, C., and Cook, E.H. (2007). Association of the oxytocin receptor gene (OXTR) in Caucasian children and adolescents with autism. Neuroscience Letters 417, 6-9.

Jahng, J.W., Kim, N.Y., Ryu, V., Yoo, S.B., Kim, B.T., Kang, D.W., and Lee, J.H. (2008). Dexamethasone reduces food intake, weight gain and the hypothalamic 5-HT concentration and increases plasma leptin in rats. European Journal of Pharmacology 581, 64-70.

James, R., Adams, R.R., Christie, S., Buchanan, S.R., Porteous, D.J., and Millar, J.K. (2004). Disrupted in Schizophrenia 1 (DISC1) is a multicompartmentalized protein that predominantly localizes to mitochondria. Molecular and Cellular Neuroscience 26, 112-122.

Jarvis, E.D., Gunturkun, O., Bruce, L., Csillag, A., Karten, H., Kuenzel, W., Medina, L., Paxinos, G., Perkel, D.J., Shimizu, T., et al. (2005). Avian brains and a new understanding of vertebrate brain evolution. Nature Reviews Neuroscience 6, 151-159.

Jego, S., Glasgow, S.D., Herrera, C.G., Ekstrand, M., Reed, S.J., Boyce, R., Friedman, J., Burdakov, D., and Adamantidis, A.R. (2013). Optogenetic identification of a rapid eye movement sleep modulatory circuit in the hypothalamus. Nature Neuroscience 16, 1637-1643.

Jesuthasan, S. (2012). Fear, anxiety, and control in the zebrafish. Developmental Neurobiology 72, 395-403.

Jinek, M., Chylinski, K., Fonfara, I., Hauer, M., Doudna, J.A., and Charpentier, E. (2012). A Programmable Dual-RNA-Guided DNA Endonuclease in Adaptive Bacterial Immunity. Science 337, 816-821.

Jordi, J., Guggiana-Nilo, D., Bolton, A.D., Prabha, S., Ballotti, K., Herrera, K., Rennekamp, A.J., Peterson, R.T., Lutz, T.A., and Engert, F. (2018). High-throughput screening for selective appetite modulators: A multibehavioral and translational drug discovery strategy. Science Advances 4, eaav1966.

Jordi, J., Guggiana-Nilo, D., Soucy, E., Song, E., Wee, C., and Engert, F. (2015). A high-throughput assay for quantifying appetite and digestive dynamics. American Journal of Physiology 309, R345.

Joung, J.K., and Sander, J.D. (2013). INNOVATION TALENs: a widely applicable technology for targeted genome editing. Nature Reviews Molecular Cell Biology 14, 49-55.

Juan, L.-W., Liao, C.-C., Lai, W.-S., Chang, C.-Y., Pei, J.-C., Wong, W.-R., Liu, C.-M., Hwu, H.-G., and Lee, L.-J. (2014). Phenotypic characterization of C57BL/6J mice carrying the Disc1 gene from the 129S6/SvEv strain. Brain Structure and Function 219, 1417-1431.

Kakuda, K., Niwa, A., Honda, R., Yamaguchi, K., Tomita, H., Nojebuzzaman, M., Hara, A., Goto, Y., Osawa, M., and Kuwata, K. (2019). A DISC1 point mutation promotes oligomerization and impairs information processing in a mouse model of schizophrenia. Journal of Biochemistry 165, 369-378.

Kalueff, A.V., Stewart, A.M., and Gerlai, R. (2014). Zebrafish as an emerging model for studying complex brain disorders. Trends in Pharmacological Sciences 35, 63-75.

Kamiya, A., Kubo, K., Tomoda, T., Takaki, M., Youn, R., Ozeki, Y., Sawamura, N., Park, U., Kudo, C., Okawa, M., et al. (2005). A schizophrenia-associated mutation of DISC1 perturbs cerebral cortex development. Nature Cell Biology 7, 1167-1178.

Kandel, E.R., Frazier, W.T., and Coggeshall, R.E. (1967). Opposite synaptic actions mediated by different branches of an identifiable interneuron in Aplysia. Science 155, 346-349.

Kang, U.G., Seo, M.S., Roh, M.S., Kim, Y., Yoon, S.C., and Kim, Y.S. (2004). The effects of clozapine on the GSK-3-mediated signaling pathway. Febs Letters 560, 115-119.

Kaplan, K.A., McGlinchey, E.L., Soehner, A., Gershon, A., Talbot, L.S., Eidelman, P., Gruber, J., and Harvey, A.G. (2015). Hypersomnia subtypes, sleep and relapse in bipolar disorder. Psychological Medicine 45, 1751-1763.

Kapsimali, M., Caneparo, L., Houart, C., and Wilson, S.W. (2004). Inhibition of Wnt/Axin/beta-catenin pathway activity promotes ventral CNS midline tissue to adopt hypothalamic rather than floorplate identity. Development 131, 5923-5933.

Karl, T., Duffy, L., Scimone, A., Harvey, R., and Schofield, P. (2007). Altered motor activity, exploration and anxiety in heterozygous neuregulin 1 mutant mice: implications for understanding schizophrenia. Genes Brain Behav 6, 677-687.

Kegeles, L.S., Abi-Dargham, A., Frankle, W.G., Gil, R., Cooper, T.B., Slifstein, M., Hwang, D.-R., Huang, Y., Haber, S.N., and Laruelle, M. (2010). Increased Synaptic Dopamine Function in Associative Regions of the Striatum in Schizophrenia. Archives of General Psychiatry 67, 231-239.

Kelly, J.P., Wrynn, A.S., and Leonard, B.E. (1997). The olfactory bulbectomized rat as a model of depression: An update. Pharmacology and Therapeutics 74, 299-316.

Khan, I., Tantray, M.A., Hamid, H., Alam, M.S., Kalam, A., Shaikh, F., Shah, A., and Hussain, F. (2016). Synthesis of Novel Pyrimidin-4-One Bearing Piperazine Ring-Based Amides as Glycogen Synthase Kinase-3 Inhibitors with Antidepressant Activity. Chemical Biology & Drug Design 87, 764-772.

Khandaker, G.M., Barnett, J.H., White, I.R., and Jones, P.B. (2011). A quantitative meta-analysis of population-based studies of premorbid intelligence and schizophrenia. Schizophrenia Research 132, 220-227.

Kilpinen, H., Ylisaukko-Oja, T., Hennah, W., Palo, O.M., Varilo, T., Vanhala, R., Wendt, T.N.V., von Wendt, L., Paunio, T., and Peltonen, L. (2008). Association of DISC1 with autism and Asperger syndrome. Molecular Psychiatry 13, 187-196.

Kim, J.Y., Liu, C.Y., Zhang, F., Duan, X., Wen, Z., Song, J., Feighery, E., Lu, B., Rujescu, D., St Clair, D., et al. (2012). Interplay between DISC1 and GABA Signaling Regulates Neurogenesis in Mice and Risk for Schizophrenia. Cell 148, 1051-1064.

Kim, M.A., Kim, D.S., and Sohn, Y.C. (2011). Characterization of two functional glucocorticoid receptors in the marine medaka Oryzias dancena. General and Comparative Endocrinology 171, 341-349.

Kimmel CB, Ballard WW, Kimmel SR, Ullmann B & Schilling TF. (1995). Stages of embryonic development of the zebrafish. Dev. Dyn. 203, 253-310.

Kinch, C.D., Ibhazehiebo, K., Jeong, J.H., Habibi, H.R., and Kurrasch, D.M. (2015). Low-dose exposure to bisphenol A and replacement bisphenol S induces precocious hypothalamic neurogenesis in embryonic zebrafish. Proceedings of the National Academy of Sciences of the United States of America 112, 1475-1480.

Kinyua, A.W., Yang, D.J., Chang, I., and Kim, K.W. (2016). Steroidogenic Factor 1 in the Ventromedial Nucleus of the Hypothalamus Regulates Age-Dependent Obesity. Plos One 11, e0162352.

Koike, H., Arguello, P.A., Kvajo, M., Karayiorgou, M., and Gogos, J.A. (2006). Disc1 is mutated in the 129S6/SvEv strain and modulates working memory in mice. Proceedings of the National Academy of Sciences of the United States of America 103, 3693-3697.

Kokoeva, M.V., Yin, H.L., and Flier, J.S. (2005). Neurogenesis in the hypothalamus of adult mice: Potential role in energy balance. Science 310, 679-683.

Kovacs, A., Telegdy, G., Toth, G., and Penke, B. (1999). Neurotransmitter-mediated open-field behavioral action of CGRP. Life Sciences 64, 733-740.

Kozikowski, A.P., Gunosewoyo, H., Guo, S.P., Gaisina, I.N., Walter, R.L., Ketcherside, A., McClung, C.A., Mesecar, A.D., and Caldarone, B. (2011). Identification of a Glycogen Synthase Kinase-3 beta Inhibitor that Attenuates Hyperactivity in CLOCK Mutant Mice. Chemmedchem 6, 1593-1602.

Kozlovsky, N., Belmaker, R., and Agam, G. (2000). Low GSK-3(beta) immunoreactivity in postmortem frontal cortex of schizophrenic patients. The American Journal of Psychiatry 157, 831-833.

Kroeger, D., Absi, G., Gagliardi, C., Bandaru, S.S., Madara, J.C., Ferrari, L.L., Arrigoni, E., Munzberg, H., Scammell, T.E., Saper, C.B., and Vetrivelan, R. (2018). Galanin neurons in the ventrolateral preoptic area promote sleep and heat loss in mice. Nature Communications 9, 4129.

Kume, K., Kume, S., Park, S.K., Hirsh, J., and Jackson, F.R. (2005). Dopamine is a regulator of arousal in the fruit fly. Journal of Neuroscience 25, 7377-7384.

Kuroda, K., Yamada, S., Tanaka, M., Iizuka, M., Yano, H., Mori, D., Tsuboi, D., Nishioka, T., Namba, T., Iizuka, Y., et al. (2011). Behavioral alterations associated with targeted disruption of exons 2 and 3 of the Disc1 gene in the mouse. Human Molecular Genetics 20, 4666-4683.

Kurrasch, D.M., Cheung, C.C., Lee, F.Y., Tran, P.V., Hata, K., and Ingraham, H.A. (2007). The neonatal ventromedial hypothalamus transcriptome reveals novel markers with spatially distinct patterning. Journal of Neuroscience 27, 13624-13634.

Kvajo, M., McKellar, H., Arguello, P.A., Drew, L.J., Moore, H., MacDermott, A.B., Karayiorgou, M., and Gogos, J.A. (2008). A mutation in mouse Disc1 that models a schizophrenia risk allele leads to specific alterations in neuronal architecture and cognition. Proceedings of the National Academy of Sciences of the United States of America 105, 7076-7081.

Kvajo, M., McKellar, H., Drew, L.J., Lepagnol-Bestel, A.M., Xiao, L., Levy, R.J., Blazeski, R., Arguello, P.A., Lacefield, C.O., Mason, C.A., et al. (2011). Altered axonal targeting and short-term plasticity in the hippocampus of Disc1 mutant mice. Proceedings of the National Academy of Sciences of the United States of America 108, E1349-E1358.

Kyzar, E., Stewart, A.M., Landsman, S., Collins, C., Gebhardt, M., Robinson, K., and Kalueff, A.V. (2013). Behavioral effects of bidirectional modulators of brain monoamines reserpine and d-amphetamine in zebrafish. Brain Research 1527, 108-116.

Labuschagne, I., Phan, K.L., Wood, A., Angstadt, M., Chua, P., Heinrichs, M., Stout, J.C., and Nathan, P.J. (2010). Oxytocin Attenuates Amygdala Reactivity to Fear in Generalized Social Anxiety Disorder. Neuropsychopharmacology 35, 2403-2413.

Lang, P.J., Herring, D.R., Duncan, C., Richter, J., Sege, C.T., Weymar, M., Limberg-Thiesen, A., Hamm, A.O., and Bradley, M.M. (2018). The Startle-Evoked Potential: Negative Affect and Severity of Pathology in Anxiety/Mood Disorders. Biological Psychiatry-Cognitive Neuroscience and Neuroimaging 3, 626-634.

Leal, E., Fernandez-Duran, B., Guillot, R., Rios, D., and Cerda-Reverter, J.M. (2011). Stress-induced effects on feeding behavior and growth performance of the sea bass (Dicentrarchus labrax): a self-feeding approach. Journal of Comparative Physiology B-Biochemical Systemic and Environmental Physiology 181, 1035-1044.

Lebestky, T., Chang, J.-S.C., Dankert, H., Zelnik, L., Kim, Y.-C., Han, K.-A., Wolf, F.W., Perona, P., and Anderson, D.J. (2009). Two Different Forms of Arousal in Drosophila Are Oppositely Regulated by the Dopamine D1 Receptor Ortholog DopR via Distinct Neural Circuits. Neuron 64, 522-536.

Lee, J.E., Wu, S.F., Goering, L.M., and Dorsky, R.I. (2006). Canonical Wnt signaling through Lef1 is required for hypothalamic neurogenesis. Development 133, 4451-4461.

Lee, M.R., Sheskier, M.B., Farokhnia, M., Feng, N., Marenco, S., Lipska, B.K., and Leggio, L. (2018). Oxytocin receptor mRNA expression in dorsolateral prefrontal cortex in major psychiatric disorders: A human post-mortem study. Psychoneuroendocrinology 96, 143-147.

Lee, M.R., Wehring, H.J., McMahon, R.P., Linthicum, J., Cascella, N., Liu, F., Bellack, A., Buchanan, R.W., Strauss, G.P., Contoreggi, C., and Kelly, D.L. (2013). Effects of adjunctive intranasal oxytocin on olfactory identification and clinical symptoms in schizophrenia: Results from a randomized double blind placebo controlled pilot study. Schizophrenia Research 145, 110-115.

Lett, T.A.P., Wallace, T.J.M., Chowdhury, N.I., Tiwari, A.K., Kennedy, J.L., and Muller, D.J. (2012). Pharmacogenetics of antipsychotic-induced weight gain: review and clinical implications. Molecular Psychiatry 17, 242-266.

Leung, L.C., Wang, G.X., Madelaine, R., Skariah, G., Kawakami, K., Deisseroth, K., Urban, A.E., and Mourrain, P. (2019). Neural signatures of sleep in zebrafish. Nature 571, 198–204.

Levin, E.D. (2011). Zebrafish assessment of cognitive improvement and anxiolysis: filling the gap between in vitro and rodent models for drug development. Reviews in the Neurosciences 22, 75-84.

Lewis, D.A., and Levitt, P. (2002). Schizophrenia as a disorder of neurodevelopment. Annual Review of Neuroscience 25, 409-432.

Li, W., Zhou, Y., Jentsch, J.D., Brown, R.A.M., Tian, X., Ehninger, D., Hennah, W., Peltonen, L., Lonnqvist, J., Huttunen, M.O., et al. (2007). Specific developmental disruption of disrupted-in-schizophrenia-1 function results in schizophrenia-related phenotypes in mice. Proceedings of the National Academy of Sciences of the United States of America 104, 18280-18285.

Lin, L., Faraco, J., Li, R., Kadotani, H., Rogers, W., Lin, X., Qiu, X., de Jong, P.J., Nishino, S., and Mignot, E. (1999). The Sleep Disorder Canine Narcolepsy Is Caused by a Mutation in the Hypocretin (Orexin) Receptor 2 Gene. Cell 98, 365-376.

Link, V., Shevchenko, A., and Heisenberg, C.P. (2006). Proteomics of early zebrafish embryos. Bmc Developmental Biology 13, 6:1.

Lipina, T.V., Haque, F.N., McGirr, A., Boutros, P.C., Berger, T., Mak, T.W., Roder, J.C., and Wong, A.H.C. (2012). Prophylactic Valproic Acid Treatment Prevents Schizophrenia-Related Behaviour in Disc1-L100P Mutant Mice. Plos One 7, e51562.

Lipina, T.V., Kaidanovich-Beilin, O., Patel, S., Wang, M., Clapcote, S.J., Liu, F., Woodgett, J.R., and Roder, J.C. (2011). Genetic and pharmacological evidence for schizophrenia-related Disc1 interaction with GSK-3. Synapse 65, 234-248.

Lipina, T.V., Niwa, M., Jaaro-Peled, H., Fletcher, P.J., Seeman, P., Sawa, A., and Roder, J.C. (2010). Enhanced dopamine function in DISC1-L100P mutant mice: implications for schizophrenia. Genes Brain and Behavior 9, 777-789.

Lipina, T.V., Zai, C., Hlousek, D., Roder, J.C., and Wong, A.H.C. (2013). Maternal Immune Activation during Gestation Interacts with Disc1 Point Mutation to Exacerbate Schizophrenia-Related Behaviors in Mice. Journal of Neuroscience 33, 7654-7666.

Lipska, B.K., Peters, T., Hyde, T.M., Halim, N., Horowitz, C., Mitkus, S., Weickert, C.S., Matsumoto, M., Sawa, A., Straub, R.E., et al. (2006). Expression of DISC1 binding partners is reduced in schizophrenia and associated with DISC1 SNPs. Human Molecular Genetics 15, 1245-1258.

Lisman, J. (2012). Excitation, inhibition, local oscillations, or large-scale loops: what causes the symptoms of schizophrenia? Current Opinion in Neurobiology 22, 537-544.

Liu, H.H., Liu, Z.N., Liang, M., Hao, Y.H., Tan, L.H., Kuang, F., Yi, Y.H., Xu, L., and Jiang, T.Z. (2006a). Decreased regional homogeneity in schizophrenia: a resting state functional magnetic resonance imaging study. Neuroreport 17, 19-22.

Liu, K.S., and Fetcho, J.R. (1999). Laser ablations reveal functional relationships of segmental hindbrain neurons in zebrafish. Neuron 23, 325-335.

Liu, X.Z., Chen, W., Tu, Y.H., Hou, H.T., Huang, X.Y., Chen, X.L., Guo, Z.W., and Bai, G.H. (2018). The Abnormal Functional Connectivity between the Hypothalamus and the Temporal Gyrus Underlying Depression in Alzheimer's Disease Patients. Frontiers in Aging Neuroscience 10, 37.

Liu, Y.-L., Fann, C.S.-J., Liu, C.-M., Chen, W.J., Wu, J.-Y., Hung, S.-I., Chen, C.-H., Jou, Y.-S., Liu, S.-K., Hwang, T.-J., et al. (2006b). A Single Nucleotide Polymorphism Fine Mapping Study of Chromosome 1q42.1 Reveals the Vulnerability Genes for Schizophrenia, GNPAT and DISC1: Association with Impairment of Sustained Attention. Biological Psychiatry 60, 554-562.

Liu, Y.W., Carmer, R., Zhang, G.N., Venkatraman, P., Brown, S.A., Pang, C.P., Zhang, M.Z., Ma, P., and Leung, Y.F. (2015). Statistical Analysis of Zebrafish Locomotor Response. Plos One 10, e0139521.

Lohr, H., Ryu, S., and Driever, W. (2009). Zebrafish diencephalic A11-related dopaminergic neurons share a conserved transcriptional network with neuroendocrine cell lineages. Development 136, 1007-1017.

Lovett-Barron, M., Chen, R., Bradbury, S., Andalman, A., Wagle, M., Guo, S., and Deisseroth, K. (2019). Multiple overlapping hypothalamus-brainstem circuits drive rapid threat avoidance. BioRxiv.

Lovett-Barron, M., Andalman, A.S., Allen, W.E., Vesuna, S., Kauvar, I., Burns, V.M., and Deisseroth, K. (2017). Ancestral Circuits for the Coordinated Modulation of Brain State. Cell 171, 1411-1423.

Lu, F., Kar, D., Gruenig, N., Zhang, Z.W., Cousins, N., Rodgers, H.M., Swindell, E.C., Jamrich, M., Schuurmans, C., Mathers, P.H., and Kurrasch, D.M. (2013). Rax Is a Selector Gene for Mediobasal Hypothalamic Cell Types. Journal of Neuroscience 33, 259-272.

Machon, R.A., Mednick, S.A., and Huttunen, M.O. (1997). Adult major affective disorder after prenatal exposure to an influenza epidemic. Archives of General Psychiatry 54, 322-328.

MacPhail, R.C., Brooks, J., Hunter, D.L., Padnos, B., Irons, T.D., and Padilla, S. (2009). Locomotion in larval zebrafish: Influence of time of day, lighting and ethanol. Neurotoxicology 30, 52-58.

Madison, J.M., Zhou, F., Nigam, A., Hussain, A., Barker, D.D., Nehme, R., van der Ven, K., Hsu, J., Wolf, P., Fleishman, M., et al. (2015). Characterization of bipolar disorder patient-specific induced pluripotent stem cells from a family reveals neurodevelopmental and mRNA expression abnormalities. Molecular Psychiatry 20, 703-717.

Mahabir, S., Chatterjee, D., and Gerlai, R. (2014). Strain dependent neurochemical changes induced by embryonic alcohol exposure in zebrafish. Neurotoxicology and Teratology 41, 1-7.

Maillard, A.M., Ruef, A., Pizzagalli, F., Migliavacca, E., Hippolyte, L., Adaszewski, S., Dukart, J., Ferrari, C., Conus, P., Mannik, K., et al. (2015). The 16p11.2 locus modulates brain structures common to autism, schizophrenia and obesity. Molecular Psychiatry 20, 140-147.

Majdic, G., Young, M., Gomez-Sanchez, E., Anderson, P., Szczepaniak, L.S., Dobbins, R.L., McGarry, J.D., and Parker, K.L. (2002). Knockout mice lacking steroidogenic factor 1 are a novel genetic model of hypothalamic obesity. Endocrinology 143, 607-614.

Malhi, G.S., Lagopoulos, J., Ward, P.B., Kumari, V., Mitchell, P.B., Parker, G.B., Ivanovski, B., and Sachdev, P. (2004). Cognitive generation of affect in bipolar depression: an fMRI study. European Journal of Neuroscience 19, 741-754.

Mao, Y., Ge, X., Frank, C.L., Madison, J.M., Koehler, A.N., Doud, M.K., Tassa, C., Berry, E.M., Soda, T., Singh, K.K., et al. (2009). Disrupted in Schizophrenia 1 Regulates Neuronal Progenitor Proliferation via Modulation of GSK3 beta/beta-Catenin Signaling. Cell 136, 1017-1031.

Martinek, S., Inonog, S., Manoukian, A.S., and Young, M.W. (2001). A role for the segment polarity gene shaggy/GSK-3 in the Drosophila circadian clock. Cell 105, 769-779.

Mathuru, Ajay s., Kibat, C., Cheong, Wei f., Shui, G., Wenk, Markus r., Friedrich, Rainer w., and Jesuthasan, S. (2012). Chondroitin Fragments Are Odorants that Trigger Fear Behavior in Fish. Current Biology 22, 538-544.

Maximino, C., de Brito, T.M., Batista, A.W.D., Herculano, A.M., Morato, S., and Gouveia, A. (2010). Measuring anxiety in zebrafish: A critical review. Behavioural Brain Research 214, 157-171.

Maximino, C., Lima, M.G., Oliveira, K.R.M., Batista, E.D.O., and Herculano, A.M. (2013). "Limbic associative" and "autonomic" amygdala in teleosts: A review of the evidence. Journal of Chemical Neuroanatomy 48-49, 1-13.

McGhie, A., and Chapman, J. (1961). Disorders of Attention and Perception in early schizophrenia. British Journal of Medical Psychology 34, 103-116.

Meng, S., Ryu, S., Zhao, B., Zhang, D., Driever, W., and McMahon, D.G. (2008). Targeting retinal dopaminergic neurons in tyrosine hydroxylase-driven green fluorescent protein transgenic zebrafish. Mol Vis 14, 2475-2483.

Meynen, G., Unmehopa, U.A., Hofman, M.A., Swaab, D.F., and Hoogendijk, W.J.G. (2007). Hypothalamic oxytocin mRNA expression and melancholic depression. Molecular Psychiatry 12, 118.

Miano, S., Donfrancesco, R., Bruni, O., Ferri, R., Galiffa, S., Pagani, J., Montemitro, E., Kheirandish, L., Gozal, D., and Villa, M.P. (2006). NREM sleep instability is reduced in children with attention-deficit/hyperactivity disorder. Sleep 29, 797-803.

Millar, J.K., Pickard, B.S., Mackie, S., James, R., Christie, S., Buchanan, S.R., Malloy, M.P., Chubb, J.E., Huston, E., Baillie, G.S., et al. (2005). DISC1 and PDE4B are interacting genetic factors in schizophrenia that regulate cAMP signaling. Science 310, 1187-1191.

Millar, J.K., Wilson-Annan, J.C., Anderson, S., Christie, S., Taylor, M.S., Semple, C.A.M., Devon, R.S., St Clair, D.M., Muir, W.J., Blackwood, D.H.R., and Porteous, D.J. (2000). Disruption of two novel genes by a translocation co-segregating with schizophrenia. Human Molecular Genetics 9, 1415-1423.

Miyaoka, T., Seno, H., and Ishino, H. (1999). Increased expression of Wnt-1 in schizophrenic brains. Schizophrenia Research 38, 1-6.

Miyoshi, K., Honda, A., Baba, K., Taniguchi, M., Oono, K., Fujita, T., Kuroda, S., Katayama, T., and Tohyama, M. (2003). Disrupted-In-Schizophrenia 1, a candidate gene for schizophrenia, participates in neurite outgrowth. Molecular Psychiatry 8, 685-694.

Moir, L., Bochukova, E.G., Dumbell, R., Banks, G., Bains, R.S., Nolan, P.M., Scudamore, C., Simon, M., Watson, K.A., Keogh, J., et al. (2017). Disruption of the homeodomain transcription factor orthopedia homeobox (Otp) is associated with obesity and anxiety. Molecular Metabolism 6, 1419-1428.

Molinoff, P.B., and Axelrod, J. (1971). Biochemistry of Catecholamines. Annual Review of Biochemistry 40, 465-500.

Monti, J.M., BaHammam, A.S., Pandi-Perumal, S.R., Bromundt, V., Spence, D.W., Cardinali, D.P., and Brown, G.M. (2013). Sleep and circadian rhythm dysregulation in schizophrenia. Progress in Neuro-Psychopharmacology & Biological Psychiatry 43, 209-216.

Moon, R.T., Brown, J.D., and Torres, M. (1997). WNTs modulate cell fate and behavior during vertebrate development. Trends in Genetics 13, 157-162.

Moravec, C.E., Samuel, J., Weng, W., Wood, I.C., and Sirotkin, H.I. (2016). Maternal Rest/Nrsf Regulates Zebrafish Behavior through snap25a/b. Journal of Neuroscience 36, 9407-9419.

Morris, J.A., Kandpal, G., Ma, L., and Austin, C.P. (2003). DISC1 (Disrupted-In-Schizophrenia 1) is a centrosome-associated protein that interacts with MAP1A, MIPT3, ATF4/5 and NUDEL: regulation and loss of interaction with mutation. Human Molecular Genetics 12, 1591-1608.

Mrosovsky, N., Redlin, U., Roberts, R.B., and Threadgill, D.W. (2005). Masking in Waved-2 Mice: EGF Receptor Control of Locomotion Questioned. Chronobiology International 22, 963-974.

Mu, Y., Li, X.Q., Zhang, B., and Du, J.L. (2012). Visual Input Modulates Audiomotor Function via Hypothalamic Dopaminergic Neurons through a Cooperative Mechanism. Neuron 75, 688-699.

Mueller, T., and Wullimann, M.F. (2002). BrdU-, neuroD (nrd)- and Hu-studies reveal unusual non-ventricular neurogenesis in the postembryonic zebrafish forebrain. Mechanisms of Development 117, 123-135.

Mueller, T., Wullimann, M.F., and Guo, S. (2008). Early teleostean basal ganglia development visualized by zebrafish Dlx2a, Lhx6, Lhx7, Tbr2 (eomesa), and GAD67 gene expression. Journal of Comparative Neurology 507, 1245-1257.

Muthu, V., Eachus, H., Ellis, P., Brown, S., and Placzek, M. (2016). Rx3 and Shh direct anisotropic growth and specification in the zebrafish tuberal/anterior hypothalamus. Development 143, 2651-2663.

Muto, A., Lal, P., Ailani, D., Abe, G., Itoh, M., and Kawakami, K. (2017). Activation of the hypothalamic feeding centre upon visual prey detection. Nature Communications 8, 15029.

Muto, A., Ohkura, M., Kotani, T., Higashijima, S.-I., Nakai, J., and Kawakami, K. (2011). Genetic visualization with an improved GCaMP calcium indicator reveals spatiotemporal activation of the spinal motor neurons in zebrafish. Proceedings of the National Academy of Sciences 108, 5425.

Nadri, C., Kozlovsky, N., Agam, G., and Bersudsky, Y. (2002). GSK-3 parameters in lymphocytes of schizophrenic patients. Psychiatry Research 112, 51-57.

Nakata, K., Lipska, B.K., Hyde, T.M., Ye, T., Newburn, E.N., Morita, Y., Vakkalanka, R., Barenboim, M., Sei, Y., Weinberger, D.R., and Kleinman, J.E. (2009). DISC1 splice variants are upregulated in schizophrenia and associated with risk polymorphisms. Proceedings of the National Academy of Sciences of the United States of America 106, 15873-15878.

Negoias, S., Croy, I., Gerber, J., Puschmann, S., Petrowski, K., Joraschky, P., and Hummel, T. (2010). Reduced olfactory bulb volume and olfactory sensitivity in patients with acute major depression. Neuroscience 169, 415-421.

Newburn, E.N., Hyde, T.M., Ye, T., Morita, Y., Weinberger, D.R., Kleinman, J.E., and Lipska, B.K. (2011). Interactions of human truncated DISC1 proteins: implications for schizophrenia. Translational Psychiatry 1, e30

Ng, M.C., Hsu, C.P., Wu, Y.J., Wu, S.Y., Yang, Y.L., and Lu, K.T. (2012). Effect of MK-801-induced impairment of inhibitory avoidance learning in zebrafish via inactivation of extracellular signal-regulated kinase (ERK) in telencephalon. Fish Physiology and Biochemistry 38, 1099-1106.

Niwa, M., Jaaro-Peled, H., Tankou, S., Seshadri, S., Hikida, T., Matsumoto, Y., Cascella, N.G., Kano, S.-i., Ozaki, N., Nabeshima, T., and Sawa, A. (2013). Adolescent Stress-Induced Epigenetic Control of Dopaminergic Neurons via Glucocorticoids. Science 339, 335-339.

Niwa, M., Kamiya, A., Murai, R., Kubo, K.-i., Gruber, A.J., Tomita, K., Lu, L., Tomisato, S., Jaaro-Peled, H., Seshadri, S., et al. (2010). Knockdown of DISC1 by In Utero Gene Transfer Disturbs Postnatal Dopaminergic Maturation in the Frontal Cortex and Leads to Adult Behavioral Deficits. Neuron 65, 480-489.

Nutt, D., Wilson, S., and Paterson, L. (2008). Sleep disorders as core symptoms of depression. Dialogues in clinical neuroscience 10, 329-336.

O'Brien, W.T., Harper, A.D., Jove, F., Woodgett, J.R., Maretto, S., Piccolo, S., and Klein, P.S. (2004). Glycogen synthase kinase-3 beta haploinsufficiency mimics the behavioral and molecular effects of lithium. Journal of Neuroscience 24, 6791-6798.

O'Malley, D.M., Kao, Y.-H., and Fetcho, J.R. (1996). Imaging the Functional Organization of Zebrafish Hindbrain Segments during Escape Behaviors. Neuron 17, 1145-1155.

O'Tuathaigh, C.M.P., O'Connor, A.-M., O'Sullivan, G.J., Lai, D., Harvey, R., Croke, D.T., and Waddington, J.L. (2008). Disruption to social dyadic interactions but not emotional/anxiety-related behaviour in mice with heterozygous 'knockout' of the schizophrenia risk gene neuregulin-1. Progress in Neuropsychopharmacology & Biological Psychiatry 32, 462-466.

Okuyama, T., Suehiro, Y., Imada, H., Shimada, A., Naruse, K., Takeda, H., Kubo, T., and Takeuchi, H. (2011). Induction of c-fos transcription in the medaka brain (Oryzias latipes) in response to mating stimuli. Biochemical and Biophysical Research Communications 404, 453-457.

O'Tuathaigh, C.M.P., Fumagalli, F., Desbonnet, L., Perez-Branguli, F., Moloney, G., Loftus, S., O'Leary, C., Petit, E., Cox, R., Tighe, O., et al. (2017). Epistatic and Independent Effects on Schizophrenia-Related Phenotypes Following Co-disruption of the Risk Factors Neuregulin-1 × DISC1. Schizophrenia Bulletin 43, 214-225.

Pariante, C.M., and Miller, A.H. (2001). Glucocorticoid receptors in major depression: Relevance to pathophysiology and treatment. Biological Psychiatry 49, 391-404.

Patton, G.C., Olsson, C.A., Skirbekk, V., Saffery, R., Wlodek, M.E., Azzopardi, P.S., Stonawski, M., Rasmussen, B., Spry, E., Francis, K., et al. (2018). Adolescence and the next generation. Nature 554, 458–466.

Perry, W., Minassian, A., Feifel, D., and Braff, D.L. (2001). Sensorimotor gating deficits in bipolar disorder patients with acute psychotic mania. Biological Psychiatry 50, 418-424.

Pezawas, L., Meyer-Lindenberg, A., Drabant, E.M., Verchinski, B.A., Munoz, K.E., Kolachana, B.S., Egan, M.F., Mattay, V.S., Hariri, A.R., and Weinberger, D.R. (2005). 5-HTTLPR polymorphism impacts human cingulate-amygdala interactions: a genetic susceptibility mechanism for depression. Nature Neuroscience 8, 828-834.

Pfaff, D., Martin, E.M., Weingarten, W., and Vimal, V. (2008). The central neural foundations of awareness and self-awareness. Progress of Theoretical Physics Supplement, 79-98.

Pfaff, D.W. (2006). Brain arousal and information theory [electronic resource]: neural and genetic mechanisms (Cambridge, Mass.: Cambridge, Mass. Harvard University Press

Pfaff, D.W., Martin, E.M., and Ribeiro, A.C. (2007). Relations between mechanisms of CNS arousal and mechanisms of stress. Stress-the International Journal on the Biology of Stress 10, 316-325.

Pierce, A.A., and Xu, A.W. (2010). De Novo Neurogenesis in Adult Hypothalamus as a Compensatory Mechanism to Regulate Energy Balance. Journal of Neuroscience 30, 723-730.

Pittman, J.T., and Lott, C.S. (2014). Startle response memory and hippocampal changes in adult zebrafish pharmacologically induced to exhibit anxiety/depression-like behaviors. Physiology & Behavior 123, 174-179.

Pletnikov, M.V., Ayhan, Y., Nikolskaia, O., Xu, Y., Ovanesov, M.V., Huang, H., Mori, S., Moran, T.H., and Ross, C.A. (2008). Inducible expression of mutant human DISC1 in mice is associated with brain and behavioral abnormalities reminiscent of schizophrenia. Molecular Psychiatry 13, 173-186.

Pletnikov, M.V., Xu, Y., Ovanesov, M.V., Kamiya, A., Sawa, A., and Ross, C.A. (2007). PC12 cell model of inducible expression of mutant DISC1: New evidence for a dominant-negative mechanism of abnormal neuronal differentiation. Neuroscience Research 58, 234-244.

Portavella, M., Vargas, J.P., Torres, B., and Salas, C. (2002). The effects of telencephalic pallial lesions on spatial, temporal, and emotional learning in goldfish. Brain Research Bulletin 57, 397-399.

Porteous, D.J., and Millar, J.K. (2006). Disrupted in schizophrenia 1: building brains and memories. Trends in Molecular Medicine 12, 255-261.

Porteous, D.J., Thomson, P.A., Millar, J.K., Evans, K.L., Hennah, W., Soares, D.C., McCarthy, S., McCombie, W.R., Clapcote, S.J., Korth, C., et al. (2014). DISC1 as a genetic risk factor for schizophrenia and related major mental illness: response to Sullivan. Molecular Psychiatry 19, 141-143.

Prober, D.A., Rihel, J., Onah, A.A., Sung, R.J., and Schier, A.F. (2006). Hypocretin/orexin overexpression induces an insomnia-like phenotype in zebrafish. Journal of Neuroscience 26, 13400-13410.

Purba, J.S., Hoogendijk, W.J.G., Hofman, M.A., and Swaab, D.F. (1996). Increased Number of Vasopressin- and Oxytocin-Expressing Neurons in the Paraventricular Nucleus of the Hypothalamus in Depression. Archives of General Psychiatry 53, 137-143.

Raadsheer, F.C., Hoogendijk, W.J.G., Stam, F.C., Tilders, F.J.H., and Swaab, D.F. (1994). Increased numbers of corticotropin-releasing hormone expressing neurons in the hypothalamic paraventricular nucleus of depressed-patients. Neuroendocrinology 60, 436-444.

Raichle, M.E., MacLeod, A.M., Snyder, A.Z., Powers, W.J., Gusnard, D.A., and Shulman, G.L. (2001). A default mode of brain function. Proceedings of the National Academy of Sciences of the United States of America 98, 676-682.

Randlett, O., Wee, C.L., Naumann, E.A., Nnaemeka, O., Schoppik, D., Fitzgerald, J.E., Portugues, R., Lacoste, A.M.B., Riegler, C., Engert, F., and Schier, A.F. (2015). Whole-brain activity mapping onto a zebrafish brain atlas. Nature Methods 12, 1039-1046.

Rayner, E., Durin, M.A., Thomas, R., Moralli, D., O'Cathail, S.M., Tomlinson, I., Green, C.M., and Lewis, A. (2019). CRISPR-Cas9 Causes Chromosomal Instability and Rearrangements in Cancer Cell Lines, Detectable by Cytogenetic Methods. Crispr Journal 2, 406-416.

Rennekamp, A., J., Huang, X.-P., Wang, Y., Patel, S., Lorello, P., J., Cade, L., Gonzales, A., P. W., Yeh, J.-R.J., Caldarone, B., J., Roth, B., L., et al. (2016). σ1 receptor ligands control a switch between passive and active threat responses. Nature Chemical Biology 12.

Riedel, G. (1997). The forebrain of the blind cave fish Astyanax hubbsi (Characidae) .1. General anatomy of the telencephalon. Brain Behavior and Evolution 49, 20-38.

Ring, D.B., Johnson, K.W., Henriksen, E.J., Nuss, J.M., Goff, D., Kinnick, T.R., Ma, S.T., Reeder, J.W., Samuels, I., Slabiak, T., et al. (2003). Selective glycogen synthase kinase 3 inhibitors potentiate insulin activation of glucose transport and utilization in vitro and in vivo. Diabetes 52, 588-595.

Rink, E., and Wullimann, M.F. (2001). The teleostean (zebrafish) dopaminergic system ascending to the subpallium (striatum) is located in the basal diencephalon (posterior tuberculum). Brain Research 889, 316-330.

Rink, E., and Wullimann, M.F. (2002). Development of the catecholaminergic system in the early zebrafish brain: an immunohistochemical study. Developmental Brain Research 137, 89-100.

Ripke, S., Neale, B.M., Corvin, A., Walters, J.T.R., Farh, K.H., Holmans, P.A., and Lee, P. (2014). Biological insights from 108 schizophrenia-associated genetic loci. Nature 511, 421–427.

Robillard, R., Naismith, S.L., and Hickie, I.B. (2013). Recent Advances in Sleep-Wake Cycle and Biological Rhythms in Bipolar Disorder. Current Psychiatry Reports 15, 402.

Robu, M.E., Larson, J.D., Nasevicius, A., Beiraghi, S., Brenner, C., Farber, S.A., and Ekker, S.C. (2007). p53 activation by knockdown technologies. Plos Genetics 3, 787-801.

Rossi, A., Kontarakis, Z., Gerri, C., Nolte, H., Hölper, S., Krüger, M., and Stainier, D., Y. R. (2015). Genetic compensation induced by deleterious mutations but not gene knockdowns. Nature 524, 230.

Rossi, M.A., and Stuber, G.D. (2018). Overlapping Brain Circuits for Homeostatic and Hedonic Feeding. Cell Metabolism 27, 42-56.

Russell, J.A. (1980). A circumplex model of affect. Journal of Personality and Social Psychology 39, 1161-1178.

Sachs, N.A., Sawa, A., Holmes, S.E., Ross, C.A., DeLisi, L.E., and Margolis, R.L. (2005). A frameshift mutation in Disrupted in Schizophrenia 1 in an American family with schizophrenia and schizoaffective disorder. Molecular Psychiatry 10, 758-764.

Sato, T., Sato, F., Kamezaki, A., Sakaguchi, K., Tanigome, R., Kawakami, K., and Sehara-Fujisawa, A. (2015). Neuregulin 1 Type II-ErbB Signaling Promotes Cell Divisions Generating Neurons from Neural Progenitor Cells in the Developing Zebrafish Brain. Plos One 10, e0127360.

Sawamura, N., Ando, T., Maruyama, Y., Fujimuro, M., Mochizuki, H., Honjo, K., Shimoda, M., Toda, H., Sawamura-Yamamoto, T., Makuch, L.A., et al. (2008). Nuclear DISC1 regulates CRE-mediated gene transcription and sleep homeostasis in the fruit fly. Molecular Psychiatry 13, 1138-1148.

Schindler, S., Schmidt, L., Stroske, M., Storch, M., Anwander, A., Trampel, R., Strauss, M., Hegerl, U., Geyer, S., and Schonknecht, P. (2019). Hypothalamus enlargement in mood disorders. Acta Psychiatrica Scandinavica 139, 56-67.

Schirmer, A., Jesuthasan, S., and Mathuru, A.S. (2013). Tactile stimulation reduces fear in fish. Frontiers in Behavioral Neuroscience 7, 167.

Schloesser, R.J., Chen, G., and Manji, H.K. (2007). Neurogenesis and neuroenhancement in the pathophysiology and treatment of bipolar disorder. Pharmacology of Neurogenesis and Neuroenhancement 77, 143-178.

Schlosser, R.G.M. (2010). Fronto-Cingulate Effective Connectivity in Major Depression: A Study with fMRI and Dynamic Causal Modeling. Biological Psychiatry 67, 7S-8S.

Schmidt, S.J., Mueller, D.R., and Roder, V. (2011). Social Cognition as a Mediator Variable Between Neurocognition and Functional Outcome in Schizophrenia: Empirical Review and New Results by Structural Equation Modeling. Schizophrenia Bulletin 37, S41-S54.

Schmitt, A., Hasan, A., Gruber, O., and Falkai, P. (2011). Schizophrenia as a disorder of disconnectivity. European Archives of Psychiatry and Clinical Neuroscience 261, 150-154.

Schneider, S., Götz, K., Birchmeier, C., Schwegler, H., and Roskoden, T. (2017). Neuregulin-1 mutant mice indicate motor and sensory deficits, indeed few references for schizophrenia endophenotype model. Behavioural Brain Research 322, 177-185.

Schreck, C.B. (2010). Stress and fish reproduction: The roles of allostasis and hormesis. General and Comparative Endocrinology 165, 549-556.

Schurov, I.L., Handford, E.J., Brandon, N.J., and Whiting, P.J. (2004). Expression of disrupted in schizophrenia 1 (DISC1) protein in the adult and developing mouse brain indicates its role in neurodevelopment. Molecular Psychiatry 9, 1100-1110.

Schwabe, K., and Krauss, J.K. (2018). What rodent models of deep brain stimulation can teach us about the neural circuit regulation of prepulse inhibition in neuropsychiatric disorders. Schizophrenia Research 198, 45-51.

Scutt, L.E., Chow, E.W.C., Weksberg, R., Honer, W.G., and Bassett, A.S. (2001). Patterns of dysmorphic features in schizophrenia. American Journal of Medical Genetics 105, 713-723.

Seeman, P., Lee, T., Chauwong, M., and Wong, K. (1976). Antipsychotic drug doses and neuroleptic-dopamine receptors. Nature 261, 717-719.

Seibt, K.J., Oliveira, R.D., Zimmermann, F.F., Capiotti, K.M., Bogo, M.R., Ghisleni, G., and Bonan, C.D. (2010). Antipsychotic drugs prevent the motor hyperactivity induced by psychotomimetic MK-801 in zebrafish (Danio rerio). Behavioural Brain Research 214, 417-422.

Selevan, S., Kimmel, C., and Mendola, P. (2000). Identifying Critical Windows of Exposure for Children's Health. Environmental Health Perspectives 108, 451-451.

Semmelhack, J.L., Donovan, J.C., Thiele, T.R., Kuehn, E., Laurell, E., and Baier, H. (2014). A dedicated visual pathway for prey detection in larval zebrafish. Elife 3, e04878.

Seshadri, S., Faust, T., Ishizuka, K., Delevich, K., Chung, Y., Kim, S.-H., Cowles, M., Niwa, M., Jaaro-Peled, H., Tomoda, T., et al. (2015). Interneuronal DISC1 regulates NRG1-ErbB4 signalling and excitatory-inhibitory synapse formation in the mature cortex. Nature Communications 6.

Shen, S., Lang, B., Nakamoto, C., Zhang, F., Pu, J., Kuan, S.-L., Chatzi, C., He, S., Mackie, I., Brandon, N.J., et al. (2008). Schizophrenia-Related Neural and Behavioral Phenotypes in Transgenic Mice Expressing Truncated Disc1. Journal of Neuroscience 28, 10893-10904.

Shevelkin, A.V., Terrillion, C.E., Abazyan, B.N., Kajstura, T.J., Jouroukhin, Y.A., Rudow, G.L., Troncoso, J.C., Linden, D.J., and Pletnikov, M.V. (2017). Expression of mutant DISC1 in Purkinje cells increases their spontaneous activity and impairs cognitive and social behaviors in mice. Neurobiology of Disease 103, 144-153.

Shu, T.Z., Ayala, R., Nguyen, M.D., Xie, Z.G., Gleeson, J.G., and Tsai, L.H. (2004). Ndel1 operates in a common pathway with LIS1 and cytoplasmic dynein to regulate cortical neuronal positioning. Neuron 44, 263-277.

Singh, Karun k., De Rienzo, G., Drane, L., Mao, Y., Flood, Z., Madison, J., Ferreira, M., Bergen, S., King, C., Sklar, P., et al. (2011). Common DISC1 Polymorphisms Disrupt Wnt/GSK3β Signaling and Brain Development. Neuron 72, 545-558.

Sink, K.S., Walker, D.L., Yang, Y., and Davis, M. (2011). Calcitonin Gene-Related Peptide in the Bed Nucleus of the Stria Terminalis Produces an Anxiety-Like Pattern of Behavior and Increases Neural Activation in Anxiety-Related Structures. Journal of Neuroscience 31, 1802-1810.

Sitaram, N., Wyatt, R.J., Dawson, S., and Gillin, J.C. (1976). REM-sleep induction by physostigmine infusion during sleep. Science 191, 1281-1283.

Soares, D.C., Carlyle, B.C., Bradshaw, N.J., and Porteous, D.J. (2011). DISC1: Structure, Function, and Therapeutic Potential for Major Mental Illness. Acs Chemical Neuroscience 2, 609-632.

Speedie, N., and Gerlai, R. (2008). Alarm substance induced behavioral responses in zebrafish (Danio rerio). Behavioural Brain Research 188, 168-177.

Srikanth, P., Han, K., Callahan, D.G., Makovkina, E., Muratore, C.R., Lalli, M.A., Zhou, H.L., Boyd, J.D., Kosik, K.S., Selkoe, D.J., and Young-Pearse, T.L. (2015). Genomic DISC1 Disruption in hiPSCs Alters Wnt Signaling and Neural Cell Fate. Cell Reports 12, 1414-1429.

Stednitz, S.J., Freshner, B., Shelton, S., Shen, T., Black, D., and Gahtan, E. (2015). Selective toxicity of L-DOPA to dopamine transporter-expressing neurons and locomotor behavior in zebrafish larvae. Neurotoxicology and Teratology 52, 51-56.

Stefansson, H., Petursson, H., Sigurdsson, E., Steinthorsdottir, V., Bjornsdottir, S., Sigmundsson, T., Ghosh, S., Brynjolfsson, J., Gunnarsdottir, S., Ivarsson, O., et al. (2002). Neuregulin 1 and Susceptibility to Schizophrenia. The American Journal of Human Genetics 71, 877-892.

Stephan, K.E., Magnotta, V.A., White, T., Arndt, S., Flaum, M., O'Leary, D.S., and Andreasen, N.C. (2001). Effects of olanzapine on cerebellar functional connectivity in schizophrenia measured by fMRI during a simple motor task. Psychological Medicine 31, 1065-1078.

Sternson, S.M., Shepherd, G.M.G., and Friedman, J.M. (2005). Topographic mapping of VMH -> arcuate nucleus microcircuits and their reorganization by fasting. Nature Neuroscience 8, 1356-1363.

Stewart, A., Wu, N., Cachat, J., Hart, P., Gaikwad, S., Wong, K., Utterback, E., Gilder, T., Kyzar, E., Newman, A., et al. (2011). Pharmacological modulation of anxiety-like phenotypes in adult zebrafish behavioral models. Progress in Neuro-Psychopharmacology & Biological Psychiatry 35, 1421-1431.

Su, P., Li, S.P., Chen, S., Lipina, T.V., Wang, M., Lai, T.K.Y., Lee, F.H.F., Zhang, H.L., Zhai, D.X., Ferguson, S.S.G., et al. (2014). A Dopamine D2 Receptor-DISC1 Protein Complex may Contribute to Antipsychotic-Like Effects. Neuron 84, 1302-1316.

Sullivan, P.F. (2013). Questions about DISC1 as a genetic risk factor for schizophrenia. Molecular Psychiatry 18, 1050-1052.

Swaab, D.F., Bao, A.M., and Lucassen, P.J. (2005). The stress system in the human brain in depression and neurodegeneration. Ageing Research Reviews 4, 141-194.

Swerdlow, N.R., Geyer, M.A., and Braff, D.L. (2001). Neural circuit regulation of prepulse inhibition of startle in the rat: current knowledge and future challenges. Psychopharmacology 156, 194-215.

Tamura, M., Mukai, J., Gordon, J.A., and Gogos, J.A. (2016). Developmental Inhibition of Gsk3 Rescues Behavioral and Neurophysiological Deficits in a Mouse Model of Schizophrenia Predisposition. Neuron 89, 1100-1109.

Tang, W.L., Davidson, J.D., Zhang, G.Q., Conen, K.E., Fang, J., Serluca, F., Li, J.Y., Xiong, X.R., Coble, M., Tsai, T.W., et al. (2020). Genetic Control of Collective Behavior in Zebrafish. Iscience 23, 100942.

Tay, T.L., Ronneberger, O., Ryu, S., Nitschke, R., and Driever, W. (2011). Comprehensive catecholaminergic projectome analysis reveals single-neuron integration of zebrafish ascending and descending dopaminergic systems. Nature Communications 2, 171.

Thisse, C., and Thisse, B. (2008). High-resolution in situ hybridization to whole-mount zebrafish embryos. Nature Protocols 3, 59-69.

Thompson, W.A., Arnold, V.I., and Vijayan, M.M. (2017). Venlafaxine in Embryos Stimulates Neurogenesis and Disrupts Larval Behavior in Zebrafish. Environmental Science & Technology 51, 12889-12897.

Thomson, P.A., Duff, B., Blackwood, D.H.R., Romaniuk, L., Watson, A., Whalley, H.C., Li, X., Dauvermann, M.R., Moorhead, T.W.J., Bois, C., et al. (2016). Balanced translocation linked to psychiatric disorder, glutamate, and cortical structure/function. Npj Schizophrenia 2, 16024.

Thyme, S.B., Pieper, L.M., Li, E.H., Pandey, S., Wang, Y.Q., Morris, N.S., Sha, C., Choi, J.W., Herrera, K.J., Soucy, E.R., et al. (2019). Phenotypic Landscape of Schizophrenia-Associated Genes Defines Candidates and Their Shared Functions. Cell 177, 478-491.

Tong, Q., Ye, C., McCrimmon, R.J., Dhillon, H., Choi, B., Kramer, M.D., Yu, J., Yang, Z., Christiansen, L.M., Lee, C.E., et al. (2007). Synaptic glutamate release by ventromedial hypothalamic neurons is part of the neurocircuitry that prevents hypoglycemia. Cell Metabolism 5, 383-393.

Toyama, B.H., and Hetzer, M.W. (2013). OPINION Protein homeostasis: live long, won't prosper. Nature Reviews Molecular Cell Biology 14, 55-61.

Troop, N.A., Holbrey, A., and Treasure, J.L. (1998). Stress, coping, and crisis support in eating disorders. International Journal of Eating Disorders 24, 157-166.

Tsai, P.T., Hull, C., Chu, Y.X., Greene-Colozzi, E., Sadowski, A.R., Leech, J.M., Steinberg, J., Crawley, J.N., Regehr, W.G., and Sahin, M. (2012). Autistic-like behaviour and cerebellar dysfunction in Purkinje cell Tsc1 mutant mice. Nature 488, 647-651.

Tsai, P.T., Rudolph, S., Guo, C., Ellegood, J., Gibson, J.M., Schaeffer, S.M., Mogavero, J., Lerch, J.P., Regehr, W., and Sahin, M. (2018). Sensitive Periods for Cerebellar-Mediated Autistic-like Behaviors. Cell Reports 25, 357-367.

Tsuboi, D., Kuroda, K., Tanaka, M., Namba, T., Iizuka, Y., Taya, S., Shinoda, T., Hikita, T., Muraoka, S., Iizuka, M., et al. (2015). Disrupted-in-schizophrenia 1 regulates transport of ITPR1 mRNA for synaptic plasticity. Nature Neuroscience 18, 698-707.

Tsuchimine, S., Hattori, K., Ota, M., Hidese, S., Teraishi, T., Sasayama, D., Hori, H., Noda, T., Yoshida, S., Yoshida, F., and Kunugi, H. (2019). Reduced plasma orexin-A levels in patients with bipolar disorder. Neuropsychiatric Disease and Treatment 15, 2221-2230.

Turetsky, B.I., Moberg, P.J., Yousem, D.M., Doty, R.L., Arnold, S.E., and Gur, R.E. (2000). Reduced Olfactory Bulb Volume in Patients With Schizophrenia. American Journal of Psychiatry 157, 828-830.

Unger, J.L., and Glasgow, E. (2003). Expression of isotocin-neurophysin mRNA in developing zebratish. Gene Expression Patterns 3, 105-108.

van den Bos, R., Althuizen, J., Tschigg, K., Bomert, M., Zethof, J., Filk, G., and Gorissen, M. (2019). Early life exposure to cortisol in zebrafish (Danio rerio): similarities and differences in behaviour and physiology between larvae of the AB and TL strains. Behavioural Pharmacology 30, 260-271.

Van den Bos, R., Mes, W., Galligani, P., Heil, A., Zethof, J., Flik, G., and Gorissen, M. (2017). Further characterisation of differences between TL and AB zebrafish (Danio rerio): Gene expression, physiology and behaviour at day 5 of the larval stage. Plos One 12, e0175420.

Van Swinderen, B., and Andretic, R. (2011). Dopamine in Drosophila: setting arousal thresholds in a miniature brain. Proceedings of the Royal Society B 278, 906-913.

van Venrooij, J.A.E.M., Fluitman, S.B.A.H.A., Lijmer, J.G., Kavelaars, A., Heijnen, C.J., Westenberg, H.G.M., Kahn, R.S., and Gispen-de Wied, C.C. (2012). Impaired Neuroendocrine and Immune Response to Acute Stress in Medication-Naive Patients With a First Episode of Psychosis. Schizophrenia Bulletin 38, 272-279.

van-Hover, C., and Li, C. (2015). Stress-activated afferent inputs into the anterior parvicellular part of the paraventricular nucleus of the hypothalamus: Insights into urocortin 3 neuron activation. Brain Research 1611, 29-43.

Vardy, E., Sassano, M.F., Rennekamp, A.J., Kroeze, W.K., Mosier, P.D., Westkaemper, R.B., Stevens, C.W., Katritch, V., Stevens, R.C., Peterson, R.T., and Roth, B.L. (2015). Single Amino Acid Variation

Underlies Species-Specific Sensitivity to Amphibian Skin-Derived Opioid-like Peptides. Chemistry & Biology 22, 764-775.

Veldman, M., Zhao, C., Gomez, G., Lindgren, A., Huang, H., Yang, H., Yao, S., Martin, B., Kimelman, D., and Lin, S. (2013). Transdifferentiation of Fast Skeletal Muscle Into Functional Endothelium in Vivo by Transcription Factor Etv2. PLoS Biology 11, e1001590.

Viaud-Delmon, I., Venault, P., and Chapouthier, G. (2011). Behavioral models for anxiety and multisensory integration in animals and humans. Progress in Neuropsychopharmacology & Biological Psychiatry 35, 1391-1399.

Viskaitis, P., Irvine, E.E., Smith, M.A., Choudhury, A.I., Alvarez-Curto, E., Glegola, J.A., Hardy, D.G., Pedroni, S.M.A., Pessoa, M.R.P., Fernando, A.B.P., et al. (2017). Modulation of SF1 Neuron Activity Coordinately Regulates Both Feeding Behavior and Associated Emotional States. Cell Reports 21, 3559-3572.

Volkoff, H., Canosa, L.F., Unniappan, S., Cerda-Reverter, J.M., Bernier, N.J., Kelly, S.P., and Peter, R.E. (2005). Neuropeptides and the control of food intake in fish. General and Comparative Endocrinology 142, 3-19.

vom Berg-Maurer, C.M., Trivedi, C.A., Bollmann, J.H., De Marco, R.J., and Ryu, S. (2016). The Severity of Acute Stress Is Represented by Increased Synchronous Activity and Recruitment of Hypothalamic CRH Neurons. Journal of Neuroscience 36, 3350-3362.

Waldman, B. (1982). Quantitative and developmental analyses of the alarm reaction in the zebra danio, brachydanio-rerio. Copeia, 1-9.

Wang, A.-L., Fazari, B., Chao, O.Y., Nikolaus, S., Trossbach, S.V., Korth, C., Sialana, F.J., Lubec, G., Huston, J.P., Mattern, C., and de Souza Silva, M.A. (2017). Intra-nasal dopamine alleviates cognitive deficits in tgDISC1 rats which overexpress the human DISC1 gene. Neurobiology of Learning and Memory 146, 12-20.

Wang, D.L., Xue, S.W., Tan, Z.L., Wang, Y., Lian, Z.Z., and Sun, Y.K. (2019). Altered hypothalamic functional connectivity patterns in major depressive disorder. Neuroreport 30, 1115-1120.

Wang, Q., Charych, E.I., Pulito, V.L., Lee, J.B., Graziane, N.M., Crozier, R.A., Revilla-Sanchez, R., Kelly, M.P., Dunlop, A.J., Murdoch, H., et al. (2011). The psychiatric disease risk factors DISC1 and TNIK interact to regulate synapse composition and function. Molecular Psychiatry 16, 1006-1023.

Wang, S.K., Liang, Q.L., Qiao, H.M., Li, H., Shen, T.J., Ji, F., and Jiao, J.W. (2016). DISC1 regulates astrogenesis in the embryonic brain via modulation of RAS/MEK/ERK signaling through RASSF7. Development 143, 2732-2740.

Warrier, V., Toro, R., Chakrabarti, B., Borglum, A.D., Grove, J., Hinds, D.A., Bourgeron, T., Baron-Cohen, S., i, P.-B.A.G., and andMe Res, T. (2018). Genome-wide analyses of self-reported empathy: correlations with autism, schizophrenia, and anorexia nervosa. Translational Psychiatry 8, 35.

Wee, C.L., Nikitchenko, M., Wang, W.-C., Luks-Morgan, S.J., Song, E., Gagnon, J.A., Randlett, O., Bianco, I.H., Lacoste, A.M.B., Glushenkova, E., et al. (2019a). Zebrafish oxytocin neurons drive nocifensive behavior via brainstem premotor targets. Nature neuroscience 22, 1477-1492.

Wee, C.L., Song, E.Y., Johnson, R.E., Ailani, D., Randlett, O., Kim, J.Y., Nikitchenko, M., Bahl, A., Yang, C.T., Ahrens, M.B., et al. (2019). A bidirectional network for appetite control in larval zebrafish. eLife 8, e43775.

Weinberger, D.R., Torrey, E.F., Neophytides, A.N., and Wyatt, R.J. (1979). Lateral Cerebral Ventricular Enlargement in Chronic Schizophrenia. Archives of General Psychiatry 36, 735-739.

Welham, J., Isohanni, M., Jones, P., and McGrath, J. (2009). The Antecedents of Schizophrenia: A Review of Birth Cohort Studies. Schizophrenia Bulletin 35, 603-623.

Whitfield-Gabrieli, S., Thermenos, H.W., Milanovic, S., Tsuang, M.T., Faraone, S.V., McCarley, R.W., Shenton, M.E., Green, A.I., LaViolette, P., Wojcik, J., et al. (2008). Hyperactivity and hyperconnectivity of the default network in schizophrenia and in first degree relatives of persons with schizophrenia. Biological Psychiatry 63, 1279–1284.

Wiedenheft, B., Sternberg, S.H., and Doudna, J.A. (2012). RNA-guided genetic silencing systems in bacteria and archaea. Nature 482, 331-338.

Wolfe, F.H., Auzias, G., Deruelle, C., and Chaminade, T. (2015). Focal atrophy of the hypothalamus associated with third ventricle enlargement in autism spectrum disorder. Neuroreport 26, 1017-1022.

Wood, J.D., Bonath, F., Kumar, S., Ross, C.A., and Cunliffe, V.T. (2009). Disrupted-in-schizophrenia 1 and neuregulin 1 are required for the specification of oligodendrocytes and neurones in the zebrafish brain. Human Molecular Genetics 18, 391-404.

Woodgett, J.R. (1994). Regulation and functions of the glycogen-synthase kinase-3 subfamily. Seminars in Cancer Biology 5, 269-275.

Woods, I.G., Schoppik, D., Shi, V.J., Zimmerman, S., Coleman, H.A., Greenwood, J., Soucy, E.R., and Schier, A.F. (2014). Neuropeptidergic Signaling Partitions Arousal Behaviors in Zebrafish. Journal of Neuroscience 34, 3142-3160.

Workman, A.D., Charvet, C.J., Clancy, B., Darlington, R.B., and Finlay, B.L. (2013). Modeling Transformations of Neurodevelopmental Sequences across Mammalian Species. Journal of Neuroscience 33, 7368-7383.

Wu, D.-M., Ma, L.-P., Song, G.-L., Long, Y., Liu, H.-X., Liu, Y., and Ping, J. (2017a). Steroidogenic factor-1 hypermethylation in maternal rat blood could serve as a biomarker for intrauterine growth retardation. Oncotarget 8, 96139-96153.

Wu, Q., Tang, W., Luo, Z., Li, Y., Shu, Y., Yue, Z., Xiao, B., and Li, F. (2017b). DISC1 Regulates the Proliferation and Migration of Mouse Neural Stem/Progenitor Cells through Pax5, Sox2, Dll1 and Neurog2. Frontiers in Cellular Neuroscience 11, 114-116.

Wu, S.P., Jia, M.X., Ruan, Y., Liu, J., Guo, Y.Q., Shuang, M., Gong, X.H., Zhang, Y.B., Yang, X.L., and Zhang, D. (2005). Positive association of the oxytocin receptor gene (OXTR) with autism in the Chinese Han population. Biological Psychiatry 58, 74-77.

Wulff, K., Gatti, S., Wettstein, J.G., and Foster, R.G. (2010). Sleep and circadian rhythm disruption in psychiatric and neurodegenerative disease. Nature Reviews Neuroscience 11, 589-599.

Xi, Y.W., Ryan, J., Noble, S., Yu, M., Yilbas, A.E., and Ekker, M. (2010). Impaired dopaminergic neuron development and locomotor function in zebrafish with loss of pink1 function. European Journal of Neuroscience 31, 623-633.

Xing, B., Li, Y.C., and Gao, W.J. (2016). GSK3 beta Hyperactivity during an Early Critical Period Impairs Prefrontal Synaptic Plasticity and Induces Lasting Deficits in Spine Morphology and Working Memory. Neuropsychopharmacology 41, 3003-3015.

Xu, Y., Tamamaki, N., Noda, T., Kimura, K., Itokazu, Y., Matsumoto, N., Dezawa, M., and Ide, C. (2005). Neurogenesis in the ependymal layer of the adult rat 3rd ventricle. Experimental Neurology 192, 251-264.

Yalla, K., Elliott, C., Day, J.P., Findlay, J., Barratt, S., Hughes, Z.A., Wilson, L., Whiteley, E., Popiolek, M., Li, Y., et al. (2018). FBXW7 regulates DISC1 stability via the ubiquitin-proteosome system. Molecular Psychiatry 23, 1278-1286.

Yang, X., Tang, Y., Wei, Q., Lang, B., Tao, H., Zhang, X., Liu, Y., and Tang, A.G. (2017). Up-regulated expression of oxytocin mRNA in peripheral blood lymphocytes from first-episode schizophrenia patients. Oncotarget 8, 78882-78889.

Yao, Y., Li, X., Zhang, B., Yin, C., Liu, Y., Chen, W., Zeng, S., and Du, J. (2016). Visual Cue-Discriminative Dopaminergic Control of Visuomotor Transformation and Behavior Selection. Neuron 89, 598-612.

Ye, F., Kang, E., Yu, C., Qian, X., Jacob, F., Yu, C., Mao, M., Poon, R.Y.C., Kim, J., Song, H., et al. (2017). DISC1 Regulates Neurogenesis via Modulating Kinetochore Attachment of Ndel1/Nde1 during Mitosis. Neuron 96, 1204-1204.

Yeh, C.M., Glock, M., and Ryu, S. (2013). An Optimized Whole-Body Cortisol Quantification Method for Assessing Stress Levels in Larval Zebrafish. Plos One 8, e79406.

Yokogawa, T., Marin, W., Faraco, J., Pezeron, G., Appelbaum, L., Zhang, J., Rosa, F., Mourrain, P., and Mignot, E. (2007). Characterization of sleep in zebrafish and insomnia in hypocretin receptor mutants. Plos Biology 5, 2379-2397.

Yue, L., Karr, T.L., Nathan, D.F., Swift, H., Srinivasan, S., and Lindquist, S. (1999). Genetic analysis of viable Hsp90 alleles reveals a critical role in Drosophila spermatogenesis. Genetics 151, 1065-1079.

Zellner, D., Padnos, B., Hunter, D.L., Macphail, R.C., and Padilla, S. (2011). Rearing conditions differentially affect the locomotor behavior of larval zebrafish, but not their response to valproate-induced developmental neurotoxicity. Neurotoxicology and Teratology 33, 674-679.

Zhang, X.H., Tee, L.Y., Wang, X.G., Huang, Q.S., and Yang, S.H. (2015). Off-target Effects in CRISPR/Cas9-mediated Genome Engineering. Molecular Therapy-Nucleic Acids 4, e264.

Zheng, X.Z., and Sehgal, A. (2010). AKT and TOR Signaling Set the Pace of the Circadian Pacemaker. Current Biology 20, 1203-1208.

Zhou, M., Li, W., Huang, S., Song, J., Kim, J.Y., Tian, X., Kang, E., Sano, Y., Liu, C., Balaji, J., et al. (2013). mTOR Inhibition Ameliorates Cognitive and Affective Deficits Caused by Disc1 Knockdown in Adult-Born Dentate Granule Neurons. Neuron 77, 647-654.

Ziv, L., Muto, A., Schoonheim, P.J., Meijsing, S.H., Strasser, D., Ingraham, H.A., Schaaf, M.J.M., Yamamoto, K.R., and Baier, H. (2013). An affective disorder in zebrafish with mutation of the glucocorticoid receptor. Molecular Psychiatry 18, 681-691.

Zuo, D.-Y., Cao, Y., Zhang, L., Wang, H.-F., and Wu, Y.-L. (2009). Effects of acute and chronic administration of MK-801 on c-Fos protein expression in mice brain regions implicated in schizophrenia with or without clozapine. Progress in Neuropsychopharmacology & Biological Psychiatry 33, 290-295.